

Noradrenergic Deficits Contribute to Impairment in the TgCRND8 Mouse Model of Alzheimer's Disease

by

Beverly M. Francis

A thesis submitted in conformity with the requirements
for the degree of Doctor of Philosophy

Department of Physiology
University of Toronto

© Copyright by Beverly M. Francis (2013)

Noradrenergic Deficits Contribute to Impairment in the TgCRND8 Mouse Model of Alzheimer's Disease

Beverly M. Francis

Doctor of Philosophy

Department of Physiology
University of Toronto

2013

Abstract

Autosomal-dominant mutations in the amyloid precursor protein (APP) gene increase the production and aggregation of toxic amyloid- β (A β) peptides and cause early-onset Alzheimer's disease (AD). Noradrenergic cell loss is well documented in AD and has been posited to play a role in cognitive symptoms as well as disease progression. We investigated memory and affect, tissue levels of catecholamines, brain-derived neurotrophic factor (BDNF) mRNA and bioenergetic homeostasis in TgCRND8 mice that express a double mutant (K670N/M671L + V717F) human *APP*₆₉₅ transgene. We found that TgCRND8 mice develop object memory impairment and behavioural despair, as well as reductions in noradrenaline and BDNF expression in the hippocampus and cortex, before the appearance of A β plaques. Animals with more advanced A β pathology exhibit disruptions in energetic status, along with diminished complex I+III activity in the electron transport chain. To test whether the AD-like phenotypes of TgCRND8 mice might be due to altered noradrenergic tone, pre-plaque mice were treated with dexefaroxan, an antagonist of presynaptic inhibitory α_2 -adrenoceptors that are highly expressed on both noradrenergic and cholinergic terminals. Effects of

dexefaroxan were compared to those of rivastigmine, a cholinesterase inhibitor. Both dexefaroxan and rivastigmine improved behavioural phenotypes and BDNF expression without affecting tissue A β load. Drug treatments also restored complex I+III mitochondrial activity and increased ATP levels. Reductions in noradrenergic tone appear to underlie A β -induced functional impairment in TgCRND8 mice, in addition to BDNF deficits and bioenergetic stress. These studies suggest that α_2 -adrenoceptor targeting may warrant consideration as a therapeutic strategy in AD.

To Leo and Moira,
with love.

Acknowledgments

I extend my deepest gratitude to my supervisor, Dr. Howard Mount, for guiding me both professionally and personally. Howard is a wonderful role model, teacher and mentor. His advice set me on the right path and helped me achieve my best.

I would also like to thank my thesis committee members, Dr. JoAnne McLaurin and Dr. Linda Mills, whose support and recommendations were crucial to the completion of this work. I also thank Dr. Paul Frankland, Dr. James Eubanks, Dr. Sheena Josselyn, Dr. Jason Lerch and Dr. Douglas Feinstein for evaluating my thesis. I am grateful to our collaborators, Dr. Margaret Fahnestock, Dr. Brian Robinson, Dr. Yeni Yücel and Dr. Richard Bazinet, for sharing their technical expertise and passion for neuroscience.

It has been a pleasure working in the Mount lab, due in large part to Dr. Jennifer Griffin, Keith Ho, Emily Lam, Jimmy Yang, Elizabeth Cumyn, Valeriya Larskova and Zohar Weinbrand, who have provided me with assistance, encouragement and laughter. I also thank Dr. Janice Robertson, Dr. Cheryl D'Souza, Dr. Jesse McLean, Dr. Vivian Ng, Dr. Christopher Bohm, Dr. John Sévalle, Robert Chen and Rosemary Ahrens, for their comradeship and advice. I treasure these friendships formed at the CRND. To my dear friends outside of the lab, particularly Anna Stasienko and Sunil Rao, thank-you for giving me much needed perspective, coffee and companionship during stressful times.

I also gratefully acknowledge support from the Ontario Graduate Scholarship (OGS), the Peterborough K.M. Hunter Alzheimer's Graduate Studentship and the Ontario Graduate Scholarship in Science and Technology (OGSST) programs.

I am indebted to my loving family for their unwavering support. This thesis is dedicated to my beloved father Leo (Nov. 25th 1953 – April 22nd, 2012), who would have read every word in it and been all the more proud, and mother Moira, who refuses to read it but has given me all I need to accomplish it. I thank my brother Dalton, for leading me to the finish line and teaching me more than I could ever teach him. Finally, I thank my fiancé Ian Aranja, for enduring the worst of me and inspiring the best in me. I love you.

Contributions

This thesis consists of 4 original research studies. Chapter 3 was published in the journal *Neurobiology of Aging* (Francis *et al.*, 2012a) and Chapter 4 was published in the journal *Neuropsychopharmacology* (Francis *et al.*, 2012b). Research described in Chapters 5, 6 and 8 has yet to be published.

The author performed all experiments described in the thesis, except as noted below:

Mr. Jimao Yang – HPLC analyses of monoamines and high-energy tissue phosphates in mouse brain tissue

Dr. Margaret Fahnestock – guidance in RT-PCR measurement of BDNF mRNA in mouse brain tissue (performed jointly with Ms. Bernadeta Michalski)

Dr. JoAnne McLaurin – assessment of spatial memory in mice (performed by Dr. Meredith Barakat) and guidance with western blot analyses of holoAPP and β -CTF (assistance provided by Ms. Mary Brown)

Dr. Brian Robinson – guidance in planning and analyses of mitochondrial enzymatic activities and tissue expression in mouse brain (assistance provided by Dr. Mary Maj)

Dr. Yeni Yücel – assessment of visual function in mice (performed by Dr. Stephan Fraenkl and Mr. John Kim in the Mount laboratory)

Dr. Richard Bazinet – TLC measurement of cardiolipin in mouse brain (performed by Mr. Chris Song)

Ms. Enid Hajderi – artwork for the microwave dissection procedure

Table of Contents

ACKNOWLEDGMENTS	V
CONTRIBUTIONS	VI
TABLE OF CONTENTS	VII
LIST OF TABLES	XIII
LIST OF FIGURES	XIV
LIST OF ABBREVIATIONS	XVI
PREFACE	1
CHAPTER 1 LITERATURE REVIEW	2
1.1 Alzheimer's Disease	3
1.1.1 Clinical Presentation	3
1.1.1.1 Cognition	4
1.1.1.2 Affect	5
1.1.2 Neuropathology	5
1.1.2.1 Amyloid Plaques	6
1.1.2.2 Neurofibrillary Tangles	6
1.1.3 Neurotransmitter System Involvement	7
1.1.3.1 The Cholinergic Hypothesis	8
1.1.3.2 Damage to the Locus Coeruleus Noradrenergic System	9
1.1.4 Neurotrophic Mechanisms	10
1.1.5 Bioenergetic Factors in Disease Progression	12
1.1.5.1 The Electron Transport Chain and ATP Homeostasis	12
1.1.5.2 Oxidative Stress and Mitochondrial Dysfunction	14
1.1.5.3 Decreased Metabolic Activity	16
1.2 The Amyloid Cascade Hypothesis	18
1.2.1 Early-Onset Familial Mutations	18
1.2.2 APP Processing, A β Production and Fibrillogenesis	19
1.2.3 Toxicity of A β	22
1.2.3.1 Distal Axonopathy and Synaptic Dysfunction	22
1.2.3.2 A β Downregulation of BDNF Signaling	23
1.2.3.3 A β Interactions with Mitochondria	25

1.3 Noradrenergic Mechanisms in Alzheimer’s Disease	26
1.3.1 Noradrenaline in the Brain	27
1.3.1.1 Anatomical Locus	27
1.3.1.2 Synthesis and Metabolism	29
1.3.1.3 Receptors and Signal Transduction Pathways	30
1.3.1.4 Functions	32
1.3.2 Noradrenergic Depletion Potentiates Amyloid Toxicity	33
1.3.2.1 Decreased Clearance of A β and Increased Inflammation	33
1.3.2.2 Decreased Cholinergic Transmission	35
1.3.2.3 Decreased Trophic Support	38
1.3.2.4 Increased Oxidative and Energetic Stress	38
1.4 APP-Transgenic Mouse Models of Alzheimer’s Disease	40
1.4.1 Mouse Models of A β Deposition	41
1.4.2 Limitations in Modeling Late-Stages of Disease	43
1.4.3 Noradrenergic Involvement in APP-Tg mice	45
1.4.3.1 Noradrenaline Depletion Studies	46
1.4.3.2 Noradrenaline Enhancement Studies	48
1.4.4 The TgCRND8 Mouse	49
1.4.4.1 Neuropathological and Neurochemical Changes	50
1.4.4.2 Behavioral Profile	53
1.4.4.3 Validity as a Model of Alzheimer’s Disease	54
 CHAPTER 2 HYPOTHESES AND EXPERIMENTAL APPROACH	 56
2.1 Thesis Aims	57
2.2 Hypotheses	57
2.2.1 Object Memory Impairment is an Early Endophenotype	57
2.2.2 Noradrenaline Content is Reduced in Major Terminals and Antagonism of α_2 -Adrenoceptors Mitigates Functional Impairment	57
2.2.3 Bioenergetic Homeostasis is Disrupted by Mitochondrial Dysfunction	58
2.2.4 Blockade of α_2 -Adrenoceptors Alleviates Mitochondrial Impairment	58
 CHAPTER 3 OBJECT RECOGNITION MEMORY AND BDNF EXPRESSION ARE REDUCED IN YOUNG TgCRND8 MICE	 59
3.1 Abstract	60

3.2 Introduction	61
3.3 Methods	63
3.3.1 Mice	63
3.3.2 Object Recognition	63
3.3.3 Visual Function	65
3.3.4 Spatial Memory	66
3.3.5 Measurement of BDNF mRNA	66
3.3.6 Statistical Analysis	67
3.4 Results	68
3.4.1 Progressive Object Recognition Deficits Precede Amyloid Plaque Accumulation	68
3.4.2 Pre-plaque TgCRND8 Mice are Not Impaired in the Morris Water Maze Task	70
3.4.3 BDNF mRNA is Reduced in the Hippocampus and Frontal Cortex of Young TgCRND8 Mice	71
3.5 Discussion	73
CHAPTER 4 REDUCED TISSUE LEVELS OF NORADRENALINE ARE ASSOCIATED WITH BEHAVIORAL PHENOTYPES OF THE TgCRND8 MOUSE MODEL OF ALZHEIMER'S DISEASE	77
4.1 Abstract	78
4.2 Introduction	79
4.3 Materials and Methods	81
4.3.1 Transgenic Mice	81
4.3.2 Brain Fixation and Microdissection	81
4.3.3 Tissue Catecholamines	83
4.3.4 Tail Suspension Test	84
4.3.5 Assessing Forelimb Coordination with the Tape Removal Task	84
4.3.6 Drug Treatments, Behavioral Testing and Tissue Processing	84
4.3.7 A β Immunoassays	86
4.3.8 Western Blotting	86
4.3.9 Measurement of BDNF mRNA	87

4.3.10 Statistical Analysis	88
4.4. Results	89
4.4.1 TgCRND8 Mice Exhibit Early Reductions in Noradrenaline Content Within Major Terminal Fields	89
4.4.2 TgCRND8 Mice Display Behavioral Despair in the Tail Suspension Test	90
4.4.3 Desipramine Alleviates Behavioral Despair	91
4.4.4 TgCRND8 Mice are Not Impaired in a Test of Forelimb Coordination	92
4.4.5 Dexefaroxan and Rivastigmine Reduce Object Memory Impairment and Behavioral Despair	93
4.4.6 Treatments Do Not Affect Amyloid Burden	95
4.4.7 Dexefaroxan and Rivastigmine Increase BDNF mRNA	97
4.4.8 Dexefaroxan and Rivastigmine Differentially Affect Noradrenaline Turnover in the Hippocampus	98
4.5 Discussion	99
CHAPTER 5 SELECTIVE TARGETING OF MITOCHONDRIAL COMPLEX I IN AGED APP-TRANSGENIC TgCRND8 MICE	105
5.1 Abstract	106
5.2 Introduction	107
5.3 Methods	109
5.3.1 Transgenic Mice	109
5.3.2 Metabolic Enzyme Activities	109
5.3.3 Western Blot Analysis	112
5.3.4 Heat-Inactivated Tissue Preparation	112
5.3.5 Measurement of Cardiolipin	113
5.3.6 High-Energy Phosphate Donors	113
5.3.7 Statistical Analysis	114
5.4 Results	115
5.4.1 Linked Complex I+III Activity and NDUFB8 Complex I Subunit Expression are Reduced in Aged TgCRND8 Mice	115
5.4.2 Cardiolipin is Unaltered in TgCRND8 Mice	118

5.4.3	ATP is Maintained While Creatine is Upregulated at End-Stages of Disease	119
5.5	Discussion	120
CHAPTER 6	DEXEFAROXAN IMPROVES MITOCHONDRIAL FUNCTION IN A MOUSE MODEL OF ALZHEIMER'S DISEASE	123
6.1	Abstract	124
6.2	Introduction	125
6.3	Methods	127
6.3.1	Mice	127
6.3.2	Drug Treatments	127
6.3.3	Metabolic Enzyme Activities	128
6.3.4	Western Blotting	131
6.3.5	Measurement of Tissue ATP and Creatine	132
6.3.6	Statistical Analysis	132
6.4	Results	133
6.4.1	Cortical Complex I+III Activity is Increased in Young TgCRND8 Mice...	133
6.4.2	Key Subunits of Complexes I and III are Not Differentially Expressed in Young TgCRND8 Mice	134
6.4.3	ATP is Transiently Depleted in the Hippocampus of Plaque-Bearing Mice, but Maintained in Cortical Regions with Increased Creatine Content	136
6.4.4	Dexefaroxan and Rivastigmine Increase ATP and Complex I+III Activity	137
6.5	Discussion	140
CHAPTER 7	CONCLUSIONS	143
7.1	General Discussion	144
7.2	Translational Impact	157

CHAPTER 8 FUTURE DIRECTIONS160

8.1 Are Protective Effects of α_2 -Adrenoceptor Blockade Mediated through Increased β -Adrenoceptor Activation?161

8.2 Does α_2 -Adrenoceptor Blockade Improve Metabolic State in TgCRND8 Mice by Stabilizing Mitochondrial Respirasomes?.....162

8.3 Does α_2 -Adrenoceptor Antagonism Reduce Oxidative Stress?.....163

8.4 Is Serotonergic Transmission Altered, and if so, How does this Influence Anxiety in TgCRND8 mice?164

CONCLUDING STATEMENT169

REFERENCES170

List of Tables

Table 1-1. APP-Transgenic mouse models of AD	42
Table 4-1. Tissue levels of dopamine and metabolites in the TgCRND8 brain	90
Table 6-1. Cortical and hippocampal complex IV activity in TgCRND8 mice	134

List of Figures

Figure 1-1.	Proteolysis of APP.....	20
Figure 1-2.	Nomenclature and coupling of adrenergic receptors	30
Figure 1-3.	Schematic of noradrenergic regulation of cortical acetylcholine release	36
Figure 3-1.	Object recognition memory assessed at pre-plaque and plaque Ages	69
Figure 3-2.	Exploration of objects and visual function examined in pre-plaque mice at 8 – 9 weeks of age	70
Figure 3-3.	Spatial reference memory in the <i>Morris</i> water maze assessed in 8-week-old mice	71
Figure 3-4.	Hippocampal BDNF mRNA levels measured by absolute quantitative real-time reverse transcriptase polymerase chain reaction (RT-PCR)	72
Figure 3-5.	Cortical BDNF mRNA levels in pre-plaque mice	72
Figure 4-1.	Dissection of a microwave-fixed brain is performed so as to allow for the crumbly nature of the cooked tissue	82
Figure 4-2.	Tissue levels of noradrenaline are reduced in major terminal fields of the TgCRND8 brain	89
Figure 4-3.	TgCRND8 mice exhibit pronounced behavioural despair in the tail suspension test	91
Figure 4-4.	Desipramine reduces immobility in the tail suspension test	92
Figure 4-5.	Forelimb use is not affected in TgCRND8 mice	92
Figure 4-6.	Dexefaroxan and rivastigmine affect memory, but not exploration of objects	94
Figure 4-7.	Dexefaroxan and rivastigmine reduce behavioural despair	95
Figure 4-8.	Dexefaroxan and rivastigmine do not affect A β , APP or β -CTF Levels	96
Figure 4-9.	Dexefaroxan and rivastigmine rescue BDNF mRNA levels in	

	TgCRND8 mice	97
Figure 4-10.	Dexefaroxan and rivastigmine differentially affect tissue levels of noradrenaline and normetanephrine in the hippocampus of 16-week-old TgCRND8 and non-Tg mice	98
Figure 5-1.	Complex I+III activity is reduced in aged TgCRND8 brains	116
Figure 5-2.	Expression of the complex I NDUFB8 subunit is decreased in aged TgCRND8 brains	117
Figure 5-3.	Neither cardiolipin nor its fatty acid constituents are altered in TgCRND8 mice	118
Figure 5-4.	Tissue levels of ATP are maintained while those of creatine are upregulated in the cortex and hippocampus of aged TgCRND8 mice	119
Figure 6-1.	Hemispheric mitochondrial enzyme activities are not altered in 9-week-old TgCRND8 mice	133
Figure 6-2.	Complex I+III activity is increased in the cortex, but not in the hippocampus at early stages of disease progression	134
Figure 6-3.	Expression of key nuclear-DNA encoded subunits of complexes I and III is unaltered in the hippocampus and cortex of 9-week-old mice.....	135
Figure 6-4.	Plaque-bearing mice exhibit reduced ATP tissue content in the hippocampus, but not in the cortex where creatine content is increased	137
Figure 6-5.	Dexefaroxan and rivastigmine restore hippocampal ATP levels in young TgCRND8 mice	138
Figure 6-6.	Dexefaroxan and rivastigmine increase complex I+III activity without altering citrate synthase activity	139
Figure 8-1.	Tissue content of 5-HIAA is increased in the striatum and frontal cortex of TgCRND8 brains.....	165
Figure 8-2.	TgCRND8 mice are less anxious than non-Tg controls in the zero Maze	166
Figure 8-3.	Dexefaroxan and rivastigmine do not alter performance in the zero Maze	167

List of Abbreviations

3-MT	3-methoxytyramine
5-HIAA	5-hydroxyindolacetic acid
5-HT	5-hydroxytryptamine; serotonin
α -KGDH	α -ketoglutarate dehydrogenase
β -CTF	β -C-terminal fragment
A β	Amyloid- β
ABAD	A β -binding alcohol dehydrogenase
ACh	Acetylcholine
AD	Alzheimer's disease
AICD	APP intracellular domain
ANOVA	Analysis of variance
Aph-1	Anterior pharynx defective 1
APLP	Amyloid precursor-like protein
APP	Amyloid precursor protein
ADP	Adenosine diphosphate
AMP	Adenosine monophosphate
APOE	Apolipoprotein E
ARA	Arachidonic acid
ATP	Adenosine triphosphate
BACE1	β -site APP-cleaving enzyme 1
BDNF	Brain-derived neurotrophic factor
cAMP	Cyclic AMP
ChAT	Choline acetyltransferase
CNS	Central nervous system
CoA	Coenzyme A
COMT	Catechol-O-methyltransferase
CREB	Cyclic AMP response element binding protein
CS	Citrate synthase
CXCL1	Chemokine (C-X-C motif) ligand 1
DA	Dopamine
DAG	Diacylglycerol
DHA	Docosahexaenoic acid
DHMA	3,4-Dihydroxymadelic acid
DHPG	3,4-Dihydroxyphenylglycol
DNA	Deoxyribonucleic acid
DOPAC	Dihydrophenylacetic acid
DOPEGAL	3,4-Dihydroxyphenylglycoaldehyde
DSP-4	<i>N</i> -(2-chloroethyl)- <i>N</i> -ethyl-2-bromobenzylamine
DTNB	5,5'-Dithio-bis-2-nitrobenzoic acid
EC	Enzyme complex

EDTA	Ethylenediaminetetraacetic acid
ETC	Electron transport chain
FADH ₂	Flavin adenine dinucleotide
FAME	Fatty acid methyl ester
FE	Frequency of extinction
FPR2	Formyl-peptide receptor 2
GABA	γ-aminobutyric acid
GAPDH	Glyceraldehyde-3-phosphate dehydrogenase
GSH	Glutathione
hAPP	Human APP
HPLC	High-performance liquid chromatography
HSV	High speed video
HVA	Homovanillic acid
IDE	Insulin degrading enzyme
IL-1β	Interleukin-1β
iNOS	Inducible nitric oxide synthase
IP ₃	Inositol triphosphate
L-DOPS	L-threo-3,4-dihydroxyphenylserine
LSD	Least significant difference
LTD	Long term depression
LTP	Long term potentiation
MAO	Monoamine oxidase
MCI	Mild cognitive impairment
MCP-1	Monocyte chemoattractant protein
MHPG	3-Methoxy-4-hydroxyphenylglycol
MI	Memory index
mRNA	Messenger ribonucleic acid
NA	Noradrenaline
NADH	Nicotinamide adenine dinucleotide
NET	Noradrenaline transporter
NGF	Nerve growth factor
NMDA	<i>N</i> -methyl- <i>D</i> -aspartate
NMN	Normetanephrine
OXPPOS	Oxidative phosphorylation
p75NTR	p75 Neurotrophin receptor
PBS	Phosphate buffered saline
PCR	Polymerase chain reaction
P-CREB	Phosphorylated CREB
PDH	Pyruvate dehydrogenase
Pen-2	Presenilin enhancer 2
PKC	Protein kinase C
PLCβ	Phospholipase Cβ
PrP	Prion promoter
PS1	Presenilin 1

PS2	Presenilin 2
RAGE	Receptor for advanced glycation end products
RNA	Ribonucleic acid
ROS	Reactive oxygen species
RT-PCR	Real-time PCR
SEM	Standard error of the mean
TBS	Tris buffered saline
TCA	Tricarboxylic acid
Tg	Transgenic
TLC	Thin-layer chromatography
TOM	Translocase of the outer membrane
Trk	Tropomyosin receptor kinase
VMA	Vanillylmandelic acid

Preface

Alzheimer's disease (AD) is often characterized as a disorder of progressive cholinergic dysfunction. However, therapies aimed at improving cholinergic transmission have had limited success in treating the behavioural and pathological indices of AD. This may be because treatments are initiated outside the therapeutic window of opportunity and/or because the noradrenergic system is more severely affected (Zarow *et al.*, 2003). Loss of cortical noradrenergic innervation and its modulatory influences on other transmitters, especially the cholinergic system, are implicated in several behavioural symptoms of AD, including depression, poor attention and memory impairments (Herrmann *et al.*, 2004; Marien *et al.*, 2004; Decker and Gallagher, 1987). Reductions in noradrenaline may also hinder the brain's capacity to fight injuries caused by the toxic amyloid- β ($A\beta$), that accumulates in the disease (reviewed in Marien *et al.*, 2004). We examined the influence of reduced brain noradrenaline in facilitating AD-like phenotypes of TgCRND8 mice, a genetically engineered robust model of $A\beta$ deposition.

Chapter 1 Literature Review

1.1 Alzheimer's Disease

At a meeting in Tübingen, Dr. Alois Alzheimer first presented clinical and histological findings from his case study of Auguste D., a middle-aged, female psychiatric patient. Auguste was institutionalized in Frankfurt in 1901 and over the next 4 and half years had shown progressive deterioration of comprehension and memory, as well as severe psychosocial impairments. At autopsy, Alzheimer noted 2 types of inclusions in her brain, which still serve as the cardinal features to definitely diagnose AD. His lecture titled "*A characteristic serious disease of the cerebral cortex*" was published in 1907. In it, he described intracellular neurofibrillary tangles: "*In the center of an otherwise almost normal cell there stands out one or several fibrils due to their characteristic thickness and peculiar impregnability*" and amyloid plaques: "*Numerous small miliary foci are found in the superior layers. They are determined by the storage of a peculiar material in the cortex*" (translated and reprinted in Maurer *et al.*, 1997). Today, AD is recognized as the most common neurodegenerative disorder and type of dementia in the elderly.

1.1.1 Clinical Presentation

AD is thought to begin decades before symptoms are first detected (Price and Morris, 1999; Braak and Del Tredici, 2011). Rare autosomal-dominant, inherited cases usually develop symptoms before the age of 60, whereas the more common, sporadic cases have later onset. Despite different initial pathways, both inherited and sporadic AD exhibit similar cognitive features and pathophysiology. Thus, studying presymptomatic individuals with these causative mutations can provide key insights into the mechanisms and treatment of AD (reviewed in Bateman *et al.*, 2011). Dementia is diagnosed when cognitive deficits interfere with daily living, at which point the pathology in AD brains may be extensive. The focus of this thesis is on early stages of disease, during a phase of mild cognitive impairment (MCI), and on the transition to dementia.

1.1.1.1 *Cognition*

MCI represents a transitional state between aging and dementia. Individuals with amnesic MCI exhibit clinically significant memory impairment beyond that of normal aging and are more likely to progress to a diagnosis of AD dementia. Cognitive deficits in MCI patients are sufficiently mild that they do not interfere with social or occupational functioning, and thus do not meet the criteria for dementia (reviewed in Petersen *et al.*, 1999; Morris *et al.*, 2001; Albert *et al.*, 2011; Petersen, 2011). For a clinical diagnosis of AD, cognitive decline must be progressive. AD dementia has an insidious onset. Disruption of episodic memory is the primary early complaint. Learning and memory deficits are usually accompanied by impairment in other cognitive domains including language, visuospatial abilities and executive function (revised clinical criteria by the National Institute on Aging and the Alzheimer's Association in McKhann *et al.*, 2011). Longitudinal neuropsychological assessment of patients with MCI and early AD dementia suggests anterograde amnesia is followed by semantic and language impairments, attention deficits and difficulty in completing complex visuospatial tasks (Lambon Ralph *et al.*, 2003).

The staging of psychological deficits reflects the distribution of pathology in typical AD brains. This starts in the medial temporal lobe then spreads to the temporal neocortex, frontal and parietal association areas and the basal forebrain (Braak and Braak, 1991; reviewed in Serrano-Pozo *et al.*, 2011). Atrophy of entorhinal cortex, and damage to the entorhinal-hippocampal circuitry that relays processed multimodal information to and from the neocortex, is highly predictive of conversion from MCI to AD (Chetelat and Baron, 2003; von Gunten *et al.*, 2006; Devanand *et al.*, 2007; Harris *et al.*, 2010; Gallagher and Koh, 2011; Devanand *et al.*, 2012). Tests of object recognition and visual attention rely heavily on the temporo-parietal cortex. For this reason, they are useful for detecting AD before it progresses to clinical dementia (Viggiano *et al.*, 2008; Alegret *et al.*, 2009; Bublak *et al.*, 2011).

1.1.1.2 *Affect*

Dr. Alzheimer's observations of Auguste included unpredictable behaviour, paranoia and auditory hallucinations. He noted that Auguste presented, "*as one of her first disease symptoms a strong feeling of jealousy towards her husband*" (reprinted in Maurer *et al.*, 1997). Non-cognitive disturbances occur in more than 50% of AD patients. Behavioural symptoms in AD can be grouped into those with psychotic features (hallucinations and delusions) and those without. The latter include apathy, depression, agitation and aggression (reviewed in Lanari *et al.*, 2006).

Affective changes are observed early and become more prevalent as the disease progresses. Depression and apathy may emerge prior to the onset of cognitive dysfunction, while psychotic behaviours are typically seen at late stages of dementia (Cummings, 2000; Bruen *et al.*, 2008; Fernández *et al.*, 2010). An imbalance in cholinergic-monoaminergic transmission may contribute to behavioural disturbances. Cholinergic deficits and degeneration of the nucleus basalis can impair corticolimbic interactions that regulate mood states (reviewed in Cummings and Kaufer, 1996). Loss of noradrenergic neurons in the locus coeruleus and of their cortical projections are associated with depressive and aggressive symptoms in AD (reviewed in Herrmann *et al.*, 2004).

1.1.2 Neuropathology

Histopathological hallmarks of the AD brain include extracellular senile plaques, intracellular neurofibrillary tangles and the loss of multiple neuronal populations.

1.1.2.1 *Amyloid Plaques*

The principal component of senile plaques, purified and sequenced by Glenner and Wong in 1984, is the amyloid- β ($A\beta$) peptide. This peptide varies from 38 to 43 amino acids in length and assumes multiple assembly states that differ in neurotoxicity. The deposition of $A\beta$ in the AD brain progresses regionally in 5 stages: (1) exclusively in the neocortex, (2) expanding into the transentorhinal cortex and CA1 region of the hippocampus, (3) into the dentate gyrus of the hippocampus, basal forebrain and the rest of the diencephalon, (4) extending through the rest of the hippocampus, striatum and brainstem nuclei, (5) to the cerebellum (Thal *et al.*, 2002). Amyloid plaques are categorized as diffuse or dense-cored deposits of $A\beta$. Dense-cored plaques contain $A\beta$ aggregates at the center of clustered dystrophic neuronal processes (i.e. dendrites or axons), hypertrophic astrocytes and activated microglia. These dense plaques are associated with synaptic loss. Diffuse plaques are non-neuritic amorphous $A\beta$ deposits that are not associated with glial inflammation or synaptic loss. They are often observed in brains of the non-demented elderly (reviewed in Serrano-Pozo *et al.*, 2011). Dystrophic neurites develop retrogradely from focal $A\beta$ aggregates, which may contribute to somatic and dendritic degeneration and to the formation of neurofibrillary tangles (Su *et al.*, 1998). The severity of AD dementia does not correlate well with plaque burden, but rather with the concentration of soluble $A\beta$ (Lue *et al.*, 1999; Näslund *et al.*, 2000).

1.1.2.2 *Neurofibrillary Tangles*

Neurofibrillary tangles are intracellular inclusions consisting of hyperphosphorylated tau, a microtubule-associated protein. Tau promotes the assembly and stabilization of microtubules in the cytoskeleton. When tau is abnormally phosphorylated, it detaches from microtubules and polymerizes into straight and paired helical filaments that

assemble into neurofibrillary tangles. Tau filaments destabilize the microtubules, disrupting axonal transport and causing axonal degeneration (reviewed in Götz *et al.*, 2004; Ballatore *et al.*, 2007; Alonso *et al.*, 2010). The degree of neurofibrillary pathology in cortical regions correlates well with the severity of dementia. The topographic distribution of tangles spreads in a predictable manner, described in the Braak staging for AD-neurofibrillary lesions. Tangles are first found in transentorhinal cortices, spread to entorhinal and hippocampal regions, progress widely to limbic areas and finally accumulate in associative cortices (Braak and Braak, 1991; Braak *et al.*, 2006).

Hyperphosphorylation and filamentous deposits of tau can cause dysfunction and degeneration in the absence of A β and are observed in several neurodegenerative dementing diseases. Abnormally phosphorylated tau appears to be a common mediator of neurodegeneration in response to upstream toxic events in AD and other tauopathies (reviewed in Ballatore *et al.*, 2007). In AD, the A β accumulation predates tau pathology and frank neuronal injury (reviewed in Hardy and Selkoe, 2002). Exposure to A β has been shown to induce tau phosphorylation and neurofibrillary tangle formation, both *in vivo* and *in vitro* (Götz *et al.* 2001; Lewis *et al.*, 2001; Gamblin *et al.*, 2003; Oddo *et al.*, 2003; reviewed in Götz *et al.* 2004). Moreover, A β immunotherapy has been shown to reduce not only A β levels but also early tau pathology (Oddo *et al.*, 2004). These findings lend credence to the amyloid cascade hypothesis (discussed in section 2.2), which posits A β accumulation to be the primary pathogenic event in AD.

1.1.3 Neurotransmitter System Involvement

Neuronal populations that project to or from regions burdened with plaques are especially vulnerable to A β toxicity (reviewed in Kar *et al.*, 2004). The clinical profile of AD is related to disturbances in multiple neurotransmitter systems, chief among which is

the atrophy of cholinergic and noradrenergic subcortical nuclei and their projections (reviewed in Lyness *et al.*, 2003).

1.1.3.1 *The Cholinergic Hypothesis*

Cholinergic neurons in the basal forebrain project to the cortex and hippocampus. The role of central cholinergic transmission in learning and memory was first advanced by Deutsch in 1971, and was soon confirmed pharmacologically by Drachman and colleagues who observed that cholinergic blockade impaired while cholinergic enhancement improved memory and cognitive performance in humans (Drachman and Leavitt, 1974; Drachman, 1977). Around the same time, researchers began reporting of severe presynaptic cholinergic deficits in the hippocampus and cortex of AD brains. The evidence presented included: decreased activity of choline acetyltransferase, the enzyme responsible for acetylcholine synthesis (Bowen *et al.*, 1976; Davies and Maloney, 1976; Perry *et al.*, 1977), reduced choline uptake (Rylett *et al.*, 1983) and acetylcholine release (Nilsson *et al.*, 1986), and loss of cholinergic cell bodies in the nucleus basalis of Meynert (Whitehouse *et al.*, 1982). These early studies helped establish the cholinergic hypothesis, which posits that the degeneration of basal forebrain cholinergic neurons is primarily responsible for cognitive decline in AD (Bartus *et al.*, 1982; Bartus, 2000). In support of this, cholinergic deficits have been found to correlate with the severity of dementia and amyloid load (Perry *et al.*, 1978; Wilcock *et al.*, 1982).

The cholinergic hypothesis has led to FDA approval of several cholinesterase inhibitors, which prevent the catabolism of acetylcholine, for the symptomatic treatment of AD. However, therapies aimed at improving cholinergic transmission have had modest efficacy in treating behavioural indices of the disease (reviewed in Francis *et al.*, 1999; Mesulam *et al.*, 2004; Schliebs and Arendt, 2006; Francis *et al.*, 2010; Contestabile, 2011). Cortical cholinergic denervation and cell loss in the nucleus basalis is evident in patients with advanced stages of disease, but may not occur in patients with MCI or

early stages of AD. In fact, choline acetyltransferase activity has been found stable or even upregulated in the hippocampus and cortex of patients with mild dementia (Davis *et al.*, 1999; DeKosky *et al.*, 2002). These cholinergic alterations may be associated with behavioural and psychotic features of AD and could be caused by altered trophic factor expression and damage to postsynaptic cholinergic signaling mechanisms (reviewed in Mesulam *et al.*, 2004; Francis *et al.*, 2010; Contestabile, 2011). In sum, it is now thought that cholinergic lesions may not play as prominent a role in the pathogenesis or clinical manifestations of AD as previously believed. They are nonetheless crucially involved in the progression of the disease.

1.1.3.2 *Damage to the Locus Coeruleus Noradrenergic System*

Noradrenergic cell bodies in the locus coeruleus are the major source of noradrenaline in the brain. They project widely to the entire cerebral cortex, thalamic nuclei, limbic areas and hippocampus, but spare the basal ganglia. These widespread noradrenergic projections regulate dynamic interactions among forebrain networks involved in attention, memory and mood (reviewed in Sara 2009). The anatomical arrangement of noradrenergic neurons in the locus coeruleus and its role in cognitive processes are discussed in section 2.3.

Forno reported moderate to severe loss of locus coeruleus cells in a majority of pre-senile AD cases (Forno 1966, 1978). Since 1980, many researchers have documented substantial neuronal losses in the locus coeruleus of AD patients (Mann *et al.*, 1980, 1982, 1984a,b; Bondareff *et al.*, 1981, 1982; Perry *et al.*, 1981b; Tomlinson *et al.*, 1981; Iversen *et al.*, 1983; Marcyniuk *et al.*, 1986; Zweig *et al.*, 1988; Chan-Palay and Asan, 1989; Strong *et al.*, 1991; German *et al.*, 1992; Förstl *et al.*, 1992; Szot *et al.*, 2000; Matthews *et al.*, 2002; Grudzien *et al.*, 2007). The magnitude of locus degeneration in AD is considerable. On average 60% loss is reported (reviewed in Busch *et al.*, 1997), and the extent of loss correlates with age of onset, severity of dementia (Mann *et al.*, 1984b; Bondareff *et al.*, 1987; Zweig *et al.*, 1988; Förstl *et al.*, 1992; German *et al.*,

1992; Matthews *et al.*, 2002) and extent of AD pathology (Tomlinson *et al.*, 1981; Bondareff *et al.*, 1987; German *et al.*, 1987; Grudzien *et al.*, 2007). Indeed, neuronal loss in the locus coeruleus has been found to be more profound and to correlate better with the duration of AD than does the loss of cholinergic cells in the nucleus basalis (Mann *et al.*, 1984a; Zarow *et al.*, 2003).

Damage to the locus coeruleus is observed at early stages of AD and in cases of MCI. AD brains exhibit preferential loss of noradrenergic cell bodies that project to the cortex and hippocampus (Marcyniuk *et al.*, 1986; German *et al.*, 1992; Hoogendijk *et al.*, 1995; Busch *et al.*, 1997; Szot *et al.*, 2000), along with reductions in tissue levels of noradrenaline (Adolfsson *et al.*, 1979; Mann *et al.*, 1981; Tomlinson *et al.*, 1981; Palmer *et al.*, 1987a) and in the enzymes that synthesize noradrenaline (Cross *et al.*, 1981; Perry *et al.*, 1981a; Palmer *et al.*, 1987b). However, reductions in transmitter level do not correlate with the degree of neuronal cell loss. Surviving neurons in the locus coeruleus compensate for the loss of noradrenergic innervation. Compensatory changes include increased expression of tyrosine hydroxylase, the rate-limiting enzyme in the synthesis of noradrenaline and sprouting of axonal projections into the hippocampus and prefrontal cortex (Szot *et al.*, 2006, 2007). Collectively, neuropathological studies reveal degeneration of noradrenergic projections, decreased noradrenaline concentrations and enhanced noradrenaline turnover in terminal fields highly burdened with plaques and tangles (reviewed in Herrmann *et al.*, 2004; McMillan *et al.*, 2011). Locus coeruleus neurons and their projections are vulnerable to A β and denervation of this system potentiates neurodegeneration (reviewed in Marien *et al.*, 2004).

1.1.4 Neurotrophic Mechanisms

A deficiency in neurotrophic support might contribute to neurodegeneration in AD. Neurotrophins are a family of structurally and functionally related proteins that promote

the development, differentiation and survival of neurons. During development, neurotrophins stimulate axonal growth and help establish synaptic contacts. Axonal transport is crucial for neurotrophin function, as they are usually synthesized distal from their site of action. Developing neurons that do not receive adequate neurotrophic signals from cellular targets undergo apoptosis. While levels drop in maturity, neurotrophins continue to maintain survival as well as enhance synaptic plasticity and memory (reviewed in Siegel and Chauhan, 2000; Hennigan *et al.*, 2007).

The neurotrophin consists of nerve growth factor (NGF, Levi-Monatalcini and Hamburger, 1951), brain-derived neurotrophic factor (BDNF, Barde *et al.*, 1982) and the neurotrophins-3 and -4/5 (NT-3 and NT-4/5, Maisonpierre *et al.*, 1990; Hallbook *et al.*, 1991; Ip *et al.*, 1992). Neurotrophin effects are mediated via two classes of receptor: the Trk (tropomyosin receptor kinase) family of tyrosine kinase receptors and the p75 neurotrophin receptor (p75NTR), which is a member of the tumor necrosis factor receptor family. Each neurotrophin preferentially binds to a subtype of Trk receptor: NGF activates TrkA, BDNF and NT-4 activates TrkB and NT-3 activates TrkC. All neurotrophins bind to p75NTR, which has intrinsic signaling function but also binds neurotrophins in heteromeric signaling complexes with Trk family members. Neurotrophin activation of Trk receptors and its downstream signaling cascades promote neuronal survival and enhances synaptic transmission whereas activation of p75NTR initiates programmed cell death (reviewed in Friedman, 2000; Hennigan *et al.*, 2007; Schindowski *et al.*, 2008; Allen *et al.*, 2011).

BDNF plays a major role in synaptic plasticity and is the most highly expressed neurotrophin in brain regions that are functionally disrupted in early AD. Decreases in BDNF mRNA (Phillips *et al.*, 1991; Murray *et al.*, 1994; Connor *et al.*, 1997; Holsinger *et al.*, 2000; Garzon *et al.*, 2002) and protein (Narisawa-Saito *et al.*, 1996; Ferrer *et al.*, 1999; Murer *et al.*, 1999; Hock *et al.*, 2000; Michalski and Fahnstock, 2003; Peng *et al.*, 2005) levels have been documented in the hippocampus as well as in the entorhinal, temporal, frontal and parietal cortices of AD brains. Progressive reductions in the expression of both pro- (uncleaved, precursor) and mature BDNF were observed in the parietal cortex of patients with MCI and AD, and were found to correlate with the

rate of cognitive decline (Michalski and Fahnstock, 2003; Peng *et al.*, 2005). Furthermore, the expression of full-length, catalytically active TrkB receptor was found to be reduced in the hippocampus and frontal cortex of AD brains (Allen *et al.*, 1999; Ferrer *et al.*, 1999). A balance between signaling pathways activated by Trk or p75NTR may regulate neuronal survival or death. The ratio of TrkB and p75NTR is thought to be decreased during the progression of AD (reviewed in Ye *et al.*, 2012). Reductions in BDNF and TrkB may have wide-ranging consequences for the ongoing function and survival of neurons that degenerate in AD.

1.1.5 Bioenergetic Factors in Disease Progression

Neuronal atrophy can result from bioenergetic failure. Mitochondrial dysfunction is implicated in the increased oxidative stress, free radical damage and compromised cellular bioenergetics documented in AD. Defects in energy metabolism occur early in the progression of the disease and suggest a central role for mitochondrial malfunction in the pathophysiology of AD (reviewed in Maruszak and Zekanowski, 2011).

1.1.5.1 *The Electron Transport Chain and ATP Homeostasis*

The brain is distinguished from other organs by its disproportionately large consumption of energy. The human brain is approximately 2% of the body's weight, but receives 15% of cardiac output and accounts for 20% of its basal metabolism. This intense energy expenditure is continuous and necessary to maintain ionic gradients critical for neurotransmission. The limited glycolytic capacity (metabolism of glucose to pyruvate) of neurons makes the brain highly dependent on mitochondrial oxidative phosphorylation (OXPHOS) to meet its bioenergetic demands (reviewed in Attwell and Laughlin, 2001; Moreira *et al.*, 2010). Recently, it was demonstrated in rat hippocampal

slices that the steps in information processing, including generation of presynaptic action potentials, transmitter release, postsynaptic currents and postsynaptic action potentials, are powered initially and mainly by ATP generated through OXPHOS, but not glycolysis (Hall *et al.*, 2012). Even slight periods of oxygen deprivation result in neuronal dysfunction and death.

OXPHOS is an aerobic metabolic pathway that provides most of the cell's energy. It couples the electron transfer and proton pumping activities of mitochondrial respiratory complexes to generate an electrochemical proton gradient that drives ATP synthesis. The oxidoreductase reactions are carried out by respiratory complexes I (NADH: ubiquinone oxidoreductase), II (succinate: ubiquinone oxidoreductase), III (ubiquinol: ferricytochrome *c* oxidase) and IV (cytochrome *c* oxidoreductase). These enzyme complexes transfer high-energy electrons from reduced nicotinamide adenine dinucleotide (NADH) and flavin adenine dinucleotide (FADH₂) to molecular oxygen, so as to form water. The energy liberated from this electron transport is used by complexes I, III and IV to pump protons from the mitochondrial matrix into the intermembrane space. This generates a proton-motive force across the inner mitochondrial membrane that can be harnessed by ATP synthase (complex V) for the phosphorylation of ADP to ATP. The 5 multi-protein complexes, together with electron carriers cytochrome *c* and ubiquinone, form the electron transport chain (ETC).

The ETC is embedded in the inner membrane of mitochondria. OXPHOS is the most efficient means of producing ATP within a cell. The yield of ATP by OXPHOS depends on the permeability properties of the mitochondrial inner membrane, the catalytic capacity of ATP synthase and the proton/electron stoichiometry of the proton-pumping respiratory complexes. There are tissue-specific differences in mitochondrial bioenergetics. Brain mitochondria have the lowest OXPHOS efficiency but the highest respiration rate, when compared with heart and liver mitochondria. Dysfunction of mitochondrial membrane properties and/or any one of the ETC complexes severely affects bioenergetic homeostasis. However, complex I, the principal entry point of electrons into the ETC, is the most responsible for physiological regulation of OXPHOS efficiency (Cocco *et al.*, 2009; reviewed in Papa *et al.*, 2008).

Creatine kinase activity plays a central role in brain bioenergetic homeostasis. It buffers cellular ATP stores by acting as a temporal and spatial phosphate transfer system. Creatine kinase is highly expressed in the hippocampus, a region with heightened and fluctuating energy demands. The enzyme catalyzes the reversible transfer of a phosphoryl group from phosphocreatine (PCr) to ADP, producing ATP and creatine. Isoforms of creatine kinase are compartmentalized within cells, forming an energy circuit between sites of ATP generation and consumption. Creatine kinase is located in the inner membrane as well as in the intermembrane space of the mitochondrion. Its function is to transphosphorylate ATP produced by OXPHOS to yield PCr. PCr can then be exported into the cytosol. PCr has a higher diffusion capacity than ATP and is an efficient energy carrier. The creatine kinase/PCr shuttle can rapidly synthesize ATP where it is needed. The shuttle is integral to maintaining cellular bioenergetics during times of stress. It maintains cellular ratios of ATP/ADP and prevents acidification caused by ATP breakdown during high metabolic activity (reviewed in Wallimann *et al.*, 1992; Bürklen *et al.*, 2006; Adhietty and Beal, 2008). An exogenous supply of creatine has been shown to bolster the intracellular phosphocreatine reservoir and protect neurons against glutamate excitotoxicity and A β insults (Brewer and Wallimann, 2000).

1.1.5.2 *Oxidative Stress and Mitochondrial Dysfunction*

The brain is very vulnerable to oxidative stress due to its dependence on OXPHOS, high polyunsaturated lipid content and low expression of antioxidant enzymes. Mitochondria are the primary consumers of oxygen and producers of reactive oxygen species (ROS) in the cell. The ETC is inherently “leaky,” with electrons escaping from electron donors, binding to oxygen and forming superoxides. Pathophysiological inhibition of OXPHOS and/or damage to the inner mitochondrial membrane potentiates superoxide production (Parihar and Brewer, 2007). Hyperpolarization of the membrane inhibits proton pumping, resulting in impaired electron transport and intermediates that are abundantly charged. This increases the potential energy for electron transfer to oxygen and the generation of superoxide anions. Oxidative stress arises when the

production of ROS outstrips the cell's antioxidant abilities, damaging DNA, RNA, proteins and lipids (reviewed in Sullivan and Brown, 2005; Lin and Beal, 2006).

As the major source of cellular ROS, mitochondria are also prime targets of cumulative oxidative damage. The lack of protective histones in mitochondrial DNA and the limited capacity for mitochondrial DNA repair render the mitochondrion vulnerable to ROS (reviewed in Moreira *et al.*, 2010). Oxidative modification of phospholipids in the mitochondrial inner membrane can compromise the ETC machinery. Cardiolipin, a tetra-acyl anionic phospholipid found almost exclusively in the inner mitochondrial membrane and comprising 25% of its total lipid content, plays a key role in maintaining mitochondrial membrane fluidity and osmotic stability. Cardiolipin is necessary for the assembly and function of the ETC and electrostatically anchors cytochrome *c* to the inner mitochondrial membrane. It is very sensitive to free radical damage because of its unsaturated side chains and its association with ROS-producing respiratory complexes. Peroxidation of cardiolipin can lead to loss in content and/or changes in its fatty acid composition. These changes have been linked with OXPHOS dysfunction and initiation of the apoptotic cascade via cytochrome *c* release from mitochondria (reviewed in Chicco and Sparagna, 2007; Pope *et al.*, 2008). ROS can also oxidize proteins in respiratory complexes. Complex I is particularly sensitive to hydroxyl radicals and superoxide anions (Zhang *et al.*, 1990). It is also the major site of electron leakage and formation of superoxides in the ETC (Votyakova and Reynolds, 2001; Liu *et al.*, 2002; Papa *et al.*, 2008). A positive feedback loop can ensue when ROS induced injury to the ETC machinery causes electrons to leak, increasing superoxide formation and further inhibiting OXPHOS (reviewed in Bowling and Beal, 1995).

Oxidative stress and mitochondrial dysfunction are well documented in AD. The expression of oxidative stress markers, indicating damage to proteins, lipids and nucleic acids, is pronounced in the brains of AD and MCI patients in comparison to healthy-aged matched controls. These markers track with the topographical distribution of pathology and neuronal loss in AD and thus are most prevalent in the hippocampus and temporoparietal cortices (reviewed in Maruszak and Zekanowski, 2011). ROS may contribute to and/or result from disruptions in energy metabolism. It is unclear whether

oxidative damage or a pathophysiological inhibition of the ETC leads mitochondrial dysfunction. Regardless of the initiating event, once the ETC is disrupted, a futile cycling between ROS and OXPHOS insults accelerate bioenergetic stress in AD.

1.1.5.3 *Decreased Metabolic Activity*

Multiple defects in energy metabolism have been documented in the AD brain. With the advent of positron emission tomography, rates of cerebral glucose metabolism can be investigated in AD patients and provide *in situ* measures of brain functional activity. AD patients exhibit significantly decreased glucose utilization within the neocortex, especially in the temporoparietal cortices. The topography of compromised glucose metabolism reflects the distribution of AD pathology. Glucose hypometabolism can precede the onset of clinical symptoms in patients at risk of developing AD (Kennedy *et al.*, 1995; Small *et al.*, 2000) and track with cognitive decline, increasing in magnitude as visuospatial and language deficits worsen (reviewed in Pietrini *et al.*, 1993; Pettegrew *et al.*, 1994; Mosconi *et al.*, 2008; Maruszak and Zekanowski, 2011). Disturbances in glycolytic metabolism within the AD brain may be associated with diminished transport and phosphorylation of glucose. While total energy consumption was found to be reduced in the temporoparietal cortices, the ratio of oxidative to glucose metabolism is abnormally high, suggesting a metabolic shift from anaerobic to aerobic respiration (Fukuyama *et al.*, 1994; Hoyer, 1993). Reductions in glucose utilization lead to a heavier dependence on oxidative metabolism, which increases the possibility of free radical damage and the uncoupling of OXPHOS.

Several key mitochondrial enzymes involved in the oxidation of glucose are deficient in AD brains. The following are the most consistent of the reported metabolic defects:

- Decreased activity of pyruvate dehydrogenase (PDH) complex, the enzyme that catalyzes the oxidative decarboxylation of the glycolytic end-product pyruvate to acetyl-CoA, which is used to initiate the tricarboxylic acid (TCA) cycle (Perry *et al.*, 1980; Sorbi *et al.*, 1983; Butterworth and Besnard, 1990; Yates *et al.*, 1990).

- Decreased activity of α -ketoglutarate dehydrogenase (α -KGDH) complex, the rate-limiting enzyme in the TCA cycle that catalyzes the reduction of NAD⁺ to NADH and the oxidation of α -ketoglutarate to succinyl-CoA (Gibson *et al.*, 1988; Mastrogiacomo *et al.*, 1993; Butterworth and Besnard, 1990; Terwel *et al.*, 1998; reviewed in Gibson *et al.*, 1998).
- Decreased activity of complex IV of the ETC both in brain and in peripheral tissue of AD patients (Parker *et al.*, 1990, 1994; Mutisya *et al.*, 1994; Davis *et al.*, 1997; Bosetti *et al.*, 2002; Cardoso *et al.*, 2004; Valla *et al.*, 2006).

The reductions in PDH and α -KGDH activity correlate with clinical dementia rating scores in AD patients. Inhibition of PDH and α -KGDH results in increased ROS production, diminished flux through the TCA cycle and production of ATP, as well as reduced synthesis of acetylcholine and glutamate. Moreover, disruptions in α -KGDH activity can incite the release of apoptotic factor cytochrome *c*, limit the availability of NADH for OXPHOS and hyperpolarize the inner mitochondrial membrane (reviewed in Bubber *et al.*, 2005). OXPHOS deficiency in AD is associated with reduced expression of mitochondrial and nuclear genes encoding polypeptide subunits of respiratory complexes I and IV (reviewed in Parihar and Brewer, 2007).

Oxidative damage to creatine kinase is thought to contribute to bioenergetic stress in AD. The cysteine residue in creatine kinase is easily oxidized, rendering the enzyme very vulnerable to free radical damage. Creatine kinase activity is diminished in the AD brain (Hensley *et al.*, 1995; David *et al.*, 1998; Aksenov *et al.*, 2000). Brain tissue levels of PCr and ADP (the immediate precursors of ATP) are reduced, while oxidative metabolic rate is increased early in the disease. The decreased energy reserve and increase in metabolic rate suggest that the AD brain is under energy duress. As the disease progresses, oxidative metabolism also declines (Pettegrew *et al.*, 1994). Focal creatine deposits have been found in the hippocampus of *post-mortem* AD brains (Gallant *et al.*, 2006) and this suggests dysfunction of the creatine kinase/PCr energy buffering system. Inhibition of creatine kinase reduces PCr formation at mitochondria. To sustain energetic charge in the energetically stressed AD brain, the limited PCr pool may be quickly depleted to convert ADP to ATP, resulting in the accumulation of creatine (reviewed in Bürklen *et al.*, 2006).

1.2 The Amyloid Cascade Hypothesis

Hardy and Higgins (1992) hypothesized that the deposition of A β triggers a pathogenic cascade that leads to the formation of neurofibrillary tangles, neurodegeneration and clinical symptoms of AD. The hypothesis was driven by the identification of A β as the main component of plaques and by the discovery that autosomal-dominant mutations, causing early onset AD, increase the production of A β (Hardy and Selkoe, 2002).

1.2.1 Early-Onset Familial Mutations

Familial AD with autosomal-dominant inheritance is rare, accounting for less than 5% of all cases. Mutations in the amyloid precursor protein (*APP*) gene on chromosome 21, presenilin 1 and 2 (*PS1*; *PS2*) genes on chromosome 14 and 1, respectively, are 100% penetrant and cause early-onset AD (reviewed in Tanzi and Bertram, 2005). Currently, 32 mutations in *APP*, 185 in *PS1* and 13 in *PS2* have been identified in familial AD (Cruts *et al.*, 2012). These causative mutations, occurring in genes that encode either the substrate APP or proteins involved in its proteolytic processing, produce an accelerated A β pathology.

The clinical presentation and neuropathology of familial AD and sporadic AD are remarkably similar, with age at onset being the exception. Typically, individuals with sporadic AD develop symptoms after 60 years of age. Patients with *PS1* mutations have the youngest age at onset, with clinical symptoms appearing between ages 30 to 50 years. *APP* mutations manifest at 45 to 60 years of age, while rare *PS2* mutations are associated with a wider and usually later age of onset. Despite differences in age of onset, both inherited and sporadic forms of AD develop plaques, tangles and selective neuronal loss (reviewed in La Ferla, 2002; Bateman *et al.*, 2011).

Sporadic AD is a multifactorial disease with complex environmental, genetic and lifestyle factors contributing to its pathogenesis. Susceptibility to late-onset AD is associated with polymorphisms in the apolipoprotein E (*APOE*) gene on chromosome 19, which is involved in lipid homeostasis. Carriers of the *APOE* ϵ 4 allele have a dose-dependent increase in risk of developing AD and exhibit more extensive A β burden than individuals with other *APOE* alleles (Schmechel *et al.*, 1993). The accumulation of A β in the brain is posited as driving the disease process in both familial and sporadic AD (reviewed in Bateman *et al.*, 2011). Recently, genome-wide association studies have identified 9 novel loci associated with late-onset AD: *CLU*, *PICALM*, *CR1*, *BIN1*, *ABCA7*, *MS4A4/MS4A6E*, *CD2AP*, *CD33* and *EPHA1*. The role of these genes in the pathogenesis of AD has yet to be resolved. *APOE* and these genes account for roughly 50% of the total genetic variance and implicate pathways of immune response, synaptic function and cholesterol metabolism in late-onset AD (reviewed in Morgan, 2011).

1.2.2 APP Processing, A β Production and Fibrillogenesis

A β is generated from proteolysis of the APP protein, a member of a family of related proteins that include amyloid precursor-like protein 1 (APLP1) and 2 (APLP2). Only APP contains the A β domain. The *APP* gene can be alternately spliced to generate multiple isoforms varying in length. The *APP695* amino acid variant is highly expressed in the brain. APP is a type I transmembrane protein, consisting of a large amino (N)-terminal glycosylated ectodomain, a helical membrane spanning segment and a short cytoplasmic domain. Full-length APP may participate in cell adhesion, neurite outgrowth, signal transduction, axonal transport and protein trafficking (reviewed in Sisodia and St. George-Hyslop, 2002; Zhang *et al.*, 2011).

APP is proteolytically processed via discrete amyloidogenic and non-amyloidogenic pathway (Figure 1-1). In the non-amyloidogenic pathway, α -secretase cleaves APP

within the A β sequence, thus precluding A β formation. This cleavage releases a large N-terminal ectodomain containing residues 1-16 of A β (sAPP α), leaving a carboxy (C)-terminal fragment of 83 residues in the membrane (C83). The activity of α -secretase is attributed to one or more enzymes in the ADAM (a disintegrin and metalloproteinase) family of proteases. APP cleavage by β -secretase, mediated by the BACE1 (β -site APP-cleaving enzyme 1) type I aspartyl protease, generates a shorter N-terminal fragment (sAPP β) and an amyloidogenic membrane-retained stub consisting of 99 residues (C99). The C-terminal fragments undergo further proteolysis by γ -secretase, a multi-protein complex composed of at least PS1 or PS2, presenilin enhancer 2 (Pen-2), nicastrin and anterior pharynx defective 1 (Aph-1). Nicastrin, Aph-1 and Pen-2 facilitate substrate recognition and activity of the complex while the aspartyl residues on PS1 and PS2 mediate intramembranous cleavage of C-terminal stubs at various sites, but most commonly at residue 40 or 42. Proteolysis of C83 by γ -secretase produces the non-amyloidogenic p3 peptide and an APP intracellular domain (AICD), whereas cleavage of C99 yields A β ₄₀ or A β ₄₂ and the corresponding AICDs (reviewed in Chow *et al.*, 2010).

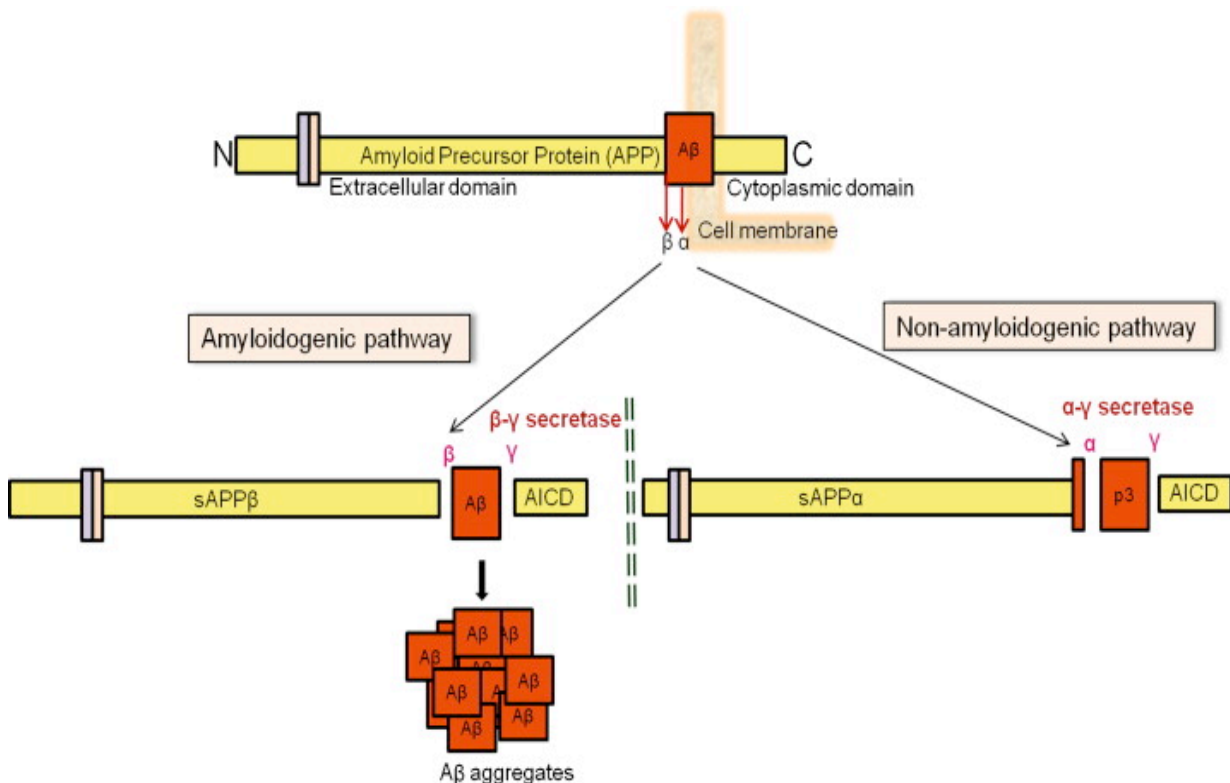


Figure 1-1. Proteolysis of APP (Reprinted from Brain Research Bulletin, 86, Mathew *et al.*, Alzheimer's disease: Cholesterol a menace?, pages 1-12, copyright (2011), with permission from Elsevier: License # 3136611194172).

The proteolytic processing of APP and generation of the soluble ~4kDa A β peptide, especially the A β_{40} isoform, occurs during normal cellular metabolism (Haass *et al.*, 1992). APP that is not cleaved at the plasma membrane is trafficked into endosomes, and has been found within the trans-Golgi network, endoplasmic reticulum, lysosomal and mitochondrial membranes. The low pH in endosomes provides an optimal environment for β -secretase cleavage of APP and A β generation. A β may also be produced along the secretory pathway in the endoplasmic reticulum and the trans-Golgi network. Although the bulk of A β is secreted outside the neuron, extracellular A β can be internalized for degradation. A β has been shown to bind to numerous cell surface receptors, such as $\alpha 7$ nicotinic acetylcholine receptors, receptor for advanced glycation end products (RAGE) and APOE receptors, causing internalization of the receptor and intracellular accumulation of A β (reviewed in La Ferla *et al.*, 2007).

Enhanced amyloidogenic processing of APP and/or decreased clearance of A β could lead to a toxic build-up within neurons and deposition in extracellular plaques. All autosomal-dominant mutations in *APP* and/or in presenilin genes affect the production or biophysical properties of A β . Increased dosage of APP, as in Down's syndrome (Trisomy 21), also results in A β accumulation. Mutations that flank the β -secretase cleavage site in APP, such as the double mutation (KM670/671NL) identified in a Swedish kindred, increase BACE activity and thus the formation of all amyloid species (38-43 amino acids in length). Point mutations within or near the hydrophobic core of the A β sequence (including Arctic, Dutch, Iowa and Flemish mutations) enhance the aggregation kinetics, or stability of A β . Mutations that cluster around the C-terminus of the A β sequence, for example London (V717I) and Indiana (V717F) mutations, alter γ -secretase cleavage of APP to favour production of the more fibrillogenic A β_{42} variant. Similarly, point mutations in the presenilins increase the amount of A β_{42} relative to A β_{40} (summarized in Walsh and Teplow, 2012). While A β_{40} is the most abundant amyloid species, longer A β_{42} and A β_{43} isoforms are more prone to aggregation and are highly concentrated in plaques. Enzymes that degrade monomeric A β , such as neprilysin and

insulin degrading enzyme (IDE), are less capable of catabolizing larger assemblies of A β (reviewed in Sisodia and St. George-Hyslop, 2002; Haass and Selkoe, 2007).

Increasing the ratio of A β_{42} to A β_{40} can drive the seeding of plaques. The additional hydrophobic residues at the C-terminus of A β_{42} promote fibrillogenesis. Monomeric A β aggregates into various assembly states: starting from low weight oligomers (dimers and trimers), growing to mid-size spherical oligomers that aggregate into protofibrils, and finally maturing to fibrils with a cross β -sheet conformation that deposit as insoluble plaques. Small A β oligomers have been found to be the most toxic and are considered the major culprit of AD pathogenesis (reviewed in McGowan *et al.*, 2005; Larson and Lesné, 2012; Benilova *et al.*, 2012).

1.2.3 Toxicity of A β

A β has long been recognized as central to AD. However, it has remained unclear how it causes neuronal dysfunction and cognitive abnormalities. There is now compelling evidence that soluble, oligomeric A β species induce progressive synaptic dysfunction, impair neurotrophin signaling and damage mitochondria.

1.2.3.1 *Distal Axonopathy and Synaptic Dysfunction*

The loss of synapses and impaired microtubule-dependent axonal transport are early features of the AD brain (Coleman and Yao, 2003; Cash *et al.*, 2003). Synaptic loss is observed in the association cortices and hippocampus and is the best correlate of cognitive decline in AD. Markers of pre- and postsynaptic components are reduced well before the onset of plaques (reviewed in Selkoe, 2002; Shankar and Walsh, 2009). Synaptic degeneration is associated with swollen axons that contain abnormal

accumulations of organelles and vesicles. Axonal swellings in cholinergic terminals are observed at early Braak stages of AD pathology, and may lead to dystrophic neurites (Stokin *et al.*, 2005). A bottleneck in axonal transport leads to synaptic collapse and retrograde 'dying-back' of axons (reviewed in Coleman, 2005).

Axonal transport is integral to neuronal communication. APP and its proteolytic enzymes are trafficked along axons and dendrites. Soluble oligomeric pools of A β inhibit bidirectional axonal transport (Pigino *et al.*, 2009) and contribute to axonal blockages. Blockages in turn promote abnormal A β generation, further disrupting vesicle traffic and transmitter release (Stokin *et al.*, 2005). A β in synaptic terminals/distal axons initiates retrograde degeneration particularly in vulnerable neurons that project to cortex and hippocampus (reviewed in Götz *et al.*, 2006).

Exogenous application of A β , especially oligomeric A β_{42} , disrupts basal transmission and synaptic plasticity. The disruption of synaptic plasticity by oligomeric A β is the likely basis of cognitive dysfunction in AD. A β has been shown to induce long-term depression (LTD) and inhibit long-term potentiation (LTP). LTP is the physiological correlate of memory and it requires the activation of postsynaptic *N*-methyl-D-aspartate (NMDA) receptors. LTP is associated with enlarged dendritic spines. The balance between LTP and LTD regulates neural connectivity, postsynaptic density and the strength of neurotransmission. A β facilitates endocytosis of NMDA receptors, shifting the LTP/LTD balance towards more LTD, resulting in synaptic depression, dendritic spine loss and synaptic collapse (reviewed in Koffie *et al.*, 2011).

1.2.3.2 *A β downregulation of BDNF signaling*

The loss of synapses in AD begins in the entorhinal-hippocampal circuitry, which is considered the seat of short-term memory. BDNF is produced in the adult entorhinal cortex and is anterogradely trafficked into the hippocampus (Yan *et al.*, 1997), where it

is released in an activity-dependent manner to modulate neuronal plasticity processes underlying memory formation (reviewed in Nagahara and Tuszynski, 2011). BDNF, via TrkB signaling, facilitates dendritic spine formation, LTP, vesicular-docking and neurotransmitter release within hippocampus. In turn, induction of LTP in the hippocampus stimulates BDNF production (reviewed in Bramham and Messaoudi, 2005; Tapia-Arancibia *et al.*, 2008; Cunha *et al.*, 2010). BDNF also fosters neurogenesis in the adult hippocampus and stimulates the non-amyloidogenic processing of APP (Sairanen *et al.*, 2005; Scharfman *et al.*, 2005; Henry *et al.*, 2007; Diniz and Teixeira, 2011). These trophic effects make BDNF an especially relevant molecule in the pathophysiology of AD.

The effects of oligomeric A β on LTP and memory may be mediated via BDNF. Once BDNF binds to TrkB on the plasma membrane, the receptor-ligand complex is internalized. Endocytosis of the BDNF-TrkB complex requires Ca²⁺ influx and activation of NMDA receptors (Du *et al.*, 2003). The internalized complex is retrogradely transported to the soma, where it activates signaling cascades that foster neuronal survival and plasticity and regulates gene transcription including *Arc*, an immediate-early gene that is involved in learning (Zheng *et al.*, 2009). A β oligomers inhibit BDNF signaling by impairing the retrograde trafficking of BDNF/TrkB (Poon *et al.*, 2011). A β ₄₂ can also modulate levels of BDNF and TrkB, reduce BDNF-induced *Arc* expression and block the nuclear translocation of phosphorylated CREB (cyclic AMP response element-binding protein; reviewed in Tapia-Arancibia *et al.*, 2008). Phosphorylated CREB (P-CREB), binds to cyclic AMP response elements on certain genes, including *BDNF*, to regulate transcription. BDNF signaling through TrkB leads to phosphorylation of CREB. CREB activation is reduced in AD hippocampi (Yamamoto-Sasaki *et al.*, 1999). Oligomeric A β ₄₂ has been found to decrease P-CREB and BDNF mRNA in human neuroblastoma cells (Garzon and Fahnstock, 2007). BDNF administration provides dose-dependent protection against A β *in vivo* and *in vitro*. However, other TrkB- and/or p75NTR-mediated effects of BDNF, including exacerbation of pain and weight loss, can limit the therapeutic potential of systemic BDNF administration (reviewed in Nagahara and Tuszynski, 2011; Tapia-Arancibia *et al.*, 2008).

1.2.3.3 *A β Interactions with Mitochondria*

Mitochondria are trafficked to synapses and provide energy for neural communication. In cultured hippocampal cells, A β was found to impair mitochondrial transport (especially in the anterograde direction), reduce the mass, length and motility of mitochondria, induce mitochondria fragmentation and decrease synaptic growth (Calkins and Reddy, 2011).

APP in mitochondria triggers dysfunction. APP contains a mitochondrial targeting sequence and undergoes incomplete import into mitochondria leaving the N-terminus inside the matrix and C-terminus in the cell cytosol (Anandatheerthavarada *et al.*, 2003; Devi *et al.*, 2006). The translocational arrest of APP in mitochondrial membranes hinders import of nuclear-encoded subunits of the electron transport chain.

Mitochondrial docking of APP is observed in vulnerable regions of the AD brain and was selectively found to inhibit the import of proteins in complex IV, decreasing complex IV activity and increasing oxidative stress (Devi *et al.*, 2006). APP may also act as a cytosolic chaperone for creatine kinase, binding to and stabilizing pro-protein forms of creatine kinase that are destined for mitochondria. Mutations in *APP* compromise its ability to shuttle creatine kinase to mitochondria, resulting in decreased PCr synthesis, creatine deposits in cells and disrupted energetic homeostasis (Bürklen *et al.*, 2006).

The presence of A β within mitochondria of brains from AD patients has been well documented (Yamaguchi *et al.*, 1992; Fernandez-Vizarra *et al.*, 2004; Lustbader *et al.*, 2004; Caspersen *et al.*, 2005; Devi *et al.*, 2006). However, the source of intra-mitochondrial A β is unclear. While active γ -secretase complexes exist in mitochondria (Hansson *et al.*, 2004; Pavlov *et al.*, 2011), there are no reports of mitochondria-associated β -secretase. The direction and aborted import of APP into mitochondria does not support a model whereby intra-mitochondrial generation of A β occurs. Rather, it is thought that intra-mitochondrial A β is taken-up by mitochondria via the translocase

of the outer membrane (TOM), allowing it to accrue in the cristae, where the respiratory complexes reside (Hansson Petersen *et al.*, 2008).

A β within mitochondria may disrupt function in multiple ways. In neuronal cell culture, sub-lethal doses of A β were found to inhibit protein import to mitochondria, decrease mitochondrial membrane potential, increase susceptibility to oxygen glucose deprivation, alter mitochondrial morphology and increase ROS (Sirk *et al.*, 2007). In the cerebral cortex of AD patients, A β was shown to bind to the mitochondrial matrix protein A β -binding alcohol dehydrogenase (ABAD). The A β -ABAD interaction induces leakage of ROS, DNA fragmentation and apoptosis (Lustbader *et al.*, 2004). In turn, oxidative stress further potentiates A β toxicity. Lipid peroxidation and ROS can promote A β aggregation and protofibril assembly. A β also interacts with cyclophilin D, a component of the mitochondrial permeability transition pore, resulting in increased membrane permeability, altered calcium homeostasis and pro-apoptotic signaling (reviewed in Crouch *et al.*, 2008; Tillement *et al.*, 2011). In mitochondria isolated from rat brain, direct exposure to increasing concentrations of A β caused dose-dependent increases in membrane viscosity, decreases in ATP synthesis, release of cytochrome *c* and inhibition of complexes I, III and IV of the ETC (Aleari *et al.*, 2005). Similarly, oxygen consumption and the activities of complexes I, III and IV were reduced in cells exposed to A β_{40} peptides (Pereira *et al.*, 1998). The effects of A β on mitochondrial respiration have yet to be resolved. A β may disrupt ETC function by directly binding to and inhibiting enzyme complexes, clogging of mitochondrial import machinery, and/or indirectly via increasing ROS.

1.3 Noradrenergic Mechanisms in Alzheimer's Disease

Noradrenergic deficits may be key to the pathogenesis of AD. There is ample evidence that degeneration of the locus coeruleus and its forebrain projections critically mediates A β -induced pathogenic cascades (reviewed in Marien *et al.*, 2004).

1.3.1 Noradrenaline in the Brain

Noradrenaline, also known as norepinephrine, is a catecholamine neurotransmitter and hormone. The catecholamines include dopamine and its metabolites, noradrenaline and adrenaline, that contain a catechol moiety (benzene ring with two contiguous hydroxyl units) and an amine group. In 1946, Ulf von Euler chemically isolated noradrenaline as the major catecholamine in mammalian postganglionic sympathetic nerve endings. Soon thereafter, Peter Holtz demonstrated that noradrenaline is highly concentrated in the brain and in the adrenal gland (reviewed in Flatmark, 2000). In the brain, noradrenaline is synthesized by pontine locus coeruleus neurons and by dorsal and lateral tegmental nuclei in the medulla. These noradrenergic systems differ in the morphology and distribution of their efferent fibers. The medullary nuclei project to the hypothalamus, thalamus, brainstem and spinal cord and regulate endocrine and autonomic functions. The locus coeruleus is the largest cluster of noradrenergic cell bodies in the brain. It innervates the entire neuroaxis and is the sole source of noradrenergic projections to the neocortex, hippocampus and cerebellum. Locus coeruleus efferents are thin with small beaded varicosities. The longer and thinner locus coeruleus projections appear to be more susceptible to toxic insults (Fritschy and Grzanna, 1989). This noradrenergic system preferentially degenerates in AD, leaving forebrain circuits particularly vulnerable to A β (reviewed in Marien *et al.*, 2004).

1.3.1.1 *Anatomical Locus*

The locus coeruleus is named for its dark blue appearance that is imparted by the neuromelanin pigment. The region was first identified in the human brain by Reil in 1809 and named by Wenzel and Wenzel in 1812 (reviewed in Maeda, 2000). It constitutes the most rostral nucleus of noradrenergic cell bodies in the brainstem, and is located in the pontine tegmentum, adjacent to the floor of the fourth ventricle. The location and structural organization of the locus coeruleus is largely conserved across

mammalian species. The human locus coeruleus has been described as “tube-like”: it extends rostrocaudally for approximately 16 mm and is bilaterally symmetrical with respect to the numbers and distribution of its cells (German *et al.*, 1988). Quantitative estimates of the noradrenergic cell population in human locus coeruleus reveal roughly 45,000 neurons in the healthy adult. Average cell counts range from 12,000 to 25,000 per hemisphere (Vijayashankar and Brody, 1979; German *et al.*, 1988; Baker *et al.*, 1989; Chan Palay and Asan, 1989; Manaye *et al.*, 1995; Ohm *et al.*, 1997; Sharma *et al.*, 2010). Although few in number, noradrenergic neurons have highly ramified axons that project broadly, along well-defined tracks. Locus coeruleus efferents form two main ascending fiber systems, the dorsal bundle and the smaller rostral limb of the dorsal periventricular pathway. These ascending tracts are largely ipsilateral. They innervate the entire forebrain, with the notable exception of the basal ganglia. Other efferents project to the cerebellar cortex, or course caudally to the medulla and spinal cord (reviewed in Gesi *et al.*, 2000; Marien *et al.*, 2004; Sara, 2009).

Retrograde tracer studies revealed the topographic organization of neurons in the locus coeruleus with respect to their terminal fields. The locus is loosely compartmentalized along the dorsoventral and rostrocaudal axes. The spinal cord and cerebellum are innervated by neurons in the ventral segment; the hypothalamus by neurons in the rostral pole; the cortex by neurons in central and somewhat dorsal portions, and the hippocampus by neurons in the dorsal pole of the nucleus (Loughlin *et al.*, 1986; Foote *et al.*, 1983). Noradrenergic neurons have axons that collateralize profusely to innervate multiple distant sites. The locus coeruleus is further organized according to the functions of its efferent targets. Individual locus coeruleus neurons tend to send axonal collaterals to multiple targets that process the same sensory information. These widely collateralized axons generally arise from neurons that are located centrally in the nucleus. The wiring of the locus coeruleus permits selective and coordinated activation of efferent networks to influence the collection and processing of sensory information in the brain (Berridge and Waterhouse, 2003).

Distinct topographic patterns of cell loss in the locus coeruleus have been described for various neurodegenerative diseases (German *et al.*, 1992). In AD, neuronal loss and

the concentration of neurofibrillary tangles in the locus coeruleus are most extensive in the dorsal and central segments of the rostral pole (Marcyniuk *et al.*, 1986; Busch *et al.*, 1997; Szot *et al.*, 2000). The preferential loss of neurons that project to the hippocampus and temporoparietal cortex matches the regional distribution of plaque load in the AD brain. In contrast, the caudal locus coeruleus degenerates in Parkinson's disease. The loss of caudal cells that project to the cerebellum and spinal cord may be related to the akinesia and postural instability symptoms in these patients. If the disease is comorbid with dementia, there is comparable cell loss throughout the rostrocaudal pole of the nucleus (Chan-Palay and Asan, 1989; German *et al.*, 1992).

1.3.1.2 *Synthesis and Metabolism*

The biosynthesis of catecholamines begins with the amino acid tyrosine and follows a series of enzymatic steps that are initiated by the rate-limiting enzyme tyrosine hydroxylase. In brief, tyrosine hydroxylase converts tyrosine to dihydroxyphenylalanine, which is then rapidly decarboxylated to dopamine by the aromatic amino-acid decarboxylase. In dopaminergic neurons, no further enzymatic modification occurs. Noradrenergic neurons contain an additional enzyme, dopamine β -hydroxylase, which converts dopamine to noradrenaline. Noradrenaline is sequestered into synaptic vesicles by a vesicular monoamine transporter and thereby protected from intraneuronal degradation. The actions of noradrenaline, once it is released into the synapse, are terminated by reuptake into the presynaptic neuron via the plasma membrane bound noradrenaline transporter (NET). Many antidepressants inhibit NET, thereby increasing noradrenaline levels in the synaptic cleft (reviewed in Ressler and Nemeroff, 1999).

Noradrenaline is degraded by monoamine oxidase (MAO) and catechol-O-methyltransferase (COMT). MAO is found within neurons and glia, on mitochondrial outer membranes. It catalyzes the oxidative deamination of catecholamines that have not been taken up into storage vesicles. MAO converts noradrenaline to its aldehyde, 3,4-dihydroxyphenylglycoaldehyde (DOPEGAL). DOPEGAL is a highly reactive and

toxic metabolite and is thus rapidly oxidized to 3,4-dihydroxymandelic acid (DHMA) or reduced to 3,4-dihydroxyphenylglycol (DHPG) by aldehyde dehydrogenase or reductase enzymes, respectively. The β -hydroxyl group on noradrenaline and its metabolite DOPEGAL favours reduction by reductase enzymes, making DHPG the major metabolite produced by deamination. COMT exists in membrane-bound and soluble forms in cells and catalyzes the conversion of DHPG to 3-methoxy-4-hydroxyphenylglycol (MHPG), which is the major breakdown pathway of noradrenaline in the central nervous system. Another minor pathway is the O-methylation of noradrenaline to normetanephrine (NMN) by COMT. This is followed by oxidative deamination of NMN to vanillylmandelic acid (VMA), the principal end product of noradrenaline in the periphery (reviewed in Eisenhofer *et al.*, 2004).

1.3.1.3 Receptors and Signal Transduction Pathways

The effects of noradrenaline are mediated by metabotropic G-protein coupled receptors. Adrenergic receptors can be classified into three families, α_1 , α_2 , and β receptors, based on their distinct signal transduction pathways. Each of these major classes is further divided into three subtypes of receptors (Bylund *et al.*, 1994; Figure 1-2).

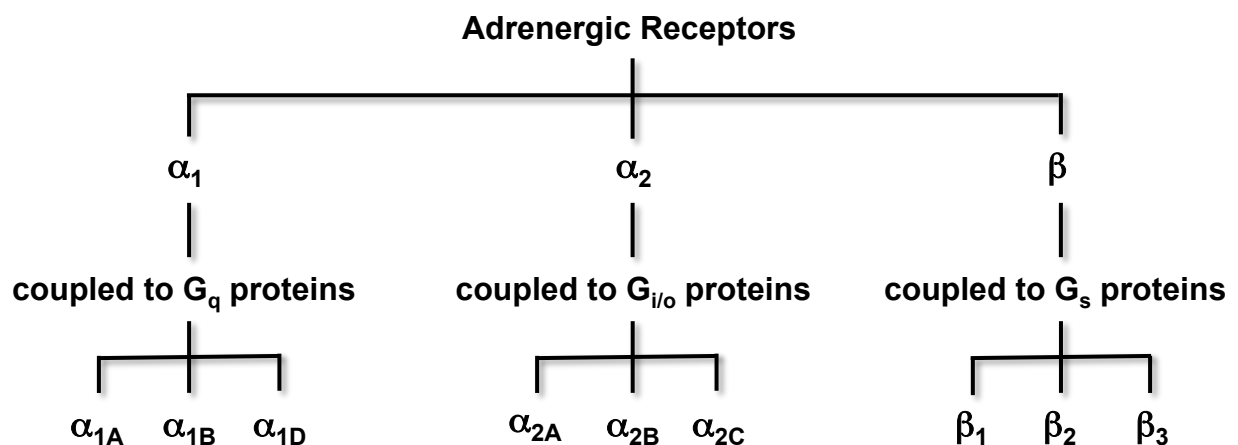


Figure 1-2. Nomenclature and coupling of adrenergic receptors.

The α_1 (α_{1A} , α_{1B} , α_{1D}) adrenoceptors are found on postsynaptic terminals in the hippocampus, cerebral cortex and brainstem. The α_{1A} receptors are preferentially expressed in the thalamus and in the deep layers of the frontal and parietal cortices. All α_1 receptors are coupled to G_q proteins, which when stimulated activates the phospholipase C β (PLC β)- inositol triphosphate (IP $_3$) – diacylglycerol (DAG) signal transduction pathway, resulting in increased cytosolic calcium concentrations and activation of protein kinase C (PKC) (reviewed in Marzo *et al.*, 2009). This class of adrenoceptors exerts a general excitatory effect in the central nervous system and has been associated with the modulation of memory consolidation, pain perception and motor coordination (reviewed in Gilsbach and Hein, 2008).

The α_2 class of adrenoceptors includes α_{2A} , α_{2B} , α_{2C} subtypes and exist at both pre- and postsynaptic terminals. In the brain, α_{2A} is the predominant subtype and is expressed in the cerebral cortex, locus coeruleus, hippocampus and hypothalamus; α_{2B} is primarily concentrated in the thalamus; α_{2C} is found in the hippocampus, prefrontal cortex, basal ganglia and olfactory bulbs. All α_2 receptor subtypes mediate inhibitory effects. They decrease adenylyl cyclase activity, open protein-gated potassium channels and inhibit calcium channels through coupling with $G_{i/o}$ proteins (reviewed in Gilsbach and Hein, 2008). Presynaptic α_2 receptors on locus coeruleus noradrenergic neurons, also known as autoreceptors, inhibit noradrenaline release via negative feedback while α_2 heteroreceptors mediate the inhibitory effect of noradrenaline on the release of other transmitters, including dopamine (Bücheler *et al.*, 2002), serotonin (Scheibner *et al.*, 2001) and acetylcholine (Tellez *et al.*, 1999).

The β adrenoceptors, β_1 , β_2 , β_3 , are primarily located at postsynaptic sites and are coupled to stimulatory G_s proteins. Stimulation of β adrenoceptors activates adenylyl cyclase and increases intracellular concentrations of cyclic AMP (cAMP). β_1 and β_2 adrenoceptors are highly expressed in the brain and play prominent roles in memory and stress, while β_3 receptors are densely expressed in adipose tissue (reviewed in Yu *et al.*, 2011). In the brain, β_1 and β_2 receptors are concentrated in the cerebral cortex,

thalamus and pineal gland. β_2 Receptors are also highly expressed in olfactory bulbs and hippocampi (reviewed in Gilsbach and Hein, 2008). The activation of β adrenoceptors and subsequent increase of intracellular cAMP triggers signaling cascades and new protein synthesis in the hippocampus and amygdala, increasing synaptic plasticity and LTP, that are required for learning and memory (reviewed in Benarroch *et al.*, 2009; Tully and Bolshakov, 2010). In addition, β_3 receptors in the hippocampus have been found to enhance the proliferation of hippocampal neural precursors (Jhaveri *et al.*, 2010).

1.3.1.4 *Functions*

The widespread projections of the locus coeruleus noradrenergic system influence a variety of physiological and behavioural states. In general, the system facilitates neural responses to salient information by boosting evoked excitatory and inhibitory transmission while dampening spontaneous activity. Locus coeruleus neurons fire in tonic and phasic modes. Tonic discharge increases from sleep to waking and supports arousal and exploratory behaviour. In response to novel stimuli, the locus coeruleus adjusts its firing pattern to phasic bursts that are time-locked with presentation of the salient stimulus. Thus, noradrenaline increases the signal to noise information transfer in efferent circuits so as to coordinate shifts in attention and optimize task-related behavioural responses. The fine-tuning of these responses in efferent circuits is mediated in part by inhibitory α_2 adrenoceptors (reviewed in Berridge and Waterhouse, 2003; Aston-Jones and Cohen, 2005; Sara and Bouret, 2012).

Noradrenergic transmission in forebrain circuits that degenerate in AD regulate mood, attention and memory (reviewed in Ressler and Nemeroff, 1999). Optimal levels of noradrenaline, mainly maintained by α_2 autoreceptors, acting on thalamic and sensory cortical nuclei influence attention and processing of salient stimuli. Reciprocal projections between the prefrontal cortex and the locus coeruleus modulate noradrenergic transmission in a context-dependent manner to facilitate focused

attention and memory (reviewed in Sara and Bouret, 2012). Noradrenergic innervation of the hippocampus facilitates LTP through β adrenoceptor activation of the intracellular cAMP cascade (Harley, 2007). In concert with other neuromodulators, such as acetylcholine, noradrenaline regulates LTP and synaptic plasticity in circuits that include the basal lateral amygdala, medial septum and dentate gyrus of the hippocampus so as to promote memory consolidation and retrieval in response to contextual cues (Marzo et al., 2009; Sara, 2009; Benarroch, 2009; Tully and Bolshakov 2010).

Noradrenergic terminals are capable of both synaptic and non-synaptic release (via boutons en passage). The latter allows noradrenaline to act as a paracrine agent, influencing neurons, astrocytes, microglia and the vasculature in the microenvironment (reviewed in Marien *et al.*, 2004). The roles of central noradrenergic transmission in modulating stress (Glavin, 1985; Morilak *et al.*, 2005), pain (Pertovaara, 2006), cerebral blood flow (Bekar *et al.*, 2012), neuroinflammation and energy metabolism (O'Donnell *et al.*, 2012) have been extensively reviewed. Dysregulation of this system in the AD brain may contribute to wide-ranging behavioural and pathological features of the disease.

1.3.2 Noradrenergic Depletion Potentiates Amyloid Toxicity

Noradrenergic transmission may offer protection against A β toxicity by improving A β metabolism and inflammation, increasing cholinergic transmission, promoting trophic support and alleviating bioenergetic stress (reviewed in Marien *et al.*, 2004). Conversely, loss of noradrenaline may exacerbate A β -induced pathogenic cascades.

1.3.2.1 *Decreased Clearance of A β and Increased Inflammation*

Microglia are first responders to injury in the brain. Once activated by pathogenic stimuli, they proliferate, migrate to sites of damage and clear away cellular debris. Activated microglia are often associated with dense-cored amyloid plaques and are involved in the phagocytosis of fibrillar A β . Microglia express receptors that promote the endocytosis of A β and secrete the proteolytic enzymes neprilysin and IDE, that degrade A β . However, prolonged microglial activation increases inflammatory cytokines, ROS, complement factors and nitrous oxide. A β can activate microglia and trigger an inflammatory response by binding to RAGE and other scavenger receptors. Activated microglia recruit astrocytes, compounding inflammation in the AD brain. As the disease progresses, microglia lose the ability to clear A β , but continue to produce pro-inflammatory cytokines. These inflammatory molecules may contribute to degeneration by stimulating A β formation and aggregation, oxidative stress and neurotrophic factor withdrawal (reviewed in Heneka and O'Banion, 2007; Hickman *et al.*, 2008).

Noradrenaline is a key orchestrator of the microglial response to A β . It acts as an anti-inflammatory agent, suppressing the transcription of inflammatory genes in microglia and astrocytes via β_2 -adrenergic receptors (Mori *et al.*, 2002; Feinstein *et al.*, 2002). Noradrenaline has been shown to dose-dependently decrease A β_{42} -induced cytokine and chemokine production and to increase migration to and phagocytosis of fibrillar A β in primary murine microglial cells (Heneka *et al.*, 2010). The G-protein coupled receptor formyl-peptide receptor 2 (FPR2) mediates endocytosis of A β in microglia.

Noradrenaline binds β_2 -adrenergic receptors in microglia, activating downstream mitogen-activated protein kinase signaling cascades and inducing the expression of FPR2 both *in vivo* and *in vitro*. β_2 -Adrenoceptor stimulation increases microglial chemotaxis, A β_{42} endocytosis via FPR2, expression of IDE and degradation of A β_{42} (Kong *et al.*, 2010). In rats with experimentally induced locus coeruleus degeneration, the inflammatory response to cortical injections of aggregated A β_{42} is potentiated (Heneka *et al.*, 2002). By extension, loss of noradrenergic innervation in AD may aggravate the inflammatory reaction to A β and impair its degradation.

1.3.2.2 *Decreased Cholinergic Transmission*

Loss of cholinergic neurons in the basal forebrain and reductions in choline acetyltransferase (ChAT) activity, choline uptake and acetylcholine release within the hippocampus and neocortex are well documented in AD. Cholinergic transmission is especially vulnerable to A β toxicity. A β inhibits acetylcholine synthesis, impairs trophic support to basal forebrain cholinergic neurons and disrupts cholinergic receptor signaling (reviewed in Kar *et al.*, 2004; Francis *et al.*, 2010). Cholinergic transmission in the brain is mediated by G-protein coupled muscarinic and ligand-gated cation channel nicotinic receptors. Acetylcholine participates in the non-amyloidogenic processing of APP. Reduced availability of acetylcholine and chronic suppression of cortical muscarinic signaling may tip the balance of APP processing towards the amyloidogenic pathway. Selective activation of M1 and M3 muscarinic subtypes has been shown to increase sAPP α secretion and decrease A β formation both *in vitro* and *in vivo* in AD patients (reviewed in Mesulam, 2004; Kar *et al.*, 2004; Schliebs and Arendt, 2006). Nicotinic signaling may also protect neurons against A β . Activation of nicotinic receptors has been shown to favour α -secretase APP processing and inhibit the formation of A β fibrils in cell culture (reviewed in Schliebs and Arendt, 2006). Inhibition of acetylcholinesterase, the enzyme that degrades acetylcholine, results in increased sAPP α secretion in rodent brain and in cell culture. Acetylcholinesterase has been shown to interact with A β to promote its aggregation and toxicity. In turn, A β ₄₂ can bind to α 7-nicotinic receptors on terminals surrounding dense-cored plaques and increase acetylcholinesterase locally (reviewed in Schliebs and Arendt, 2006). Collectively, these studies suggest that acetylcholine depletion facilitates the production and toxicity of A β , which can in turn further disrupt cholinergic transmission.

Degeneration of the locus coeruleus can exacerbate cholinergic hypofunction in the AD brain. Anatomical and pharmacological evidence suggests that noradrenergic tone regulates basalocortical cholinergic transmission. In the human, primate and rodent brain, cholinergic cell bodies in the nucleus basalis of Meynert receive substantial and

direct synaptic input from the locus coeruleus. Interactions between noradrenergic and cholinergic efferents throughout the basal forebrain and in their overlapping terminal fields are implicated in learning, memory and arousal (reviewed in Smiley *et al.*, 1999; Zaborszky *et al.*, 2004; Marien *et al.*, 2004). Noradrenaline can modulate acetylcholine release via presynaptic α_2 adrenergic heteroreceptors that are located on cholinergic cell bodies and terminals. Systemic administration of various α_2 adrenoceptor antagonists, including dexefaroxan, idazoxan, atipamezole and fluparoxan, increase while the α_2 adrenoceptor agonists guanabenz and UK14 304, reduce acetylcholine microdialysis outflow in the medial prefrontal cortex of conscious rats (Tellez *et al.*, 1997). Tellez *et al.* (1999) consolidated results of these and other pharmacological studies on the noradrenergic regulation of basalcortical cholinergic transmission (see Figure 1-3).

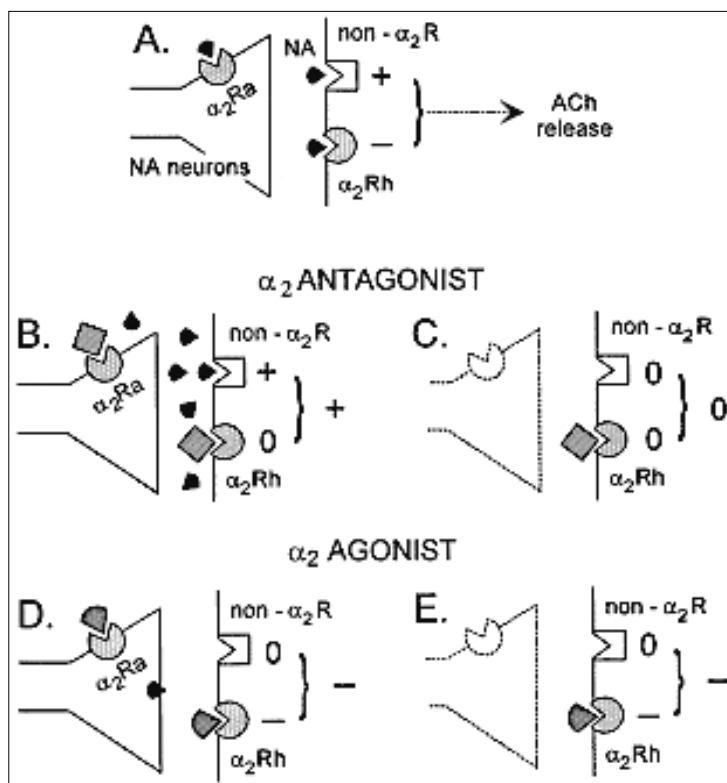


Figure 1-3. Schematic of noradrenergic regulation of cortical acetylcholine release.

Panel **A** depicts basal noradrenaline (NA) and acetylcholine (ACh) synaptic activity. The rest of the panels illustrate the effects of α_2 adrenoceptor antagonism on NA and ACh transmission in intact brains (**B**) and in brains induced with locus coeruleus denervation (**C**) as well as the effects of α_2 adrenoceptor agonists on NA and ACh transmission in intact (**D**) and in locus coeruleus damaged brains (**E**). α_2 Ra, α_2 autoreceptor; α_2 Rh, α_2 heteroreceptor; non- α_2 R; non α_2 -adrenoceptor; +, facilitation; -, inhibition; 0, inactive.

(Reprinted from Neuroscience, 89, Tellez *et al.*, α_2 -Adrenoceptor modulation of cortical acetylcholine release *in vivo*, pages 1041-1050, copyright (1999), with permission from Elsevier: License # 3136640382091).

Noradrenergic tone regulates basal acetylcholine release via inhibitory α_2 adrenergic heteroreceptors and excitatory non- α_2 adrenergic receptors, such as α_1 and β receptors on

cholinergic terminals (Figure 1-3, panel A). Dexefaroxan, a selective antagonist of α_2 adrenoceptors that has no effect on cholinesterase, inhibits α_2 autoreceptors on noradrenergic terminals. The effect of this presynaptic inhibition is to increase noradrenaline synthesis and release. Dexefaroxan simultaneously blocks α_2 heteroreceptors on cholinergic terminals. The net effect is thus increased acetylcholine release (panel B). Dexefaroxan has no effect on cholinergic transmission in animals that undergo lesions of the locus coeruleus (panel C). An α_2 agonist, such as UK 14 304, activates α_2 autoreceptors, inhibiting noradrenaline release and excitatory adrenergic receptor activation while concurrently activating α_2 heteroreceptors and inhibiting acetylcholine release (panel D). The inhibitory effect of the α_2 agonist on cholinergic transmission is maintained in animals with damage to the locus coeruleus (panel E). Thus, the loss of locus coeruleus neurons and its facilitatory effects on basalocortical cholinergic transmission may worsen cholinergic deficits in AD (reviewed in Tellez *et al.*, 1999).

Dexefaroxan can reverse memory deficits in aged rats with bilateral lesions of the nucleus basalis magnocellularis and in rats with cognitive deficits induced by various anti-cholinergic amnesic agents (Chopin *et al.*, 2002). In a rat model of unilateral cortical devascularization, retrograde degeneration of basal forebrain cholinergic projections and the loss of cell bodies in the nucleus basalis ensued. For these animals, chronic dexefaroxan treatment abrogated cholinergic atrophy at both somatic and synaptic terminal levels (Debeir *et al.*, 2002). It also ameliorated spatial memory deficits (Chopin *et al.*, 2004). The protective effect of dexefaroxan on the basalocortical cholinergic system of the devascularized rats was associated with a local and sustained increase in NGF and TrkA receptor levels (Debeir *et al.*, 2004). These findings indicate that pharmacological activation of the locus coeruleus noradrenergic system can both enhance cholinergic transmission and related behaviours as well as provide neurotrophic support to forebrain cholinergic innervation.

1.3.2.3 *Decreased Trophic Support*

The neuroprotective effects of noradrenaline are largely mediated by BDNF. Several *in vivo* studies in rodents have revealed a mutually trophic relationship between BDNF and noradrenergic neurons with forebrain terminal fields. Dexefaroxan was found to enhance cellular survival and neurogenesis in the olfactory bulb (Bauer *et al.*, 2003; Veyrac *et al.*, 2005) and hippocampus (Rizk *et al.*, 2006), whereas noradrenergic depletion drastically reduced the proliferation of dentate gyrus progenitor cells (Kulkarni *et al.*, 2002) in adult rats. A stimulatory effect of dexefaroxan on the long-term survival and differentiation of new granule cells in the dentate gyrus was associated with an upregulation of BDNF expression in the hippocampus (Rizk *et al.*, 2006). Noradrenergic neurons synthesize and secrete BDNF in the neocortex. This in turn regulates the survival of developing and injured neurons (Fawcett *et al.*, 1998). BDNF has been shown to induce the phenotypic differentiation of noradrenergic neurons in locus coeruleus cultures (Traver *et al.*, 2006) and to maintain forebrain noradrenergic innervation in the aged rat brain (Matsunaga *et al.*, 2004). The facilitatory effect of dexefaroxan on neurogenesis can be ascribed to an increase in the activity-dependent synthesis, anterograde transport and secretion of BDNF by noradrenergic terminals (Rizk *et al.*, 2006). As reviewed earlier, reductions in BDNF occur at pre-clinical stages of AD, preceding deficits in basal forebrain cholinergic transmission, but corresponding with the expression of cognitive decline (Peng *et al.*, 2005). The loss of forebrain noradrenergic activity and BDNF trophic support in AD may play a permissive role in the degeneration of vulnerable neuronal populations within locus coeruleus terminal fields.

1.3.2.4 *Increased Oxidative and Energetic Stress*

Degeneration of the locus coeruleus can disrupt energetic homeostasis and functional interactions between neurons and astrocytes. Adrenergic receptors on astrocytes have been linked to various housekeeping roles that include glycogen metabolism and the

transport of energy and transmitter substrates to neurons during periods of intense activity. Furthermore, stimulation of the locus coeruleus results in the release of co-factors such as BDNF and ATP. A deficiency in noradrenergic transmission in the AD brain could lead to a failure in energy utilization and homeostasis in both neurons and astrocytes and impair other transmitter systems (reviewed in Marien *et al.*, 2004; O'Donnell *et al.*, 2012).

Noradrenaline has been shown to protect cultured neurons from oxygen-glucose deprivation and excitotoxicity (Madrigal *et al.*, 2009), oxidative stress (Troadece *et al.*, 2001; Traver *et al.*, 2005) and A β injury (Madrigal *et al.*, 2007; Counts and Mufson, 2010). In human neuronal and rat primary hippocampal cultures, noradrenaline prevented A β -induced oxidative stress, depolarization of the mitochondrial membrane and the activation of apoptotic cascades. These effects were mediated through β adrenergic stimulation of cAMP and P-CREB and the subsequent increased production of NGF and BDNF (Counts and Mufson, 2010). In astrocytic cultures, noradrenaline and cAMP induced expression of the protective chemokine MCP-1 (monocyte chemoattractant protein). MCP-1 reduced lactate dehydrogenase release and prevented the loss of ATP in neurons challenged with oxidative-glucose deprivation and glutamate (Madrigal *et al.*, 2009). Noradrenaline and cAMP also reduced A β_{42} -induced damage in primary cultures of rat cortical neurons (Madrigal *et al.*, 2007). Some protective effects of noradrenaline against A β and oxidative insults may be mediated through adrenoceptor-independent mechanisms. Noradrenaline increases the synthesis and expression of the antioxidant GSH in neurons (Madrigal *et al.*, 2007). It also has antioxidant properties. It promoted the long-term survival and function of dopaminergic neurons in rat mesencephalic cultures, independent of adrenoceptor activation or glutathione synthesis (Troadece *et al.*, 2001). In an *in vitro* model of septal cholinergic cell death induced by low-level oxidative stress, noradrenaline rescued cholinergic neurons by neutralizing hydroxyl radicals (Traver *et al.*, 2005). Like noradrenaline, other 1,2-dihydroxybenzene derivatives have been found to reduce ROS and to promote survival of cholinergic and dopaminergic neurons *in vitro*, suggesting that the catechol moiety may confer antioxidant and neuroprotective properties. Some

of these effects may involve synergistic interaction with other trophic molecules. For example, in the septal neuron culture model, BDNF and NGF only prevented oxidative stress and stimulated the cholinergic phenotype when tested in the presence of noradrenaline (Traver *et al.*, 2005). The protective effects of noradrenaline against A β toxicity and oxidative stress, together with its stimulatory effects on transmission and on the synthesis and release of trophic factors, draw attention to the AD-associated noradrenergic deficits as targets for therapeutic intervention.

1.4 APP-Transgenic Mouse Models of Alzheimer's Disease

AD-like cerebral A β pathology occurs spontaneously in aged nonhuman primates, bears and dogs. Primates, bears and sheep can also develop neurofibrillary tangles. There are no reports of these pathological indices spontaneously occurring in lower-order species (reviewed in Jucker, 2010). The dog is an especially relevant model of AD. Canine *APP* and its proteolytic machinery share considerable homology with the human equivalents. Dogs develop age-related cognitive dysfunction, the extent of which correlates with cortical A β load and the loss of noradrenergic neurons (Insua *et al.*, 2010). These findings in the plaque-bearing dog brain affirm the interplay of A β toxicity and noradrenergic deficits in driving disease progression. Despite these similarities to human AD, the dog is not a practical choice for most AD research. Mice offer several advantages. They are comparatively easy, fast and inexpensive to breed in large numbers. Moreover, procedures for transgenic manipulation and phenotyping of the mouse are well described in the biomedical literature. For these reasons, numerous lines of genetically engineered mice expressing a variety of AD-associated human mutations have been created over the past 15 years (reviewed in Jucker, 2010).

1.4.1 Mouse Models of A β Deposition

Increased A β biogenesis and aggregation is the common pathogenic denominator in both familial and sporadic AD (see section 2.2). Consequently, initial attempts at creating a transgenic (Tg) mouse model of AD focused on inducing expression of the entire human *APP* (h*APP*) gene. However, overexpression of wild-type h*APP*, either the *APP695* or *APP751* isoforms, was insufficient to produce A β plaque pathology. Subsequent attempts at producing amyloid pathology led to the creation of Tg mice overexpressing familial AD-causing mutations in *APP*, *PS1* or *PS2*. Such mutant APP-Tg mice exhibit robust A β deposition, whereas mice expressing only *PS1* or *PS2* mutations exhibit increased production of A β_{42} but not cerebral plaques. Differences in murine and human sequences and/or processing of APP may explain the failure of presenilin over-expression to cause significant A β pathology in mice. However, combining mutant h*APP* with presenilin over-expression can accelerate cerebral A β pathology and exacerbate behavioural deficits in APP-Tg mice (reviewed in Dodart *et al.*, 2002; Bateman *et al.*, 2011; Kokjohn and Roher, 2009). APP-Tg mice have proven invaluable tools for studying the toxicity of A β *in vivo*. Table 1-1 summarizes the main characteristics of the most widely used APP-Tg lines.

Table 1-1. APP transgenic mouse models of AD

Transgenic Mouse	Strain	Gene, Mutation(s)	Promoter	Plaque Onset	Neuropathology	Behavioural Phenotype	Primary Reference
PDAPP	C57BL/6J x DBA/2 x Swiss-Webster	hAPP minigene, Indiana: V717F	platelet-derived growth factor β (PDGFB)	6-9 months in hippocampus and cingulate cortex	dystrophic neurites, gliosis, loss of synaptic and dendritic spine density, oxidative stress, tau hyperphosphorylation	reference working and spatial memory deficits	Games <i>et al.</i> , 1995
Tg2576	C57BL/6 x SJL x C57BL/6	hAPP 695, Swedish: K670N/M671L	hamster prion protein promoter (PrP)	9-12 months in hippocampus, cortex, subiculum and cerebellum	intracellular A β , dystrophic neurites, gliosis, decreased dendritic spine density in hippocampus, mitochondrial dysfunction, tau hyperphosphorylation	perseverative behaviour, reference working, contextual and spatial memory deficits	Hsiao <i>et al.</i> , 1996
APP23	C57BL/6 x DBA/2	hAPP 751, Swedish: K670N/M671L	murine Thy-1.2	6 months in the cortex	intracellular A β , loss of pyramidal neurons in the hippocampus CA1 region, dystrophic neuritis and gliosis, hyperphosphorylated tau	reference working, recognition and spatial memory deficits, passive avoidance impairments	Sturchler-Pierrat <i>et al.</i> , 1997
TgCRND8 *extensively reviewed in section 2.4.4	C57BL/6 x C3H	hAPP 695, Swedish: K670N/M671L and Indiana: V717F	Syrian hamster PrP	3 months in hippocampus and cortex	loss of cortical cholinergic neurons, nitrosative stress, gliosis, hyperphosphorylated tau	working and spatial memory impairment	Chisti <i>et al.</i> , 2001
APP/PS1	Tg2576 mice x mutated PS1 lines	hAPP 695, Swedish: K670N/M671L PS1: M146L	hamster PrP and PDGFB	4-6 months in hippocampus and cortex	Accelerated A β deposition, intracellular A β , gliosis, elevated A β ₄₂ /A β ₄₀ ratios compared to Tg2576 mice, minor neuron loss	Impaired spatial and working memory	Holcomb <i>et al.</i> , 1998
3xTg-AD	129/C57BL/6	hAPP 695, Swedish: K670N/M671L PS1: M146L Tau: P301L	murine Thy-1.2, PS1 knock-in	9 months in hippocampus and cortex followed by tau pathology	intracellular A β , A β pathology begins in the cortex and spreads to the hippocampus, synaptic dysfunction, neurofibrillary tangles in the hippocampus spreading to the cortex, gliosis	deficits in long-term retention and spatial memory	Oddo <i>et al.</i> , 2003
5xFAD (Tg6799)	C57BL/6 x SJL	hAPP 695, Swedish: K670N/M671L, Florida: I716V, London: V717I PS1: M156L, L286V	murine Thy1	2 months in deep layers of cortex and subiculum	intracellular Ab by 1.5 months, neuron loss in cortex and subiculum by 9 months, synaptic dysfunction, axonopathy, gliosis	working memory and spatial memory deficits, decreased anxiety, growth retardation, motor impairment	Oakley <i>et al.</i> , 2006

The features summarized in Table 1-1 are drawn from seven key reviews of APP-Tg mouse models (Dodart *et al.*, 2002; Spires *et al.*, 2005; Crews *et al.*, 2010; Wirths *et al.*, 2010; Balducci *et al.*, 2011; Jawhar *et al.*, 2012; Li *et al.*, 2013). They indicate that expression of hAPP mutations in Tg mice reliably leads to A β accumulation and to development of senile plaques. Plaques are associated with cognitive and synaptic dysfunction, dystrophic neurites, reactive gliosis as well as hyperphosphorylation of tau. Soluble oligomeric species of A β are believed to mediate the toxicity. Alterations in synaptic plasticity, axonal swellings and hippocampal atrophy are present well before plaque deposition can be discerned (reviewed in Elder *et al.*, 2010).

Neurofibrillary tangles are not encountered in these models. However, in the case of 3xTg mice that express mutant forms of human APP, PS1 and tau, intraneuronal A β deposits appear before somatodendritic accumulation of tau. These findings support the hypothesis that amyloid accumulation precedes and fosters hyperphosphorylation of tau, in turn leading to tangle formation. Consistent with this notion, A β immunotherapy was found to reduce tau pathology in 3xTg mice (Oddo *et al.*, 2004).

1.4.2 Limitations in Modeling Late-Stages of Disease

APP-Tg mice reliably mimic age-dependent A β deposition and cognitive impairment, though not neurofibrillary tangles and extensive neuronal loss exhibited in the human disease. Thus, these constitute partial models, best suited for studying the role of amyloid pathology in isolation. In this sense, APP-Tg mice are particularly useful for examining early, prodromal phases of the human disease, when interventions might serve to prevent disease progression (Zahs and Ashe, 2010). Clearly other factors that may play a role in the sporadic human disease, including the influence of ageing, social and environmental factors, as well as comorbidities such as diabetes can be approached experimentally, but cannot be fully recapitulated in transgenic mice (reviewed in Li *et al.*, 2013).

Several confounding artifacts may arise with transgenesis. APP-Tg mice express mutated *APP* transgenes and accumulate A β by mechanisms that are not under normal physiological control. This may trigger unanticipated tissue responses that are unrelated to the disease process in AD. The level and topography of transgene expression is dependent on the transcriptional promoter used. The genetic background and gender of the mouse can also substantially influence pathology and behaviour (reviewed in Duyckaerts *et al.*, 2008). The use of different promoters, murine genetic backgrounds and *APP* isoforms in creating APP-Tg mice has led to some heterogeneity in the expression of amyloid pathology and cognitive phenotypes. Of the three major isoforms of APP expressed in the brain (APP₆₉₅, APP₇₅₁, APP₇₇₀), only the AICD produced from β - and γ -secretase cleavage of APP₆₉₅ is transcriptionally active. AICD up-regulates the expression of neprilysin. AICD produced from the Swedish mutant form of APP₆₉₅ is more transcriptionally active than that produced from wild-type APP₆₉₅ (Belyaev *et al.*, 2010). Increased expression of the amyloid degrading enzyme neprilysin in mice expressing the Swedish variant of APP695 may lead to differences in the development of amyloid pathology among APP-transgenic lines. Levels of soluble A β , especially of the toxic oligomeric kind, differ among transgenic lines. For example, Tg2576 mice exhibit lower levels of soluble A β than APP23 mice. Both of these lines express the Swedish mutation, but do so on distinct murine genetic backgrounds and with different hAPP isoforms and transcriptional promoters (refer to Table 1-1). Background strain critically influences the overall phenotypic profile. Mice bred from the DBA/2J and SJL lines, such as the PDAPP and Tg2576 mice, display aggressive and neophobic tendencies that can hinder the interpretation of their performance in behavioural tasks (reviewed in Kobayashi and Chen, 2005; Balducci and Forloni, 2011). These differences and the co-existence of human and murine A β in transgenic mice can confound translation of results to the human disease.

Typically, the A β plaques produced in APP-Tg mice are less dense, more soluble and less resistant to degradation than are those observed in AD patients. Compared with human A β , mouse A β has three amino acid substitutions in the *N*-terminal region.

These sequence differences do not prevent murine A β from aggregating into β -sheet structures and fibrils *in vitro*. In fact, mixed human and murine A β fibrils were found to be more insoluble than homogenous human A β fibers (Fung *et al.*, 2004). Differences between the amyloid aggregates observed in APP-Tg mice and in AD patients may arise from the lack of post-translational modifications of A β in mice. More extensive amino-terminal truncation, aspartate isomerization, methionine oxidation, intermolecular cross-linking and an increased glycosylation in humans may underlie the greater insolubility and resistance to proteolysis of human A β plaques. Such species differences may explain the resilience of APP-Tg mice to A β burdens that cause neuronal death in humans (reviewed in Kokjohn and Roher, 2009). Despite these caveats, APP-Tg mice have provided the first *in vivo* demonstration that *APP* familial mutations cause amyloidogenesis similar to that observed in AD and are thus useful for examining how A β initiates the disease (reviewed in Dodart *et al.*, 2002).

1.4.3 Noradrenergic Involvement in APP-Tg mice

Progressive damage to noradrenergic terminals and degeneration of the locus coeruleus have been observed in several strains of APP-Tg mice. Aged PDAPP mice exhibit selective shrinkage of locus coeruleus cells that project to cortical or hippocampal regions with extensive A β pathology (German *et al.*, 2005). In APP_{swe}/PS1 Δ E9 mice, progressive A β deposition in the forebrain is associated with distal axonopathy and loss of noradrenergic neurons in the locus coeruleus (Liu *et al.*, 2008). These mice also exhibit a late-onset, gradual loss of noradrenaline in the hippocampus (Szapacs *et al.*, 2004). A decrease in the volume and number of cells was also observed in the locus coeruleus of the Tg2576 mouse. This degeneration in Tg2576 mice coincided with impairments in olfactory memory and neurogenesis (Guérin *et al.*, 2009). Finally, damage to the locus coeruleus is evident in the 5xFAD APP-Tg mouse. At 6 months of age, male 5xFAD mice exhibit increased astrocyte activation, increased inflammatory gene expression, neuronal hypertrophy and reduced catecholaminergic

markers in the locus coeruleus (Kalinin *et al.*, 2012). In all of these transgenic mouse studies, locus coeruleus damage was observed late in disease progression and appeared to result from retrograde degeneration that was initiated by A β in forebrain terminal fields (Liu *et al.*, 2008).

1.4.3.1 *Noradrenaline Depletion Studies*

Degeneration of the locus coeruleus appears to be driven by A β . In turn, a deficiency in noradrenergic transmission can aggravate A β pathology and toxicity (see section 2.3.2). Several research groups have experimentally lesioned the locus coeruleus in APP-Tg mice to investigate the effects of noradrenergic depletion on A β mediated dysfunction *in vivo*. The neurotoxin *N*-(2-chloroethyl)-*N*-ethyl-2-bromobenzylamine (DSP-4) is routinely used. It accumulates intraneuronally and irreversibly inhibits noradrenaline uptake (Wenge and Bönisch, 2009). Although the precise mechanism of DSP-4 action is unknown, it is thought to produce retrograde degeneration in noradrenergic terminals by alkylation of neuronal structures (Fritschy and Grzanna, 1989). In rodents, systemic administration of DSP-4 causes dose-dependent denervation of fibers arising mainly from the locus coeruleus (reviewed in Marien *et al.*, 2004). This results in reduced noradrenaline tissue content and NET levels, as well as increased α_2 adrenoceptor binding sites in the forebrain (reviewed in Szot *et al.*, 2010).

To study the interplay between noradrenergic depletion and A β toxicity, Heneka and colleagues (2006) administered acute high dose DSP-4 treatments (2 intraperitoneal injections of 50 mg/kg separated by a week) to 10 month-old APP23 mice. Normally, APP23 mice do not exhibit degeneration of the locus coeruleus. However, DSP-4 caused 50-60% loss of neurons in the locus coeruleus and > 70% loss of tissue noradrenaline content within the cortex and hippocampus. Loss of noradrenergic fibers exacerbated glial inflammation and A β load in terminal fields. DSP-4 treatment significantly increased neuronal loss, decreased the density of cholinergic boutons,

attenuated cholinesterase activity and reduced cerebral glucose metabolism. The neurochemical and pathological changes were associated with increased cognitive deterioration. Compared to non-lesioned APP23 mice, the DSP-4 treated animals performed worse in tests of spatial learning and exhibited no ability to recognize a social partner. Although DSP-4 treatment in wild-type mice induced noradrenergic depletion, it did not affect neuronal integrity in terminal fields, inflammatory markers, cholinergic function or cognitive performance. These findings suggest that amyloid and noradrenergic deficits induce dysfunction synergistically (Heneka *et al.*, 2006). Chronic low doses of DSP-4 (5 mg/kg; intraperitoneally, every 2 weeks for 6 months) administered to 3 month-old APP-Tg mice overexpressing the Indiana mutation, increased A β burden 5-fold and decreased both expression and activity of neprilysin (Kalinin *et al.*, 2007). Repeated injections of DSP-4 (5 mg/kg monthly from 5 to 11 months of age) were administered to APP/PS1 mice bearing *APP* Swedish and PS1 M146V mutations (TASTPM mouse line). These animals exhibited reductions in forebrain noradrenaline levels greater than those associated with normal ageing. The injections increased glial activation and inflammatory markers but did not affect the severity of A β pathology or memory deficits (Pugh *et al.*, 2007). Finally, in APP_{swe}/PS1 Δ E9 mice with endogenous noradrenergic deficits, chronic intraperitoneal injections of 50 mg/kg DSP-4 (monthly from 3 to 6.5, or 3 to 12.5 months of age) accelerated A β pathology, neuroinflammation and cognitive impairment (Jardanhazi-Kurutz *et al.*, 2010) and altered the relative expression of α - and β -adrenoceptors in terminal fields (Jardanhazi-Kurutz *et al.*, 2011). These studies collectively reveal that the effects of DSP-4 on A β and related dysfunction depend on the dosing regime, transgenic model and age at which treatments are initiated.

The selectivity and efficacy of DSP-4 as a noradrenergic toxin has been questioned. In rats, DSP-4 rapidly and transiently depletes noradrenaline and NET levels in forebrain terminal fields, without causing obvious degeneration of the locus coeruleus (Szot *et al.*, 2010). Though mice may be more sensitive to DSP-4 than rats (Fornai *et al.*, 1996), experimental lesions of the locus coeruleus are reversible. Surviving noradrenergic neurons exhibit robust sprouting and compensatory increases in noradrenaline release.

Upregulation of postsynaptic adrenergic receptors also occurs in response to presynaptic deficits. The immediate effects of systemic administration of DSP-4 include an acute increase in noradrenaline release in the cortex. This effect is assumed to result from DSP-4 inactivation of NET. Depending on the extent of denervation and the time after DSP-4 treatment, noradrenaline release may be maintained at normal levels because of the compensatory capacity of this system (reviewed in Marien *et al.*, 2004). Moreover, DSP-4 decreases not only noradrenaline but also co-factors such as galanin and BDNF. To isolate the effects of a specific noradrenaline deficiency, APP_{swe}/PS1ΔE9 mice were crossbred with dopamine β-hydroxylase knock-out animals, unable to synthesize noradrenaline but with intact locus coeruleus neurons, projection fibers and co-transmitters. Selectively ablating noradrenaline in APP_{swe}/PS1ΔE9 mice potentiated impairments in spatial memory and hippocampal LTP and reduced levels of learning-associated postsynaptic receptors without increasing Aβ pathology or impairing its clearance (Hammerschmidt *et al.*, 2013). Collectively, these studies suggest that a disruption in forebrain noradrenergic transmission exacerbates phenotypes in APP-Tg mice and that locus coeruleus degeneration triggers inflammation and Aβ deposition.

1.4.3.2 *Noradrenaline Enhancement Studies*

Deficiency in forebrain noradrenergic transmission exacerbates Aβ-induced impairment in APP-Tg mice. Thus, enhancing noradrenergic function might mitigate disease progression. Noradrenaline stimulates microglial phagocytosis of Aβ. Loss of this phagocytic activity in DSP-4 treated APP-Tg mice can be restored with the noradrenaline precursor, L-threo-3,4-dihydroxyphenylserine (L-DOPS) (Heneka *et al.*, 2010). In 5xFAD APP-Tg mice with noradrenergic degeneration and inflammation, chronic treatment with L-DOPS elevated noradrenaline levels in the brain, reduced glial activation and Aβ burden, increased mRNA levels of the amyloid-degrading enzymes neprilysin and IDE, upregulated BDNF expression and improved spatial memory (Kalinin *et al.*, 2012). However, the noradrenaline-reuptake inhibitor, atomoxetine, did

not reduce plaque burden in 5xFAD mice and did not improve clinical scores in AD patients (reviewed in Kalinin *et al.*, 2012). A related reuptake inhibitor, reboxetine, failed to improve cognitive deficits in APP/PS1 mice. In contrast, chronic treatment with the α_2 -adrenoceptor antagonist fluparoxan prevented age-related spatial working memory deficits in APP/PS1 TASTPM mice without altering A β load or astrocytic activation (Scullion *et al.*, 2011). These results suggest that increasing noradrenaline tissue levels alone may not correct the full complement of AD-like changes in the brain. In particular, improving cognitive endpoints may rely on improving cholinergic and/or serotonergic tone through heteroceptor blocking actions of α_2 -adrenoceptor antagonism. Differences in drug treatment paradigms, mouse strain and A β load may also contribute to the outcome of drug treatment studies in AD models. Despite these caveats, it appears that enhancing forebrain noradrenergic transmission (see section 1.3.2) can mitigate both symptoms and progression of amyloid pathology.

1.4.4 The TgCRND8 Mouse

The TgCRND8 mouse is a robust, early-onset model of amyloidogenesis in a hybrid C57BL/6 x C3H genetic background strain. TgCRND8 mice overexpress a hAPP695 transgene bearing Swedish (KM670/671NL) and Indiana (V717F) familial AD mutations, under the control of the pan-neuronal Syrian hamster prion promoter. Expression of the doubly mutated hAPP protein is ~5-fold higher than that of endogenous murine APP (Chishti *et al.*, 2001). The Swedish mutation promotes the β -secretase proteolysis of APP, while the Indiana mutation increases the A β_{42} /A β_{40} proportion of amyloid peptides produced (reviewed in Walsh and Teplow, 2012).

1.4.4.1 *Neuropathological and Neurochemical Changes*

TgCRND8 mice develop A β accumulation preferentially in the cortex and hippocampus (Chishti *et al.*, 2001; Ma *et al.*, 2011). From 4 to 10 weeks of age, A β_{40} levels are low and stable. A β_{42} levels rise slowly from 4 to 8 weeks and sharply increase at 10 weeks, at which point, A β_{42} peptide levels are ~5X those of A β_{40} . At 6 months of age, overall levels of A β in TgCRND8 brains are equivalent to those observed in sporadic AD brains (Chishti *et al.*, 2001). A β_{42} /A β_{40} ratios in TgCRND8 mice are highest in the regions wherein insoluble A β accumulates most. These include the hippocampus, cortex and olfactory bulbs (Ma *et al.*, 2011). The spatiotemporal progression of A β deposition in TgCRND8 brains is similar to that in AD patients (see section 1.1.2.1). In the mice, A β plaques emerge in cortical regions surrounding the hippocampus (subiculum) shortly after 9 weeks of age. Robust plaque pathology is consistently present throughout cortex and hippocampus by 15 weeks of age. From the cortex, plaques spread to the hippocampus proper, dentate gyrus, olfactory bulbs and thalamus. At 28 weeks of age, A β deposits are observed in the cerebral vasculature and striatum. By 35 weeks, the cerebellum and brainstem are also burdened with A β (Chishti *et al.*, 2001). At 40 weeks, extensive A β pathology occupies ~4% of total cortical area in TgCRND8 brains (Hyde *et al.*, 2005). TgCRND8 mice exhibit both dense-core and diffuse plaques. Infrared microspectroscopy has revealed that the dense core plaques assume a highly aggregated β -sheet structure and are surrounded by an increase in phospholipids, that likely come from membranes of dystrophic neurites and microglial processes. In contrast, diffuse amyloid plaques lack the β -sheet structure and do not appear to disrupt tissue morphology (Rak *et al.*, 2007). Dense-cored A β plaques in TgCRND8 mice are closely associated with dystrophic neurites and a focal inflammatory response (Chishti *et al.*, 2001).

At early stages of A β deposition, inflammatory markers are unchanged in TgCRND8 mice. At 28 weeks of age, the pro-inflammatory cytokine IL-1 β , was found to be upregulated in the cortex, hippocampus and olfactory bulbs. By 36 weeks, IL-1 β levels

were increased in the striatum as well. At that age, TgCRND8 mice also were found to exhibit increased expression of the astrocytic chemokine, CXCL1, in the hippocampus and olfactory bulbs (Ma *et al.*, 2011). A β plaques in TgCRND8 mice are surrounded by hypertrophic astrocytes and are infiltrated by activated microglia. Moreover, neurons and microglia in the vicinity of A β deposits express inducible nitric oxide synthase (iNOS) (Bellucci *et al.*, 2006). The induction of iNOS fosters production of nitrous oxide, leading to protein nitration and oxidative damage. Indeed, nitrotyrosine immunostaining was observed in the neocortex and hippocampus of the TgCRND8 brain (Bellucci *et al.*, 2007). Nitrosative stress may contribute to the formation of tau filaments by promoting tau hyperphosphorylation and disassembly from microtubules (Zhang *et al.*, 2005a,b). TgCRND8 mice do not develop neurofibrillary tangles (Chishti *et al.*, 2001), but do exhibit hyperphosphorylated (Bellucci *et al.*, 2007; Greco *et al.*, 2010) and nitrosylated tau in the vicinity of plaques (Bellucci *et al.*, 2007). Neuroinflammation and abnormal processing of tau in TgCRND8 mice were found to occur after the development of cerebral amyloidosis.

Signs of bioenergetic stress emerge with A β accumulation in TgCRND8 brains. Focal microcrystalline deposits of creatine have been observed in the hippocampus of 5 month-old mice and have been found to progressively increase with A β burden (Kuzyk *et al.*, 2010). Creatine deposits are also evident in the hippocampus of AD patients (Gallant *et al.*, 2006) and may reflect disruption in the creatine kinase/PCr energy shuttle and/or an unmet need in maintaining tissue bioenergetics (reviewed in section 1.1.5.3). The significance of creatine deposits in TgCRND8 mice is unknown, as is their state of bioenergetic homeostasis and mitochondrial function.

Amyloidosis in TgCRND8 brains is accompanied by autophagic-lysosomal pathology, as observed in AD (Nixon *et al.*, 2005; reviewed in Nixon and Yang, 2011). Neurons in the cortex and hippocampus of TgCRND8 mice were found to contain enlarged autophagic vacuoles filled with A β . Autophagic pathways are probable sites of A β generation. Disruption of autophagy/ proteolytic clearance may contribute to intracellular A β buildup

(reviewed in Nixon, 2007). Reversal of autophagic deficits in TgCRND8 mice reduced intraneuronal A β and extracellular A β deposition (Yang *et al.*, 2011).

A β accumulation induces some degeneration in TgCRND8 brains. A β deposits in this mouse are highly axonopathic, causing localized displacement or termination of apical dendrite segments (Woodhouse *et al.*, 2009). Despite severe dystrophy, axons and apical dendrites remain continuous and their corresponding cell bodies are metabolically active throughout disease progression. However, dystrophic axons are associated with impaired axonal transport and a loss of presynaptic machinery. Localized disruption of synaptic function in TgCRND8 mice is thought to reflect early stages of axonopathy and synaptic loss in AD (Adalbert *et al.*, 2009). Frank neuronal loss has also been reported. At 6 months of age, TgCRND8 mice exhibit a significant reduction in the number of hippocampal neurons immunoreactive for glutamate decarboxylase 67, the enzyme responsible for synthesizing GABA. The loss of GABAergic neurons is localized to the CA1-3 hippocampal fields and occurs in the absence of alterations in glutamatergic transmission (Krantic *et al.*, 2012). Neuronal damage and extensive white matter demyelination has been observed in plaque-riddled brain regions that receive heavy cholinergic innervation. By 7 months, TgCRND8 mice exhibit a significant loss of cholinergic neurons (39% reduction) in the nucleus basalis magnocellularis and reduced M2 muscarinic receptor immunoreactivity in the cortex. The cell bodies and dendrites of the remaining cholinergic neurons are shrunken. Moreover, levels of basal and potassium-evoked extracellular acetylcholine were significantly reduced in the prefrontal cortex (Bellucci *et al.*, 2006).

A β_{42} has been associated with increased levels of the ryanodine receptor-3 and altered calcium homeostasis in neurons from TgCRND8 mice (Supnet *et al.*, 2006). Ryanodine receptors regulate the release of calcium from endoplasmic reticulum and play a critical role in regulating intracellular calcium levels. The increase in ryanodine receptor-3 levels in the cortex and hippocampus of TgCRND8 mice was associated with disruption of this intraneuronal calcium control. Alterations in GABAergic tone and/or calcium homeostasis may underlie reported increases in hippocampal excitability, abnormal synaptic plasticity (Jolas *et al.*, 2002) and lowered seizure threshold (Del Vecchio *et al.*,

2004). As in AD, the dendritic morphology of hippocampal pyramidal CA1 neurons is grossly simplified in TgCRND8 brains. Specifically, the basal dendrites of CA1 pyramidal neurons were shorter, with fewer intersections and nodes (Yiu *et al.*, 2011). Decreases in spine density and dendritic morphology were associated with reductions in activation of CREB and transcription of Arc (Yiu *et al.*, 2011). These studies suggest disruptions in synaptic efficacy and neuronal activity in hippocampal networks that may be important for memory.

Decreased P-CREB expression, reduced GABAergic and cholinergic markers, disrupted calcium homeostasis and creatine deposits reflect bioenergetic stress and reveal potential pathways to degeneration in the TgCRND8 brain.

1.4.4.2 *Behavioural Profile*

TgCRND8 mice exhibit a range of behavioural phenotypes. These include well-characterized learning and memory deficits in explicit hippocampus-dependent spatial navigation tasks, such as the Morris water maze (Chishti *et al.*, 2001, Janus, 2004; Hyde *et al.*, 2005; Hanna *et al.*, 2009), the 6-arm radial water maze (Lovasic *et al.*, 2005) and the Barnes maze (Görtz *et al.*, 2008; Richter *et al.*, 2008; Ambrée *et al.*, 2009; Walker *et al.*, 2011). These mice also exhibit memory deficits in hippocampus-independent implicit associative learning tasks, such as conditioned taste aversion (Janus *et al.*, 2004; Hanna *et al.*, 2009) and step-down inhibitory avoidance (Bellucci *et al.*, 2006).

TgCRND8 mice also model other behavioural manifestations of AD. They demonstrate reduced sensory gating to auditory startle stimuli in a prepulse inhibition paradigm (McCool *et al.*, 2003). TgCRND8 mice also display increased stereotypic behaviour (ex. jumping, circling, hanging) in their home cages. Altered 24-hour activity rhythms and stereotypies precede plaque deposition and progress with age, but do not correlate with A β burden (Ambrée *et al.*, 2006). Others have observed that TgCRND8 mice are

hyperactive (Hyde *et al.*, 2005; Walker *et al.*, 2011), very sensitive or irritable to touch (Walker *et al.*, 2011) and show altered anxiety-related behaviour (Görtz *et al.*, 2008; Walker *et al.*, 2011). Behavioural disturbances in TgCRND8 mice have been described as analogues of non-cognitive symptoms often seen in AD patients, such as agitation, irritability and sundowning (Walker *et al.*, 2011; Ambrée *et al.*, 2006).

The behaviour of TgCRND8 mice has rarely been assessed prior to plaque formation. One study has noted that emergence of cognitive dysfunction follows the appearance of amyloid plaques, at around 16 weeks of age (Hyde *et al.*, 2005). However, profound spatial memory deficits were recently reported in 10-week-old mice (Yiu *et al.*, 2011). These memory deficits were associated with reductions in P-CREB levels within the dorsal hippocampus. Acutely increasing CREB function restored spatial memory, as well as dendritic spine density and CA1 network activity without affecting plaque load or total A β levels (Yiu *et al.*, 2011). Thus, TgCRND8 behavioural dysfunction may not correlate with levels of insoluble A β (Hanna *et al.*, 2009), but as in the human disease (described in section 2.2.3), it may be triggered by soluble, intracellular accumulations of A β . A build-up of intracellular A β may result from autophagic defects. Autophagic vacuoles and deficiencies in the autophagic-lysosomal degradation pathway have been observed in the hippocampus and cortex of TgCRND8 brains (Lai and McLaurin, 2012). Markedly reducing intraneuronal and total A β levels in TgCRND8 mice, by restoring autolysosomal proteolysis, rescues memory in hippocampus-dependent contextual fear conditioning and olfactory habituation tasks (Yang *et al.*, 2011). Thus, cognitive and behavioural dysfunction likely results from accrual of soluble A β and its downstream effects on transmission, trophic support and/or energetic homeostasis.

1.4.4.3 *Validity as a Model of Alzheimer's Disease*

The high basal synthesis of A β , which is skewed towards production of the longer and more fibrillogenic A β_{42} peptide, contributes to the early onset and aggressive nature of

A β pathology in TgCRND8 mice. As summarized earlier, these mice recapitulate many relevant behavioural, neurochemical and pathological features of AD. However, the molecular determinants of A β -induced functional impairment have yet to be resolved. Cholinergic deficits and most other reported biochemical changes emerge after plaques and behavioural dysfunction. Thus, a major goal of this thesis work was to identify pathways that might lead to these changes in TgCRND8 mice.

Chapter 2 Hypotheses and Experimental Approach

2.1 Thesis Aims

The TgCRND8 phenotype is driven by the production and accumulation of A β . How A β leads to neuronal dysfunction and behavioural abnormalities has yet to be determined. The central objective of this thesis was to investigate neurochemical changes that lead to A β -induced functional impairment. To achieve this, it was first necessary to pinpoint what behavioural changes emerge and when they appear. This provided the 'when' and 'where' to identify pathogenically significant events that unfold in the TgCRND8 brain. With the therapeutic window defined, suitable measures for assessing functional improvements were then determined. The experimental work included four discrete studies, which tests the following hypotheses.

2.2 Hypotheses

2.2.1 Object memory impairment is an early endophenotype

Object recognition is dependent on the integrity of the hippocampus, entorhinal and frontal cortices. These are brain regions that are targeted first by A β . We hypothesized that object memory is affected early in the development of TgCRND8 dysfunction. Mice were tested on a non-spatial, object memory task at pre-plaque, early and advanced plaque stages. We also investigated whether changes in hippocampal and cortical BDNF mRNA levels coincide with memory impairment.

2.2.2 Noradrenaline content is reduced in major terminals and antagonism of α_2 -adrenoceptors mitigates functional impairment

We hypothesized that a progressive loss of noradrenergic innervation to major terminal fields in TgCRND8 mice facilitates A β toxicity. We performed a longitudinal

measurement of catecholamine transmitter and metabolite content in major terminal fields. We hypothesized that reductions in tissue noradrenaline contribute to AD-like phenotypes in TgCRND8 mice. To test this, we examined the effects of increasing noradrenergic transmission on behaviour, BDNF mRNA levels and amyloid burden. We treated mice with the α_2 -adrenoceptor antagonist dexefaroxan, because it has been shown to increase BDNF levels and stimulate cholinergic parameters in addition to increasing locus coeruleus neuronal activity and noradrenaline synthesis (reviewed in Marien *et al.*, 2004). The therapeutic effects of dexefaroxan were compared to that of rivastigmine, a clinically used cholinesterase inhibitor.

2.2.3 Bioenergetic homeostasis is disrupted by mitochondrial dysfunction

We hypothesized that the accumulation of A β metabolically stresses the cell, impairing mitochondrial enzyme function and disrupting energy homeostasis. We examined activities of complex I+III and complex IV of the electron transport chain, as well as those of α -ketoglutarate dehydrogenase and pyruvate dehydrogenase in mice with advanced plaque pathology. To determine how alterations in metabolic enzyme rates affect mitochondrial output, we measured tissue levels of high-energy phosphate donors in behaviourally relevant brain regions.

2.2.4 Blockade of α_2 -adrenoceptors alleviates mitochondrial impairment

Perturbations in energy homeostasis may provide a progressive end-point for therapeutic evaluation in TgCRND8 mice. We revisited mitochondrial enzyme activities and tissue levels of ATP and creatine in younger mice at pre-plaque and nascent plaque pathology stages. Finally, we assessed the therapeutic effects of dexefaroxan on mitochondrial enzyme activity and output. To test whether any positive effect on these parameters might be mediated through a cholinomimetic action of α_2 -adrenoceptor antagonism, effects of dexefaroxan were compared to rivastigmine.

Chapter 3 Object Recognition Memory and BDNF Expression are Reduced in Young TgCRND8 Mice

This chapter has been published:

Reprinted from *Neurobiology of Aging*, 33, Francis BM, Kim J, Barakat ME, Fraenkl S, Yücel YH, Peng S, Michalski B, Fahnstock, M, McLaurin J, Mount HTJ, Object recognition memory and BDNF expression are reduced in young TgCRND8 mice, pages 555-563, Copyright (2012), with permission from Elsevier: License # 3136650486489.

3.1 Abstract

The TgCRND8 mouse model of Alzheimer's disease exhibits progressive cortical and hippocampal β -amyloid accumulation, resulting in plaque pathology and spatial memory impairment by 3 months of age. We tested whether TgCRND8 cognitive function is disrupted prior to the appearance of macroscopic plaques in an object recognition task. We found profound deficits in 8 week-old mice. Animals this age were not impaired on the Morris water maze task. TgCRND8 and littermate controls did not differ in their duration of object exploration or optokinetic responses. Thus, visual and motor dysfunction did not confound the phenotype. Object memory deficits point to the frontal cortex and hippocampus as early targets of functional disruption. Indeed, we observed altered levels of brain-derived neurotrophic factor (BDNF) mRNA in these brain regions of pre-plaque TgCRND8 mice. Our findings suggest that object recognition provides an early index of cognitive impairment associated with amyloid exposure and reduced BDNF expression in the TgCRND8 mouse.

3.2 Introduction

Alzheimer's disease (AD) presents as a progressive loss in memory and general cognitive abilities. A crucial pathogenic factor is the accumulation of amyloid- β ($A\beta$) peptide. Processing of amyloid precursor protein (APP) into $A\beta$ through sequential β - and γ -secretase cleavage results in the deposition of aggregated $A\beta$ in plaques that are first observed in the temporal neocortex, hippocampus and entorhinal cortex of the AD brain (Braak and Braak, 1991; Braak and Del Tredici, 2004; Thal *et al.*, 2006).

Transgenic mice expressing human *APP* are widely used to study how $A\beta$ accumulation leads to neuronal dysfunction and cognitive impairment. The APP-transgenic TgCRND8 mouse develops a pattern of $A\beta$ deposition similar to human AD. Plaques appear in the hippocampus and frontal cortex by 3 months and are eventually found throughout the brain, sparing the cerebellum until late in the disease (Chishti *et al.*, 2001).

The cognitive performance of TgCRND8 mice has been widely studied (Janus *et al.*, 2000; Chishti *et al.*, 2001; Bellucci *et al.*, 2006; Ambree *et al.*, 2006). However, it remains unclear just how early relevant impairments occur. It was reported that the onset of progressive spatial memory deficits in TgCRND8 mice coincides with plaque deposition (Hyde *et al.*, 2005). In humans, plaque burden is poorly correlated with severity of dementia (Terry *et al.*, 1991; Dickson *et al.*, 1992) and it has been suggested that neurotoxic oligomeric $A\beta$ likely causes cognitive decline prior to plaque formation (reviewed in Westerman *et al.*, 2002; Hardy and Selkoe, 2002; Van Dam *et al.*, 2003; Hanna *et al.*, 2009). To pinpoint when cognitive dysfunction first emerges in TgCRND8 mice, we sought a sensitive assay that relies on brain regions targeted by $A\beta$ early in the pathogenic process. Among the earliest symptoms of AD is the disruption of object recognition (Done and Hajilou, 2005; Viggiano *et al.*, 2008), a form of memory that is dependent upon reciprocal interconnections that relay multimodal sensory information between the neocortex, entorhinal cortex and the hippocampus (Charles *et al.*, 2004; Hammond *et al.*, 2004; Parron *et al.*, 2006; Sipos *et al.*, 2007; Vannuci *et al.*, 2008; and reviewed in Dere *et al.*, 2007).

A β may disrupt neural function in these regions, in part, by down-regulating brain derived neurotrophic factor (BDNF) (Garzon and Fahnstock, 2007; Christensen *et al.*, 2008). BDNF is heavily expressed in the hippocampus and cerebral cortex (Hofer *et al.*, 1990; Yan *et al.*, 1997), where it plays important roles in synaptic plasticity and long-term potentiation (reviewed in Nagahara *et al.*, 2009). Decreases in BDNF are evident at preclinical stages of AD, and these reductions correlate with the rate of cognitive decline (Peng *et al.*, 2005). We previously reported decreased levels of BDNF mRNA in the brains of aged, plaque-bearing TgCRND8 mice (Peng *et al.*, 2009). To determine whether BDNF down-regulation is an early correlate of object recognition impairment, we measured BDNF mRNA levels in the hippocampus and frontal cortex of pre-plaque TgCRND8 mice.

3.3 Methods

3.3.1 Mice

TgCRND8 mice express a double mutant (Swedish: KM670/671NL + Indiana: V717F) form of the human *APP*₆₉₅ transgene under control of the Syrian hamster PrP gene promoter (Chishti *et al.*, 2001). These mice, created by Dr. David Westaway at the Centre for Research in Neurodegenerative diseases (Janus *et al.*, 2000), exhibit progressive plaque pathology beginning at 3 months. By 7 months, they exhibit hyperphosphorylation and nitrosylation of tau (Bellucci *et al.*, 2007) along with cholinergic cell loss (Bellucci *et al.*, 2006). The animals were maintained on a hybrid C57BL/6/C3H background and backcrossed with C57BL/6 wild-type mice. Behavioral studies were performed on mice of the F1 generation. TgCRND8 and non-transgenic (non-Tg) littermates were housed in groups of 2 to 4 in ventilated polycarbonate clear cages under standard laboratory conditions (12/12-h light/dark cycle with lights on at 0700-h; room temperature of 21°C). Food and water were available *ad libitum*. Tests were carried out during the light phase of the cycle in accordance with the Canadian Council on Animal Care guidelines and the Animal Care Committee at the University of Toronto.

Experiments were performed on pre-plaque mice at 4 – 6 weeks or 8 – 9 weeks of age and on mice with advanced plaque pathology (6 – 8 months old). Groups were matched for gender and the genotype was unknown to experimenters. Genotypes were determined by dot-blot hybridization analysis of genomic DNA extracted from tail clippings using a human *APP* probe as described previously (Chishti *et al.*, 2001).

3.3.2 Object Recognition

Cohorts of TgCRND8 ($n \geq 10$) and non-Tg ($n \geq 10$) littermates at 4 weeks, 8 weeks and 6 – 8 months of age were tested for object recognition. This is a test of non-spatial, episodic memory that is independent of neuromotor deficits and emotional cues. It is based on the spontaneous tendency of rodents to explore a novel object over a familiar one (Ennaceur and Delacour, 1988). Entorhinal and perirhinal regions of the cortex (the rhinal cortex) are implicated in object recognition, as is the hippocampus, although involvement of the latter is temporally delayed. The rhinal cortex is thought to support short-term retention of object familiarity in concert with neocortical areas (Mumby and Pinel, 1994; Steckler *et al.*, 1998). With delay intervals longer than 15 min, retention becomes dependent upon reactivation of memory traces in the hippocampus (Hammond *et al.*, 2004). To differentiate between cortical and hippocampal components of task performance, we adapted the object memory paradigm used previously in our laboratory (Vaucher *et al.*, 2002) by varying delay intervals. Mice were habituated to the testing arena (clear plastic mouse cages) for 15 min over 7 daily sessions, and were considered successfully habituated if they consumed a small piece of breakfast cereal within 2 min. On the test day, each animal was exposed for 10 min to a LEGO[®] construct (LEGO Group, Billund, Denmark) and a Hot Wheels[®] car (Mattel, Inc., El Segundo, CA, USA). The objects were predetermined to be of matched saliency to mice. Objects were fixed to the floor of the mouse cage with Velcro tape. Time spent exploring the objects was recorded. Exploration was scored when the mouse touched an object with its forepaws or snout, bit, licked, or sniffed the object from a distance of no more than 1.5 cm. Five min, 1-h, or 3-h later, mice were re-exposed for 5 min to one object from the original test pair and to a novel object. Separate cohorts ($n \geq 10$ for either genotype) were tested at each retention interval. Between tests, the objects and testing cage were wiped with Virox5[™] (Johnson Diversey, Inc., Sturtevant, WI, USA) to eliminate odor cues. The possible confound of mice exhibiting preference for the right or left side of the cage was addressed by counterbalancing the placements of new object between mice in a test group. A “memory index” (MI) was calculated as: $MI = (t_n - t_f) / (t_n + t_f)$, wherein ‘ t_n ’ represents time exploring a novel object and ‘ t_f ’ the duration of familiar object exploration.

3.3.3 Visual Function

Visual function was assessed non-invasively in 9-week-old TgCRND8 ($n=7$) and non-Tg ($n=10$) littermates by testing a head tracking response to a rotating whole field stimulus. Head-tracking behaviour has been used to rapidly quantify spatial vision in rodents (Prusky *et al.*, 2004) and is consistent with electrophysiology results (Thomas *et al.*, 2004). The optokinetic apparatus was custom-made and consisted of a stationary platform on which the animal was placed and where it could move freely (diameter 5 cm), surrounded by a drum (diameter 30.5 cm, height 61 cm). The inner surface of the drum was lined with alternating black and white vertical stripes covering the entire visual field. Two visual patterns with spatial frequencies of 0.13 cycle/degree and 0.26 cycle/degree were used. The Weber contrast of white and black stripes ($L_{max} - L_{min} / L_{min}$; L =luminance) was 7.55, as measured by a luminance meter (Minolta, LS-100, Japan). A video camera was mounted on a stand overlooking the platform (Olympus digital camera, C-3000, Japan). The drum was rotated at angular velocities ranging from 1 degree/sec to 60 degrees/sec either clockwise or anticlockwise using a motor (GM9413-4, Pittman, Harleysville, PA, USA,). Angular velocity of the drum was measured with a contact tachometer (High-Accuracy Digital Contact Tachometer, McMaster-Carr, Dayton, NJ, USA). Once a mouse was placed on the platform within the drum, the light was turned on and the drum was rotated clockwise or anticlockwise until head tracking was observed for a maximum of 30 sec. A movement of the head corresponding to the direction and speed of the optokinetic stimulus was defined as head tracking. Experimenters were blind to each animal's genotype, and all mice were tested on the same day by the same experimenters. The optokinetic stimulus was repeated 3 times in alternating directions. If a head tracking response was not observed, the stimulus was repeated 2 more times. The angular velocity of the drum was increased stepwise until a 50% response rate was achieved (Bonaventure *et al.*, 1983; Yücel *et al.*, 1990). Visual function was assessed by determining the optokinetic frequency at which head-tracking behaviour was extinguished. Frequency of Extinction (FE) was calculated by multiplying spatial frequency of the visual pattern with the specific angular velocity at which a mouse responded at chance level.

3.3.4 Spatial Memory

Behaviourally naïve TgCRND8 ($n=5$) and non-Tg ($n=5$) mice were tested at 8 weeks of age in the reference memory version of the Morris Water Maze test. The maze apparatus and testing procedure were described previously (Janus *et al.*, 2000). All mice underwent a day of non-spatial pre-training during which the mice learn that a submerged platform is present, how to climb onto the platform and to perform random swim search for the platform. The pre-training consisted of 4 trials, in each of which the mouse was released from a different quadrant and swam to a visible platform. This cued platform test was conducted to assess whether motoric or motivational factors might have confounded maze performance. One day following pre-training, mice underwent 5 days of place discrimination training with the platform hidden in the center of a single quadrant, over 4 trials per day. Following the last trial on the fifth day, the platform was removed and the mouse received a 60 sec probe trial. Mean latency to platform, swim path length and swim speed were measured with an on-line HSV video tracking system. An annulus-crossing index (number of passes over platform site, minus the mean of passes over sites in other quadrants) was calculated to determine the place preference during the probe trial.

3.3.5 Measurement of BDNF mRNA

TgCRND8 and non-Tg littermates were sacrificed at 6 weeks, 9 weeks and 6 – 8 months of age by decapitation several days following behavioural testing. Brains were removed and the hippocampus and cortex were dissected. Tissues were flash frozen in liquid nitrogen and stored at -80°C until analysis. RNA isolation, DNase treatment, reverse transcription and absolute quantitative real-time PCR for measurement of BDNF mRNA in frozen cortical and hippocampal samples were completed as previously described (Peng *et al.*, 2009). The forward and reverse primers used for total mouse BDNF mRNA were: 5'CAG CGG CAG ATA AAA AGA and 5'TCA GTT GGC CTT TGG ATA, product 87 bp. β -actin mRNA was used to normalize results. The forward and

reverse primers used for β -actin mRNA were: 5' CTG ACA GGA TGC AGA AGG and 5' GAG TAC TTG CGC TCA GGA, product 85 bp. Purified PCR products derived from use of these primers were used as standards for total BDNF and β -actin. Only experiments with an $R^2 > 0.995$ and PCR efficiency $> 90\%$ were used for analysis. All unknowns and controls were run in triplicate. A dissociation curve was created to verify that no secondary products had formed. Results were obtained as copies per ng total RNA and expressed as a ratio of BDNF/ β -actin mRNA.

3.3.6 Statistical Analysis

Object recognition and BDNF mRNA data were analyzed by unpaired Student's *t* tests. Morris water maze data were analyzed by 2-way analysis of variance (ANOVA) with genotype as between subject factor and test day as repeated measure factor. The Mann-Whitney *U* test was applied to the non-parametric FE optokinetic testing scores. A significance level (α) was set to 0.05, and the 2-tailed variants of all tests were used. Data are presented as means \pm standard error of the mean (SEM). All calculations were performed using GraphPad Prism version 4.0c for Macintosh (Mac OS X version by Software MacKiev™, GraphPad Software, Inc., San Diego, CA, USA).

3.4 Results

3.4.1 Progressive Object Recognition Deficits Precede Amyloid Plaque Accumulation

TgCRND8 and non-Tg mice were tested for object recognition memory with retention intervals of 5 min, 1-h or 3-h. We calculated a memory index, wherein a score of zero indicates no preference for novel or familiar objects. TgCRND8 mice exhibited progressive object memory deficits that could be discerned by 8 weeks of age (Figure 3-1). The performance of 4 – 6-week-old TgCRND8 mice was indistinguishable from that of non-Tg littermates in all delay interval versions of the task ($P>0.05$). Performance of 8-week-old TgCRND8 mice was impaired at the 5 min delay interval ($t(18)=2.96$, $P<0.01$), trended toward impairment at the 1-h delay interval ($t(18)=1.76$, $P=0.095$) and was profoundly impaired when assayed with a 3-h delay interval ($t(18)=5.92$, $P<0.001$). TgCRND8 mice with advanced plaque pathology (6 – 8 months of age) were impaired at delays of 5 min ($t(38)=4.78$, $P<0.001$), 1-h ($t(24)=4.37$, $P=0.001$) and 3-h ($t(25)=7.74$, $P<0.001$). Reductions in object recognition performance were not explained by differences between TgCRND8 and non-Tg animals in time spent exploring the initial object pairs (Figure 3-2A, $t(33)=0.07$, $P>0.05$). The sets of object pairs were previously demonstrated to be of matched saliency (Vaucher *et al.*, 2002), and we observed no group differences in object preference at any age during the retention phase (data not shown). Similarly, it is unlikely that our data can be explained by differences in visual function. Frequency of extinction (FE) scores of head-tracking behaviour in 9 week-old TgCRND8 mice were comparable to those of age-matched non-Tg controls (Figure 3-2B, $U=22.50$, $P>0.05$). Even at 6 – 8 months of age, TgCRND8 mice ($FE=4.55 \pm 0.56$) and littermate controls ($FE=5.67 \pm 0.41$) were indistinguishable by this task (Mann-Whitney $U=8.5$, $P=0.214$).

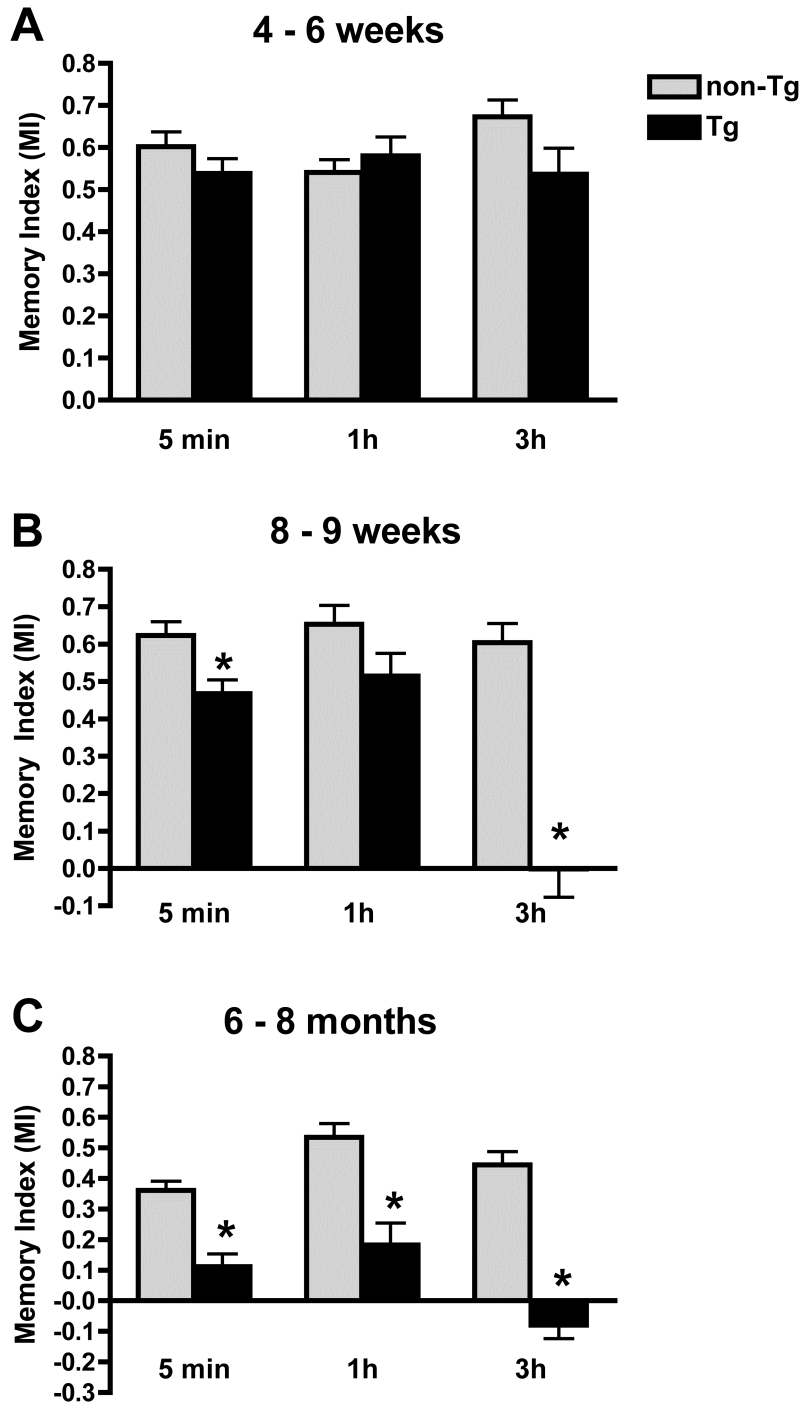


Figure 3-1. Object recognition memory assessed at pre-plaque and plaque ages. TgCRND8 mice exhibit no discernable memory impairment at 4 weeks (**A**), but a profound deficit in 3-h object recognition memory by 8 weeks (**B**). By 6 – 8 months of age, TgCRND8 are impaired at delays of 5 min, 1-h, and 3-h following initial exposure to objects (**C**). Values are means \pm SEM of memory index (MI) scores, with $n \geq 10$ for each genotype at each delay interval. * $P < 0.01$ by unpaired Student *t* test.

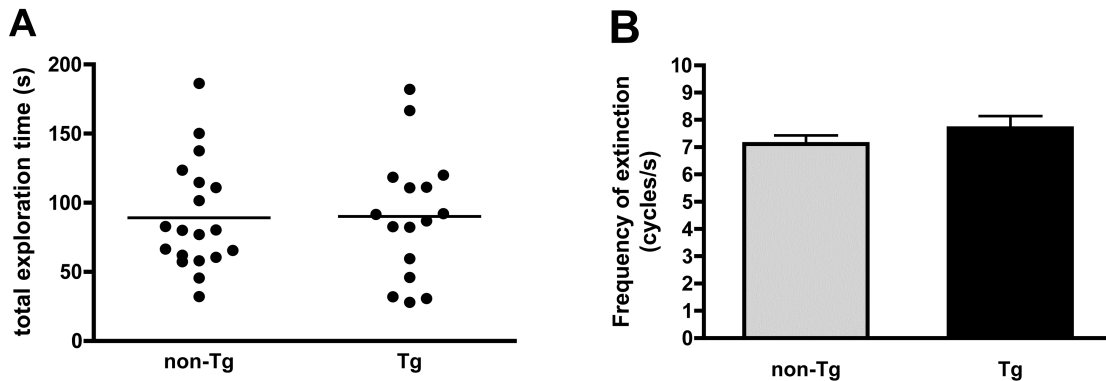


Figure 3-2. Exploration of objects and visual function examined in pre-plaque mice at 8 – 9 weeks of age. Time in seconds (s) spent exploring both left and right objects during the initial exposure period are compared (**A**). TgCRND8 mice ($n=16$) and non-Tg mice ($n=19$) did not differ in duration of object exploration ($P>0.05$, unpaired Student t test). Visual function was assessed by examination of head-tracking behaviour (**B**). Animals were placed on a stationary platform within a patterned surface drum. The speed of the drum rotation was varied stepwise. The maximal angular speed at which an optokinetic response was detected greater than 50% of the time was calculated (frequency of extinction; FE). The FE (cycle/second) was calculated by multiplying spatial frequency of the drum visual pattern with angular velocity. TgCRND8 mice ($n=7$) were compared to non-Tg mice ($n=10$) in their FE scores ($P>0.05$, Mann-Whitney U test). Values are means \pm SEM.

3.4.2 Pre-plaque TgCRND8 mice are NOT impaired in the *Morris Water Maze Task*

TgCRND8 mice were tested on the spatial reference memory version of the Morris water maze task at 8 weeks of age (Figure 3-3). Consistent with previous reports (Hyde *et al.*, 2005; Janus *et al.*, 2000), we did not detect any differences in swim path length ($F(1,9)=0.67$, $P>0.05$), escape latency ($F(1,9)=0.003$, $P>0.05$), or swim speed ($t(8)=1.44$, $P=0.187$ for data from day 2, by unpaired Student's t test) between pre-plaque TgCRND8 and control mice. Probe trial results were equivalent for TgCRND8 and non-Tg mice (data not shown).

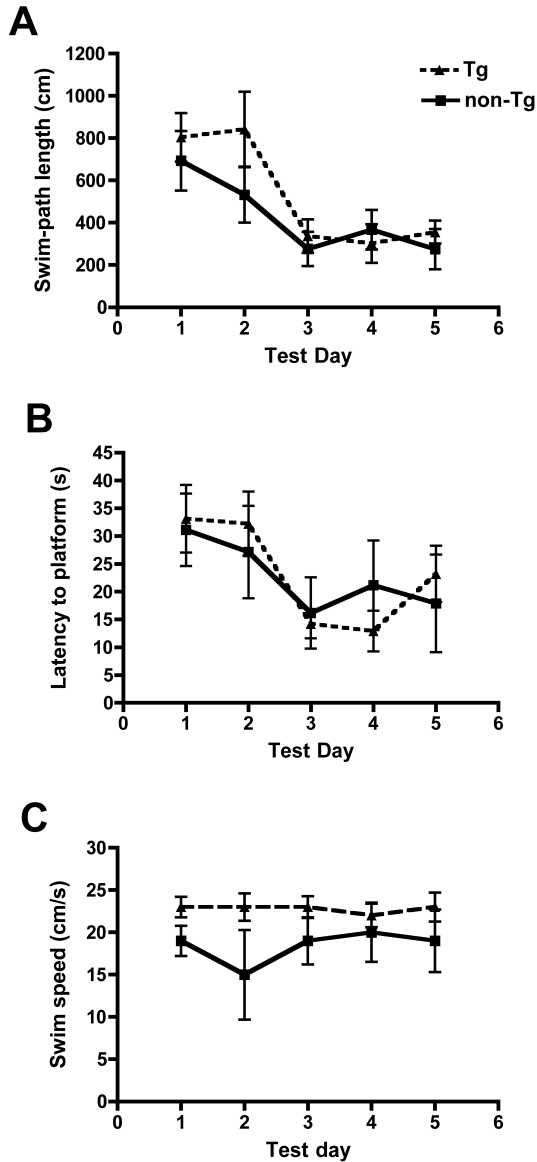


Figure 3-3. Spatial reference memory in the *Morris* water maze assessed in 8-week-old mice. TgCRND8 mice ($n=5$) were indistinguishable from non-Tg littermates ($n=5$) in terms of their swim-path length (**A**), escape latency (**B**), and swim-speed (**C**). Data are means \pm SEM of all trials performed on each test day and were evaluated by repeated measures ANOVA ($P>0.05$).

3.4.3 BDNF mRNA is Reduced in the Hippocampus and Frontal Cortex of Young TgCRND8 Mice

We measured total BDNF mRNA and β -actin mRNA by real-time quantitative RT-PCR in the hippocampus (Figure 3-4) and frontal cortex (Figure 3-5) of TgCRND8 mice. These brain regions exhibit extensive plaque pathology in mature TgCRND8 mice and are crucial for object recognition memory. Hippocampal and cortical mRNA levels for the housekeeping gene β -actin did not differ between TgCRND8 and non-Tg littermates and thus were used to normalize levels of BDNF mRNA. BDNF mRNA was significantly

reduced in the hippocampus ($t(7)=2.86$, $P<0.05$), but not in the cortex ($t(10)=0.90$, $P=0.40$) of 6-week-old TgCRND8 mice. By 9 weeks, BDNF mRNA levels were also reduced in the cortex of TgCRND8 mice ($t(15)=2.22$, $P<0.05$). Hippocampal BDNF mRNA levels did not differ between groups at 9 weeks of age ($t(14)=1.78$, $P>0.05$). However, in 6 – 8 month-old TgCRND8 samples, the downregulation of hippocampal BDNF mRNA was clearly evident ($t(14)=1.78$, $P<0.05$).

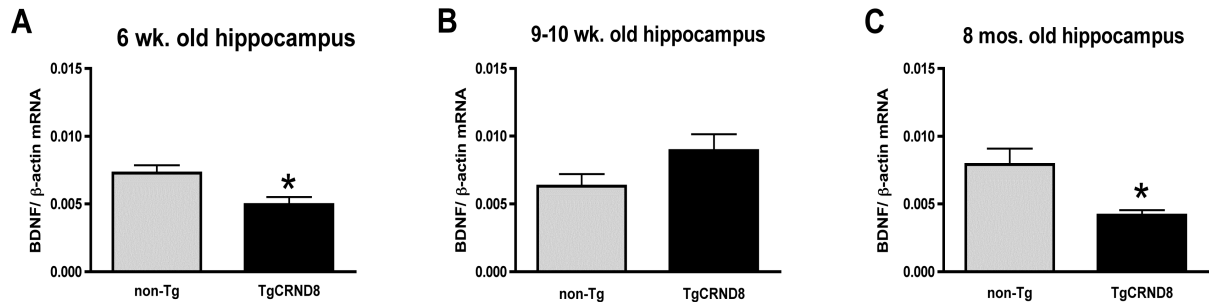


Figure 3-4. Hippocampal BDNF mRNA levels measured by absolute quantitative real-time reverse transcriptase polymerase chain reaction (RT-PCR). At 6 weeks of age, TgCRND8 mice ($n=5$) had reduced BDNF mRNA levels in the hippocampus compared with non-Tg mice ($n=4$) (A). However at 9 weeks, there was no significant difference between TgCRND8 mice ($n=7$) and non-Tg littermates ($n=9$) (B). By 6 – 8 months, hippocampal BDNF mRNA was reduced in TgCRND8 mice ($n=4$) in comparison with littermate controls ($n=4$) (C). Data are expressed as a ratio of copies of BDNF mRNA/copies of β -actin mRNA. Values are means \pm SEM. * $P<0.05$ by unpaired Student t test.

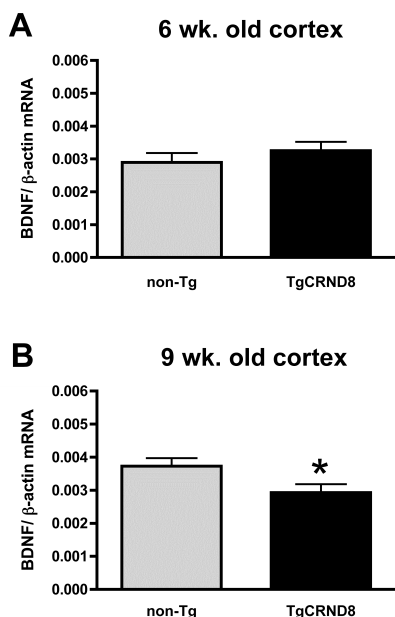


Figure 3-5. Cortical BDNF mRNA levels in pre-plaque mice. At 6 weeks of age, TgCRND8 mice ($n=6$) and non-Tg littermates ($n=6$) had equivalent levels of BDNF mRNA in the cortex (A). By 9 weeks of age, TgCRND8 mice ($n=7$) had reduced BDNF expression compared with non-Tg mice ($n=10$) (B). Data are expressed as a ratio of copies of BDNF mRNA/copies of β -actin mRNA. Values are means \pm SEM. * $P<0.05$ by unpaired Student t test.

3.5 Discussion

We have used an object recognition test of non-spatial, hippocampal and cortical short-term memory to determine when cognitive deficits first occur in TgCRND8 mice. We found that object memory deficits emerge several weeks prior to the appearance of macroscopic amyloid plaques in the brain. This is the earliest cognitive deficit reported in an APP-transgenic mouse. The onset of object recognition impairment coincides with reductions in BDNF mRNA in the hippocampus and cortex of pre-plaque TgCRND8 mice.

Uncovering subtle phenotypes well before widespread neurodegeneration has occurred is crucial for early diagnosis and treatment. Performance in the object recognition test is dependent on brain regions first targeted by β -amyloid and thus provides a sensitive measure of early cognitive disruption (Dodart *et al.*, 2002; Sipos *et al.*, 2007). Ennaceur and Delacour developed a spontaneous object recognition task for rats in 1988. Since then it has been successfully modified for use in the mouse (reviewed in Sik *et al.*, 2003). Various object recognition paradigms may be used to investigate slightly different aspects of memory (Dodart *et al.*, 1997; Capsoni *et al.*, 2000; Chopin *et al.*, 2002; Hammond *et al.*, 2004; Winters *et al.*, 2004; Broadbent *et al.*, 2004; Dere *et al.*, 2007; Heldt *et al.*, 2007; Benice and Raber, 2008; Yuede *et al.*, 2009).

The one-trial, non-spatial test that we used is based on the rodent's innate preference for novelty. Performance of the task is not associated with positive or negative reinforcement. We also undertook measures to assess the potential confounding influence of contextual, motor or visual factors. Mice were habituated to the testing arena so as to reduce stress and novelty associated with the testing environment. The location of a novel object within the testing box was always identical to that of the replaced object.

We observed no difference between TgCRND8 mice and non-Tg controls in the duration of object exploration, and TgCRND8 mice did not differ from non-Tg littermates

in swim speed. Thus, it does not appear that memory deficits were confounded by differences in motor ability. Similarly, visual dysfunction was not a factor, as TgCRND8 performance was equivalent to that of non-Tg littermates in optokinetic testing. We conclude that the object recognition deficit of TgCRND8 mice can be ascribed to impaired memory.

The disruption of object recognition over short (5 min) and long (3-h) retention intervals suggests that both cortical and hippocampal structures are functionally disrupted early in the disease process. Steckler and coworkers (1998) described two neural networks for recognition memory in the rodent: one for spatial memory is encoded by the hippocampus and one for non-spatial memory involves the rhinal cortex and cortical association areas. Whether the hippocampus is truly irrelevant for non-spatial object memory has been questioned (Dere *et al.*, 2007). When short delay intervals (<15 min) are used, entorhinal, perirhinal and frontal cortices are sufficient for object recognition. With longer retention intervals, the hippocampus is recruited (Hammond *et al.*, 2004). Baker and Kim (2002) blocked LTP with a *N*-methyl-*D*-aspartate receptor antagonist in the dorsal hippocampus of rats. They reported a selective impairment of object memory when tested with a 3-h delay but not with a 5 min delay.

Although the profound deficit we observed in mice tested with a 3-h delay underscores functional impairment of hippocampus in pre-plaque TgCRND8 mice, the water maze spatial reference memory of these mice was normal. The hippocampus is important for both spatial and non-spatial recognition memory, but the two tasks may differ in the degree of integrated hippocampal function required. Hippocampal lesion studies in rats have shown that more hippocampal tissue is involved in spatial memory performance than in non-spatial recognition memory (Broadbent *et al.*, 2004). Conversely, object recognition is more sensitive to disruption of the entorhinal-hippocampal circuitry (Burwell *et al.*, 2004; Parron *et al.*, 2006). The entorhinal cortex relays processed information from the surrounding neocortex to the dentate gyrus of the hippocampus via the medial perforant pathway. Damage to this circuitry is a specific and reliable distinguishing factor between healthy aged subjects and mild/early stage AD (Chetelat and Baron, 2003; Gunten *et al.*, 2006). As A β deposition is first noted in cortical and

hippocampal structures of TgCRND8 mice, the object recognition task is an especially relevant and efficient method for assessing early cognitive changes in TgCRND8 mice.

Downregulation of BDNF expression may be a factor linking A β exposure with cognitive impairment. Site-specific deletion of the BDNF gene in dorsal hippocampus of adult mice can result in object recognition deficits (Heldt *et al.*, 2007). Moreover, BDNF delivery to the entorhinal cortex has been shown to both mitigate degeneration in the entorhinal cortex and hippocampus, and to rescue learning and memory impairments in rodent and primate models of AD (Nagahara *et al.*, 2009). *In vitro* studies have confirmed the deleterious influence of soluble A β on BDNF expression and signaling (Tong *et al.*, 2004; Garzon and Fahnstock, 2007). Moreover, we previously reported that aged, plaque-bearing TgCRND8 mice exhibit very high levels of the more fibrillogenic A β_{42} relative to A β_{40} and that the relative increase in A β_{42} was inversely correlated with BDNF mRNA in the cortex (Peng *et al.*, 2009).

We now report that BDNF is altered at earlier stages of TgCRND8 dysfunction. From 4 to 8 weeks of age tissue levels of A β_{42} double in TgCRND8 mice, and the A β_{42} /A β_{40} ratio increases 1.5-fold (Chishti *et al.*, 2001). Over the same timeframe, we observed decreased BDNF mRNA in the hippocampus and cortex. Decreases were evident at 6 weeks in the hippocampus and by 9 weeks in the cortex of pre-plaque mice. A slight, non-significant increase in hippocampal BDNF mRNA was observed in TgCRND8 mice at 9 weeks. However, BDNF mRNA subsequently decreased again and low levels were observed at 6 – 8 months.

Such phasic fluctuations in BDNF may occur in response to progression through stages of amyloid pathology. Sub-lethal concentrations of soluble oligomeric A β functionally disrupt neurons, causing suppression of cAMP-response element-binding protein (CREB) phosphorylation and downstream BDNF expression (Tong *et al.*, 2001, Garzon and Fahnstock, 2007). Decreases in BDNF at 6 weeks in the hippocampus and at 9 weeks in the cortex of TgCRND8 mice are consistent with the onset of A β -induced dysfunction in brain regions crucial for object recognition. However, this acute reduction

in BDNF mRNA may be short-lived. Tissue levels of CREB and BDNF mRNA may rebound in response to a moderate load of intracellular A β (Arvanitis *et al.*, 2007). In support of this notion, BDNF mRNA was found to be upregulated in glial cells surrounding plaques in APP23 transgenic mice (Burbach *et al.*, 2004). This increase may reflect a compensatory neuroprotective response after CNS injury (Lindvall *et al.*, 1992). Human studies also indicate increased BDNF expression during early stages of Alzheimer's disease and a decline as disease progresses (Laske *et al.*, 2006). It has been suggested that continuing exposure to increasing levels of central nervous system A β leads to the neuropathology and decreased neuronal BDNF expression (Burbach *et al.*, 2004; Arvanitis *et al.*, 2007). In the TgCRND8 mouse, the second phasic decrease of BDNF mRNA that we observed at 6 – 8 months coincides with significant cholinergic cell loss (Bellucci *et al.*, 2006).

In summary, the TgCRND8 mouse recapitulates early and relevant cognitive symptoms of Alzheimer's disease. Object recognition deficits in TgCRND8 mice precede plaque accumulation and coincide with a 2-fold increase in A β_{42} levels. The early alterations in BDNF mRNA seen in pre-plaque TgCRND8 mice suggest that dysregulation of BDNF expression contributes to A β -induced cognitive impairment.

Chapter 4 Reduced Tissue Levels of Noradrenaline are Associated with Behavioral Phenotypes of the TgCRND8 Mouse Model of Alzheimer's Disease

This chapter has been published:

Francis BM, Yang J, Hajderi E, Brown ME, Michalski B, McLaurin J, Fahnstock M, Mount HTJ (2012). Reduced tissue levels of noradrenaline are associated with behavioural phenotypes of the TgCRND8 mouse model of Alzheimer's disease. *Neuropsychopharmacology* **37**: 1934-1944.

4.1 Abstract

Noradrenergic cell loss is well documented in Alzheimer's disease (AD). We have measured the tissue levels of catecholamines in an amyloid precursor protein-transgenic 'TgCRND8' mouse model of AD and found reductions in noradrenaline within hippocampus, temporoparietal and frontal cortices and cerebellum. An age-related increase in cortical noradrenaline levels was observed in non-Tg controls, but not in TgCRND8 mice. In contrast, noradrenaline levels declined with aging in the TgCRND8 hippocampus. Dopamine levels were unaffected. Reductions in tissue content of noradrenaline were found to coincide with altered expression of brain-derived neurotrophic factor (BDNF) mRNA and to precede the onset of object memory impairment and behavioral despair. To test whether these phenotypes might be associated with diminished noradrenaline, we treated mice with dexefaroxan, an antagonist of presynaptic inhibitory α_2 -adrenoceptors on noradrenergic and cholinergic terminals. Mice 12 weeks of age were infused systemically for 28 days with dexefaroxan or rivastigmine, a cholinesterase inhibitor. Both dexefaroxan and rivastigmine improved TgCRND8 behavioral phenotypes and increased BDNF mRNA expression without affecting amyloid- β peptide levels. Our results highlight the importance of noradrenergic depletion in AD-like phenotypes of TgCRND8 mice.

4.2 Introduction

The temporal neocortex, entorhinal cortex and hippocampus are the earliest sites of amyloid- β (A β) deposition and the first to become functionally disrupted in the Alzheimer's disease (AD) brain (Braak and Braak, 1991; DeToledo-Morrell *et al.*, 1997; Thal *et al.*, 2000, 2002; Braak and Del Tredici, 2004; Stoub *et al.*, 2010). Subcortical neurons that project to these areas are especially vulnerable to A β toxicity (Gonzalo-Ruiz *et al.*, 2003). Degeneration of basal forebrain cholinergic neurons in AD was initially described in 1976 (Davies and Maloney, 1976), and the corresponding role of these neurons in the pathology and behavioral presentation of the disease has been well documented (Coyle *et al.*, 1983; Francis *et al.*, 1999). Less well appreciated has been the profound loss of noradrenergic innervation from the locus coeruleus (Zarow *et al.*, 2003). Forno (1966) was first to report severely reduced cell counts in the locus coeruleus of AD patients. Subsequent studies revealed more than 60% loss of noradrenergic cells (Mann *et al.*, 1982; Bondareff *et al.*, 1982; German *et al.*, 1992) and depleted tissue levels of noradrenaline in cortical and limbic terminal fields (Adolfsson *et al.*, 1979; Palmer *et al.*, 1987a,b; Matthews *et al.*, 2002). The extent of noradrenergic degeneration was found to correlate with the tissue load of amyloid plaques and neurofibrillary tangles, as well as with the severity of dementia (Bondareff *et al.*, 1987; Grudzien *et al.*, 2007).

The locus coeruleus projects widely in the brain and is the sole source of noradrenaline in the neocortex and hippocampus (Foote *et al.*, 1983). The loss of cortical noradrenergic innervation and its influence on basalocortical cholinergic neurons may contribute to behavioral symptoms of AD including depression and memory impairment (reviewed by Marien *et al.*, 2004). In rats treated with scopolamine to block cholinergic function, enhancing noradrenaline release facilitated memory retention (Chopin *et al.*, 2002), whereas ablating the locus coeruleus exacerbated working memory deficits (Ohno *et al.*, 1997). Non-selectively targeting the locus coeruleus of human amyloid precursor protein (APP) mice with the neurotoxin *N*-(2-chloroethyl)-*N*-ethyl-2-bromobenzylamine (DSP-4) potentiated amyloid pathology, glial inflammation, neuronal

loss and cognitive impairment (Heneka *et al.*, 2006; Kalinin *et al.*, 2007; Jardanhazi-Kurutz *et al.*, 2010, 2011). Collectively, these data point to a likely role for noradrenergic dysfunction in the pathogenesis of AD and an interaction with the basal forebrain cholinergic system.

We investigated if and when noradrenergic deficits might spontaneously occur in the TgCRND8 (Janus *et al.*, 2000; Chishti *et al.*, 2001) APP-transgenic mouse. These mice exhibit deficits in memory and BDNF mRNA as early as 2 months (Francis *et al.*, 2012a), significant plaque loads within hippocampus and cortex by 3 months (Chishti *et al.*, 2001) and cholinergic dysfunction by 7 months of age (Bellucci *et al.*, 2006). We now report that reductions in tissue noradrenaline precede the appearance of plaques and cholinergic dysfunction and strongly contribute to behavioral phenotypes and decreased BDNF expression.

4.3 Materials and Methods

4.3.1 Transgenic Mice

TgCRND8 mice express a double mutant (Swedish: KM670/671NL plus Indiana: V717F) human APP₆₉₅ transgene under control of the pan-neuronal Syrian hamster prion gene promoter. Transgenic mice were maintained on a hybrid C57BL/6/C3H background and were backcrossed with C57BL/6 wild-type mice. Mice were housed in groups of 2 to 4 on a 12-h light-dark cycle. Food and water were available *ad libitum*. All tests were in accordance with the Canadian Council on Animal Care guidelines and were approved by the Animal Care Committee at the University of Toronto.

4.3.2 Brain Fixation and Microdissection

TgCRND8 and non-transgenic (non-Tg) littermates ($n \geq 8$ per group) were sacrificed at 4 – 5, 7 – 9 or 40 – 50 weeks of age with a brief (0.8 – 1.2 sec) head-focused pulse of microwave radiation (8 kW, 60 Hz, 56 Amp) delivered by a 10 kW Muromachi rodent brain fixation system (model TMW-4012C, Muromachi Kikai Co. Ltd., Tokyo, Japan). This procedure rapidly heat-inactivates enzymes, thereby preserving levels of labile biogenic amines at concentrations that existed *ante-mortem* (Moroji *et al.*, 1978; Wood & Altar, 1988; Mount *et al.*, 2004). The microwaved frontal, parietal and occipital cortices, anterior and posterior brainstem, hippocampus, ventral midbrain, striatum and cerebellum were dissected on ice (Figure 4-1) and stored at -80°C until analysis.

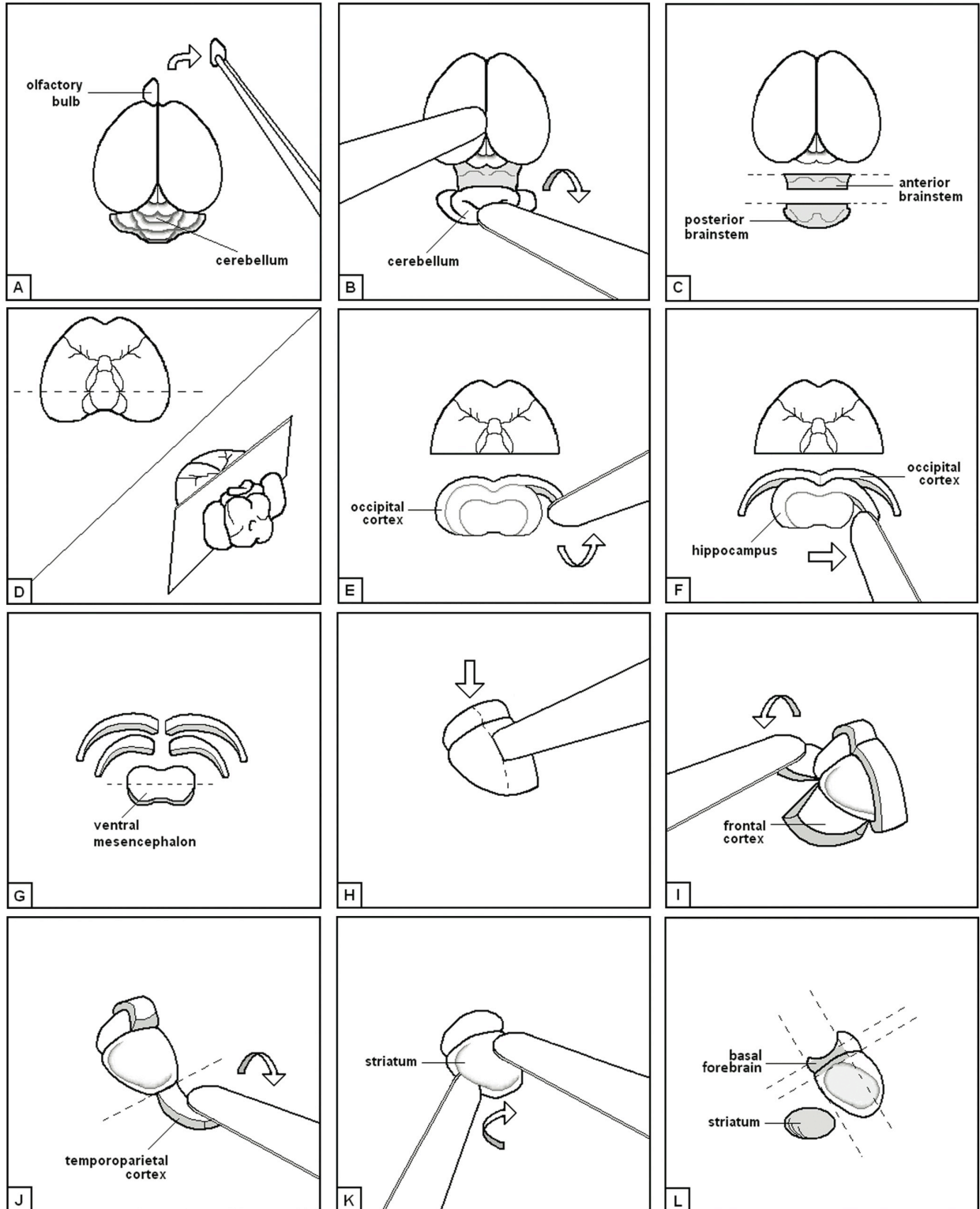


Figure 4-1. Dissection of a microwave-fixed brain is performed so as to allow for the crumbly nature of the cooked tissue. The olfactory bulbs are pinched off with forceps (A). The cerebellum is rolled away from the brain with a spatula (B). A razor is used to cut the underlying brainstem piece evenly into anterior and posterior regions

(C). The brain is flipped to expose its ventral surface, and a cut is made 1/3 the length of the remaining tissue **(D)**. The cut slice is laid flat with the anterior aspect facing up, and the outermost cortical layer is peeled away from both hemispheres, as the occipital cortex piece **(E)**. The lighter subcortical layer is removed from both hemispheres as the hippocampal sample **(F)**. Remaining tissue is cut horizontally, and the anterior piece discarded. The posterior portion, containing the substantia nigra/ventral tegmental area, is taken as the ventral mesencephalon **(G)**. A superficial cut is made horizontally with a spatula **(H)**, so as to obtain the frontal cortex **(I)** and the temporoparietal cortex **(J)**. The cortical pieces are pulled away from underlying subcortical structures to reveal the striatum, which is readily separated from the remaining tissue **(K)**. Finally, 2 horizontal and 2 vertical cuts are made to retrieve the basal forebrain **(L)**.

4.3.3 Tissue Catecholamines

Levels of dopamine, dihydrophenylacetic acid, homovanillic acid, 3-methoxytyramine, and noradrenaline were measured by HPLC, as previously described (Mount *et al.*, 2004). Regional cooked tissues were homogenized in 1 ml ice-cold 0.1 N perchloric acid. Homogenates were centrifuged at 10 000 *g* for 20 min at 4°C. The supernatants were filtered through 0.2 µm porosity membrane (PALL Corporation, Ann Arbor, MI, USA) and stored in aliquots of 50 µl at – 80°C. Equipment for isocratic reverse-phase chromatographic measurements was from Dionex and was operated with the Chromeleon® Chromatography Data Management System, version 6.8 (DIONEX Co., Sunnyvale, CA, USA). Chemicals for standards and mobile phase solutions were purchased from Sigma-Aldrich (St. Louis, MO, USA). The chromatographic conditions consisted of a C18 reverse-phase column (Acclaim® 120, 150 x 4.0 mm, 5 µm particle size) maintained at 30°C (UltiMate® 3000 Thermostatted Column Compartment). The mobile phase was sodium acetate (100 mM), tetrasodium EDTA (0.125 mM), 1-octane sulfonic acid (432 mg/L) and 5% methanol (pH 3.6) and was delivered at a flow rate of 0.75 ml/min with an UltiMate® 3000 pump. 25 µl of each sample and 20 µl of each standard were injected automatically using a refrigerated UltiMate® 3000 autosampler. The electrochemical detector (ESA Coulochem® III, 5011A analytical cell plus 5020 guard cell) was operated at a working electrode potential of – 400 mV.

4.3.4 Tail Suspension Test

Gender balanced groups of 4-, 8- and 27-week-old TgCRND8 and non-Tg mice ($n \geq 8$ per group) were tested with the tail suspension test. Mice were suspended for 6 min by affixing masking tape to the end of their tails and attaching the tape to a clamp on a ring stand. Latency to immobility and duration of immobility were scored with ODlog™ event recording software (Macropod Software, Armidale, Australia). To test how altered tissue noradrenaline levels affect measured endpoints, separate groups of experimentally naïve 30-week-old mice ($n \geq 6$) were administered the noradrenaline uptake inhibitor, desipramine (16 mg/kg, i.p.; Sigma-Aldrich Canada Ltd., Oakville, Canada), or saline 30 min prior to testing.

4.3.5 Assessing Forelimb Coordination with the Tape Removal Task

Forelimb coordination was assessed in 15-week-old TgCRND8 ($n = 12$) and non-Tg littermates ($n = 11$) with the adhesive tape removal task. This test assesses forelimb use by inducing a grooming response. It is sensitive to subtle dysfunction of the nigrostriatal dopaminergic system (Schallert *et al.*, 1982; Chen *et al.*, 2005). A round half-inch red Avery® adhesive label (Avery Dennison Canada Inc., Pickering, ON, Canada) was affixed to the forehead of the mouse. The mouse was then placed in an empty home cage and observed for up to 5 min. Time taken for an animal to remove the label was recorded as an index of forelimb coordination.

4.3.6 Drug Treatments, Behavioural Testing and Tissue Processing

We investigated effects of 28-day infusion of dexefaroxan (1.9 mg/kg/day), rivastigmine (0.48 mg/kg/day) or saline on TgCRND8 behavioral phenotypes. Dexefaroxan hydrochloride (2-[2-(2-ethyl-2,3-dihydrobenzofuranyl)]-2-imidazoline) was synthesized at

Pierre Fabre Medicament (Castres, France) and rivastigmine tartrate (Exelon[®]) was obtained from Novartis Pharma AG (Basel, Switzerland). Drugs were administered via Alzet[®] (DURECT Corporation, Cupertino, CA, USA) osmotic mini-pumps (model 1002) implanted subcutaneously in the mid-scapular region. In all, 120 mice (6 gender balanced groups of 20 mice) were fitted with pumps at 12 weeks of age and were treated chronically for 28 days. Pumps delivered 100 μ l of solution at a rate of 0.25 μ l/h for 2 weeks. Primed pumps were soaked overnight in saline at 37°C before implantation. During surgery, mice were anaesthetized via isoflurane inhalation. A second surgery was performed on treatment day 14 to replace the depleted pump. Habituation for object recognition testing began the day after the second pump was implanted (third week of chronic treatment). Habituation involved handling mice and exposing them to an empty home cage for 15 min per day over 3 days. This regimen ensured that experimentally naïve mice received 2 weeks of continuous drug treatment prior to assessment and were sufficiently habituated for measures of behavior. The object recognition test was conducted on treatment day 19, as described previously (Francis *et al.*, 2012a). Each mouse was exposed for 10 min to a LEGO[®] construct (LEGO Group, Billund, Denmark) and a Hot Wheels[®] car (Mattel Inc., El Segundo, CA, USA). Three hours later, mice were re-exposed for 5 min to 1 object from the original test pair and to a novel object. The memory index (MI) was calculated as $MI = (t_n - t_f) / (t_n + t_f)$, wherein 't_n' represents time exploring a novel object and 't_f' the duration of familiar object exploration. On the following day, we assessed behavioral despair in the tail suspension task. At the end of the drug treatment, 16-week-old mice were anaesthetized with an overdose of sodium pentobarbital (60 mg/kg) and perfused transcardially with ice-cold phosphate-buffered saline (0.1 M PBS, pH 7.4). The hippocampus and cortex were dissected, snap frozen and stored at -80°C for A β analyses and BDNF mRNA measurements. Separate cohorts of drug treated mice (n \geq 8 mice per group) were sacrificed at 16-weeks of age by microwave irradiation for the determination of noradrenaline and normetanephrine tissue content in the hippocampus.

4.3.7 A β Immunoassays

The concentration of aggregated A β in the cortex of drug treated mice ($n=7$ per group) was measured using the Amorfix A⁴ assay (Amorfix, Mississauga, Canada) as previously described (Tanghe *et al.*, 2010). Tissues were homogenized (10% w/v) in 2% (v/v) nonyl phenoxy polyethoxy ethanol (NP-40) in PBS containing 1 mM phenylmethylsulfonyl fluoride and protease inhibitor cocktail (Complete Mini, Roche, Quebec, Canada). Homogenates were centrifuged at 845 *g* for 30 sec and the supernatant was aliquotted. One aliquot was further diluted to a 1/10 000 concentration to provide a signal within the linear range of the immunoassay. Using the A⁴ proprietary enrichment protocol (Amorfix, Mississauga, Canada), only aggregated species of A β were isolated from the sample. The eluate was then disaggregated to quantify A β in its monomeric form using the Amorfix dual-bead based immunoassay using europium-fluorescent beads coupled to the N-terminal 4G10 antibody and magnetic beads coupled to 1F8 and 2H12 C-terminal antibodies recognizing A β ₄₀ and A β ₄₂, respectively. The europium-fluorescent intensity was measured using time-resolved fluorescence on triplicate samples and is directly proportional to the concentration of A β in the tissue. To measure levels of monomeric A β in the cortical samples, another aliquot of the homogenate was diluted (1/500) and loaded directly into the Amorfix immunoassay, without the A⁴ enrichment or disaggregation steps. Separate immunoassays were performed to detect monomeric A β ₄₀ and A β ₄₂. The detection limit of the immunoassay was 50 fg/well.

4.3.8 Western Blotting

Aliquots of cortical tissue homogenates used in the A β immunoassays were spun at 3000 rpm for 10 min at 4°C and the protein concentration of supernatants were determined. In all, 20 μ g of protein was prepared in sample buffer, boiled for 5 min, separated by gel electrophoresis on 10-20% Tricine gels (Invitrogen, Burlington,

Canada) and transferred to nitrocellulose membranes. Membranes were boiled in Tris-buffered saline (TBS), blocked for an hour in 8% non-fat milk powder in TBS-Tween (0.2%) at room temperature and incubated overnight at 4°C with A β ₁₋₁₆ monoclonal antibody 6E10 (1:1000; SIG-39320, Covance Inc., Montreal, Canada). After 1-h incubation with goat anti-mouse horseradish-peroxidase conjugated secondary antibody (1:5000, Thermo Scientific Pierce, Rockford, IL, USA), membranes were developed using enhanced chemiluminescence (Amersham™ ECL™ Western blotting analysis system, GE Healthcare, Quebec, Canada) and exposed to film. Blots were stripped and reprobed with anti-glyceraldehyde-3-phosphate dehydrogenase (GAPDH) antibody (1:7500; Meridian Life Sciences, Brockville, Canada). Densitometry was quantified for 3 separate blots with ImageJ 1.44V software (National Institutes of Health). Data were normalized to the corresponding expression level of GAPDH in each sample.

4.3.9 Measurement of BDNF mRNA

Ribonucleic acid (RNA) isolation, reverse transcription and absolute quantitative real-time polymerase chain reaction (RT-PCR) for measurement of BDNF mRNA in hippocampal tissues from 16-week-old drug treated mice ($n \geq 6$ per group) were performed as previously described, with minor changes (Peng *et al.*, 2009). Hippocampal BDNF mRNA was also measured in an older cohort (45 – 50 weeks old) of mice chronically infused with dexefaroxan or rivastigmine for 4 weeks. RNA extraction was performed using Trizol (Invitrogen) and RNeasy spin columns (Qiagen Inc., Toronto). DNase treatment was done on columns as per the Qiagen protocol. RNA integrity was verified by agarose gel electrophoresis. For reverse transcription, Invitrogen's protocol and reagents for Superscript III were used. The forward and reverse PCR primers used for mouse BDNF mRNA were: 5' GCG GCA GAT AAA AAG ACT GC and 5' CTT ATG AAT CGC CAG CCA AT, product 248 bp. Results were normalized to β -actin mRNA. The forward and reverse primers used for β -actin mRNA were: 5' AGC CAT GTA CGT AGC CAT CC and 5' CTC TCA GCT GTG GTG GTG AA, product 228 bp. Purified PCR products derived from use of these primers were used as

standards for BDNF and β -actin. The following thermal profile was used for PCR: 2 min at 50°C, 2 min at 95°C followed by 40 cycles of 95°C for 30 sec, 58°C for 30 sec, and 72°C for 45 sec. Unknowns, standard curve and controls were run in triplicate using SYBR Green. Only experiments with an $R^2 > 0.995$ and PCR efficiency $> 90\%$ were used in the analysis. A dissociation curve verified that no secondary products had formed.

4.3.10 Statistical Analysis

Data were evaluated by unpaired Student's *t* tests. Multiple comparisons were analyzed by a non-repeated measures 2-way analysis of variance (ANOVA). When ANOVAs yielded significant main effects of genotype and/or treatment, pairwise comparisons were evaluated by Fisher's protected least significant difference (LSD) test. Differences were significant at $P < 0.05$.

4.4 Results

4.4.1 TgCRND8 Mice Exhibit Early Reductions in Noradrenaline Content Within Major Terminal Fields

Tissue levels of noradrenaline, dopamine and their metabolites were measured across brain regions of 4 – 5, 7 – 9 and 40 – 50 week-old TgCRND8 and non-Tg littermate mice and data were analyzed by the 2-tailed Student's *t* test for independent samples. We observed an early and reliable pattern of reduced noradrenaline in the frontal and temporoparietal cortices, hippocampus and cerebellum (Figure 4-2). Neither dopamine, nor its metabolites were consistently altered (Table 4-1). With aging, noradrenaline reductions in the TgCRND8 mice worsened in hippocampus, but remained stable in cortical regions. In contrast, aging control mice exhibited increased noradrenaline levels in the temporoparietal and frontal cortices. Levels of noradrenaline in the ventral mesencephalon, striatum and brainstem were unaffected, suggesting that rostral, cortically-projecting noradrenergic cells of the locus coeruleus are the most severely disrupted in this mouse model of AD.

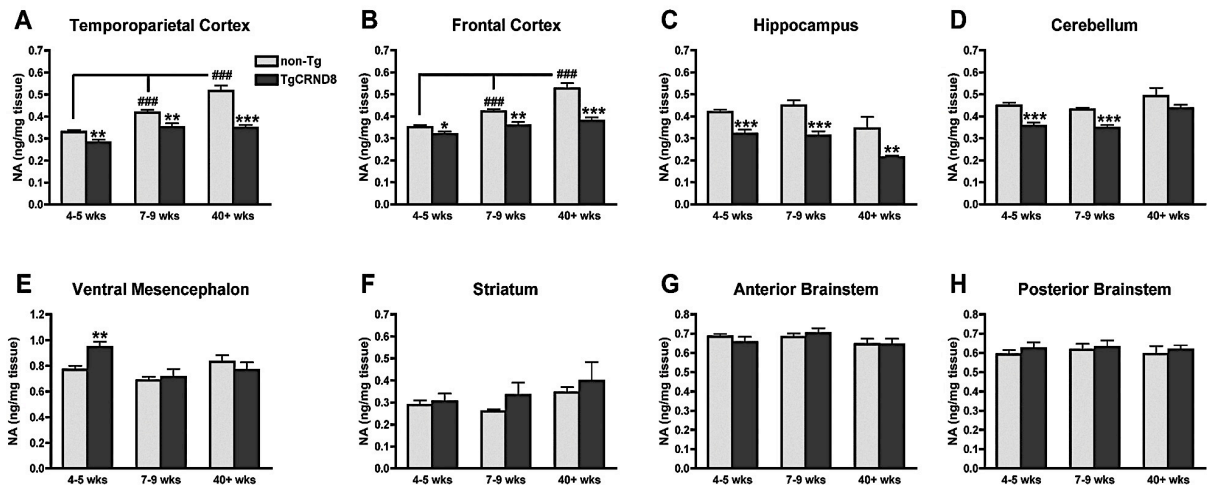


Figure 4-2. Tissue levels of noradrenaline (NA) are reduced in major terminal fields of the TgCRND8 brain. Reductions in tissue NA were observed in temporoparietal cortex (A), frontal cortex (B), hippocampus (C) and cerebellum (D). No reductions were observed within ventral mesencephalon (E), striatum (F), or anterior (G)

and posterior brainstem (**H**) regions. * $P < 0.05$, ** $P < 0.01$ and *** $P < 0.001$ versus non-Tg mice by 2-way ANOVA followed by Fisher's protected LSD test. Non-Tg mice exhibited NA tissue levels in the temporoparietal and frontal cortices that increased with aging. ### $P \leq 0.001$ versus 4 – 5 week old non-Tg mice by 2-way ANOVA followed by Fisher's protected LSD test. Values are means of NA tissue content (ng/mg tissue) \pm SEM of $n \geq 8$ mice per group.

Table 4-1. Tissue levels of dopamine and metabolites in the TgCRND8 brain.

		4-5 weeks				7-9 weeks				40+ weeks			
		DA	DOPAC	HVA	3-MT	DA	DOPAC	HVA	3-MT	DA	DOPAC	HVA	3-MT
Frontal cortex	non-Tg	602.7 \pm 76.5	83.5 \pm 12.9	189.9 \pm 7.3	ND	702.3 \pm 46.6	99.3 \pm 6.4	270.4 \pm 17.2	ND	1256.0 \pm 135.3	114.0 \pm 10.5	367.2 \pm 25.1	ND
	Tg	634.8 \pm 43.6	94.3 \pm 12.9	195.9 \pm 22.3	ND	737.0 \pm 76.7	110.5 \pm 13.8	257.0 \pm 10.5	ND	1268.0 \pm 146.5	119.1 \pm 15.2	440.3 \pm 33.3	ND
Parietal cortex	non-Tg	204.2 \pm 51.0	27.8 \pm 8.6	73.3 \pm 12.9	ND	464.0 \pm 34.7	53.2 \pm 4.1	165.2 \pm 10.7	ND	377.5 \pm 24.2	57.7 \pm 2.9	186.9 \pm 13.2	ND
	Tg	200.2 \pm 29.7	33.5 \pm 9.2	77.6 \pm 12.9	ND	481.6 \pm 59.1	65.1 \pm 6.4	194.6 \pm 16.2	ND	519.8 \pm 94.6	42.6 \pm 10.7	219.1 \pm 31.3	ND
Hippocampus	non-Tg	44.9 \pm 6.9	12.2 \pm 3.9	28.6 \pm 2.1	ND	51.7 \pm 7.0	12.3 \pm 1.9	48.9 \pm 6.5	ND	52.1 \pm 4.2	ND	92.2 \pm 15.3	ND
	Tg	63.4 \pm 11.9	17.7 \pm 7.0	36.6 \pm 3.9	ND	64.5 \pm 10.8	10.4 \pm 2.3	48.5 \pm 6.0	ND	42.4 \pm 3.6	ND	91.4 \pm 6.5	ND
Striatum	non-Tg	3555.3 \pm 169.0	368.0 \pm 21.6	747.0 \pm 39.4	59.1 \pm 3.3	4947.9 \pm 198.4	472.7 \pm 16.1	1063.4 \pm 29.9	77.2 \pm 3.2	6295.5 \pm 512.1	504.5 \pm 22.0	1758.0 \pm 87.3	115.9 \pm 8.0
	Tg	3887.8 \pm 109.0	441.4 \pm 23.7 *	847.6 \pm 30.8	63.9 \pm 8.9	5030.2 \pm 310.0	543.3 \pm 65.0	993.0 \pm 32.2	103.2 \pm 26.5	5893.4 \pm 688.2	513.5 \pm 58.6	2009.0 \pm 102.2	105.7 \pm 25.4
Cerebellum	non-Tg	15.4 \pm 3.3	5.2 \pm 0.7	17.9 \pm 1.5	ND	13.3 \pm 0.9	7.6 \pm 1.9	19.1 \pm 1.4	ND	ND	ND	ND	ND
	Tg	16.3 \pm 2.0	5.8 \pm 0.9	14.4 \pm 1.7	ND	12.3 \pm 1.3	6.9 \pm 1.9	17.2 \pm 1.2	ND	ND	ND	ND	ND
Ventral Mesencephalon	non-Tg	236.2 \pm 22.1	92.1 \pm 8.3	130.2 \pm 7.5	ND	235.4 \pm 25.9	100.9 \pm 12.1	141.2 \pm 13.9	ND	257.0 \pm 14.7	116.5 \pm 15.9	255.9 \pm 27.7	ND
	Tg	276.6 \pm 28.7	96.8 \pm 8.8	127.5 \pm 10.4	ND	296.7 \pm 45.9	103.6 \pm 13.7	161.4 \pm 21.5	ND	304.8 \pm 20.9	132.8 \pm 9.1	258.0 \pm 16.8	ND
Anterior Brainstem	non-Tg	28.4 \pm 1.8	22.5 \pm 2.0	35.2 \pm 2.0	ND	31.2 \pm 2.9	32.1 \pm 5.0	38.3 \pm 4.2	ND	34.5 \pm 1.9	ND	68.3 \pm 3.5	ND
	Tg	34.6 \pm 4.0	20.2 \pm 1.5	26.9 \pm 2.0 *	ND	31.5 \pm 4.7	28.2 \pm 3.7	36.8 \pm 4.7	ND	27.4 \pm 3.0	ND	80.3 \pm 8.5	ND
Posterior Brainstem	non-Tg	28.3 \pm 1.6	14.7 \pm 1.9	27.7 \pm 3.7	ND	29.5 \pm 1.4	22.9 \pm 3.4	25.3 \pm 2.4	ND	34.6 \pm 2.3	ND	78.9 \pm 8.8	ND
	Tg	38.1 \pm 4.3 *	18.4 \pm 2.8	25.9 \pm 2.2	ND	34.0 \pm 3.5	21.0 \pm 3.4	26.2 \pm 5.4	ND	28.3 \pm 1.2 *	ND	68.9 \pm 6.0	ND

Dopamine (DA), dihydrophenylacetic acid (DOPAC), homovanillic acid (HVA) and 3-methoxytyramine (3-MT) levels are expressed as pg/mg/tissue. Values are means \pm SEM of $n \geq 8$ mice per group. * $P \leq 0.05$ versus non-Tg littermates by Student's unpaired *t*-test. ND - not detected.

4.4.2 TgCRND8 Mice Display Behavioural Despair in the Tail Suspension Test

To determine whether reductions in tissue noradrenaline content might be accompanied by development of a depressive phenotype, we tested 4, 8 and 27-week-old TgCRND8 and littermate control mice in the tail suspension test (Figure 4-3). Behavioral despair in this task is defined as an increase in immobility in response to inescapable stress (Steru *et al.*, 1985). The hippocampus and frontal cortex are the neuroanatomical substrates of the stress-induced, depressive-like response in the tail suspension test (Galeotti and Ghelardini, 2012). Mice were considered immobile when they hung motionless with their limbs tucked against their bodies. At 4 weeks of age, TgCRND8 mice were indistinguishable from controls in their latency to immobility ($t(17)=1.49$, $P=0.156$) as well as duration of immobility ($t(17)=0.08$, $P=0.936$). At 8 weeks, TgCRND8 mice were quicker to become immobile ($t(18)=2.71$, $P=0.014$) and by 27 weeks they exhibited both reduced latency to ($t(17)=3.30$, $P=0.004$) and increased duration of ($t(17)=2.31$, $P=0.033$) immobility.

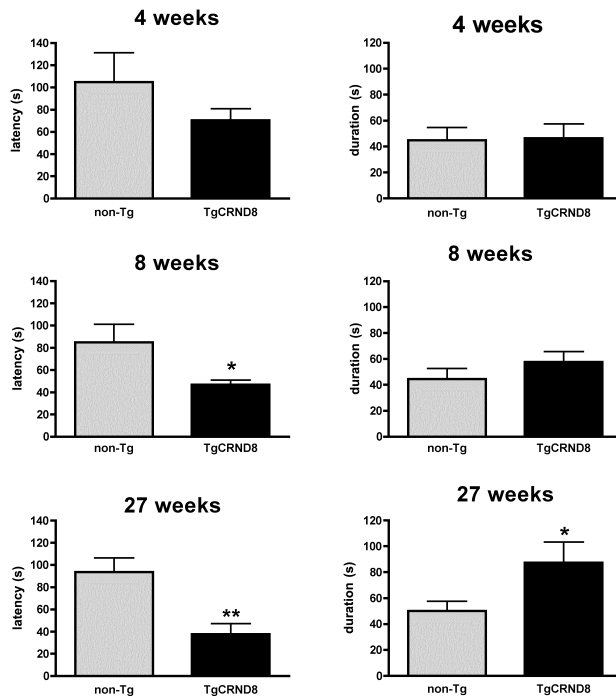


Figure 4-3. TgCRND8 mice exhibit pronounced behavioral despair in the tail suspension test. Latency to immobility (left panel) and duration of immobility (right panel) were measured in 4-, 8- and 27-week-old mice that were suspended by their tails for 6 min. At 8 weeks, TgCRND8 mice became immobile quickly. By 24 weeks, they also spent more of the test period immobile. Values are means \pm SEM of $n \geq 8$ mice per group. * $P \leq 0.05$, ** $P \leq 0.01$ versus non-Tg animals by Student's unpaired t test.

5.4.3 Desipramine Alleviates Behavioural Despair

Desipramine, a noradrenaline reuptake inhibitor, has been shown to effectively reduce behavioral despair in C57BL/6 mice in the tail suspension test (Steru *et al.*, 1985; Cryan *et al.*, 2005). We found significant main effects of both genotype ($F_{1,20}=26.30$, $P < 0.001$) and desipramine ($F_{1,20}=41.55$, $P < 0.001$) on duration of immobility. Although desipramine increased the latency to immobility in both TgCRND8 and non-Tg mice, we did not see a significant effect of genotype on latency scores (data not shown). The stress of i.p. injections may have influenced latency scores, as has been reported previously (Barfield *et al.*, 2010). Thus, duration of immobility is deemed the most reliable readout of the tail suspension test (Cryan *et al.*, 2005). Desipramine slightly reduced the duration of immobility (Figure 4-4) in non-Tg mice ($t(11)=2.23$, $P=0.048$), but profoundly reduced immobility in TgCRND8 mice ($t(9)=5.97$, $P=0.0002$), so as to render the response of these animals indistinguishable from that of saline-treated non-Tg mice ($t(10)=1.03$, $P=0.33$). These results suggest that increasing synaptic noradrenaline has an anti-depressive effect in the tail suspension test.

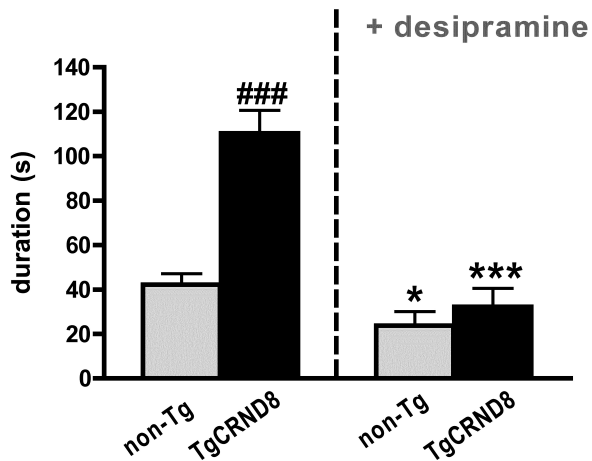


Figure 4-4. Desipramine reduces immobility in the tail suspension test. Thirty-week-old TgCRND8 and non-Tg mice received an injection of either desipramine or saline 30 min prior to the test. Desipramine reduced time mice spent immobile. Values are means \pm SEM of $n \geq 6$ mice per group. * $P \leq 0.05$; *** $P \leq 0.001$ versus saline-treated animals of matched genotype; ### $P \leq 0.001$ versus saline-treated non-Tg mice by 2-way ANOVA followed by Fisher's protected LSD test.

4.4.4 TgCRND8 Mice are Not Impaired in a Test of Forelimb Coordination

To assess subtle changes in motor function, we induced grooming behaviour in mice by affixing an adhesive label to their foreheads (Figure 4-5). To remove the stimulus, mice typically use both forelimbs to reach upwards and swipe off the label. Such fine voluntary motor skills are dependent on dopaminergic transmission in the striatum and substantia nigra (reviewed in Meredith and Kang, 2006). Consistent with their normal dopamine levels and turnover in the striatum and ventral mesencephalon, 15-week-old TgCRND8 mice do not differ from littermate controls in the time taken to remove the label ($t(21) = 1.27$, $P = 0.22$).

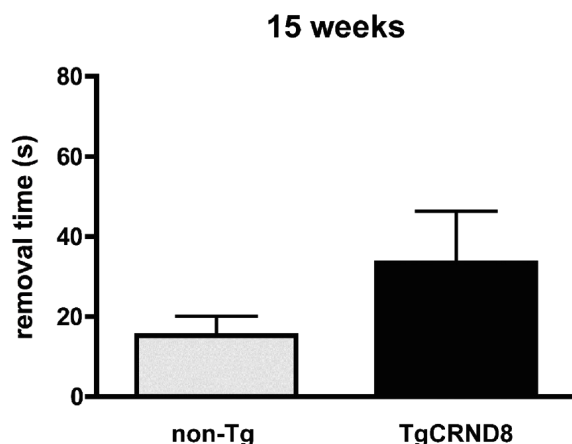


Figure 4-5. Forelimb use is not affected in TgCRND8 mice. Mice used their forelimbs to remove an adhesive label that was affixed to the forehead. No differences in removal time were observed between TgCRND8 mice ($n = 12$) and littermate controls ($n = 11$) at 15 weeks of age.

4.4.5 Dexefaroxan and Rivastigmine Reduce Object Memory Impairment and Behavioural Despair

Twelve-week-old TgCRND8 mice and non-Tg littermates were treated with dexefaroxan, rivastigmine or saline for 4 weeks and were subjected to object memory and tail suspension tests. The 12 to 16 week window is a relevant timeframe for therapeutic assessment in TgCRND8 mice as robust spatial memory impairment develops by 12 weeks and plaque deposition is evident at 15 weeks of age (Chishti *et al.*, 2001; Janus *et al.*, 2000). Dexefaroxan enhances noradrenergic transmission by antagonizing inhibitory α_2 -adrenoceptors. The dose was adopted from a study in which daily injections of dexefaroxan were found to enhance olfactory bulb neurogenesis (Veyrac *et al.*, 2005). Others have verified stable pharmacological activity of an equivalent dexefaroxan dose delivered chronically in rats via mini-osmotic pumps (Chopin *et al.*, 2002; Debeir *et al.*, 2002; Rizk *et al.*, 2006). Tolerance to a facilitatory effect of dexefaroxan on cognition was not observed even after chronic infusion for 25 days (Chopin *et al.*, 2002). We compared the effects of dexefaroxan to those of rivastigmine, a clinical cholinesterase inhibitor used to treat memory deficits in AD. The dose of rivastigmine administered in this study previously was found to improve spatial memory in APP23-Tg mice (Van Dam *et al.*, 2005).

Regardless of genotype or drug treatment, mice spent an equivalent amount of time exploring objects during the acquisition trial (Figure 4-6a). The set of objects used for this task was predetermined to ensure matched saliency and we did not observe group differences in object preference during the acquisition trial (data not shown). Object memory (Figure 4-6b) was calculated following a 3-h retention interval with a memory index, where a score of 0 indicates no preference for the novel object. Both genotype ($F_{1,50}=21.52$, $P<0.0001$) and treatment ($F_{2,50}=7.07$, $P=0.002$) significantly influenced object memory. At 14 weeks of age, TgCRND8 mice were severely impaired on this test ($t(15)=9.13$, $P<0.001$). A reversal of the memory deficit was observed in TgCRND8 mice chronically infused with either dexefaroxan ($t(18)=6.57$, $P<0.001$) or rivastigmine ($t(15)=3.59$, $P=0.003$). The performance of non-Tg mice in the object recognition test was not altered with dexefaroxan ($t(16)=1.04$, $P=0.31$) or rivastigmine ($t(16)=1.51$,

$P=0.15$) treatment. On the 20th day of infusion with either drug or saline, mice were tested on the tail suspension test (Figure 4-7). We found that both genotype ($F_{1,54}=20.35$, $P<0.0001$) and treatment ($F_{2,54}=24.80$, $P<0.0001$) significantly affected time mice spent immobile in this test. Fourteen to 15 week-old TgCRND8 mice were behaviorally depressed, with longer durations of immobility than non-Tg controls ($t(14)=6.59$, $P<0.0001$). Immobility of TgCRND8 mice was dramatically reduced with both dexefaroxan ($t(15)=9.45$, $P<0.0001$) and rivastigmine ($t(12)=5.36$, $P=0.0002$). The immobility of non-Tg mice was unaffected by either dexefaroxan ($t(19)=1.75$, $P=0.09$) or rivastigmine ($t(16)=1.21$, $P=0.24$), suggesting that a floor effect for immobility scores was achieved.

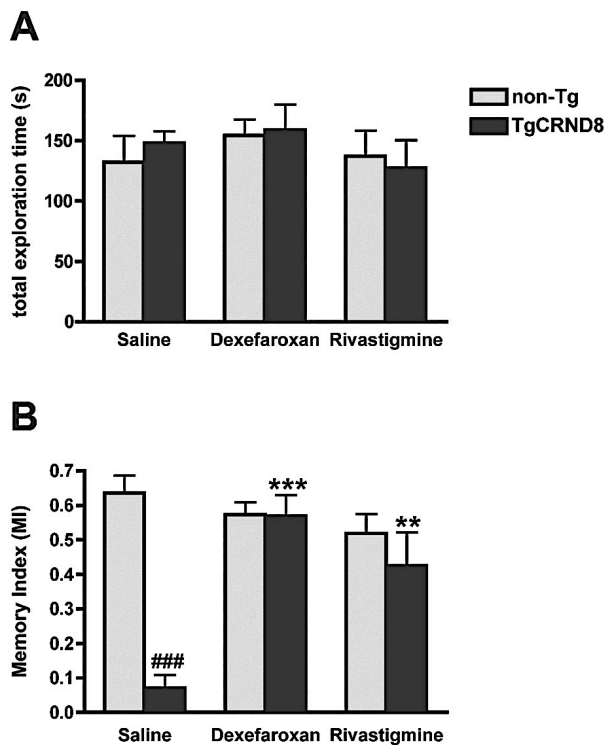


Figure 4-6. Dexefaroxan and rivastigmine affect memory, but not exploration of objects. On day 19 of treatment with dexefaroxan, rivastigmine or saline, 14-week-old TgCRND8 and littermate controls were tested on the object recognition task. Time spent exploring the objects during the initial exposure period are compared (**A**). Three hours after this initial exposure, mice were re-exposed to an object from the original test pair and to a novel object. A memory index was calculated as described in Materials and Methods. Both dexefaroxan and rivastigmine abolished object memory deficits of TgCRND8 mice (**B**). Results are means \pm SEM of 8 – 11 mice per group. ** $P\leq 0.01$; *** $P\leq 0.001$ versus saline treated controls; ### $P\leq 0.001$ versus non-Tg saline treated mice by 2-way ANOVA followed by Fisher's protected LSD test.

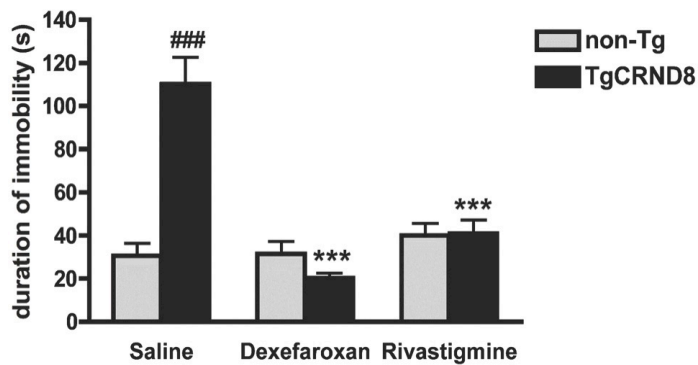


Figure 4-7. Dexefaroxan and rivastigmine reduce behavioral despair. One day after object recognition testing, 14 to 15-week-old TgCRND8 and littermate drug-treated mice were subjected to the tail suspension test. Saline-treated TgCRND8 mice exhibited behavioral despair, spending more of the test time immobile than did control animals. Dexefaroxan and rivastigmine reduced behavioral

despair to levels observed in non-Tg mice. Data are mean values \pm SEM for 6 to 13 mice per group. *** $P \leq 0.001$ versus saline treated controls; ### $P \leq 0.001$ versus non-Tg saline treated mice by 2-way ANOVA followed by Fisher's protected LSD test.

4.4.6 Treatments Do Not Affect Amyloid Burden

We investigated how dexefaroxan and rivastigmine might affect A β load in TgCRND8 mice. Levels of monomeric A β_{42} and A β_{40} were assessed with the Amorfix A β immunoassay, and the aggregated soluble and insoluble forms of A β were quantified using the Amorfix A⁴ assay. The A⁴ is a sensitive immunoassay that allows quantification of aggregated A β levels well before plaques can be detected by immunohistochemical means. The A⁴ matrix enriches for insoluble fibrils, as well as smaller soluble oligomers, up to and including trimeric A β . Neither drug treatment altered cortical levels of aggregated or monomeric A β (Figure 4-8a-c). Similar results were obtained with hippocampal samples (data not shown). We also assessed cortical levels of holoAPP and β -C-terminal fragments (β -CTF) by Western blot analysis with the monoclonal antibody, 6E10 (Figure 4-8d). 6E10 is directed toward amino acid residues 1-16 of A β , which are within the 99-residue carboxy-terminal fragment of APP that is produced by β -secretase cleavage. 6E10 also reacts with full-length APP protein. Neither drug altered APP levels (not shown) or β -CTF expression (Figure 4-8e).

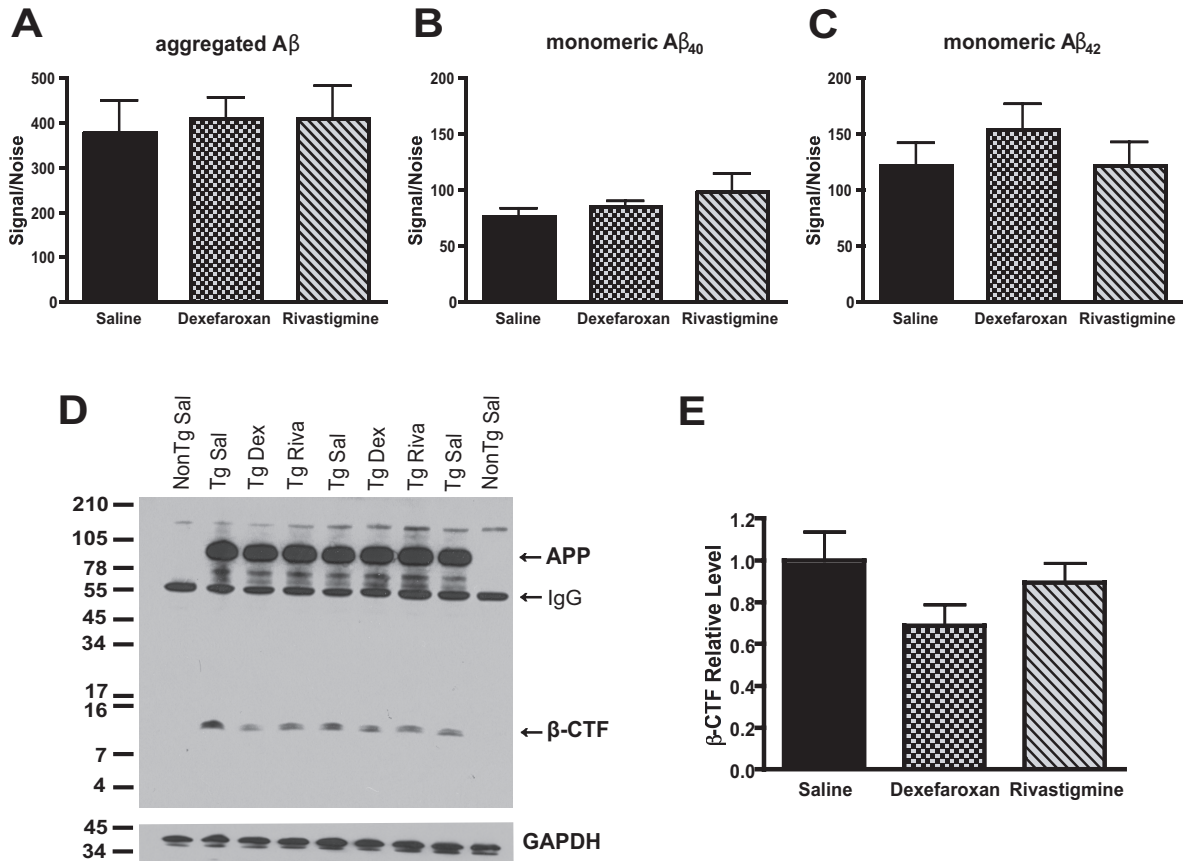


Figure 4-8. Dexefaroxan and rivastigmine do not affect A β , APP or β -CTF levels. Top panels (A – C) show that cortical levels of aggregated A β (A), monomeric A β_{40} (B) and monomeric A β_{42} (C) in 16-week-old TgCRND8 mice were unaffected by dexefaroxan or rivastigmine treatment as measured by Amorfix immunoassays with time-resolved fluorescence. Results are means \pm SEM of 7 mice per group. The signal/noise ratio was calculated by dividing the europium-fluorescent readout signal from the sample by the signal from the dilution buffer alone. Samples were scored as negative if the signal/noise ratio was <2 . All non-Tg samples scored negative (not shown). Representative immunoblot of cortical tissue homogenates from 16-week-old non-Tg saline ($n=6$), TgCRND8 saline ($n=7$), TgCRND8 dexefaroxan ($n=7$) and TgCRND8 rivastigmine ($n=7$) treated mice probed with the A β_{1-16} monoclonal antibody 6E10 (D). Blots were stripped and reprobed with GAPDH-specific antibody to ensure equal loading of protein. Densitometric analysis of β -CTF band intensities (normalized against GAPDH signal) was performed using ImageJ software (E). Effect of treatments on band intensity is shown relative to the average staining intensity obtained for TgCRND8 saline samples (which was set to 1). Neither drug altered levels of holoAPP (not shown) or β -CTF. Values are means \pm SEM, obtained from 3 independent experiments.

4.4.7 Dexefaroxan and Rivastigmine Increase BDNF mRNA

We examined whether dexefaroxan and rivastigmine treatment might alter hippocampal BDNF mRNA levels, at 2 stages of plaque pathology (Figure 4-9). Treatments were initiated in 12-week-old TgCRND8 mice, at the onset of A β deposition and in another cohort of 45 – 50-week-old mice with advanced plaque pathology. Levels of β -actin mRNA were found to be equivalent in all mice, regardless of genotype or drug treatment ($P>0.05$, data not shown). Results were obtained as copies per 50 ng total RNA and expressed as a ratio of BDNF/ β -actin mRNA. In the young mice, we found interacting effects of genotype and treatment on BDNF mRNA levels ($F_{2,50}=3.85$, $P=0.0279$). In 1-year-old mice, both genotype ($F_{1,37}=32.54$, $P<0.0001$) and drug treatment ($F_{2,37}=3.24$, $P=0.05$) were found to affect BDNF mRNA expression. BDNF mRNA was reduced in young ($t(9)=2.45$, $P=0.036$) and aged ($t(13)=4.78$, $P=0.0004$) TgCRND8 mice. Neither drug altered BDNF levels in non-Tg mice. Both drugs increased BDNF in TgCRND8 mice. However, in young mice the increase was significant only with rivastigmine treatment ($t(9)=3.63$, $P=0.005$; Figure 4-9a). By 1 year of age, dexefaroxan significantly improved BDNF mRNA levels in TgCRND8 mice ($t(12)=2.24$, $P=0.044$; Figure 4-9b).

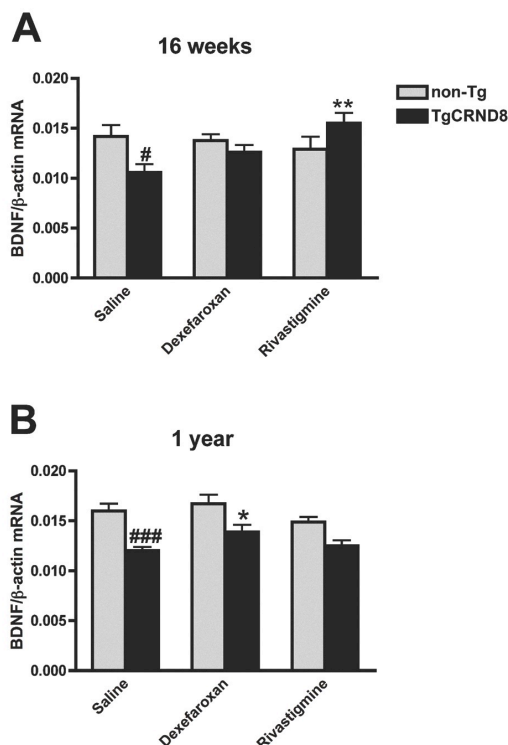


Figure 4-9. Dexefaroxan and rivastigmine rescue BDNF mRNA levels in TgCRND8 mice. BDNF mRNA levels were measured by absolute quantitative real-time reverse transcriptase polymerase chain reaction (RT-PCR). Reduced levels of BDNF mRNA in hippocampi of 16-week-old TgCRND8 mice were restored with rivastigmine treatment (**A**). In 1-year-old TgCRND8 mice, dexefaroxan increased BDNF mRNA (**B**). Data are expressed as ratio of copies of BDNF mRNA/ β -actin mRNA. Values are means \pm SEM of ≥ 6 mice per group. * $P\leq 0.05$, ** $P\leq 0.01$ versus saline treated controls; # $P\leq 0.05$, ### $P\leq 0.001$ versus non-Tg saline mice by 2-way ANOVA followed by Fisher's protected LSD test.

4.4.8 Dexefaroxan and Rivastigmine Differentially Affect Noradrenaline Turnover in the Hippocampus

We investigated the effects of dexefaroxan and rivastigmine treatment on hippocampal tissue levels noradrenaline and its extracellular metabolite, normetanephrine (Figure 4-10). *Ex vivo* tissue levels of normetanephrine directly reflect noradrenaline turnover in microwave-inactivated brain (Wood *et al.*, 1987). Dexefaroxan treatment reduced noradrenaline, but marginally increased normetanephrine in non-Tg mice ($t(23)=1.812$, $P=0.083$). Saline treated TgCRND8 mice, with decreased noradrenaline tissue content, exhibited increased normetanephrine levels ($t(13)=2.275$, $P=0.0405$). In TgCRND8 mice, both drug treatments reduced normetanephrine levels to the levels of non-Tg controls, but did not alter noradrenaline content in the hippocampus.

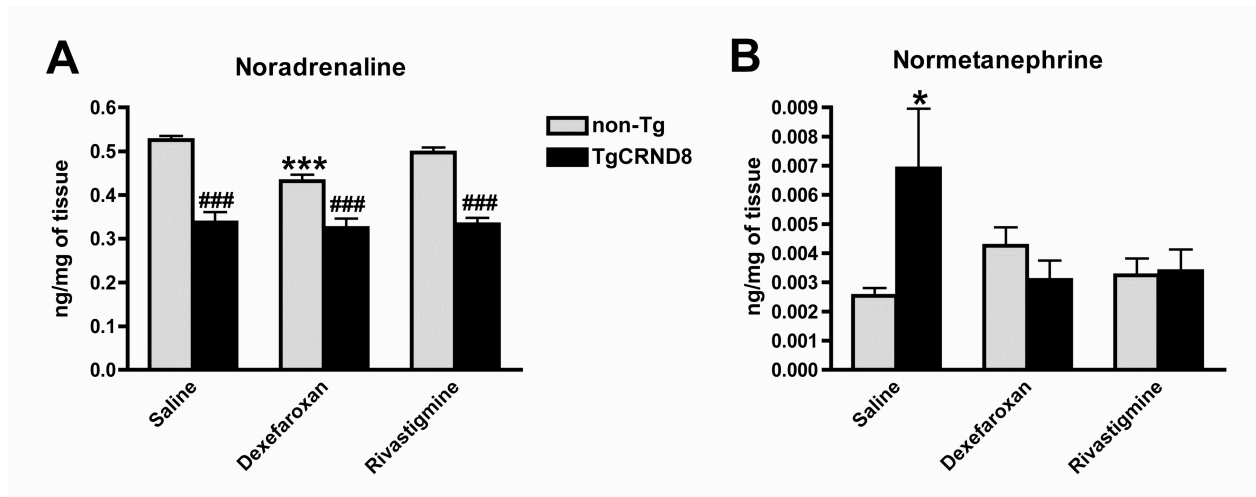


Figure 4-10. Dexefaroxan and rivastigmine differentially affect tissue levels of noradrenaline and normetanephrine in the hippocampus of 16-week-old TgCRND8 and non-Tg mice. TgCRND8 mice exhibited reductions in noradrenaline (A), but increases in normetanephrine (B) content in the hippocampus. In TgCRND8 mice, drug treatments normalized normetanephrine levels, without affecting those of noradrenaline. In non-Tg animals, dexefaroxan reduced noradrenaline content and induced a non-significant increase in tissue normetanephrine levels. Data are means \pm SEM of $n \geq 8$ mice per group. * $P \leq 0.05$; *** $P \leq 0.001$ relative to saline-treated animals of the same genotype; ### $P \leq 0.001$ versus saline-treated non-Tg mice by 2-way ANOVA and Fisher's protected LSD comparisons.

4.5 Discussion

This study provides the first longitudinal analysis of TgCRND8 brain catecholamine content and reveals that noradrenergic deficits precede amyloid deposition in an APP-transgenic mouse. These spontaneous reductions in tissue noradrenaline contribute to behavioral impairment and BDNF deficits.

TgCRND8 phenotypes are driven by the production and accumulation of A β . How A β leads to neuronal dysfunction and behavioral abnormalities is unknown. We reported previously that TgCRND8 mice develop object memory deficits by 8 weeks of age, before frank plaque pathology but coincident with a 2-fold increase in A β levels and reduced BDNF mRNA in the hippocampus and frontal cortex (Francis *et al.*, 2012a). We argued that decreased BDNF expression contributes to the functional disruption of these brain regions that are first targeted by amyloid.

BDNF is synthesized in part by noradrenergic neurons (reviewed in Marien *et al.*, 2004) and has been found to promote the survival and phenotypic maturation of these neurons during development (Holm *et al.*, 2003; Traver *et al.*, 2006). BDNF is also required for the maintenance of noradrenergic innervation in the aging brain (Matsunaga *et al.*, 2004). It is trophic for both catecholaminergic and cholinergic neurons and is transported to and from the forebrain in noradrenergic neurons (reviewed in Marien *et al.*, 2004 and Matsunaga *et al.*, 2004).

In view of the trophic relationship between BDNF and noradrenergic neurons, we anticipated finding decreased noradrenaline content in TgCRND8 brains. We found such reductions in the hippocampus, temporoparietal and frontal cortices, and cerebellum of 4-week-old mice. Analyses of older TgCRND8 mice revealed reduced levels of noradrenaline in the cortex and progressive deficits in the hippocampus. In the cerebral cortex of aged non-Tg control mice, we found tissue content of noradrenaline to be elevated relative to younger mature animals. Similar age-dependent increases in cortical noradrenaline content have been reported in the rat (Harik and McCracken,

1986). While noradrenergic projections to the frontal cortex decrease with age, axonal branching and excitability of axon terminals of locus coeruleus neurons increase to maintain noradrenaline levels (Ishida *et al.*, 2001). The higher degree of arborization and plasticity of the remaining noradrenergic axons in the frontal cortex may be mediated by BDNF (Matsunaga *et al.*, 2004). Such compensatory increases in cortical noradrenaline levels appear to be absent in the aging TgCRND8 brain. The regional specificity of noradrenergic deficits suggests that cortical- and hippocampal-projecting cells in the locus coeruleus are damaged in TgCRND8 animals. In contrast, the ventral mesencephalon, striatum and brainstem, all of which receive noradrenergic innervation from nuclei outside the locus coeruleus (Berridge and Waterhouse, 2003; Mejías-Aponte *et al.*, 2009) are unaffected. This pattern of noradrenergic tissue deficits resembles what has been described in the human disease. In AD, noradrenergic cell loss is attributed to retrograde degeneration of rostral, cortical-projecting cells of the locus coeruleus (Marcyniuk *et al.*, 1986; German *et al.*, 1992; Manaye *et al.*, 1995).

Reductions in noradrenaline and BDNF constitute pathogenically significant steps in A β -induced functional impairment and occur early in disease progression. In contrast, deleterious effects on cholinergic neurons and decreased cortical acetylcholine release have been reported in TgCRND8 animals at 7, but not 2 months of age (Bellucci *et al.*, 2006). Thus, cholinergic dysfunction may follow the development of noradrenergic deficits in the TgCRND8 mouse. The degeneration of the locus coeruleus has been reported in mild cognitive impairment and is suggested to mediate the emergence of dementia in human AD (Grudzien *et al.*, 2007). An early loss of tissue noradrenaline also appears to influence development of behavioral phenotypes in TgCRND8 mice. Eight-week-old TgCRND8 mice exhibited increased behavioral despair in the tail suspension test in addition to object memory impairment. The noradrenaline reuptake inhibitor desipramine reversed immobility, implicating noradrenergic deficits in the development of this depressive phenotype.

To test whether reduced noradrenergic tone in major terminal fields might have caused TgCRND8 behavioral dysfunction, we examined effects of enhancing noradrenergic transmission with dexefaroxan. Dexefaroxan blocks α_2 -adrenergic autoreceptors as

well as inhibitory α_2 -adrenoceptors expressed heterologously on non-noradrenergic cells, including cholinergic neurons (reviewed in Chopin *et al.*, 2002). Thus, dexefaroxan not only increases noradrenergic release (Rizk *et al.*, 2006) but can also produce dose-dependent and sustained increase in cortical acetylcholine release (Tellez *et al.*, 1999). Both dexefaroxan and rivastigmine ameliorated object memory deficits and behavioral despair of TgCRND8 animals. It is unlikely that our treatments improved behavior by eliciting a general stimulant-type, hyperkinetic effect, as neither drug influenced object exploration, or the immobility scores of non-Tg mice.

The behavioral phenotypes we observed could not be explained by frank motor differences. TgCRND8 and non-Tg mice spent equal time exploring objects in the object memory test and no gross difference in motor activity was discerned. To test motor coordination more directly, we assessed a tape removal task that is sensitive to altered dopaminergic transmission in the striatum and substantia nigra (reviewed in Meredith and Kang, 2006; Schallert *et al.*, 1982; Chen *et al.*, 2005). We found TgCRND8 mice to be unimpaired in performing this task. Moreover, we observed no differences between these mice and their non-Tg controls in tissue levels of dopamine and its metabolites within the striatum and ventral mesencephalon.

The apparent absence of dopaminergic dysfunction in our mice is consistent with findings in human AD (reviewed in Hardy, 1985; Palmer *et al.*, 1987a,b; Dringenberg, 2000), but at odds with previous results of Ambrée and co-workers (2009), who reported elevated levels of dopamine in the frontal cortex and neostriatum of TgCRND8 mice, as well as improved memory and reduced stereotypy in response to treatment with levodopa. These authors measured dopamine in freshly dissected brains. However, tissue levels of dopamine and its metabolites are strongly influenced by a *postmortem* surge in transmitter release and degradation. For this reason, we used rapid heat inactivation of tissue enzymes immediately before brain dissection. We found no differences in dopamine, or alteration in tissue levels of 3-MT, an indicator of released dopamine in the microwave-inactivated brain (Wood and Altar, 1988). As levodopa is a precursor of both dopamine and noradrenaline, we are left to speculate that it was

increasing noradrenergic, rather than dopaminergic tone that led to reported effects of this drug on TgCRND8 behavior (Ambrée *et al.*, 2009).

Rivastigmine can significantly improve mood in patients with mild to moderate AD (Finkel, 2004). However, it is now well appreciated that cholinergic deficits alone are insufficient to account for the various clinical manifestations of AD (Dringenberg, 2000). The loss of noradrenaline and its trophic effects on forebrain cholinergic activity can cause cognitive as well as depressive symptoms in AD (reviewed in Marien *et al.*, 2004; Herrmann *et al.*, 2004). In mice, dexefaroxan improves cognition (Chopin *et al.*, 2002) and can prevent cholinergic atrophy (Debeir *et al.*, 2002; Traver *et al.*, 2005) following basal forebrain cholinergic damage. Dexefaroxan may alleviate behavioral despair, by enhancing both noradrenergic and cholinergic transmission. Acetylcholine can reciprocally stimulate noradrenergic neurons in the locus coeruleus (Engberg and Svensson, 1980; Strong *et al.*, 1991). The possibility that cholinergic as well as noradrenergic mechanisms contribute to affective phenotypes is supported by the observation that both rivastigmine and dexefaroxan were active in reducing behavioral despair.

Progressive damage to noradrenergic terminals and the locus coeruleus has been described in multiple APP-Tg models (reviewed in Kalinin *et al.*, 2012). In all of these mice, degenerative changes in the locus coeruleus were observed well after the onset of plaque deposition. In contrast, we now report that TgCRND8 mice exhibit reduced terminal concentrations of noradrenaline weeks before behavioral dysfunction and plaque deposition.

We assessed the effects of chronic treatment with either dexefaroxan or rivastigmine on hippocampal levels of noradrenaline and normetanephrine. Dexefaroxan reduced noradrenaline, but marginally increased normetanephrine in non-Tg mice. This increase in noradrenaline turnover is consistent with a presynaptic action of the drug on intact noradrenergic terminals. In contrast, untreated TgCRND8 with decreased tissue noradrenaline exhibited an increase in normetanephrine levels, which likely reflect a compensatory release of transmitter. Both dexefaroxan and rivastigmine normalized

TgCRND8 normetanephrine levels, without changing tissue levels of noradrenaline. These observations suggest a loss of terminals and reduced reuptake of released transmitter, as has been described in clinical populations by Palmer *et al.*, 1987a,b. Elevated turnover and increased firing of surviving noradrenergic neurons have also been described in AD patients (Palmer *et al.*, 1987a,b; Szot *et al.*, 2006).

Neither dexefaroxan nor rivastigmine reduced the monomeric or aggregated A β burden in TgCRND8 brains. Similarly, neither drug significantly affected APP or β -CTF expression. In contrast, APP-Tg mice treated with the neurotoxin DSP-4 were found to exhibit a 5-fold increase in plaque burden and decreased expression and activity of an A β degrading protease, neprilysin (Kalinin *et al.*, 2007). This increased amyloid load was associated with inflammation and impaired microglial phagocytosis of A β . Replenishing noradrenaline in DSP-4 treated mice restored microglial migration and A β phagocytosis (Heneka *et al.*, 2010). While loss of noradrenergic innervation can promote amyloid deposition, treating with an α_2 -adrenoceptor antagonist may not affect A β levels in the brain. The therapeutic actions of our drugs are likely independent of effects on A β accumulation. By 16 weeks, A β plaques are abundant in the hippocampus and cortex, although we found cytokine expression to remain unchanged (Ma *et al.*, 2011). Only at late stages of amyloid pathology have we found IL-1 β to be upregulated in the TgCRND8 brain. It is possible that by 28 weeks, a time-point at which microglial activation is observed in this model, an effect of desipramine on neuroinflammatory measures might be discerned.

We reported previously that downregulation of BDNF mRNA can be induced by large oligomer formations of A β and high A β_{42} /A β_{40} ratios (Peng *et al.*, 2009). These conditions are achieved before the onset of plaque pathology in TgCRND8 mice and decreased BDNF mRNA is observed in mice only 6 to 8 weeks of age (Francis *et al.*, 2012a). BDNF has established roles in synaptic plasticity, mood and memory (reviewed by Coyle and Duman, 2003). Noradrenaline can induce the production of BDNF and mitigate A β -induced stress through stimulation of canonical β -adrenoceptor cAMP

pathways (Counts and Mufson, 2010). By corollary, reduction in tissue noradrenaline may exacerbate A β -induced BDNF deficits.

Dexefaroxan increases BDNF expression in afferent noradrenergic fibers and in hippocampal granule cells (Rizk *et al.*, 2006). Cholinomimetic drugs also induce BDNF expression in the brain (Srivareerat *et al.*, 2011) and can elevate serum BDNF concentrations of AD patients to levels found in healthy controls (Leyhe *et al.*, 2008). In TgCRND8 mice, both dexefaroxan and rivastigmine upregulated hippocampal BDNF mRNA. This effect of dexefaroxan persisted even at advanced stages of amyloid accumulation.

In sum, early depletion of noradrenaline within selected terminal fields constitutes a pathophysiologically relevant event in this robust mouse model of A β deposition. Dexefaroxan and rivastigmine ameliorated memory impairment and behavioral despair in addition to increasing BDNF mRNA. Our results suggest that increasing noradrenergic transmission may warrant consideration as part of a therapeutic strategy in the treatment of AD.

**Chapter 5 Selective Targeting of Mitochondrial
Complex I in Aged APP-Transgenic
TgCRND8 Mice**

5.1 Abstract

Bioenergetic failure is a feature of Alzheimer's disease (AD). We examined mitochondrial function in the amyloid precursor protein-transgenic 'TgCRND8' mouse model of AD. Activities of NADH: cytochrome *c* reductase (complex I+III) and cytochrome oxidase (complex IV) of the electron transport chain, as well as those of α -ketoglutarate dehydrogenase (α -KGDH) and pyruvate dehydrogenase (PDH) were assessed in brains of 45-week-old mice. Complex I+III activity was reduced by almost 50%, whereas complex IV, α -KGDH and PDH activities were unaffected. Reduced activity coincided with decreased expression of NDUFB8, a nuclear-DNA encoded subunit integral to the assembly of complex I. The composition and availability of cardiolipin, a major phospholipid in inner mitochondrial membranes, was not altered. To determine whether mitochondrial output is affected by the selective reduction in complex I+III activity, we examined tissue levels of high-energy phosphates. ATP was maintained whereas creatine increased in the cortex and hippocampus. These results suggest disruption of complex I function and the likely role of creatine in sustaining ATP at end-stages of dysfunction in TgCRND8 mice.

5.2 Introduction

Bioenergetic stress and mitochondrial dysfunction in Alzheimer's disease (AD) are well documented (reviewed in Bowling and Beal, 1995; Swerdlow, 2012; Ye *et al.*, 2012). Among the most consistently reported metabolic defects is the progressive reduction in glucose metabolism within cerebral cortices (Mosconi *et al.*, 2008). Decreased glucose utilization in brains of AD patients is associated with deficits in several enzymes of oxidative metabolism. Notably, activities of pyruvate dehydrogenase (PDH) and α -ketoglutarate dehydrogenase (α -KGDH), rate-limiting enzymes of the tricarboxylic acid cycle, are compromised (Bubber *et al.*, 2005). Hypometabolism in AD is also reflected in decreased expression of mitochondrial and nuclear genes encoding subunits of the electron transport chain (ETC) complexes (Chandrasekaran *et al.*, 1996; Aksenov *et al.*, 1999; Manczak *et al.*, 2004; Liang *et al.*, 2008). AD brains exhibit a generalized depression in activity of all ETC complexes (Parker *et al.*, 1994), though decreases in cytochrome *c* oxidase (complex IV) activity are the most frequent finding (reviewed in Maruszak and Zekanowski, 2011).

Compromised mitochondrial function has been ascribed to the accumulation of toxic amyloid- β (A β) peptides, a pathological hallmark of the disease. A β is produced from the sequential β - and γ -secretase cleavage of amyloid precursor protein (APP). A β , APP and functional complexes with γ -secretase activity have been found within the mitochondrion. Intra-mitochondrial A β causes bioenergetic dysfunction by decreasing membrane potential, increasing oxidative stress and inhibiting ETC activity (reviewed in Swerdlow, 2012; Ye *et al.*, 2012).

We examined mitochondrial function in the TgCRND8 mouse, which expresses a double mutant human APP₆₉₅ transgene (Swedish: KM670/671NL and Indiana: V717F), under control of the pan-neuronal Syrian hamster prion gene promoter. These mice exhibit A β deposition by 3 months of age (Chishti *et al.*, 2001) and microcrystalline deposits of creatine in the hippocampus (Gallant *et al.*, 2006). Elevations in creatine were observed at an early age and increased in parallel with plaque pathology (Kuzyk *et*

al., 2010). Creatine deposits are suggestive of disrupted bioenergetic homeostasis, although this has not been investigated in TgCRND8 mice. We examined brain activities of complexes I+III and IV of the ETC, as well activities of PDH complex and α -KGDH complex in mice with advanced A β pathology. We also measured tissue levels of high-energy phosphate donors to assess mitochondrial output in TgCRND8 mice.

5.3 Methods

5.3.1 Transgenic Mice

Mice were maintained on a hybrid genetic background (C57BL/6/C3H x C57BL/6 backcross) and communally housed under standard laboratory conditions.

Experimental groups were gender-balanced. All procedures were approved by the Animal Care Committee at the University of Toronto, in accordance with Guidelines for the Use and Treatment of Animals, put forth by the Animal Care Council of Canada.

5.3.2 Metabolic Enzyme Activities

TgCRND8 and non-Tg mice ($n \geq 5$ mice/genotype) were killed by cervical dislocation at 45 weeks of age. Brains were bisected sagittally and intact hemispheres were snap frozen in liquid nitrogen. Tissues were homogenized in 10 X w/v PDH buffer (10 mg/ml fatty acid free bovine serum albumin, 0.17 mg/ml dithiothreitol, 1 mg/ml NAD, 11 mM potassium phosphate, 3 mM $MgCl_2$, 1 mM EDTA, pH 7.4). Homogenates were centrifuged at 3000 *g* for 10 min at 4°C. The supernatant was collected and 200 μ l aliquots were flash frozen in liquid nitrogen. Two aliquots were used to analyze the activities of NADH: cytochrome *c* reductase (complexes I and III; EC 1.6.2.1) and cytochrome oxidase (complex IV; EC 1.9.3.1). The remaining aliquots were stored at -80°C for pyruvate dehydrogenase (PDH; complex of EC 1.2.4.1, EC 2.3.1.12 and EC 1.8.1.4) and α -ketoglutarate dehydrogenase determinations (α -KGDH; complex of EC 1.2.4.2, EC 2.3.1.61 and EC 1.8.1.4), and for assaying complexes I and III subunit expression. Enzyme activities were assayed in quadruplicate and expressed as nmol of product formed/ precursor converted per min per mg of wet weight brain tissue, at 37°C.

5.3.2.1 *Pyruvate Dehydrogenase Complex*

Native activity of the PDH complex was measured by adapting a $^{14}\text{CO}_2$ capture technique (Maj *et al.*, 2005). An aliquot of brain homogenate was diluted in 0.6 ml potassium phosphate (KPi) buffer (1M, pH 7.4). An incubation mixture was prepared with 8 ml PDH buffer, 1.42 mg coenzyme A, 0.91 mg sodium sulfate, 9 μl of 0.1 M thiamine pyruvate phosphate, 16 μl of 0.1 M pyruvate and 18 μl of $[1-^{14}\text{C}]$ pyruvate. The $[1-^{14}\text{C}]$ pyruvate was prepared by suspending a vial of 0.05 Ci $[1-^{14}\text{C}]$ pyruvate powder (Amersham Biosciences, Arlington Heights, IL) in 0.5 ml of 0.1 M hydrochloric acid. Before it was added to the incubation mixture, 18 μl of $[1-^{14}\text{C}]$ pyruvate was diluted in 0.2 ml H_2O and bubbled with air for 10 min, to eliminate CO_2 gas. Diluted samples (50 μl) were added to 200 μl of incubation mixture in 10ml Erlenmeyer flasks. The reaction proceeded for 10 min at 37°C and was stopped by adding 100 μl of 10% trichloroacetic acid and reducing bath temperature to 25°C . The mixture was allowed to equilibrate for an additional hour. $^{14}\text{CO}_2$ gas produced from the oxidative decarboxylation of $[1-^{14}\text{C}]$ pyruvate by tissue PDH was captured in 0.2 ml benzethonium hydroxide, contained in wells that were attached to the Erlenmeyer flask stoppers. Toluene scintillation fluid was added to the benzethonium hydroxide and radioactivity was measured with a Beckman LS 6500 scintillation counter.

5.3.2.2 *α -Ketoglutarate Dehydrogenase Complex*

Native activity of the α -KGDH complex was also determined by $^{14}\text{CO}_2$ capture. Aliquots of brain homogenate (50 μl) were added to 200 μl of radioactive incubation mixture (8 ml PDH buffer, 1.42 mg coenzyme A, 0.02 ml of 0.1M CaCl_2 , 10 μl of 200 mM ketoglutarate and 16 μl of $[1-^{14}\text{C}]$ ketoglutarate). The release of $^{14}\text{CO}_2$ gas from the oxidative decarboxylation of $[1-^{14}\text{C}]$ ketoglutarate was captured and counted, as above.

5.3.2.3 *NADH: Cytochrome c Reductase*

Rotenone-sensitive complex I+III activity was measured by assaying the rate of cytochrome *c* reduction on a Cary Bio 300 UV-Vis Spectrophotometer (Varian Instruments, Palo Alto, CA) at 550 nm, as described (Seyda *et al.*, 2001). An aliquot of brain homogenate was thawed and 10 μ l was added to experimental and reference cuvettes, each containing 1 ml of 0.1 M KPi plus 1 mM sodium azide buffer (pH 7.0) and 30 μ l of 40 mg/ml horse heart ferricytochrome *c* in H₂O (Sigma Chemical Co., St. Louis, MO). Azide in the reaction mixture inhibited complex IV, preventing the re-oxidation of cytochrome *c*. To the reference cuvette, 5 μ l of 1 mM rotenone was added to inhibit complex I. Readings were “zeroed” against the reference cuvette. Thus, the reduction of cytochrome *c* in this assay is only due to the transfer of electrons from complex I through complex III. The reaction was timed from the addition of 10 μ l of 5 mg/ml NADH (Sigma) and recorded for 2 min. The initial linear rate of increase in absorbance was used to calculate the rate of cytochrome *c* reduction with extinction coefficient $\epsilon_{550\text{nm}} = 0.0185 \text{ nmol}^{-1}\text{cm}^{-1}$.

5.3.2.4 *Cytochrome Oxidase*

Complex IV activity was determined spectrophotometrically by monitoring the decrease in absorbance during oxidation of reduced cytochrome *c* at 550 nm (Seyda *et al.*, 2001). Horse heart ferricytochrome *c* was reduced with 0.5 M ascorbate (Sigma). Excess ascorbate was removed by dialyzing against 0.1 M KPi buffer (pH 7.0) for 24-h at 4°C with 2 changes of buffer. Samples were thawed and further diluted with KPi buffer to a final concentration of 5% brain homogenate. To sample and reference cuvettes, 1 ml of 0.1 M KPi buffer and 30 μ l of 40 mg/ml reduced cytochrome *c* was added. The reaction was initiated with 5 μ l of 5% brain homogenate and was recorded for 2 min. The initial linear rate of decrease in absorbance was used to calculate complex IV activity with cytochrome *c* extinction coefficient $\epsilon_{550\text{nm}} = 0.0185 \text{ nmol}^{-1}\text{cm}^{-1}$.

5.3.3 Western Blot Analysis

Polyclonal antibodies to the human complex I 49kDa (NDUFS2) nuclear-DNA encoded subunit and citrate synthase were prepared in-house (Xu *et al.*, 2008). Mouse monoclonal antibodies to the complex III Rieske FeS (catalog # MS305) nuclear-DNA encoded subunit and the complex I NDUF8 (catalog # MS105) nuclear-DNA encoded subunit were purchased from MitoSciences (Eugene, OR). Hemispheric homogenate samples were spun at 16000 *g* for 15 min at 4°C to obtain mitochondria-enriched pellets. Protein concentrations were determined by the Lowry method and 50 µg from each sample was run on a NuPAGE® 4%-12% Bis-Tris Novex® gel (Invitrogen). Proteins were transferred onto a polyvinylidene fluoride membrane and blocked for 1-h with 5% milk powder in Tris-buffered saline with 0.1% Tween 20 (TBST). The membrane was incubated with 49KDa and Rieske FeS primary antibodies (1:1000 dilution) in 3% milk powder in TBST overnight at 4°C. After a 2-h incubation with horseradish peroxidase conjugated secondary antibodies (anti-mouse SC-2005; 1:5000 dilution, Santa Cruz Biotechnology, Santa Cruz, CA and anti-rabbit NA934; 1:10 000 dilution, GE Healthcare, Quebec, Canada), the membrane was developed by Western Lightning® enhanced chemiluminescence (Perkin Elmer, Rockford, IL) and exposed to film. Blots were stripped and reprobed with antibodies to NDUF8 (1:1000 dilution) and citrate synthase (1:3000 dilution). Expression of subunit relative to citrate synthase was quantified by densitometry with ImageJ 1.44V software (National Institutes of Health).

5.3.4 Heat-Inactivated Tissue Preparation

Aged TgCRND8 mice and non-Tg controls were sacrificed with a head-focused pulse (<1 sec) of microwave radiation (10-kW rodent brain fixation system: Muromachi, Kikai, Tokyo), as described (Francis *et al.*, 2012b). Such rapid fixation of the brain *in situ* is necessary to reliably measure basal *ex vivo* levels of lipids and high-energy phosphate donors (Murphy, 2010; McCandless *et al.*, 1984). Microwaved brains were bisected. One hemisphere was stored at -80°C for cardiolipin analysis. From the contralateral

hemisphere, the cortex and hippocampus were dissected for measurements of energetic metabolites.

5.3.5 Measurement of Cardiolipin

Total lipids were extracted from microwaved brains of 9 TgCRND8 mice and 6 non-Tg controls, aged 32 to 48 weeks, using chloroform: methanol: 0.88% potassium chloride (2: 1: 0.75 by volume) (Folch *et al.*, 1957). Cardiolipin was isolated from the total lipid extract by thin layer chromatography (TLC). Its fatty acids were converted to fatty acid methyl esters (FAMES), which were separated and identified on a Varian-430 gas chromatograph (Varian, Lake Forest, CA) equipped with a Varian FactorFour capillary column (VF-23 ms; 30 m x 0.25 mm i.d. x 0.25 μ m film thickness) and a flame ionization detector, as described (Chen *et al.*, 2009). Peaks were identified by retention times of FAME standards (Nu-Chek-Prep, Elysian). Fatty acid concentrations (nmol/g) were calculated by proportional comparison of gas chromatography peak areas to that of the heptadecanoic acid internal standard.

5.3.6 High-Energy Phosphate Donors

Levels of ATP, ADP, AMP and creatine were measured in 0.1 N perchloric acid extracts from heat-inactivated frontal cortex and hippocampus of 40 – 52-week-old TgCRND8 and non-Tg littermates ($n \geq 7$ per group) mice. Analytes were separated by isocratic reverse-phase chromatography (Dionex, Sunnyvale, CA) on a SupelcosilTM LC-18-DB, 25 cm X 4.6 mm column and were measured with a Dionex Ultimate 3000 VWD UV detector, operated at absorbance wavelengths of 215 nM and 260 nM, as described (Mount *et al.*, 2004).

5.3.7 Statistical Analysis

Data were evaluated by unpaired Student's *t* tests, and are expressed as means \pm standard error of the mean (SEM). Differences were significant at $P < 0.05$.

5.4 Results

5.4.1 Linked Complex I+III Activity and NDUF8 Complex I Subunit Expression are Reduced in Aged TgCRND8 mice

We measured native activities of PDH, α -KGDH, linked complex I+III and complex IV in brains of 45-week-old mice. Only complex I+III was compromised (Figure 5-1). Its activity was reduced ~50% in aged TgCRND8 mice, as compared to littermate controls ($t(8)=5.33$, $P=0.0007$). We investigated whether the reduction in activity might be associated with altered expression of key integral nuclear-DNA encoded subunits of complexes I or III. NDUF8, an evolutionarily conserved core subunit, nucleates the assembly of the hydrophilic peripheral/matrix arm of complex I and is essential for the hydrogenase function of the enzyme. NDUF8 is a structural subunit in the hydrophobic membrane arm of complex I, important for full assembly of the complex and for supercomplex assembly with complex III (reviewed in Vogel *et al.*, 2007). Rieske FeS is one of 3 redox subunits that constitute the catalytic center of complex III. Protein levels of the 49kDa (NDUF8) and NDUF8 complex I subunits, and Rieske FeS complex III subunit were determined by western blot analysis in the same brain homogenates that were used for enzymatic assays (Figure 5-2). Decreased complex I+III activity in TgCRND8 mice was found to coincide with reduced NDUF8 expression ($t(6)=2.69$, $P=0.0362$).

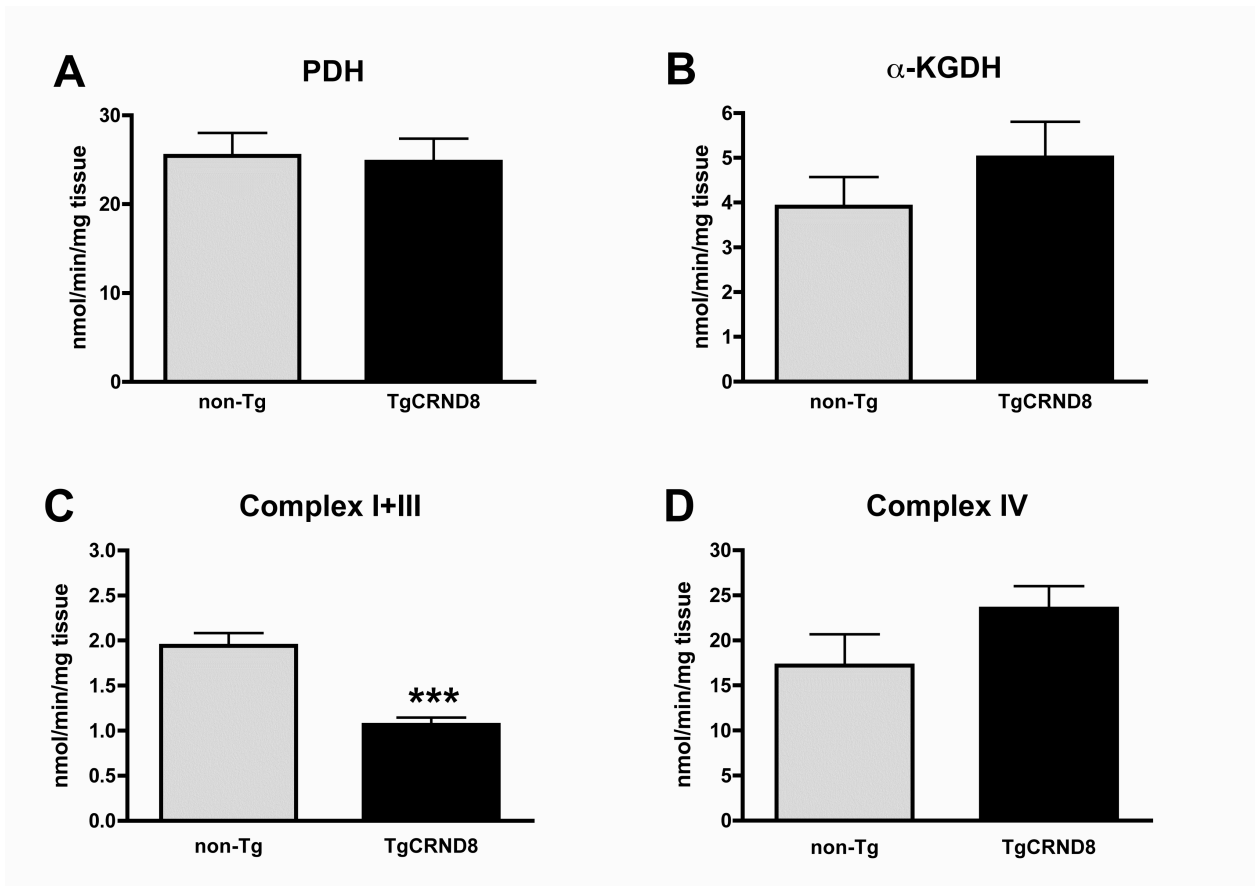


Figure 5-1. Complex I+III activity is reduced in aged TgCRND8 brains.

Hemispheric brain mitochondrial enzymatic activity was measured in 45-week-old mice. Pyruvate dehydrogenase (PDH) and α -ketoglutarate dehydrogenase (α -KGDH) complex activities were measured by $^{14}\text{CO}_2$ capture, and linked complex I+III (NADH: cytochrome *c* reductase) and complex IV (cytochrome *c* oxidase) activities were measured spectrophotometrically at 550nm. Complex I+III activity was reduced by 45% in aged TgCRND8 mice (C), whereas activities of PDH (A), α -KGDH (B) and complex IV (D) were unaffected. Values are means \pm SEM of $n \geq 5$ mice per group. *** $P \leq 0.001$ versus littermate non-Tg controls by unpaired Student's *t* test.

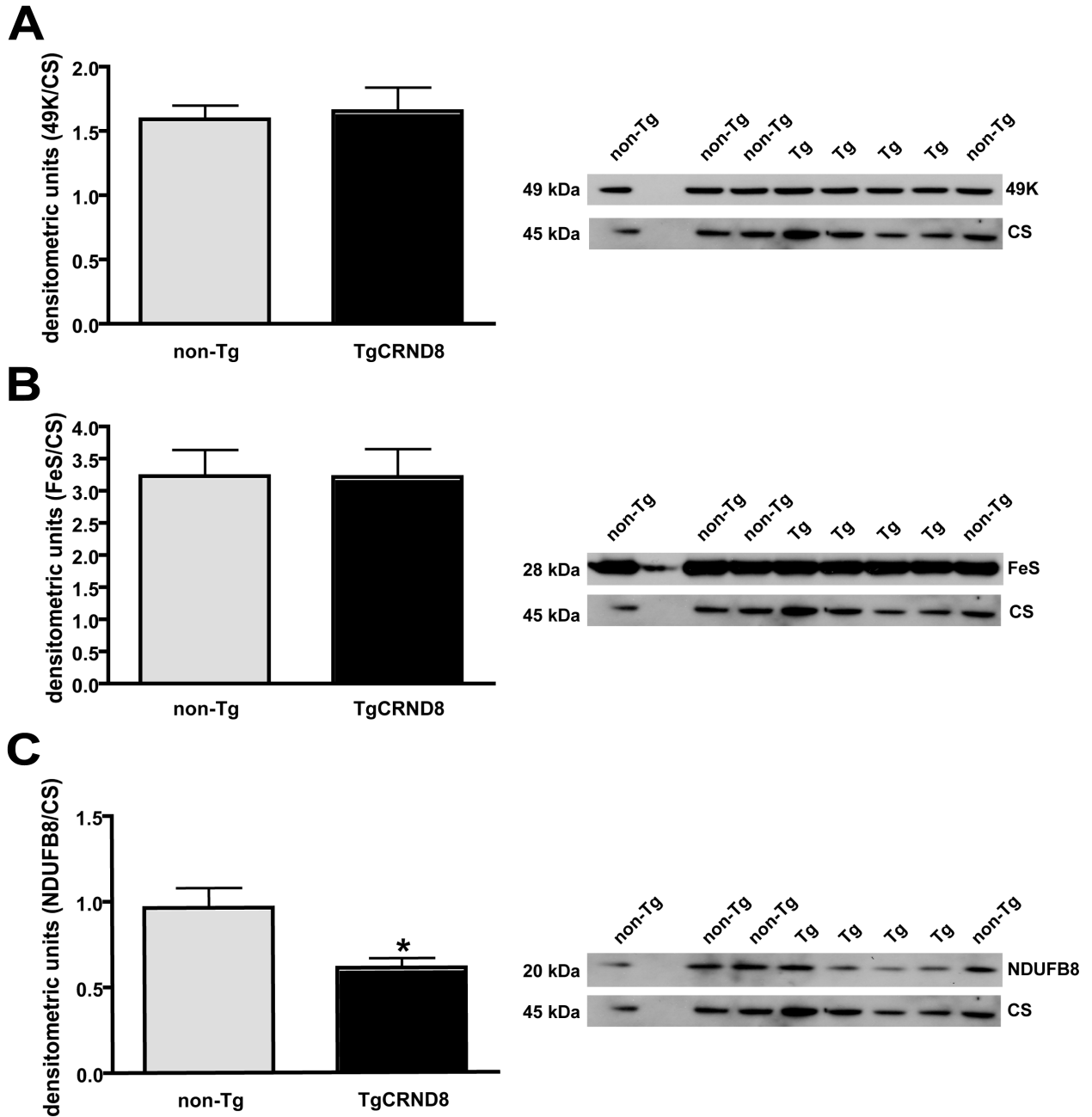


Figure 5-2. Expression of the complex I NDUF8 subunit is decreased in aged TgCRND8 brains. Immunoblots of mitochondria-enriched fractions of brain homogenates from 45 week-old mice were probed with antibodies against the complex I subunit, 49K (NDUFS2) and the complex III subunit, FeS. Blots were stripped and reprobed for the complex I subunit, NDUF8 and citrate synthase (CS). Densitometric analyses of the subunit band intensities (normalized against CS signal) were performed with ImageJ software. Expression of NDUF8 was reduced in aged TgCRND8 brains (C). * $P \leq 0.05$ versus non-Tg mice by unpaired Student's *t* test.

5.4.2 Cardiolipin is Unaltered in TgCRND8 Mice

Alterations in cardiolipin can cause reduced complex I+III activity. Cardiolipin is a tetra-acyl phospholipid found almost exclusively in the inner mitochondrial membrane, where it plays important roles in membrane fluidity and tethering of respiratory complexes (reviewed in Pope *et al.*, 2008). We found no differences between TgCRND8 and non-Tg brains in levels of total cardiolipin (Figure 5-3) ($t(13)=0.8608$, $P=0.4049$) or its fatty acid components.

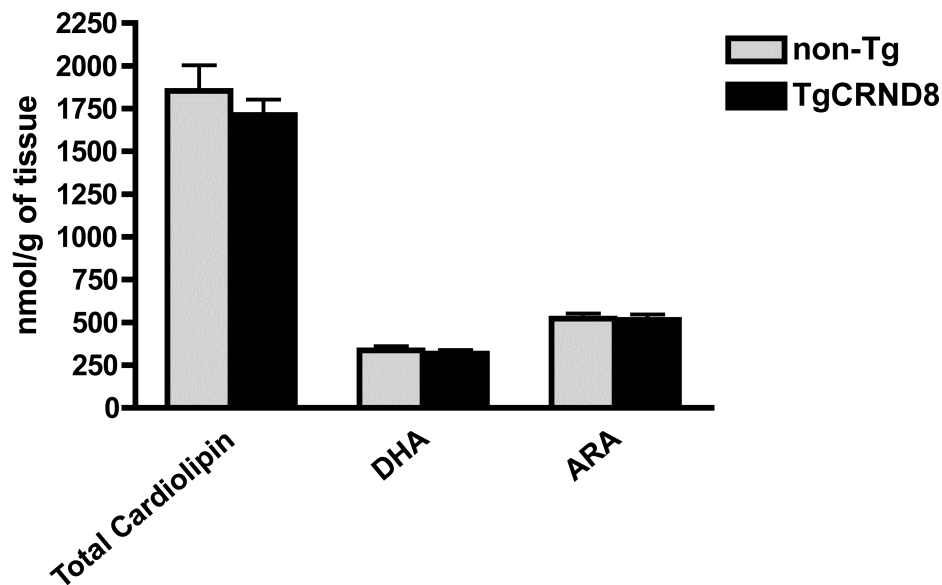


Figure 5-3. Neither cardiolipin nor its fatty acid constituents are altered in TgCRND8 mice. Aged TgCRND8 and non-Tg mice did not exhibit differences in levels of total cardiolipin (nmol/g tissue) or its fatty acid constituents, including docasahexaenoic acid (DHA; 22:6n-3) and arachidonic acid (ARA; 20:4n-6), shown here. Values are means \pm SEM of 9 TgCRND8 and 6 non-Tg mice.

5.4.3 ATP is Maintained While Creatine is Upregulated at End-Stages of Disease

To determine whether reduced brain complex I+III activity might alter bioenergetic charge, we examined the content of high-energy phosphate donors in the hippocampus and cortex of 40 to 52 week-old TgCRND8 mice. ATP levels (Figure 5-4a) and energetic charge (Figure 5-4b) were maintained. However, creatine content (Figure 5-4c) was elevated in the cortex ($t(11)=3.698$, $P=0.0035$) and hippocampus ($t(15)=2.646$, $P=0.0183$) of aged TgCRND8 mice compared to littermate controls.

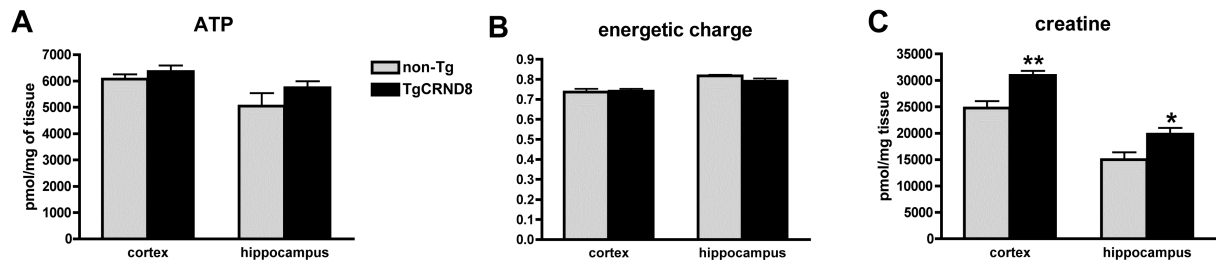


Figure 5-4. Tissue levels of ATP are maintained while those of creatine are upregulated in the cortex and hippocampus of aged TgCRND8 mice. TgCRND8 mice exhibited normal levels of ATP (A) but increased creatine (C) content in the cortex and hippocampus. No depletion of energetic charge [calculated as $(ATP+0.5 \times ADP)/(ATP+ADP+AMP)$] was observed in either brain area (B). Values are mean analyte concentrations (pmol/mg tissue) \pm SEM of $n \geq 7$. * $P \leq 0.05$, ** $P \leq 0.01$ versus non-Tg controls by unpaired Student's t test.

5.5 Discussion

We investigated activities of key mitochondrial enzymes in brains of TgCRND8 mice and observed a ~50% reduction in linked complex I+III activity at late stages of plaque pathology. The reduced activity was associated with decreased expression of the complex I subunit NDUFB8. Deficient oxidative phosphorylation (OXPHOS) was not associated with reductions in ATP brain tissue content. However, levels of creatine were elevated. Increases in creatine likely buffer tissue ATP levels in TgCRND8 mice, compensating for the severe reductions in complex I+III activity.

A β can impair mitochondrial function (reviewed in Swerdlow, 2012; Ye *et al.*, 2012). Mutation-specific alterations in levels of energy metabolites and in the trafficking, morphology and oxidative capacity of mitochondria, have been described in both APP- and presenilin (PS1)-transgenic mice (Trushina *et al.*, 2012). In the 5xFAD transgenic mouse, that harbors 5 familial AD mutations, APP, A β and the β -secretase-cleaved terminal fragment of APP (C99) were targeted to the inner membrane and matrix of mitochondria, where they contribute to oxidative DNA damage and reduced OXPHOS (Devi and Ohno, 2012). Tg2576 mice also exhibit mitochondrial dysfunction. Like TgCRND8 animals, the Tg2576 mice express mutant human APP under control of the hamster prion promoter. The Tg2576 *APP* transgene includes the Swedish double mutation, but lacks the Indiana V717F mutation. Relative to TgCRND8 mice, these animals develop similar, though relatively delayed cognitive and pathologic phenotypes. In the Tg2576 model, oligomeric A β has been associated with increased hydrogen peroxide, marginal reductions in complex IV activity (Manczak *et al.*, 2006), deregulation of protein subunits of complexes I and III, reduced electron transfer from complex I to complex IV, and decreased complex I function (Gillardon *et al.*, 2007). Collectively, these findings point to problem with complex I, though the molecular targets of this impairment have remained elusive.

In TgCRND8 brains, compromised complex I+III activity does not reflect a general decline in mitochondrial density or function. We did not observe any change in PDH, α -

KGDH or complex IV enzyme rates. Rather, deficits in complex I+III activity are likely related to the reduced expression of NDUFB8, an integral structural component of complex I. Complex I (NADH: ubiquinone oxidoreductase, EC 1.6.5.3) is the first and the largest of the OXPHOS complexes embedded in the inner mitochondrial membrane. In mammals, the L-shaped complex consists of 45 subunits, 7 of which are encoded by mitochondrial DNA and the remainder encoded by nuclear DNA (reviewed in Vogel *et al.*, 2007). Complex I is unstable alone and is usually organized into respiratory supercomplexes (respirasomes) with dimeric complex III. The membrane subunits of complexes I and III interact to assemble into functional respirasomes, which results in increased kinetic efficiency of electron transfer, stabilization of complex I, and reduced superoxide production (reviewed in Lenaz *et al.*, 2010). We investigated expression levels of NDUFS2, NDUFB8 and FeS, nuclear-DNA encoded subunits in the matrix arm of complex I, the membrane arm of complex I, and the catalytic center of complex III, respectively. Of these, only NDUFB8 was significantly decreased in aged TgCRND8 brains. NDUFB8 is not involved in the catalytic action of complex I but is an essential component of the nuclear-DNA encoded membrane anchor needed for full assembly of the holoenzyme and for supercomplex assembly with complex III (Lazarou *et al.*, 2007). NDUFB8 was identified as a candidate gene involved in neurodegenerative disorders (Emahazion *et al.*, 1999); its gene expression level was significantly downregulated in AD (Li *et al.*, 2003).

Davis and colleagues (2010) demonstrated the importance of the NDUFB8 subunit in mitochondrial function. They found that mitochondrial-derived superoxides promote the nitration of NDUFB8, thereby reducing complex I activity. Overexpression of mitochondrial superoxide dismutase significantly decreased NDUFB8 nitration, restored complex I activity and mitochondrial homeostasis. Furthermore, selective knockdown of NDUFB8 caused an overall reduction in mitochondrial oxygen consumption. The authors hypothesized that the selective nitration of NDUFB8 leads to disruption of supercomplex assembly and the inactivation of complex I. Inhibition of complex I increases superoxide production (Perier *et al.*, 2005). Thus the decreased complex I+III activity in TgCRND8 mice may contribute to increasing reactive oxygen species, decreasing NDUFB8 expression and potentiating OXPHOS impairment.

Compromised complex I+III activity in TgCRND8 mice was not associated with changes in cardiolipin, the major phospholipid constituent of inner mitochondrial membranes. Cardiolipin deficiency destabilizes interactions between complexes I and III, resulting in reduced levels and enzymatic activity of complex I (McKenzie *et al.*, 2006). The absence of alterations in cardiolipin in our mice is consistent with findings in the clinical disease. Total content and fatty acid composition of cardiolipin are not modified to any great extent in human AD (Guan *et al.*, 1994). Our results extend those of Kuzyk *et al.* (2010) who reported no disturbances in the overall distribution of lipids in the TgCRND8 brain.

To determine how severely decreased complex I+III activity affects mitochondrial output, we examined tissue levels of high-energy phosphate donors in the hippocampus and cortex. ATP content and energetic charge were maintained, whereas creatine was significantly upregulated. Focal microcrystalline deposits of creatine have been described in the hippocampus of AD patients and in TgCRND8 mice (Gallant *et al.*, 2006; Kuzyk *et al.*, 2010). Creatine kinase can generate ATP much faster than OXPHOS or glycolysis and is an efficient energy buffer system during stress. Creatine supplementation can fortify energy reserves and protect neurons against A β toxicity (Brewer and Wallimann, 2000). Our observations suggest that increases in creatine also contribute to preserving energetic charge, at advanced stages of A β -induced pathology and mitochondrial impairment, in the aging TgCRND8 brain.

**Chapter 6 Dexefaroxan Improves Mitochondrial
Function in a Mouse Model of
Alzheimer's Disease**

6.1 Abstract

The TgCRND8 mouse model of Alzheimer's disease (AD) exhibits progressive amyloid accumulation that has been linked to behavioural impairment and depletion of tissue noradrenaline levels. We measured activity of electron transport chain enzyme complexes as well as tissue content of ATP and creatine in the hippocampus and cortex in young TgCRND8 mice, before (7-9 weeks) and after (16 weeks) the onset of plaque pathology and spatial memory impairment. Hippocampal tissue levels of ATP were reduced in 16-week-old TgCRND8 mice whereas creatine levels and complex I+III activity were unaffected. In the cortex, creatine and complex I+III activity were both increased, but ATP levels remained unchanged. Chronic treatment with dexefaroxan, an antagonist of inhibitory α_2 -adrenoceptors on noradrenergic and cholinergic terminals, improved the hippocampal ATP deficit in 16-week-old mice. The cholinesterase inhibitor, rivastigmine, elicited a similar effect. In aged TgCRND8 mice with extensive plaque pathology (45 – 50 weeks), both dexefaroxan and rivastigmine rescued deficits in complex I+III activity. The stimulatory effects of α_2 -adrenoceptor blockade on mitochondrial function further support its use in the treatment of AD.

6.2 Introduction

Alzheimer's disease (AD) is characterized by progressive cognitive decline, by the appearance in CNS of amyloid- β ($A\beta$) plaques and neurofibrillary tangles and by neuronal loss. Intracellular $A\beta$, a 39-43 amino acid peptide derived through sequential β - and γ -secretase cleavage of amyloid precursor protein (APP), triggers neuronal dysfunction long before it is deposited in insoluble plaques (reviewed in Hardy and Selkoe, 2002; Larson and Lesné, 2012). APP and $A\beta$ have been found within the mitochondrion, causing bioenergetic depletion by inhibiting respiratory enzymes in the electron transport chain (ETC) and promoting leakage of reactive oxygen species (reviewed in Maruszak and Zekanowski, 2011). It is unclear how mitochondrial dysfunction is related to other pathophysiological features of AD. These include reduction in noradrenergic efferents from the locus coeruleus (Adolfsson *et al.*, 1979; Mann *et al.*, 1980; Marcyniuk *et al.*, 1986; German *et al.*, 1992; Matthews *et al.*, 2002; Zarow *et al.*, 2003; Grudzien *et al.*, 2007). The catechol moiety of noradrenaline makes it an endogenous antioxidant in the brain (Troadek *et al.*, 2001; Traver *et al.*, 2005). The loss of noradrenaline in AD brains may render forebrain neural circuits especially vulnerable to $A\beta$ toxicity. Indeed, noradrenergic activation of β -adrenoceptor signalling cascades has been found to induce expression of neurotrophins and to mitigate $A\beta$ -induced oxidative stress and mitochondrial dysfunction (Counts and Mufson, 2010).

We examined mitochondrial function in APP-transgenic TgCRND8 mice, expressing a double mutated APP₆₉₅ gene (Swedish: KM670/671NL and Indiana: V717F) with the pan-neuronal Syrian hamster prion gene promoter (Chishti *et al.*, 2001). This model recapitulates some cardinal features of AD. The mice develop $A\beta$ deposits in the hippocampus and cortex by 3 months (Chishti *et al.*, 2001) and cholinergic dysfunction at 7 months of age (Bellucci *et al.*, 2006). Prior to frank plaque pathology, TgCRND8 mice exhibit behavioural dysfunction, BDNF mRNA deficits and reduced noradrenaline content within major terminal fields (Francis *et al.*, 2012a,b). Reductions in noradrenaline turnover may mediate the $A\beta$ -induced impairment of object memory and behavioural despair in TgCRND8 mice. Pre-plaque mice treated with dexefaroxan, an

antagonist of inhibitory α_2 -adrenoceptors on noradrenergic terminals, exhibited a reversal of behavioural deficits and improved BDNF levels (Francis *et al.*, 2012b). In mice with advanced plaque pathology, microcrystalline deposits of creatine have been observed in the hippocampus (Gallant *et al.*, 2006). These creatine deposits are found by 5 months of age, and increase with A β burden (Kuzyk *et al.*, 2010). Elevated creatine tissue content suggests perturbed energetic status, although this possibility has not been examined in TgCRND8 mice.

We investigated mitochondrial function through stages of TgCRND8 disease progression by measuring the activities of key enzymes of oxidative metabolism as well as ATP and creatine content in the hippocampus and cortex. We focused on pre-plaque mice, both before (4 – 5 weeks) and after (7 – 9 weeks) the onset of object memory impairment, on animals exhibiting both plaques and spatial memory impairment (16 weeks) and on aged mice with advanced plaque pathology (36 – 45 weeks). We assessed the effects of increasing noradrenergic and/or cholinergic transmission on these bioenergetic parameters.

6.3 Methods

6.3.1 Mice

TgCRND8 and non-Tg mice were maintained on a hybrid C57BL/6/C3H x C57BL/6 genetic background and communally housed under standard laboratory conditions. Experimental groups were gender-balanced. Tests were approved by the Animal Care Committee at the University of Toronto, in accordance with the guidelines for the Use and Treatment of Animals, outlined by the Animal Care Council of Canada.

6.3.2 Drug Treatments

We investigated the effects of 28-day infusion of dexefaroxan (1.9 mg/kg/day), rivastigmine (0.48 mg/kg/day), or saline on mitochondrial function in young (12-week-old) and aged (40 – 45-week-old) TgCRND8 and non-Tg mice. Dexefaroxan hydrochloride (2-[2-(2-ethyl-2,3-dihydrobenzofuranyl)]-2-imidazoline) was synthesized at Pierre Fabre Medicament (Castres, France). Rivastigmine tartrate (Exelon) was obtained from Novartis Pharma AG (Basel, Switzerland). Drugs were administered via Alzet (DURECT Corporation, Cupertino, CA) osmotic mini-pumps (model 1002) implanted subcutaneously, as described (Francis *et al.*, 2012b). At the end of treatment, mice ($n \geq 6$ per group) were sacrificed by cervical dislocation for assessment of complex I+III and citrate synthase activities, or by microwave irradiation for determination of ATP and creatine levels.

6.3.3 Metabolic Enzyme Activities

TgCRND8 and non-Tg mice ($n \geq 8$ per group) were killed by cervical dislocation at 4, 9 or 16 weeks of age. Freshly removed brains were bisected sagittally. One intact hemisphere and the cortex (temporoparietal and frontal lobes) and hippocampus, dissected from the contralateral hemisphere, were snap frozen in liquid nitrogen. Tissues were homogenized in 10X w/v PDH buffer (10 mg/ml fatty acid free bovine serum albumin, 0.17 mg/ml dithiothreitol, 1 mg/ml NAD, 11 mM potassium phosphate, 3 mM $MgCl_2$, 1 mM EDTA, pH 7.4) and centrifuged at 3000 g for 10 min at 4°C. The supernatant was collected in 200 μ l aliquots and frozen in liquid nitrogen. Hemispheric homogenates from 9-week-old mice were used to analyze the activities of NADH: cytochrome c reductase (complexes I and III; EC 1.6.2.1), cytochrome oxidase (complex IV; EC 1.9.3.1), pyruvate dehydrogenase (PDH; complex of EC 1.2.4.1, EC 2.3.1.12 and EC 1.8.1.4) and α -ketoglutarate dehydrogenase (α -KGDH; complex of EC 1.2.4.2, EC 2.3.1.61 and EC 1.8.1.4). Activities of complexes I+III and IV were also determined in cortical and hippocampal homogenates from 4, 9 and 16 week-old mice. Enzyme activities were assayed in quadruplicate and expressed as nmol of product formed or precursor converted per minute per mg of wet weight brain tissue, at 37 °C.

6.3.3.1 *Pyruvate Dehydrogenase Complex*

Native activity of the PDH complex was measured via $^{14}CO_2$ capture (Maj *et al.*, 2005). An aliquot of brain homogenate was diluted in 0.6 ml potassium phosphate (KPi) buffer (1M, pH 7.4). The incubation mixture contained 8 ml PDH buffer, 1.42 mg coenzyme A, 0.91 mg sodium sulfate, 9 μ l of 0.1 M thiamine pyruvate phosphate, 16 μ l of 0.1 M pyruvate and 18 μ l of [1- ^{14}C]pyruvate. The [1- ^{14}C]pyruvate was made with 0.05 Ci [1- ^{14}C]pyruvate powder (Amersham Biosciences, Arlington Heights, IL) in 0.5 ml of 0.1 M hydrochloric acid, further diluted in 0.2 ml H_2O and bubbled with air for 10 min to eliminate CO_2 gas. The reaction was started by adding 50 μ l of sample to 200 μ l of

incubation mixture, held in 10 ml Erlenmeyer flasks in a water bath at 37°C. The reaction was stopped after 10 min with 100 µl of 10% trichloroacetic acid. The bath temperature was reduced to 25°C and the mixture equilibrated for an additional hour. $^{14}\text{CO}_2$ gas released from the oxidative decarboxylation of [1- ^{14}C]pyruvate by tissue PDH was captured in 0.2 ml benzethonium hydroxide, contained in wells attached to the Erlenmeyer flask stoppers. Radioactivity in benzethonium hydroxide was measured with a Beckman LS 6500 scintillation counter.

6.3.3.2 *α-Ketoglutarate Dehydrogenase Complex*

Native activity of the α -KGDH complex was also analyzed by $^{14}\text{CO}_2$ capture. Aliquots of brain homogenate (50 µl) were added to 200 µl of radioactive incubation mixture made with 8 ml PDH buffer, 1.42 mg of coenzyme A, 0.02 ml of 0.1M CaCl_2 , 10 µl of 200 mM ketoglutarate and 16 µl of [1- ^{14}C]ketoglutarate. $^{14}\text{CO}_2$ gas produced from the oxidative decarboxylation of [1- ^{14}C]ketoglutarate was captured and counted, as above.

6.3.3.3 *NADH: Cytochrome c Reductase*

Rotenone-sensitive complex I+III activity was determined by assessing the rate of cytochrome c reduction on a Cary Bio 300 UV-Vis Spectrophotometer (Varian Instruments, Palo Alto, CA) at 550 nm, as described (Seyda *et al.*, 2001). Brain homogenate (10µl) was added to experimental and reference cuvettes, each holding 1ml of 0.1 M KPi plus 1mM sodium azide buffer (pH 7.0) and 30 µl of 40 mg/ml horse heart ferricytochrome c in H_2O (Sigma Chemical Co., St. Louis, MO). Azide inhibited complex IV and prevented the re-oxidation of cytochrome c. 5µl of 1mM rotenone was added to reference cuvette to inhibit complex I. Readings were “zeroed” against the reference cuvette. Reduction of cytochrome c measured in this assay is due to the transfer of electrons from complex I through complex III. The reaction was timed from

the addition of 10 μl of 5 mg/ml NADH (Sigma) and recorded for 2 min. The first linear increase in absorbance was used to calculate the rate of cytochrome *c* reduction with extinction coefficient $\epsilon_{550\text{nm}} = 0.0185 \text{ nmol}^{-1}\text{cm}^{-1}$.

6.3.3.4 *Cytochrome Oxidase*

Complex IV activity was determined spectrophotometrically by measuring the oxidation of reduced cytochrome *c* at 550 nm (Seyda *et al.*, 2001). Horse heart ferricytochrome *c* was reduced with 0.5 M ascorbate (Sigma), and the excess ascorbate was removed by dialyzing against 0.1 M KPi buffer (pH 7.0) for 24-h at 4°C. Brain homogenates were further diluted with KPi buffer to 5% of its original concentration. Sample and reference cuvettes contained 1 ml of 0.1M KPi buffer and 30 μl of 40 mg/ml reduced cytochrome *c*. The reaction was initiated with 5 μl of 5% brain homogenate and recorded for 2 min. The initial linear decrease in absorbance was used to calculate the rate of cytochrome *c* oxidation with extinction coefficient $\epsilon_{550\text{nm}} = 0.0185 \text{ nmol}^{-1}\text{cm}^{-1}$.

6.3.3.5 *Citrate Synthase*

Citrate synthase (CS; EC 2.3.3.1) activity was assessed as an indicator of mitochondrial mass in tissues. CS, found in the mitochondrial matrix, catalyzes the condensation of acetyl-CoA and oxaloacetate, forming citrate and releasing CoA. CS activity was determined spectrophotometrically by measuring the reduction of 5,5'-dithio-bis-2-nitrobenzoic acid (DTNB) by freed CoA at 412 nm, as described (Maj *et al.*, 2011). Briefly, 10 μl of cortical homogenate was added to experimental and reference cuvettes, each containing 1 mL of Tris-HCL buffer (0.1M, pH 8.0), 10 μl of 4 mg/ml DTNB (Sigma Chemical Co., St. Louis, MO) and 2 μl of 30 mM acetyl-CoA (Roche). The reaction was initiated with 10 μl of oxaloacetic acid (50 mM, 6.6 mg/ml, pH 8.0, Sigma) and recorded

for 2 min. The initial linear increase in absorbance was used to calculate the rate of DTNB reduction, with extinction coefficient $\epsilon_{412\text{nm}} = 0.0136 \text{ nmol}^{-1}\text{cm}^{-1}$.

6.3.4 Western Blotting

Polyclonal antibodies to the human complex I 49kDa (NDUFS2) nuclear-DNA encoded subunit and citrate synthase were prepared, as described (Xu *et al.*, 2008). Mouse monoclonal antibodies to the complex III Rieske FeS (catalog # MS305) nuclear-DNA encoded subunit and the complex I NDUFB8 (catalog # MS105) nuclear-DNA encoded subunit were purchased from MitoSciences (Eugene, OR). Cortical and hippocampal homogenates from 9-week-old mice were spun at 16 000 g for 15 min at 4°C to obtain mitochondria-enriched pellets. Protein concentration was determined by the Lowry method and 50 µg from each sample was run on NuPAGE[®] 4%-12% Bis-Tris Novex[®] gels (Invitrogen). Proteins were transferred onto polyvinylidene fluoride membranes and blocked for 1 h with 5% milk powder in Tris-buffered saline with 0.1% Tween 20 (TBST). Membranes were incubated with 49KDa and Rieske FeS antibodies (1:1000 dilution) in 3% milk powder in TBST overnight at 4°C. Following a 2-h incubation with anti-mouse SC-2005 (1:5000 dilution, Santa Cruz Biotechnology, CA) and anti-rabbit NA934 (1:10 000 dilution, GE Healthcare, Quebec, Canada) horseradish peroxidase conjugated secondary antibodies, membranes were developed by Western Lightning[®] enhanced chemiluminescence (Perkin Elmer, Rockford, IL) and exposed to film. Blots were stripped and re probed with antibodies to NDUFB8 (1:1000 dilution) and citrate synthase (1:3000 dilution). Expression of each subunit relative to citrate synthase was analyzed by densitometry and ImageJ 1.44V (National Institutes of Health).

6.3.5 Measurement of Tissue ATP and Creatine

TgCRND8 mice and non-Tg littermates ($n \geq 6$ per group) were sacrificed at 7 – 9 or 16 weeks of age by microwave irradiation (10 kW Muromachi Brain Fixation system: Muromachi, Kikai, Tokyo), as described (Francis *et al.*, 2012b). Tissue levels of ATP and creatine were measured in 0.1 N perchloric acid extracts from cooked hippocampus and frontal cortex. Analytes were separated by isocratic reverse-phase chromatography (Dionex, Sunnyvale, CA) on a Supelcosil™ LC-18-DB, 25 cm X 4.6 mm column and measured with a Dionex Ultimate 3000 VWD UV detector at absorbance wavelengths of 215 nM and 260 nM. Analyte levels are expressed as pmol/mg of tissue.

6.3.6 Statistical Analyses

Data were evaluated by unpaired Student's *t*-tests or, in the case of multiple comparisons, by non-repeated measures 2-way analysis of variance (ANOVA). When ANOVAs yielded significant main effects of genotype and/or treatment, pairwise comparisons were assessed by Fisher's protected least significant difference (LSD) test. Differences were significant at $P < 0.05$.

6.4 Results

6.4.1 Cortical Complex I+III Activity is Increased in Young TgCRND8 Mice

We measured native activities of PDH, α -KGDH, linked complex I+III and complex IV in brain hemispheres of pre-plaque 9 week-old mice and did not find significant differences between TgCRND8 and non-Tg littermates (Figure 6-1). To investigate whether specific loci within the hemisphere might be affected at earlier stages of A β accumulation, we assessed activities of complex I+III and complex IV in the hippocampus and cortex of pre-plaque 4-5 and 9 week-old mice and of 16 week-old mice with early plaque pathology. Complex I+III activity was increased in the cortex of 9 ($t(14)=2.508$, $P=0.025$) and 16 week-old ($t(17)=3.237$, $P=0.005$) TgCRND8 mice (Figure 6-2b), but was unaltered in the hippocampus (Figure 6-2a). Complex IV enzyme rates were equivalent in TgCRND8 and non-Tg littermates at all ages tested (Table 6-1).

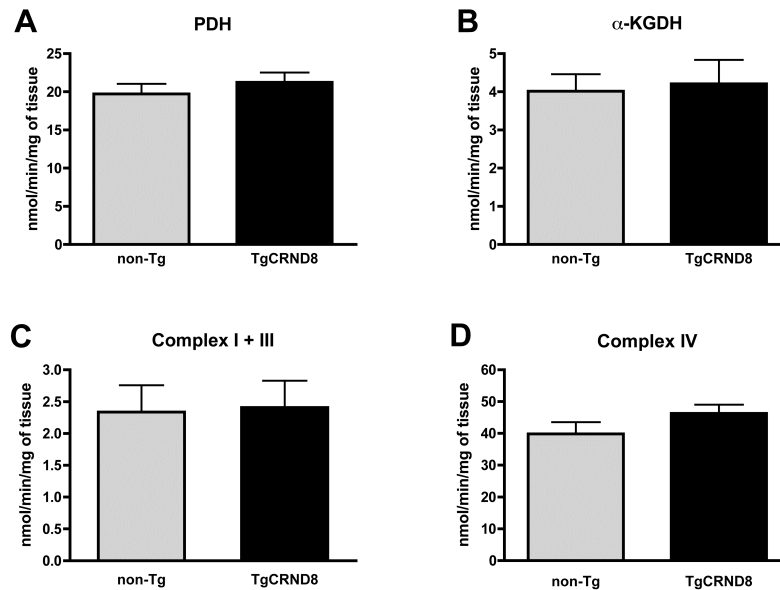


Figure 6-1. Hemispheric mitochondrial enzyme activities are not altered in 9 week-old TgCRND8 mice. Native activities of PDH (A), α -KGDH (B), linked complex I+III (C) and complex IV (D) was measured in brain hemispheres of 9 week-old mice. Activity is expressed as nmol of product formed/ precursor converted per min per mg of wet weight tissue. No differences were observed between TgCRND8 and non-Tg littermates. Values are means \pm SEM of ≥ 5 mice per group.

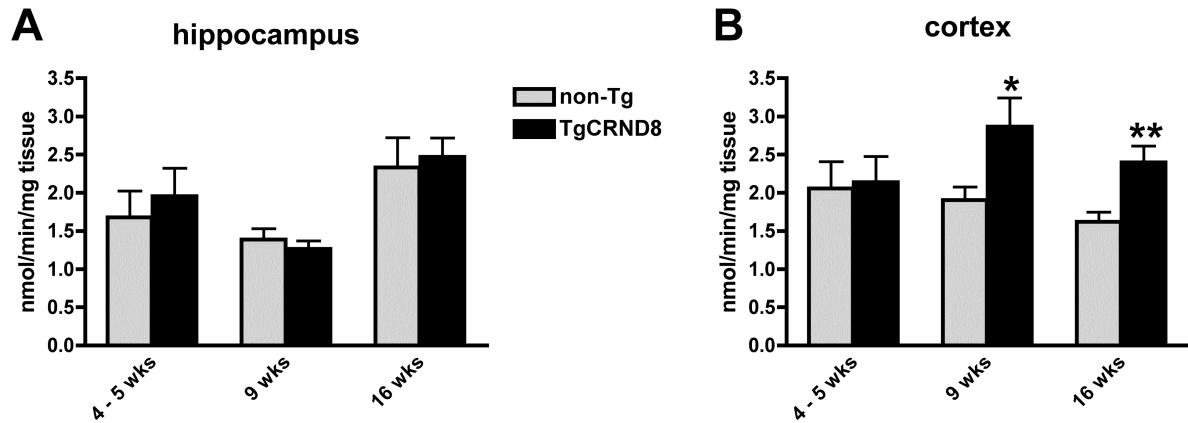


Figure 6-2. Complex I+III activity is increased in the cortex, but not in the hippocampus at early stages of disease progression. Complex I+III activity, expressed as nmol of cytochrome *c* reduced /min/mg of tissue, was measured in cortical and hippocampal samples from 4 – 5, 9 and 16 week-old TgCRND8 and non-Tg mice. Nine and 16 week-old TgCRND8 mice exhibited increased complex I+III activity in cortex (**B**), but not in the hippocampus (**A**). Values are means \pm SEM of ≥ 7 mice per group. * $P \leq 0.05$, ** $P \leq 0.01$ versus non-Tg controls by unpaired Student's *t* test.

Table 6-1. Cortical and hippocampal Complex IV activity in TgCRND8 mice

		4-5 weeks	9 weeks	27 weeks
Cortex	non-Tg	20.18 \pm 3.15	35.08 \pm 1.68	24.88 \pm 1.40
	TgCRND8	21.50 \pm 3.16	34.38 \pm 2.45	25.90 \pm 2.61
Hippocampus	non-Tg	9.63 \pm 0.41	17.76 \pm 1.99	17.06 \pm 1.66
	TgCRND8	13.08 \pm 2.53	17.98 \pm 2.17	22.07 \pm 2.29

Complex IV activity is expressed as nmol of cytochrome *c* oxidized/min/mg of wet weight tissue. Values are means \pm SEM of ≥ 6 mice per group.

6.4.2 Key Subunits of Complexes I and III are NOT Differentially Expressed in Young TgCRND8 Mice

To determine whether complex I+III activity reflected selective increase in complex I, or III expression, we examined levels of integral nuclear-DNA encoded subunits of complexes I and III. Protein levels of the 49kDa (NDUFS2) core subunit in the hydrophilic matrix arm of complex I, the NDUF8 structural subunit in the hydrophobic

membrane arm of complex I and the Rieske FeS redox complex III subunit were determined in aliquots of the same hippocampal and cortical samples that were used for enzymatic assays. Increased complex I+III activity was not reflected in altered expression of NDUFB8, NDUFS2 or Rieske FeS (Figure 6-3).

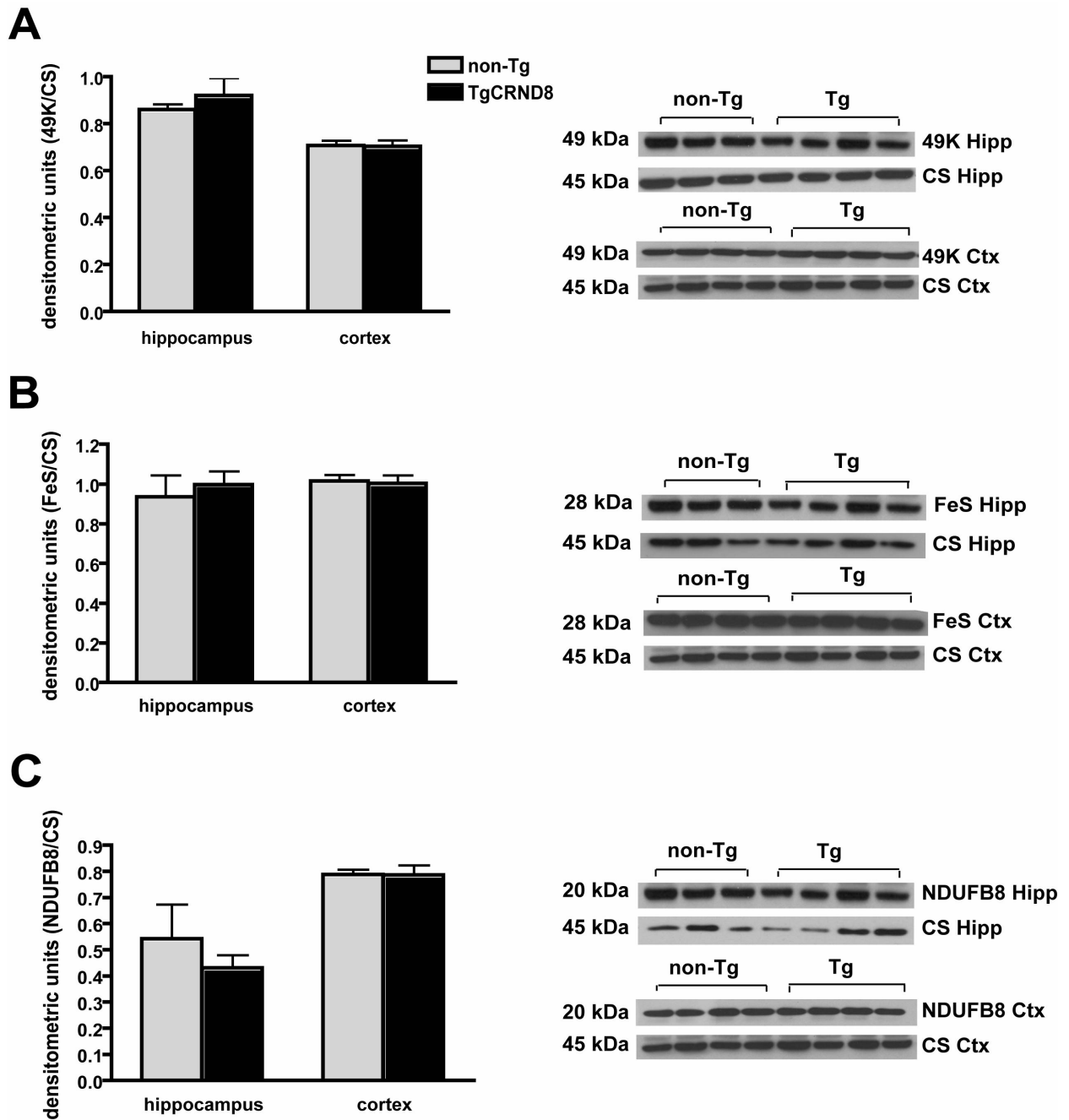


Figure 6-3. Expression of major nuclear-DNA encoded subunits of complexes I and III is unaltered in the hippocampus and cortex of 9 week-old mice.

Immunoblots of cortical and hippocampal homogenates from 9-week-old mice were probed with antibodies against the complex I subunit, 49K (NDUFS2) and complex III subunit, FeS. Blots were stripped and reprobed for the complex I subunit, NDUFB8 and for citrate synthase (CS). Densitometric analyses of the subunit band intensities were performed using ImageJ software. Data were normalized to the corresponding expression level of CS in each sample. Expression of 49K **(A)**, FeS **(B)** or NDUFB8 **(C)** was not altered in the hippocampus or cortex of the young TgCRND8 mice.

6.4.3 ATP is Transiently Depleted in the Hippocampus of Plaque-Bearing Mice, but Maintained in Cortical Regions with Increased Creatine Content

To determine whether the increase in complex I+III activity might alter tissue levels of high-energy phosphates, we measured ATP and creatine in the hippocampus and cortex of 9 and 16 week-old TgCRND8 mice. At 9 weeks of age, no differences were observed in the levels of ATP or creatine between TgCRND8 and non-Tg mice (Figure 6-4). By 16 weeks, regionally distinct changes were seen. In the hippocampus, where complex I+III activity was not altered, ATP declined at 16 weeks ($t(11)=2.428$, $P=0.033$; Figure 6-4a), while creatine remained unchanged (Figure 6-4b). In the cortex, where complex I+III activity was elevated, ATP was maintained (Figure 6-4c) as creatine increased ($t(18)=2.703$, $P=0.015$; Figure 6-4d) with A β burden.

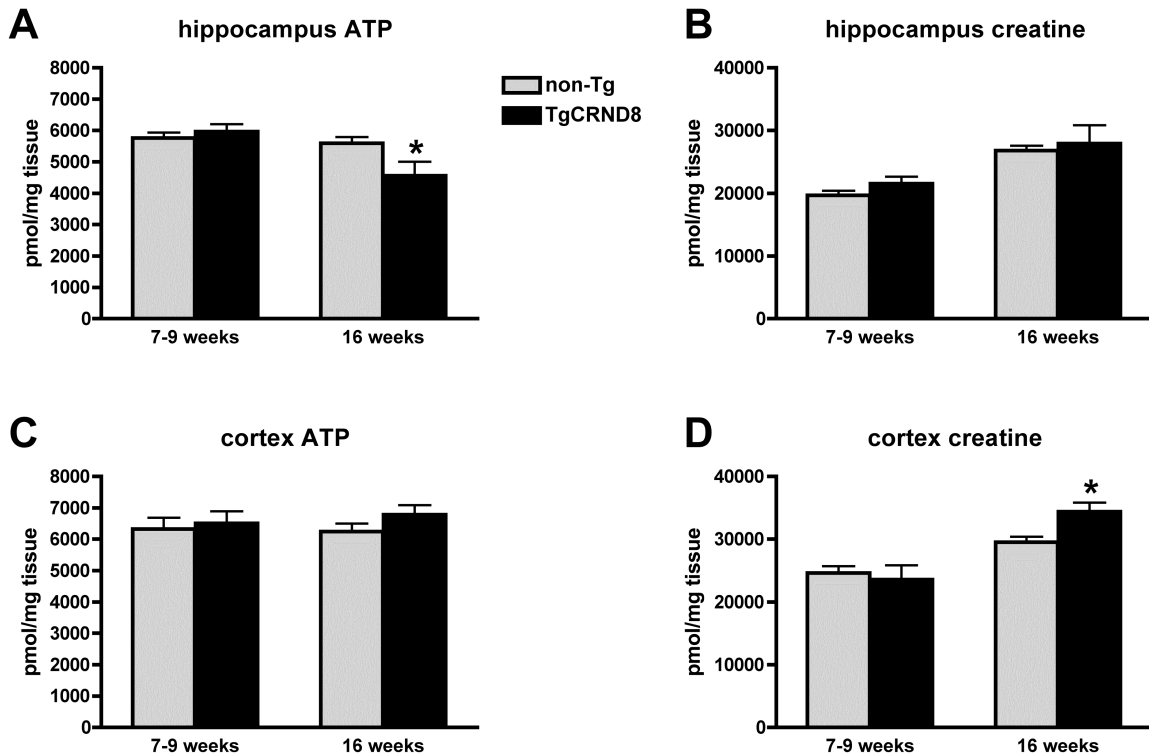


Figure 6-4. Plaque-bearing mice exhibit reduced ATP tissue content in the hippocampus, but not in the cortex where creatine content is increased.

At 16 weeks of age, ATP was depleted in the hippocampus of TgCRND8 mice (A). Cortical levels of ATP were maintained (C) while creatine increased (D) in TgCRND8 mice with plaques. Values are mean analyte concentrations (pmol/mg tissue) \pm SEM of $n \geq 6$. * $P \leq 0.05$, ** $P \leq 0.01$ versus non-Tg controls by unpaired Student's t test.

6.4.4 Dexefaroxan and Rivastigmine Increase ATP and Complex I+III Activity

We examined whether a 28-day infusion of dexefaroxan or rivastigmine might affect TgCRND8 mitochondrial phenotypes at 16 weeks. These treatments have been shown to improve behaviour and BDNF mRNA levels in TgCRND8 mice (Francis *et al.*, 2012b). Neither treatment altered creatine levels in the hippocampus ($F_{2,50}=1.08$, $P=0.346$) or cortex ($F_{2,60}=0.67$, $P=0.515$). We found interacting effects of genotype and treatment on ATP levels in the hippocampus ($F_{2,50}=8.00$, $P=0.001$; Figure 6-5a) but not in the cortex (Figure 6-5b), where complex I+III activity and creatine was increased. Both

dexefaroxan ($t(10)=2.364$, $P=0.039$) and rivastigmine ($t(12)=2.866$, $P=0.014$) reversed the hippocampal ATP deficit at 16 weeks (Figure 6-5a).

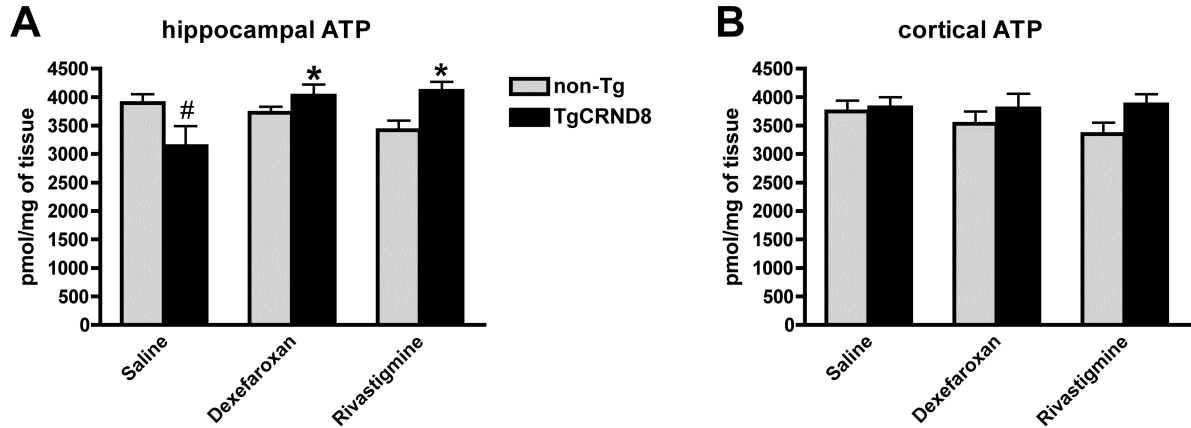


Figure 6-5. Dexefaroxan and rivastigmine restore hippocampal ATP levels in young TgCRND8 mice. ATP was depleted in the hippocampus (A) but unaltered in the frontal cortex (B) of 16-week-old TgCRND8 mice. Both dexefaroxan and rivastigmine treatments rescued ATP levels in the hippocampus (A). Values are mean ATP concentrations (pmol/mg tissue) \pm SEM of ≥ 6 mice per group. * $P \leq 0.05$ versus saline controls; # $P \leq 0.05$ versus non-Tg saline-treated mice by 2-way ANOVA followed by Fisher's protected LSD test.

We found that genotype ($F_{1,42}=5.34$, $P=0.026$) and treatment ($F_{2,42}=11.43$, $P=0.0001$) affected complex I+III activity in the cortex (Figure 6-6a) but not in the hippocampus. Cortical complex I+III activity in TgCRND8 mice was upregulated at 16 weeks ($t(17)=3.237$, $P=0.005$; Figure 6-6a). Dexefaroxan increased complex I+III activity in non-Tg controls ($t(14)=4.470$, $P=0.005$) but did not boost the already elevated activity in TgCRND8 cortices. Rivastigmine did not alter cortical complex I+III activity in these 16-week-old mice (Figure 6-6a).

With increasing age, we observed diminished complex I+III activity in both brain areas. This effect was exacerbated in animals with advanced plaque pathology. At 45 weeks of age, TgCRND8 cortical complex I+III activity was reduced in comparison to that of non-Tg animals ($t(12)=3.453$, $P=0.005$; Figure 6-6b). Both dexefaroxan ($t(12)=2.321$,

$P=0.038$) and rivastigmine ($t(11)=2.667$, $P=0.022$) restored complex I+III activity to non-Tg levels (Figure 6-6b). Neither treatment altered tissue levels of citrate synthase activity (Figure 6-6c,d), suggesting that both drugs modulated complex I+III selectively, rather than increasing mitochondrial density.

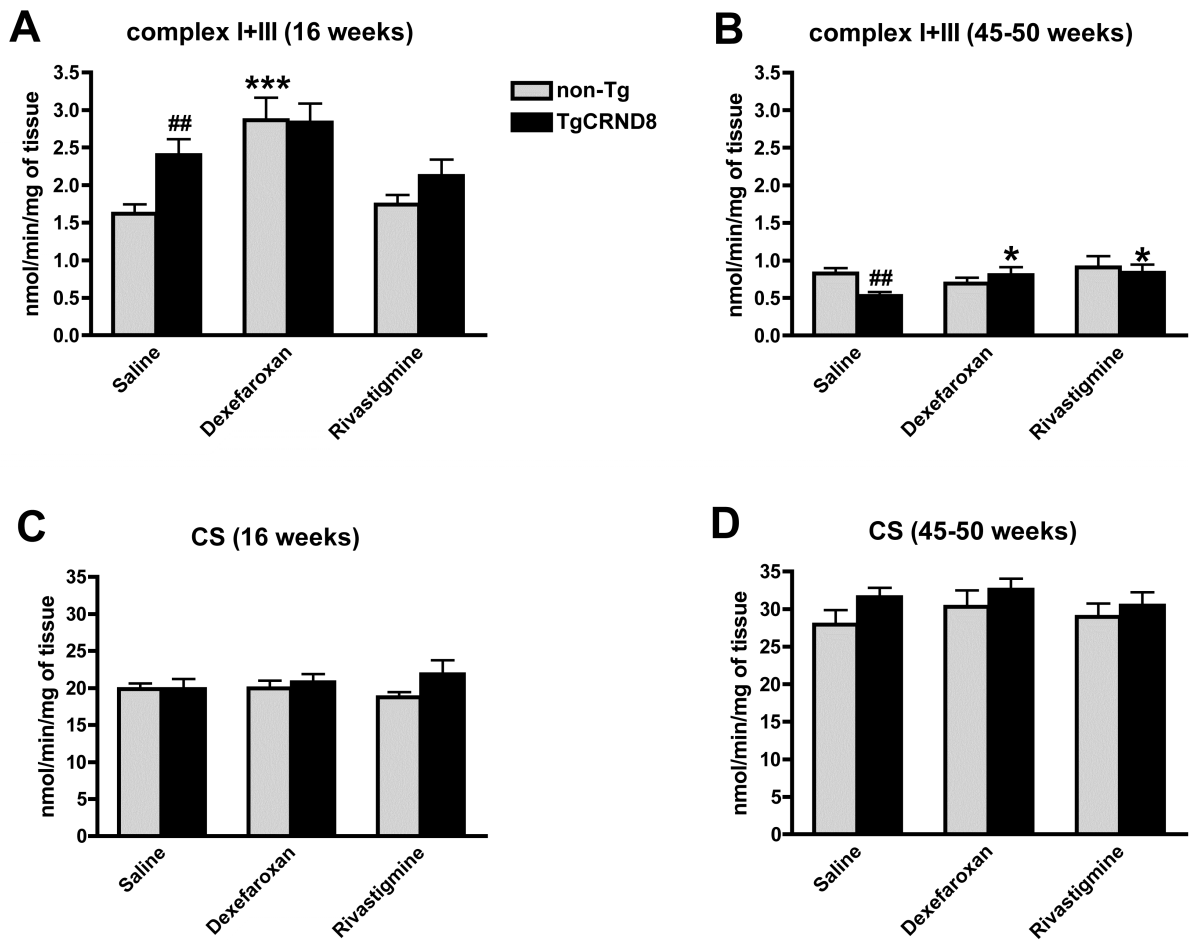


Figure 6-6. Dexefaroxan and rivastigmine increase complex I+III activity without altering citrate synthase activity. Activities of complex I+III and citrate synthase (CS) were measured in cortical tissues from 16 and 40 to 50 week-old drug treated mice. Young TgCRND8 mice exhibited increased cortical complex I+III activity (**A**). Dexefaroxan improved complex I+III activity in young non-transgenic mice, but had no effect on the already elevated levels in TgCRND8 mice. Rivastigmine did not alter activity in the younger cohort. By 45 weeks, complex I+III activity was compromised in TgCRND8 mice and both drugs rescued activity (**B**). CS activity, expressed as nmol of DTNB reduced/min/mg of tissue, was equivalent in TgCRND8 and non-Tg mice and was not altered by drug treatments (**C** and **D**). Values are means \pm SEM of $n \geq 6$. *** $P \leq 0.001$, * $P \leq 0.05$ versus saline treated controls; ## $P \leq 0.01$ versus non-Tg saline mice by 2-way ANOVA followed by Fisher's protected LSD test.

6.5 Discussion

We have found that TgCRND8 mice exhibit regionally distinct changes in tissue ATP levels and complex I+III activity at onset of A β deposition. Transient increases in complex I+III and creatine may buffer cortical ATP levels at least to the age of 16 weeks, a time point at which A β load and impairment recapitulate features of clinical disease (Ma *et al.*, 2011, Francis *et al.*, 2012b). Although the 16 week-old TgCRND8 hippocampus expresses comparable high levels of A β , tissue ATP levels fall, consistent with the observation that compensatory increases in creatine content are delayed in this area (Chapter 5). Enhancing noradrenergic and cholinergic transmission with dexefaroxan, or rivastigmine improved mitochondrial function in young mice and also in aged mice at advanced stages of disease.

Complex I+III activity levels appear to change through stages of TgCRND8 disease progression. We did not observe any changes in PDH, α -KGDH, or complex IV enzyme rates. The dissociation between effects of the APP-transgene on complex I+III and other enzymes of oxidative metabolism suggests A β exposure does not simply alter mitochondrial density. At both 9 and 16 weeks of age, complex I+III activity was increased in the cortex, but not in the hippocampus. APP and A β in mitochondria have been shown to damage the ETC, increase oxidative stress and inhibit import of nuclear-DNA encoded proteins essential for mitochondrial function (Devi *et al.*, 2006). The transient increase in cortical activity was not reflected in altered expression of several key nuclear-DNA encoded subunits of complexes I or III. This suggests that rising levels of A β may not initially impair import of nuclear-DNA encoded subunits of the ETC but rather induce a mitochondrial compensatory response. In wild-type APP stably transfected human neuroblastoma cells (SH-SY5Y), complex III activity increased in response to physiological levels of soluble A β protein (Rhein *et al.*, 2009a).

Oligomeric A β disrupts respiratory complexes of the ETC at the inner mitochondrial membrane (reviewed in Maruszak and Zekanowski, 2011). Both the cortex and the hippocampus exhibit A β deposits early in disease progression and high levels of

insoluble A β . However, A β oligomer levels progressively increase in the hippocampus (Ma *et al.*, 2011), suggesting that this region is particularly vulnerable to bioenergetic stress. Indeed, tissue levels of ATP were depleted in the hippocampus, but not in the cortex of young TgCRND8 mice. Conversely, an increase in complex I+III activity that was observed in the cortex of these 9 and 16 week-old mice may compensate for high A β levels, thus preserving ATP in this region. Similar region-specific increases in ETC activity or gene expression during early stages of A β accumulation have been noted in other APP-Tg models (Strazielle *et al.*, 2003; Reddy *et al.*, 2004) and in AD brains (Bossers *et al.*, 2010). With continuing exposure to mounting A β levels, complex I+III activity precipitously declines in the TgCRND8 brain.

ATP in the cortex may have been conserved by the upregulation of creatine at onset of A β plaques. Creatine was not altered in the hippocampus when ATP was depleted, but did increase throughout the brain at later stages of A β pathology. Despite compromised complex I+III activity, energetic charge was maintained in aged brains (Chapter 5). Creatine administration can buffer A β -induced increases in metabolic demand and sustain ATP levels (Brewer and Wallimann, 2000). This is in line with our observations in TgCRND8 brains, where ATP was maintained only when creatine was elevated.

Perturbations in bioenergetic homeostasis may be driven by noradrenergic deficits. Noradrenaline levels within major terminal fields are depleted early in TgCRND8 mice. Anti-oxidant properties of noradrenaline may be involved in maintaining energy homeostasis. In an *in vitro* model of cholinergic cell death induced by low-level oxidative stress, noradrenaline was shown to rescue cholinergic neurons by neutralizing hydroxyl radicals (Traver *et al.*, 2005).

To test whether reduced noradrenergic tone might have contributed to mitochondrial dysfunction, we examined effects of enhancing noradrenergic transmission by blocking autoinhibitory α_2 -adrenoceptors. Pre-plaque 12 week-old or aged 45 to 50 week-old mice were treated for 28 days with dexefaroxan, an α_2 -adrenoceptor antagonist or rivastigmine, a cholinesterase inhibitor. Dexefaroxan blocks inhibitory α_2 -adrenergic

receptors expressed on noradrenergic as well as cholinergic neurons, and increases the release of both noradrenaline and acetylcholine (reviewed in Chapter 5). Dexefaroxan and rivastigmine rescued complex I+III activity in aged TgCRND8 mice, although a ceiling effect may have been achieved in young mice. Furthermore, both drugs reversed the hippocampal ATP deficit in young mice. Neither treatment altered citrate synthase activity, which suggests that their stimulatory effects on metabolism are not due to proliferation of mitochondria.

Complex I+III activity declines with age, but this decline was more pronounced in TgCRND8 mice. Complex I is the principal entry point for electrons in the ETC. It has the greatest control over respiration rates and ATP generation, and shows the most sensitivity to age-related endogenous substrate depletions (Jones and Brewer, 2010; Pathak and Davey, 2008). Inhibition of complexes I and III are the main producers of reactive oxygen species in mitochondria (Li *et al.*, 2003; Chen *et al.*, 2003). The therapeutic effects of dexefaroxan and rivastigmine may be due in part to its regulation of oxidative phosphorylation. Lymphocytes from AD patients treated with rivastigmine exhibited enhanced enzymatic activities of complexes in the ETC (Casademont *et al.*, 2003). In rats administered with 3-nitropropionic acid to induce mitochondrial dysfunction, rivastigmine treatment mitigated oxidative stress and improved ETC complex activities in the cortex and hippocampus (Kumar and Kumar, 2009). Noradrenaline was shown to prevent A β -induced cell death by decreasing reactive oxygen species and stabilizing the mitochondrial membrane potential (Counts and Mufson, 2010). Dexefaroxan may rescue complex I+III activity and ATP deficits in TgCRND8 mice, by stimulating both noradrenergic and cholinergic transmission.

The TgCRND8 mouse provides a valuable model for studying causal relationships in A β -induced functional impairment. Mitochondrial dysfunction and altered energetic homeostasis provides another progressive end-point for therapeutic assessment. Dexefaroxan and rivastigmine improved ATP and complex I+III activity. These results suggest noradrenergic deficits mediate bioenergetic stress. The stimulatory effect of α_2 -adrenoceptor blockade on mitochondrial function supports the notion of improving both noradrenaline and acetylcholine transmission in treating AD.

Chapter 7 Conclusions

7.1 General Discussion

The loss of noradrenergic cells in the locus coeruleus, bioenergetic stress, altered neurotransmission and reductions in brain-derived neurotrophic factor (BDNF) are well-described features of Alzheimer's disease (AD). Yet, how these pathogenic factors jointly influence disease progression and dementia remains unknown. We investigated neurochemical correlates of behavioural impairment in the TgCRND8 mouse model of AD. Our experiments have helped us identify targets of amyloid- β (A β) toxicity and phenotypes for assessing functional improvements in TgCRND8 mice.

We have demonstrated that these mice exhibit behavioural and neurochemical abnormalities that recapitulate changes in early-stage AD. Noradrenergic tissue deficits are central to A β -induced impairment in TgCRND8 mice. Behavioural dysfunction, decreases in BDNF and bioenergetic stress are all mechanistically linked to the reductions in noradrenaline. Our results in this model confirm the vulnerability of forebrain noradrenergic projections arising from the locus coeruleus. They also raise the possibility of α_2 -adrenoceptor antagonists being used as disease-modifying drugs in the treatment of AD.

7.1.1 TgCRND8 Mice Model Early-Stage Dysfunction in AD

A valid model should resemble the clinical disease in etiology, pathophysiology, symptomatology and response to therapeutics (Van Dam and De Deyn, 2006). Compared to other amyloid precursor protein (APP)-transgenic mice, the TgCRND8 mouse exhibits especially early-onset of amyloid pathology. Amyloid plaques are evident in the cortex and hippocampus by 3 months of age. The spatiotemporal patterns of A β deposition recapitulate those seen in AD (Chishti *et al.*, 2001). Accumulation of A β in TgCRND8 brains is accompanied by other pathophysiological

features that are relevant to AD, including inflammation (Bellucci *et al.*, 2006; Ma *et al.*, 2011), as well as degeneration of hippocampal GABAergic (Krantic *et al.*, 2012) and cortical cholinergic neurons (Bellucci *et al.*, 2006). TgCRND8 mice also exhibit progressive deposits of creatine in the hippocampus, which may reflect disrupted energetic homeostasis (Kuzyk *et al.*, 2010). Neurofibrillary tangles are absent in this model (Chishti *et al.*, 2001). However, tau is hyperphosphorylated and nitrosylated in dystrophic neurites surrounding plaques (Bellucci *et al.*, 2007; Greco *et al.*, 2010). Findings of early-stage tau dysfunction support the notion that A β is the pathogenic trigger of the disease. To date, most of the reported TgCRND8 biochemical abnormalities develop after A β deposition and behavioural deficits (reviewed in section 1.4.4). We have now uncovered subtle phenotypes that emerge before frank plaque pathology and that mimic prodromal symptoms of AD.

In AD, A β deposits are a trailing indicator of cognitive decline. A leading indicator is the concentration of soluble A β (Näslund *et al.*, 2000). We determined onset of behavioural dysfunction in TgCRND8 mice by using sensitive and relevant assays that rely on brain regions that are targeted first by A β . From as early as 8 weeks of age, the mice exhibit progressive memory loss in a non-spatial, object memory task (Chapter 3) and behavioural despair in a tail suspension test (Chapter 4). These are the earliest behavioural phenotypes reported in TgCRND8 mice. They have strong face validity, as deficits in object memory and affect are also observed in patients with mild cognitive impairment (MCI). Damage to the entorhinal-hippocampal circuitry, which relays multimodal information to and from the cortex, is highly predictive of the conversion from MCI to AD. Object memory is remarkably sensitive to disruption of this circuit in both humans and mice. The hippocampus and cortex are also substrates of the stress-induced depressive response in the tail suspension test (reviewed in Chapters 3 and 4). Thus, our object memory data confirm the face validity of TgCRND8 mice as a model of early-stage AD. The tail suspension results extend utility of the model to phenotypes suggestive of the affective disturbances seen in MCI.

Behavioural disturbances in TgCRND8 mice appear to be triggered by increases in soluble A β_{42} load. Between 4 and 8 weeks of age, levels of A β_{42} double and the ratio of A β_{42} /A β_{40} increases 1.5-fold (Chishti *et al.*, 2001). We have reported that ratios of A β_{42} /A β_{40} correlate inversely with BDNF mRNA in aged, plaque-riddled TgCRND8 cortex (Peng *et al.*, 2009). BDNF is produced in the entorhinal cortex and is anterogradely trafficked into the hippocampus, where it regulates synaptic plasticity. Rising levels of A β_{42} may downregulate BDNF, thereby inducing cognitive dysfunction. We found that BDNF mRNA was reduced in the hippocampus and cortex just prior to onset of behavioural impairment. Decreases in BDNF expression were not monophasic. Rather, levels within hippocampus and cortex recovered shortly after behavioural impairment was established. BDNF levels declined again as plaque load developed to a degree observed in late-stage AD brains. Transient increases in BDNF expression have been observed in other APP-Tg mice and in AD (Burbach *et al.*, 2004; Lindvall *et al.*, 1992; Laske *et al.*, 2006). These increases are short-lived and may constitute a compensatory response to disease onset (Chapter 3). The second phasic decrease in BDNF expression is observed at 6 to 8 months. At this point, cholinergic markers are also reduced (Bellucci *et al.*, 2006). These findings in TgCRND8 mice are similar to what is observed in the clinical disease. In end-stage AD brain, neurodegeneration is widespread and BDNF expression is severely reduced. However, smaller reductions are evident in the parietal cortex at preclinical stages of AD. Reductions in BDNF expression precede cholinergic dysfunction and track with the rate of cognitive decline in patients with MCI and early AD (Peng *et al.*, 2005).

A β may have detrimental effects on BDNF transport and signaling before depositing in plaques. The phasic decreases in BDNF mRNA within the TgCRND8 brain may reflect tissue responses to different aggregation states of A β . Oligomeric A β_{42} is known to decrease BDNF mRNA and its activity-dependent transcriptional regulator, phosphorylated cyclic AMP response element binding protein (P-CREB) *in vitro* (Garzon and Fahnestock, 2007). Oligomeric A β can also disrupt BDNF signaling by impairing the axonal trafficking of BDNF and its TrkB receptor (Poon *et al.*, 2011). These findings raise questions about the nature of BDNF deficits in TgCRND8 mice. How does A β

decrease BDNF expression early in the disease? Why do BDNF levels rebound and what triggers the second phasic decrease at more advanced stages of disease? Our work did not address these questions. However, others have provided data that point to some answers. As early as 2 months of age, TgCRND8 mice exhibit focal swellings and a thickening of axons just proximal to sites of A β accumulation in the cortex. These dystrophic axons are associated with localized disruption of axonal transport (Adalbert *et al.*, 2009). Defects in axonal transport may impair the trafficking and signaling of BDNF in A β -burdened regions. The transcription of BDNF may also be downregulated. TgCRND8 mice have been shown to exhibit decreased activation of CREB (i.e. lower P-CREB levels) in the hippocampus (Yiu *et al.*, 2011). The transcription of BDNF is induced by P-CREB. In turn, BDNF signaling through TrkB leads to activation of CREB. Both P-CREB and BDNF levels are reduced in hippocampi of AD brains (reviewed in section 1.2.3.2). Decreases in P-CREB levels are observed in pre-plaque TgCRND8 mice (Yiu *et al.*, 2011) and may underlie the first phasic downregulation in BDNF mRNA. The late phase decrease in BDNF could result from neurodegeneration and other pathophysiological factors that emerge with disease progression. These findings collectively point to A β toxicity beginning upstream of BDNF, targeting factors involved in its production and/or transport.

Locus coeruleus neurons synthesize and transport BDNF along noradrenergic axons to forebrain terminals, where it regulates cortical neuronal survival and organization in the developing brain (Fawcett *et al.*, 1998). This transport of BDNF is required for maintenance of forebrain noradrenergic innervation throughout life (Matsunaga *et al.*, 2004). For this reason, it may be anticipated that decreased BDNF mRNA in TgCRND8 mice would be coupled with noradrenergic dysfunction. Indeed, we found early and consistent reductions in terminal field noradrenaline content (Chapter 5). Noradrenaline levels were decreased in the hippocampus, temporoparietal and frontal cortices, as well as in the cerebellum of 4-week-old mice. However, noradrenaline content was unaltered in regions that receive little, or no innervation from the locus coeruleus, including the ventral mesencephalon, striatum and brainstem (Berridge and Waterhouse, 2003). Non-Tg controls exhibited age-related increases in cortical noradrenaline levels. These increases did not occur in aging TgCRND8 mice and may

be related to the late-life reductions in BDNF mRNA. In the hippocampus, levels of noradrenaline progressively declined in TgCRND8 mice. Our results imply that locus coeruleus forebrain projections are especially vulnerable in TgCRND8 mice (discussed in section 7.1.3). As suggested by the mouse model, loss of neurons in the locus coeruleus was found to be more severe and to correlate better with the duration of AD than neuronal loss in the nucleus basalis (Zarow *et al.*, 2003).

Bioenergetic stress is another core, progressive feature of AD (reviewed in section 1.1.5). To investigate whether mitochondria are affected with progression of TgCRND8 pathology (Chapters 5 and 6), we measured the activities of key enzymes of oxidative metabolism. Behaviourally impaired 9 and 16 week-old mice exhibited increased complex I+III oxidoreductase activity in the cortex only. In contrast, complex I+III activity was globally reduced by nearly 50% in 45-week-old, plaque-riddled brains. Changes in complex I+III activity do not reflect a general change in mitochondrial density or function. The activities of complex IV, α -ketoglutarate dehydrogenase and pyruvate dehydrogenase were intact. While the early increase in complex I+III activity was not associated with altered expression of several important subunits of complexes I or III, the late-life decline coincided with reduced expression of the nuclear-DNA encoded complex I subunit NDUFB8.

The gene expression of NDUFB8 is significantly reduced in AD brains (Li *et al.*, 2003). Declines in NDUFB8 expression may very well account for deficient complex I+III activity in TgCRND8 mice at end-stage disease. NDUFB8 is necessary for assembly of the complex I holoenzyme and for super-complex assembly with complex III (Lazarou *et al.*, 2007). It is easily nitrated and is especially susceptible to free radical damage. Nitration of NDUFB8 hinders super-complex assembly and inactivates complex I (Davis *et al.*, 2010). Signs of nitrosative stress emerge with cerebral amyloidosis in TgCRND8 mice. Neurons and microglia surrounding plaques express inducible nitric oxide synthase (Bellucci *et al.*, 2006). At 7 and 12 months of age, a marked increase in nitrotyrosine immunostaining has been reported in dystrophic neurites within the neocortex and hippocampus (Bellucci *et al.*, 2007). What remains to be addressed is whether

nitrosative stress underlies the decreases in NDUFB8 expression and complex I+III activity in aged mice.

Markers of nitrosative stress appear at advanced stages of A β pathology and thus may not be related to the increases in complex I+III activity seen earlier in the disease process. The changes in complex I+III activity in younger mice were not associated with altered NDUFB8 expression. As with BDNF, phasic alterations in oxidative phosphorylation (OXPHOS) may occur with the progression of A β pathology. The early increase in complex I+III activity was only found in the cortex. Similar transient increases in activity or in gene expression of the electron transport chain (ETC) have been described in the cortices of other APP-Tg mice (Strazielle *et al.*, 2003; Reddy *et al.*, 2004; Rhein *et al.*, 2009b) and in AD brains (Bossers *et al.*, 2010). Such increases likely represent a compensatory mitochondrial response to low concentrations of A β (Rhein *et al.*, 2009a). A β can impair OXPHOS directly by clogging ETC machinery and preventing import of nuclear DNA-encoded subunits, or indirectly by promoting ROS (reviewed in section 1.2.3.3). As A β pathology develops, mitochondria eventually lose the capacity for adaptive response and consequently fail to meet metabolic demand. Early increases in complex I+III activity and late-phase declines in both activity and NDUFB8 levels implicate complex I malfunction in TgCRND8 disease progression.

Complex I is the largest and the 'leakiest' of the 5 complexes in the ETC. It is the major source of superoxides in mitochondria. As reviewed earlier in the thesis, ROS can in turn oxidize proteins in complex I, causing more electrons to leak and thereby further disrupt OXPHOS. Alterations in complex I+III activity may reveal bioenergetic stress in TgCRND8 mice. We examined tissue levels of creatine and ATP in cortex and hippocampi through stages of A β accumulation. In aged mice with advanced A β pathology and complex I+III deficits, energetic charge and ATP were maintained but creatine increased in the brain (Chapter 5). Younger animals exhibited regional differences in bioenergetic status. In hippocampi, ATP transiently declined at onset of plaques. Whereas in cortical tissues with enhanced complex

I+III activity, ATP was unaltered as creatine increased with A β burden (Chapter 6). Our data reveal that ATP levels are sustained when creatine is elevated, despite OXPHOS deficits in the brain.

The increased levels of creatine may maintain energetic charge despite A β -induced increases in metabolic demand (Brewer and Wallimann, 2000). In accord with this observation, we found that the transient decrease in hippocampal ATP occurred at 16 weeks, a time point at which creatine levels were not increased. Our findings extend those of Kuzyk *et al.* (2010), who reported progressive accumulation of creatine deposits in the hippocampus of TgCRND8 mice between 5 and 17 months of age. It appears that compensatory increases in creatine are delayed in this brain area. Although both cortex and hippocampus accumulate A β early in disease and although both regions exhibit extensive plaque pathology, the hippocampus is the only region in which high molecular weight A β oligomers increase with disease progression (Ma *et al.*, 2011). The hippocampus is also the only region in which progressive reductions in tissue noradrenaline are observed (Chapter 4). This regional difference may underlie the distinct mitochondrial stress responses in cortex and hippocampus. The hippocampus maintains neurogenesis throughout adulthood. It is an area with high and fluctuating metabolic demands. Decreases in P-CREB, as well as in BDNF and noradrenaline may underlie the vulnerability of the hippocampus to A β toxicity and disruptions in energy homeostasis.

Creatine deposits have also been observed in hippocampal tissues from AD brains (Gallant *et al.*, 2006), underlying the likely relevance of this molecule to the human disease. When tissue is bioenergetically stressed by A β , or during bouts of high metabolic activity, the creatine kinase/phosphocreatine shuttle maintains energetic charge. Disruption of creatine kinase activity can lead to decreased energy reserves and bioenergetic failure. Creatine kinase is sensitive to oxidative stress. Its activity is reduced in AD brains (reviewed in section 1.1.5.3). In addition to activity deficits, the transport of creatine kinase also appears to be impaired in AD. The APP protein interacts with creatine kinase and assists its translocation to

mitochondria. Mutations in *APP* impair its ability to chaperone creatine kinase to mitochondria (Li *et al.*, 2006), leading to decreased phosphocreatine synthesis and accumulations of creatine within the cell. The cytoplasmic tail of APP has been found to interact with and stabilize several mitochondrial-targeted proteins. APP expression protects the cell from endoplasmic reticulum stress (Kögel *et al.*, 2003). However, mutations in *APP*, and especially the Swedish double mutation (Haass *et al.*, 1995; Kögel *et al.*, 2003, Eckert *et al.*, 2011) increase the susceptibility of cells to oxidative stress and compromise mitochondrial function (reviewed in Bürklen *et al.*, 2006). The origin of elevated creatine content and its association with mitochondrial dysfunction and altered cellular bioenergetics in TgCRND8 brains warrant further investigation.

It is unclear why TgCRND8 mice exhibit selective dysfunction of complex I. Deficits in complex IV and other consistently reported oxidative metabolic defects of AD have been observed in various APP-Tg mice. Some of these transgenic lines also exhibit decreases in the mitochondrial membrane potential, bioenergetic depletion and oxidative stress (reviewed in Eckert *et al.*, 2011 and in Chapter 6). However, mitochondrial phenotypes of APP-Tg mice are highly variable in severity and age at onset. Mutation-specific disruptions in mitochondrial motility, morphology, oxidative capacity and functional output have been described in APP-Tg, PS1-Tg and APP/PS1-Tg mice (Trushina *et al.*, 2012). *APP* and *PS1* mutations appear to act synergistically so as to disrupt mitochondria and energy status. The murine genetic background, transcriptional promoter and expressed hAPP isoform can also influence mitochondrial phenotypes. Thus, while different transgenic mouse lines can exhibit distinct mitochondrial impairments, all demonstrate aspects of changes seen in AD (Trushina *et al.*, 2012). In this regard, complex I disruption would seem to be a feature that is particularly prominent when AD is driven by Swedish and/or Indiana *APP* mutation. Whether this is the case or not, our mice arguably model early stages of the disease. As such, they do not develop the full spectrum of mitochondrial defects seen in AD.

7.1.2 Noradrenergic Deficits are Central to TgCRND8 Impairment

We examined the effects of increasing noradrenergic transmission on behaviour, A β load, BDNF expression and mitochondrial function. In doing so, we sought to distinguish secondary factors from upstream causes of noradrenergic tissue deficits. Pre-plaque mice 12 weeks of age, or aged mice 45-50 weeks of age were treated systemically for 28 days with dexefaroxan, an α_2 -adrenoceptor antagonist.

Noradrenergic transmission is regulated by presynaptic α_2 -adrenoceptors. Blocking these autoreceptors inhibits negative feedback control of transmitter release, thereby increasing noradrenaline outflow from terminals. As reviewed previously, these inhibitory α_2 -adrenoceptors are also expressed heterologously on forebrain cholinergic terminals. Hence, using a noradrenaline reuptake inhibitor to increase extracellular levels of noradrenaline may induce inhibition of cholinergic transmission. Dexefaroxan increases noradrenergic transmission. It also increases acetylcholine outflow in the cortex and can provide trophic support to forebrain cholinergic innervation in rodents. Moreover, tolerance to these beneficial effects of dexefaroxan did not occur in rats that were chronically treated for 28 days (Debeir *et al.*, 2002). For these reasons, we opted to treat mice with dexefaroxan. To discern whether any therapeutic effects might be mediated through the cholinomimetic action of α_2 -adrenoceptor blockade, effects of dexefaroxan were compared to those of the cholinesterase inhibitor, rivastigmine.

We found that both dexefaroxan and rivastigmine reversed object memory deficits and behavioural despair. Neither drug influenced object exploration or mobility measures in non-Tg controls. Thus, it did not appear that the drugs improved behaviour by simply encouraging the mice to move more. Our findings suggest that cholinergic and noradrenergic mechanisms may both contribute to cognitive and affective phenotypes in TgCRND8 mice (Chapter 4). The locus coeruleus noradrenergic system is activated in response to novel stimuli. Reciprocal connections between the prefrontal cortex and the

locus coeruleus change noradrenergic tone in forebrain circuits to regulate shifts in attention, arousal and mood. Extensive synaptic interactions between cholinergic and noradrenergic efferents also exist in hippocampal and cortical brain regions. Our experiments did not discriminate between α_2 -autoreceptors and α_2 -heteroreceptors on cholinergic terminals, in accounting for therapeutic effects of dexefaroxan on memory and mood.

In these studies, we did not investigate drug effects at advanced stages of plaque pathology, when inflammatory markers and microglial activation are evident in TgCRND8 mice. However, in young animals, neither drug altered the CNS burden of monomeric or aggregated A β . In addition, the compounds had no effect on expression of holoAPP or β -CTF, the C-terminal fragment produced by β -secretase cleavage of APP. While the loss of noradrenergic innervation can exacerbate A β pathology, our results indicate therapeutic actions of dexefaroxan to be independent of any effects on APP processing and A β accumulation (Chapter 4). Consistent with this conclusion, chronic treatment with the α_2 -adrenoceptor antagonist fluparoxan was found to prevent memory deficits in APP/PS1 mice without altering A β burden (Scullion *et al.*, 2011).

Both dexefaroxan and rivastigmine improved hippocampal BDNF mRNA levels in TgCRND8 mice. This effect of dexefaroxan persisted even at advanced stages of A β pathology, in 1-year-old mice (Chapter 4). These results with dexefaroxan were expected given the mutually trophic relationship between noradrenergic neurons and BDNF. Likewise, boosting cholinergic transmission has been shown to prevent memory impairment and increase BDNF expression in rats infused with A β peptides (Srivareerat *et al.*, 2009). It remains to be seen how dexefaroxan and rivastigmine may alter the expression of P-CREB and the immediate-early gene *Arc*. This experiment could help determine whether therapeutic targets include transcriptional regulators of BDNF that are crucial for memory formation in the hippocampus.

The protective effects of noradrenaline against A β toxicity may depend on the activation of canonical β -adrenergic signaling cascades involving cAMP and P-CREB, and on the

consequent induction of BDNF. In cultured neurons, noradrenaline inhibited A β -induced increases in ROS, mitochondrial depolarization and caspase activation by increasing BDNF and nerve growth factor mRNA (Counts and Mufson, 2010). But, noradrenaline itself may neutralize hydroxyl radicals and prevent cholinergic cell death (reviewed in section 1.3.2.4). We found that the therapeutic effects of dexefaroxan and rivastigmine include regulation of energetic homeostasis (Chapter 6). Both dexefaroxan and rivastigmine reversed the hippocampal ATP deficit in young mice and rescued complex I+III activity in aged mice. Neither drug altered citrate synthase activity. Thus, the compounds appear to stimulate energy metabolism by some action on complex I+III activity and not by increasing mitochondrial density. The mechanism is unclear.

The drugs may have reduced energetic stress by improving BDNF expression and transmitter deficits. Conversely, reduced noradrenergic transmission could lead to failure in energy homeostasis through the loss of its neuroprotective actions against oxidative stress and of its stimulatory action on the synthesis and release of ATP and BDNF. Cholinergic as well as noradrenergic mechanisms may be involved in the generation of energetic stress, as both drugs reversed ATP and OXPHOS deficits. Rivastigmine has been shown to increase ETC complex enzymatic activities in mitochondria of AD patient lymphocytes (Casademont *et al.*, 2003), and in a rat model of oxidative stress (Kumar and Kumar, 2009). Both transmitter systems may be involved in reducing oxidative stress in the TgCRND8 model, although this has yet to be demonstrated. Effects of drug treatments on creatine levels and the energetic buffering capacity of creatine kinase also need to be determined.

In sum, dexefaroxan reversed behavioural phenotypes, increased BDNF expression and improved mitochondrial function. Similar results were attained with the clinical cholinesterase inhibitor, rivastigmine. Our work suggests that reductions in noradrenaline and its facilitatory effects on basalocortical cholinergic transmission are critical factors in TgCRND8 impairment. Blocking α_2 -adrenergic receptors may prove an especially relevant pharmacological approach for the treatment of AD.

7.1.3 Do TgCRND8 Noradrenergic Deficits Resemble those in AD?

We have demonstrated that TgCRND8 mice develop AD-like phenotypes prior to plaque formation. As in AD, a deficiency in forebrain noradrenergic tone mediates key molecular cascades of A β toxicity to drive dysfunction. An important question that remains to be answered is how noradrenergic deficits arise in AD and in APP-Tg mice.

We have reviewed studies indicating that onset and severity of AD dementia correlate with the magnitude of locus coeruleus degeneration and the reduction in noradrenaline levels. Decreases in the noradrenaline transporter (NET) have been observed in the locus coeruleus and the thalamus. These areas normally express the most NET. Decreases in NET within these regions of the AD brain progress in tandem with Braak staging of the disease (Guylás *et al.*, 2010). Loss of nuclei in the locus coeruleus is also seen in other neurodegenerative conditions, including Down syndrome, Parkinson's disease and Huntington's disease. However, the pattern of cell loss within the locus coeruleus differs, depending upon the condition. The rostral portion of the nucleus degenerates in AD brains, with preferential loss seen to be of cells that project to the cortex and hippocampus (reviewed in section 1.3.1.1). Similar topographic patterns of locus coeruleus degeneration have been described in the PDAPP (German *et al.*, 2005) and APP_{swe}/PS1 Δ E9 (Liu *et al.*, 2008) transgenic lines. Our results in TgCRND8 mice also suggest vulnerability of forebrain locus coeruleus projections. While we found reduced noradrenaline content within all major terminals, the reduction was most severe and progressive only in the hippocampus.

The pattern of noradrenergic tissue deficits in the TgCRND8 brain suggest degeneration of fibers from the locus coeruleus. Histopathological and microdialysis experiments can be performed to determine whether these reductions in noradrenaline tissue content are associated with decreases in synaptic availability of transmitter, alterations in adrenergic receptor density or sensitivity, and/or degeneration of terminals and cell bodies. It

remains possible that the tissue content deficits we observed reflect changes in transmitter synthesis, synaptic vesicle packaging or number, and that the model does not experience frank loss of noradrenergic cells. Our chromatographic measures of noradrenaline and its extracellular metabolite, normetanephrine from TgCRND8 brain extracts indicated increased transmitter turnover in the hippocampus. While noradrenaline levels were decreased, those of normetanephrine were increased. Both dexefaroxan and rivastigmine normalized normetanephrine levels, but did not alter noradrenaline content. These results likely reflect compensatory increases in noradrenergic activity and reduced reuptake of released transmitter (Chapter 4).

In the AD brain, reductions in noradrenaline tissue levels do not correlate with the degree of cell loss in the locus coeruleus. Degeneration of this nucleus is accompanied by compensatory changes in surviving noradrenergic neurons, which include increased tyrosine hydroxylase expression and sprouting of terminals in the prefrontal cortex and hippocampus. This sprouting does not reflect normal noradrenergic innervation and may even contribute to dementia. Postsynaptic α_{1D} and α_{2C} receptor levels are decreased in the hippocampus and prefrontal cortex (Szot *et al.*, 2006; 2007), while presynaptic α_2 adrenoceptors are relatively spared in the AD brain (Matthews *et al.*, 2002). Postsynaptic β receptors were reportedly increased in the prefrontal cortex and hippocampus of AD patients (Kalaria *et al.*, 1989). Selective increases in α_2 - and β -receptors have been described in the cerebellum of aggressive AD patients (Russo-Neustadt and Cotman, 1997). The exact role of each adrenergic subtype in different brain regions is still uncertain. The issue that receptors may be localized pre- and/or postsynaptically further complicates modeling of outcomes. Clearly, reduced concentrations of noradrenaline within the forebrain, aberrant sprouting or hyper-innervation by surviving noradrenergic neurons and the deregulation in the balance of adrenoceptor activation contribute to disturbances in attention, memory and affect in AD (Szot *et al.*, 2007; Herrmann *et al.*, 2004).

The topographic pattern of cell loss in the locus coeruleus of AD patients and APP-Tg mice suggest a retrograde degenerative process, whereby noradrenergic degeneration is initiated at axon terminals in the forebrain. A β deposits induce distal axonopathy in

noradrenergic terminals and cause the subsequent neurodegeneration of cortical- and hippocampal-projecting locus coeruleus cells in APP-Tg mice (Liu *et al.*, 2008; German *et al.*, 2005). We have observed noradrenergic tissue deficits in 4 week-old TgCRND8 mice, long before the deposition of A β . A β accumulation in the TgCRND8 brain is axonopathic, causing localized disruption in axonal transport and loss of presynaptic machinery early in the disease (Adalbert *et al.*, 2009; Woodhouse *et al.*, 2009). Soluble A β may initiate retrograde degeneration in vulnerable noradrenergic and cholinergic terminals within the cortex and hippocampus. Compared to afferents arising from the basalocortical cholinergic system, the longer fibers from the locus coeruleus may be more susceptible to defects in axonal transport. This greater vulnerability of the locus coeruleus system likely explains why noradrenergic tissue deficits precede cholinergic dysfunction.

In sum, our work has revealed that the TgCRND8 mouse not only provides a means by which to study the molecular mechanisms of A β toxicity, but also that testing therapeutic interventions in this model may be highly predictive of clinical outcome.

7.2 Translational Impact

While there are substantial challenges in translating findings from APP-Tg mice to the human (section 1.4.2), transgenic models have confirmed the central role that A β plays in AD-like disease. A variety of A β targeted interventions in TgCRND8 mice have been found to decrease A β burden and to ameliorate behavioural deficits (Janus *et al.*, 2000; McLaurin *et al.*, 2002, 2006; Greco *et al.*, 2010; Hawkes *et al.*, 2010). Yet, determining which A β peptides and oligomeric assembly states to therapeutically target remains a challenge. In addition, there are concerns about the safety and efficacy of inhibiting A β production, disaggregating plaques, or reducing A β tissue load in humans.

Our work suggests that treating noradrenergic deficits, an immediate downstream target and mediator of A β toxicity, can prevent or delay the onset of AD. Results in TgCRND8 mice suggest that α_2 -adrenoceptor antagonists could provide effective disease-modifying therapy. Blocking α_2 -adrenoceptors on noradrenergic and cholinergic terminals may improve both cognitive and affective disturbances in AD. Targeting this receptor may also reduce AD pathophysiology by restoring trophic support and energy metabolism in the brain. Other mechanisms involved in the progression of disease, such as inflammation and oxidative stress, can be mitigated by α_2 -adrenoceptor blockade, or by increasing noradrenaline levels. To a large extent, α_2 -adrenoceptor antagonists protect against A β insults by enhancing the trophic, metabolic or transmitter-related compensatory responses that are mediated by the locus coeruleus. However, their direct effect of improving cholinergic tone, provides an additional pathway whereby CNS deterioration in AD can be targeted.

There is already clinical evidence that α_2 -adrenoceptor blockade positively regulates mood. Mirtazapine is a second-generation noradrenergic and serotonergic tetracyclic antidepressant, with potent α_2 -adrenergic antagonism (Stimmel *et al.*, 1997). It blocks pre- and postsynaptic α_2 -adrenoceptors, postsynaptic 5-HT₂ and 5-HT₃ serotonergic receptors and histamine receptors with high affinity. Mirtazapine also marginally antagonizes α_1 -adrenoceptors. The net effect of this compound is increased noradrenergic and serotonergic tone at 5-HT₁ and β -adrenergic receptors (reviewed in Blier, 2003; Benjamin and Doraiswamy, 2011). In a randomized, double-blind, placebo controlled 4-week study, mirtazapine was found to be an effective anxiolytic in patients with anxiety as a primary complaint (Sitsen and Moors, 1994). The drug is generally well tolerated and has minimal cardiovascular and anticholinergic effects (reviewed in Benjamin and Doraiswamy, 2011). To date, there have been no randomized, controlled trials using mirtazapine to treat AD patients. However, in a case series of 3 elderly depressed AD patients, mirtazapine caused a remission of depression symptoms, anxiety, poor appetite and sleep disturbances. No effect was reported in cognition (Raji and Brady, 2001). In a larger 12-week open-label pilot study with 16 AD patients, mirtazapine effectively treated agitation without significant side-effects or impact on cognitive deterioration (Cakir and Kulaksizoglu, 2008).

The clinical efficacy of α_2 -adrenoceptor antagonists and its selectivity of action is influenced by the dose at which it is used. The non-selective α_2 -adrenoceptor antagonist, yohimbine, as well as other more recent and selective compounds such as dexefaroxan and atipamezole have a “U”-shaped dose-response curve. In addition to selecting the optimal dose, other issues related to tolerance and its action in the periphery need to be addressed in preclinical pharmacological trials (reviewed in Marien *et al.*, 2004). In the periphery, α_2 -adrenoceptors are involved in hemodynamic regulation. The off-target hypertensive effects have tempered enthusiasm for development of selective α_2 -adrenoceptor antagonists. However, rigid analogues of atipamezole were shown to have differential effects at peripheral and central α_2 -adrenoceptors (Vacher *et al.*, 2010). By incorporating methyl groups at various positions of the imidazole ring in atipamezole, it was determined that a single conformation was particularly effective at increasing cortical noradrenaline release with minimal cardiovascular effects in the rodent. This demonstration of CNS selectivity suggests a potential for targeted α_2 -adrenoceptor antagonism.

Many clinical trials have validated the efficacy and safety of cholinesterase inhibitors for the symptomatic treatment of AD. Preclinical studies suggest that cholinesterase inhibitors can also affect AD pathogenesis, however the mechanisms by which it does so may be unrelated to an increase in acetylcholine (Francis *et al.*, 2005). Our work suggests that α_2 -adrenoceptor antagonists, with its cholinomimetic action, may treat both symptoms and the underlying pathophysiology of AD.

Chapter 8 Future Directions

The results presented in this thesis highlight the contribution of noradrenergic tissue deficits to AD-like impairment in the TgCRND8 mouse. Treatment with an α_2 -adrenoceptor antagonist or a cholinesterase inhibitor improved behavioural, BDNF and metabolic deficits. Several experiments can be performed now to distinguish between noradrenergic and cholinergic mechanisms in mediating A β toxicity in TgCRND8 mice. In addition to noradrenergic and cholinergic systems, serotonergic transmission may also be affected in TgCRND8 disease. We present preliminary data on serotonin transmitter levels and turnover, as well as related anxiety behaviour in TgCRND8 mice.

8.1 Are protective effects of α_2 -adrenoceptor blockade mediated through increased β -adrenoceptor activation?

Dexefaroxan and rivastigmine treatments improved memory and affect, as well as hippocampal BDNF expression in TgCRND8 mice. It is unclear whether these effects were ultimately mediated through increase in noradrenergic tone or through a cholinomimetic action of the drugs. Counts and Mufson (2010) demonstrated that noradrenaline increases BDNF mRNA levels through β -adrenergic stimulation of cAMP production and CREB activation. Other groups have demonstrated that blockade of α_2 -adrenoceptors enhances hippocampal neurogenesis, increases mRNA for BDNF and Arc, and improves depression-related behaviour (Yanpallewar *et al.*, 2010). However, both drugs could conceivably have increased BDNF levels through cholinergic mechanisms. Chronic nicotine treatment is known to increase BDNF mRNA in the hippocampus (reviewed in Srivareerat *et al.*, 2009).

Decreases in hippocampal P-CREB and transcription of the immediate early gene *Arc* can serve as end-points to discriminate between cholinergic and noradrenergic mechanisms in A β -induced functional impairment in TgCRND8 mice. Deficits in P-CREB and Arc expression have been shown to provide measurable indices of dysfunction that coincide with spatial memory impairment in pre-plaque mice (Yiu *et al.*, 2011). Dexefaroxan, or rivastigmine would be administered for 28 days to 12-week-old

mice. As described by Yiu and coworkers, mice could then be exposed to a novel environment for 5 minutes, returned to the home cage and sacrificed 30 minutes thereafter. In this paradigm, it has been observed that TgCRND8 mice exhibit normal levels of CREB, but failure of CREB activation in response to novelty (Yiu *et al.*, 2011). Thus, western blot tracking of the hippocampal P-CREB and Arc signals would provide a proxy for behavioural improvement. If the two drugs indeed share a common pathway to influence the encoding of memory, we would hypothesize that both dexefaroxan and rivastigmine should restore this response. Drugs may have rescued behaviour and BDNF levels in TgCRND8 mice through β -adrenergic activation of CREB. Alternatively, they could increase P-CREB and BDNF levels through cholinergic signaling. In adult rats, chronic treatment with the acetylcholinesterase inhibitor donepezil was shown to enhance P-CREB expression and neurogenesis in the hippocampus. In contrast, the muscarinic antagonist scopolamine suppressed hippocampal neurogenesis, P-CREB activation and BDNF mRNA levels (Kotani *et al.*, 2008). To test whether drug effects are mediated through noradrenergic and/or cholinergic signaling, one might compare BDNF and P-CREB levels in mice that are treated with rivastigmine, dexefaroxan or the β -adrenergic agonist isoproterenol, with or without scopolamine. These experiments should help us answer the following:

1. Is the activation of CREB a therapeutic target of dexefaroxan and rivastigmine?
2. Do drugs increase CREB activation through β -adrenergic and/or muscarinic signaling?
3. Can dexefaroxan alone induce CREB activation and rescue A β -functional impairment, or is it better administered as adjunctive therapy to rivastigmine?

8.2 Does α_2 -adrenoceptor blockade improve metabolic state in TgCRND8 mice by stabilizing mitochondrial respirasomes?

Aged TgCRND8 brains exhibit increased creatine content coupled with a selective ~50% loss of complex I+III oxidoreductase activity. Reduced activity coincided with

decreased expression of the complex I subunit NDUFB8, which is required for assembly of the complex I and III respirasome (Lazarou *et al.*, 2007). Dexefaroxan and rivastigmine restored complex I+III activity in aged mice and ATP levels in young mice. Recently, β -adrenergic agonists were found to increase mitochondrial biogenesis, including NDUFB8 gene expression, in the heart and kidneys of mice (Wills *et al.*, 2012). It is likely that α_2 -adrenoceptor antagonism stabilizes the assembly of respiratory super-complexes of the electron transport chain (ETC). It will be important to test the effects of dexefaroxan and rivastigmine on respirasome assembly in TgCRND8 mice. Our aims are to answer the following:

1. Is complex I+III respirasome assembly disrupted in TgCRND8 mice?
2. Does dexefaroxan stabilize interactions between complexes I and III in aged TgCRND8 mice by increasing NDUFB8 expression and respirasome assembly?
3. Does dexefaroxan increase mitochondrial output through postsynaptic cholinergic or noradrenergic signaling?

Synaptosomal respirasomes will be isolated by blue native gel electrophoresis followed by immunodetection of specific proteins from complexes I and III in digitonin detergent-treated mitochondrial brain fractions. Aged (40 to 45 week-old) TgCRND8 mice and wild-type littermates will be treated with dexefaroxan or isoproterenol, with or without scopolamine for 28 days. At the end of treatment, cortical and hippocampal tissue will be harvested for analysis of various mitochondrial parameters, including respirasome detection, NDUFB8 expression, ATP and creatine tissue content, as well as creatine kinase and ETC oxidative phosphorylation activities.

8.3 Does α_2 -adrenoceptor antagonism reduce oxidative stress?

TgCRND8 mice exhibit nitrosative stress in the cortex and hippocampus (Bellucci *et al.*, 2007). Reactive oxygen species (ROS) are largely generated by reverse electron transport through complex I. ROS could contribute to or result from failure in oxidative phosphorylation. The loss of super-complex formation in the ETC destabilizes complex

I, potentiates inefficient electron transfer and superoxide production (reviewed in Lenaz *et al.*, 2010). The alterations in complex I+III activity and decreases in NDUFB8 expression suggest ROS is involved in the TgCRND8 disease. In addition, the loss of noradrenaline may be permissive for A β -induced oxidative stress (Counts and Mufson, 2010). Dexefaroxan and rivastigmine treatments may be improving mitochondrial function by reducing ROS. By using reactive oxidation-sensitive fluorescent probes (2,7-dichlorodihydrofluorescein diacetate), we could measure the production of mitochondrial superoxides in synaptosomal respirasomes from drug treated mice.

8.4 Is serotonergic transmission altered, and if so, how does this influence anxiety in TgCRND8 mice?

While catecholaminergic and cholinergic systems have been investigated, relatively little is known about the state of the serotonergic system in TgCRND8 mice and in the human disease. Losses of serotonergic cells from the raphe nuclei have been documented in AD brains. Less degeneration in the serotonergic system is observed, relative to the noradrenergic and cholinergic systems (reviewed in Gonzalo-Ruiz *et al.*, 2003). Most studies report a decrease in forebrain serotonin transmitter and metabolite tissue levels, as well as a loss of serotonergic receptors in the frontal and temporoparietal cortices (reviewed in Hardy *et al.*, 1985; Gonzalo-Ruiz *et al.*, 2003). Alterations in serotonergic tone have been implicated in depressed mood, anxiety, aggression and agitation in AD patients (reviewed in Lanari *et al.*, 2006). Thus, we began an investigation of serotonin transmitter levels and turnover to determine whether altered serotonergic tone might contribute to TgCRND8 behavioural phenotypes.

We measured tissue concentrations of serotonin (5-HT) and its major metabolite 5-hydroxyindoleacetic acid (5-HIAA) across brain regions, during the course of TgCRND8 disease. 5-HT content was not altered in the TgCRND8 brain at any age. However, we observed significant but inconsistent increases in 5-HIAA levels in the striatum and

frontal cortex of young and aged TgCRND8 mice (Figure 8-1). Increased content of 5-HIAA relative to 5-HT reflect elevated serotonin turnover in these brain regions.

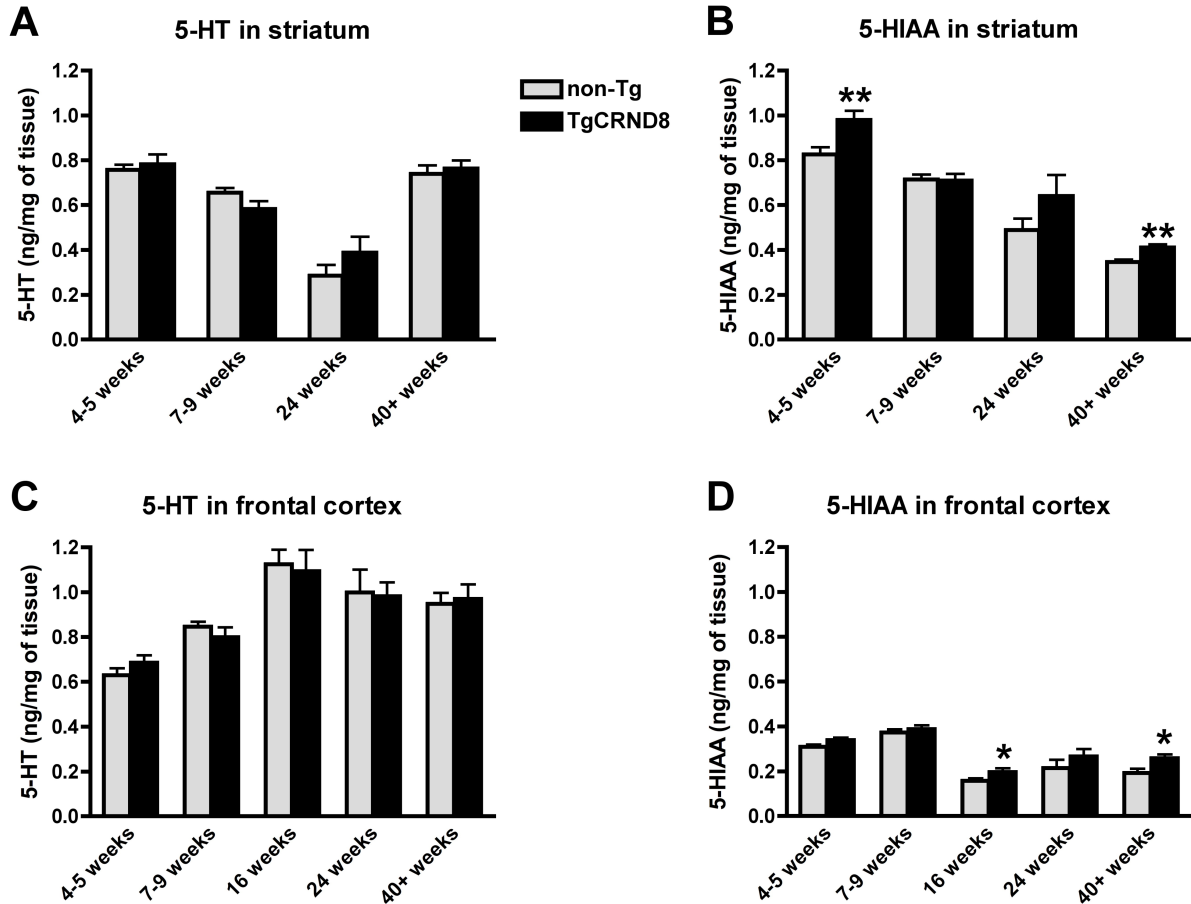


Figure 8-1. Tissue content of 5-HIAA is increased in the striatum and frontal cortex of TgCRND8 brains. Analyte concentrations (ng/mg tissue) of 5-HT and 5-HIAA (5-hydroxyindoleacetic acid) were measured by HPLC and electrochemical detection in perchloric acid tissue extracts from microwave-irradiated brains, as described (Francis *et al.*, 2012b). Levels of 5-HT were not altered in the striatum (**A**), or in the frontal cortex (**C**). 5-HIAA concentrations were increased at 4- and 40+ weeks in the striatum (**B**) and at 16- and 40+ weeks in the frontal cortex (**D**) of TgCRND8 mice. Data are means \pm SEM of $n \geq 8$ mice per group. * $P \leq 0.05$, ** $P \leq 0.01$ vs. non-Tg controls by unpaired Student's *t*-test.

Serotonergic tone in the striatum and frontal cortex can affect levels of anxiety (Ludwig and Schwarting, 2007; Adriani *et al.*, 2006). We assessed thigmotaxis of adult

TgCRND8 mice in the zero maze. Performance in this maze provides measures of anxiety that are sensitive to altered serotonergic tone (Shepherd *et al.*, 1994). Avoidance of the open sectors is considered anxiety-like behaviour. The apparatus (Stoelting Co., Wood Dale, IL) is an elevated circular platform, with two enclosed walled quadrants opposing two open quadrants. This design allows for uninterrupted exploration. It also eliminates ambiguity associated with scoring the time spent in the central open square of the classical elevated plus maze. Mice were placed in a closed quadrant and allowed to explore the maze for 5 minutes. We measured the following indices of anxiety: latency to enter an open area, total time spent in open areas, and the number of times a mouse dipped its head over an open edge. We found that 30-week-old TgCRND8 mice were less anxious than non-Tg controls in this maze (Figure 8-2).

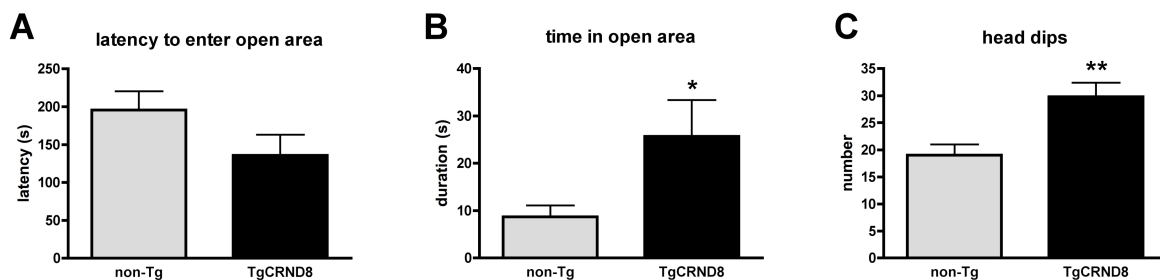


Figure 8-2. TgCRND8 mice are less anxious than non-Tg controls in the zero maze. Anxiety-like behaviour was assessed in 30 week-old mice by measuring the latency to enter (A), duration in (B) and number of head dips over (C) the open quadrants of the zero maze. TgCRND8 mice spent more time in the open area ($t(45) = 2.08$, $P = 0.043$; B) and dipped their heads over the open edge of the maze more frequently ($t(45) = 3.30$, $P = 0.002$; C) than non-Tg littermates. Data are means \pm SEM of $n \geq 23$ mice per group. * $P \leq 0.05$, ** $P \leq 0.01$ versus littermate controls by unpaired Student's t -test.

Schwartz and colleagues (1998) reported that rats with high levels of anxiety in the elevated plus maze exhibit decreased tissue concentrations of serotonin in the ventral striatum. Correspondingly, rats administered a serotonergic neurotoxin in the ventral striatum exhibited anxiogenic behaviour in the elevated plus maze and open field (Ludwig and Schwartz, 2007). By extension, the increased striatal and cortical serotonin turnover in TgCRND8 mice might be expected to account for decreased inhibition in the zero maze. Similar findings have been reported in another APP-Tg line

(Adriani *et al.*, 2006). APP₆₉₅SWE mice show reduced anxiety in the elevated plus maze and motor impulsivity. These behaviours were associated with increased serotonin turnover in the frontal cortex. The authors equate this behaviour to the loss of inhibition observed in AD patients. Similar to our mice, behavioural disinhibition in APP₆₉₅SWE mice is not related to changes in dopaminergic parameters.

We assessed whether reduced noradrenergic tone is associated with decreased anxiety in TgCRND8 mice. 12 week-old mice were treated with dexefaroxan, rivastigmine or saline for 28 days and tested in the zero maze. Neither dexefaroxan nor rivastigmine affected performance in this maze (Figure 8-3), suggesting that thigmotaxic behaviour may be more dependent on striatal serotonergic tone. The striatum is nearly devoid of locus coeruleus innervation (Berridge and Waterhouse, 2003), which may account for the lack of drug effects on anxiety-related phenotypes.

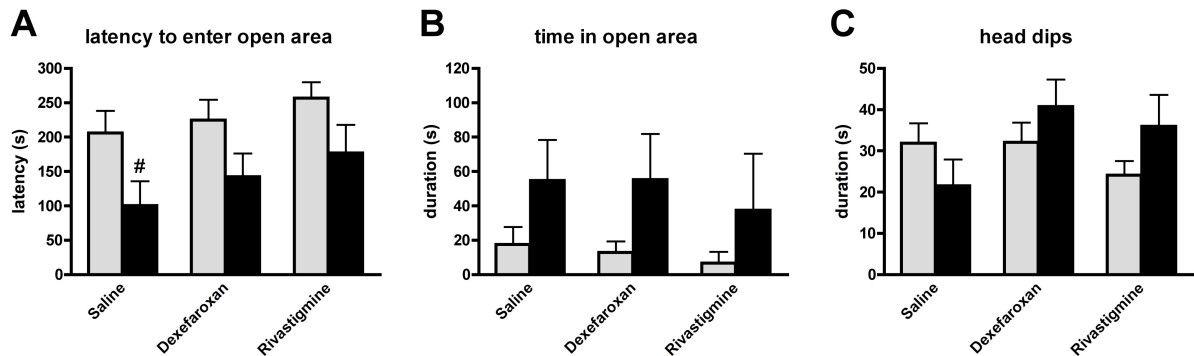


Figure 8-3. Dexefaroxan and rivastigmine do not alter performance in the zero maze. Mice at 12 weeks of age were infused with dexefaroxan, rivastigmine or saline for 28 days. In the last week of their treatment, they were tested in the zero maze. At 15 weeks of age, saline treated TgCRND8 mice were quicker to enter the open area ($t(16) = 2.13$, $P = 0.049$; **A**), but did not differ from controls in the amount of time spent in the open (**B**), or in the number of head dips over the edge of open (**C**) sectors. Neither dexefaroxan nor rivastigmine altered thigmotaxic behaviour (**A**, **B** or **C**). Data are means \pm SEM of $n > 7$ mice per group. [#] $P \leq 0.05$ versus non-Tg saline controls by unpaired Student's t -test.

Administering a serotonin reuptake inhibitor, such as fluoxetine, will help determine whether increases in serotonin turnover contribute to anxiolytic behaviour, or memory deficits and behavioural despair in TgCRND8 mice. We are currently examining whether onset of the anxiolytic response in the zero maze coincides with increased striatal 5-HIAA levels in pre-plaque mice. Rats treated with soluble A β ₄₂ peptides for 7 days, exhibited a depressive but not anxiogenic phenotype. The A β ₄₂ treatment selectively reduced 5-HT content and BDNF expression in the prefrontal cortex. These neurochemical changes were not observed in the striatum (Colaianna *et al.*, 2010). These results imply that serotonergic tone in the prefrontal cortex mediates depressive-like behaviour in rodents. They also confirm our findings of altered affect in TgCRND8 mice and suggests that A β can functionally disrupt specific brain regions to cause distinct depressive and anxiolytic behaviours. Plaque-bearing TgCRND8 mice have been found to exhibit other behavioural abnormalities, including hyperactivity, perseverative wheel-running and circling, but do not show anxiogenic responses in the elevated plus maze (Walker *et al.*, 2011). It would be worthwhile to examine aggressive responses in the isolation-induced resident-intruder test. Results from these assays may extend the face validity of this mouse in modeling non-cognitive symptoms of AD.

TgCRND8 behavioural phenotypes mirror the clinical presentation of AD. As reviewed earlier in the thesis, memory deficits and depressed mood are evident in MCI and early-stage AD. Anxiety, agitation and aggression typically emerge at later stages of dementia. The imbalance between monoaminergic and cholinergic transmission is implicated in behavioural and psychological manifestations of AD, and may very well underlie the behavioural phenotypes of the TgCRND8 mouse.

Concluding Statement

I set out to characterize the onset of behavioural impairment in the TgCRND8 mouse, and to determine the neurochemical correlates of such impairment. At the start of this investigation, TgCRND8 mice had been shown to recapitulate many behavioural and pathophysiological features of AD. However, all of these reported changes occurred late in disease and could not account for the emergence of behavioural deficits. By 2006, it was well established that cognitive decline in AD patients preceded A β deposits. Our work demonstrated that TgCRND8 mice model memory and affective disturbances seen in early-stage AD. In addition, we were the first to report that functional impairment preceded plaque formation in an APP-Tg mouse. Since then, many groups have corroborated our findings in TgCRND8 mice, as well as in other APP-Tg mice.

Our behavioural data pointed to the cortex and hippocampus as early targets of A β -functional disruption. We subsequently discovered decreased BDNF expression, noradrenergic tissue deficits and bioenergetic stress in these brain regions. Among these, noradrenergic tissue deficits were the first to emerge. Hence, we hypothesized that reductions in noradrenaline trigger the AD-like phenotypes of TgCRND8 mice. To test this, we treated mice with the α_2 -adrenoceptor antagonist dexefaroxan, and compared its effects to the cholinesterase inhibitor rivastigmine. Both drugs improved behavioural, BDNF and mitochondrial parameters in these mice. While we did not distinguish between noradrenergic and cholinergic mechanisms of the therapeutic action, it is likely that the early reduction in noradrenaline within forebrain terminals exacerbates A β toxicity and causes functional disruption. Others have demonstrated that the loss of noradrenaline may potentiate A β pathology and associated inflammation, trophic factor deficits, cholinergic hypofunction and bioenergetic stress in a variety of *in vitro* and *in vivo* models. All of these pathophysiological factors occur spontaneously in TgCRND8 mice. We have demonstrated that treating with an α_2 -adrenoceptor antagonist may prevent or delay the onset of A β -induced dysfunction.

References

- Adalbert R, Nogradi A, Babetto E, Janeckova L, Walker SA, Kerschensteiner M et al (2009). Severely dystrophic axons at amyloid plaques remain continuous and connected to viable cell bodies. *Brain* **132**: 402-16.
- Adihetty PJ, Beal MF (2008). Creatine and its potential therapeutic value for targeting cellular energy impairment in neurodegenerative diseases. *Neuromol Med* **10**: 275-290.
- Adolfsson R, Gottfries CG, Roos BE, Winblad B (1979). Changes in the brain catecholamines in patients with dementia of Alzheimer type. *Br J Psychiatry* **135**: 216-223.
- Adriani W, Ognibene E, Heuland E, Ghirardi O, Caprioli A, Laviola G (2006). Motor impulsivity in APP-SWE mice: a model of Alzheimer's disease. *Behav Pharmacol* **17**: 525-533.
- Aksenov M, Aksenova M, Butterfield DA, Markesbery WR (2000). Oxidative modification of creatine kinase BB in Alzheimer's disease brain. *J Neurochem* **74**: 2520–2527.
- Aksenov M, Tucker HM, Nair P, Aksenova M, Butterfield DA, Estus S et al (1999). The expression of several mitochondrial and nuclear genes encoding the subunits of electron transport chain enzyme complexes, cytochrome c oxidase, NADH dehydrogenase in different brain regions in Alzheimer's disease. *Neurochem Res* **24**: 767-774.
- Albert MS, DeKosky ST, Dickson D, Dubois B, Feldman HH, Fox NC et al (2011). The diagnosis of mild cognitive impairment due to Alzheimer's disease: Recommendations from the National Institute on Aging-Alzheimer's Association workgroups on diagnostic guidelines for Alzheimer's disease. *Alzheimers Dement* **7**: 270-279.
- Aleardi AM, Benard G, Augereau O, Malgat M, Talbot JC, Mazat JP et al (2005). Gradual alteration of mitochondrial structure and function by beta-amyloids: importance of membrane viscosity changes, energy deprivation, reactive oxygen species production, and cytochrome c release. *J Bioenerg Biomembr* **37**: 207-225.
- Alegret M, Boada-Rovira M, Vinyes-Junqué G, Valero S, Espinosa A, Hernández I, Modinos G et al. (2009). Detection of visuoperceptual deficits in preclinical and mild Alzheimer's disease. *J Clin Exp Neuropsychol* **31**: 860-867.
- Allen SJ, Watson JJ, Dawbarn D (2011). The neurotrophins and their role in Alzheimer's disease. *Curr Neuropharmacology* **9**: 559-573.
- Allen SJ, Wilcox GK, Dawbarn D (1999). Profound and selective loss of catalytic TrkB immunoreactivity in Alzheimer's disease. *Biochem Biophys Res Comm* **264**: 648-651.

Alonso AD, Clerico JD, Li B, Corbo CP, Alaniz ME, Grundke-Iqbal I, Iqbal K (2010). Phosphorylation of Tau at Thr212, Thr231, and Ser262 combined causes neurodegeneration. *JBC* **285**: 30851-30860.

Ambree O, Richter H, Sachser N, Lewejohann L, Dere E, de Souza Silva MA et al (2009). Levodopa ameliorates learning and memory deficits in a murine model of Alzheimer's disease. *Neurobiol Aging* **30**: 1191-1204.

Ambree O, Touma C, Gortz N, Keyvani K, Paulus W, Palme R, Sachser N (2006). Activity changes and marked stereotypic behaviour precede A β pathology in TgCRND8 Alzheimer mice. *Neurobiol Aging* **27**: 955-964.

Anandatheerthavarada HK, Biswas G, Robin MA, Avadhani NG. (2003). Mitochondrial targeting and a novel transmembrane arrest of Alzheimer's amyloid precursor protein impairs mitochondrial function in neuronal cells. *J Cell Biol* **161**: 41-54.

Arvanitis DN, Ducatenzeiler A, Ou JN, Grodstein E, Andrews SD, Trendulkar SR et al (2007). High intracellular concentrations of amyloid-beta block nuclear translocation of phosphorylated CREB. *J Neurochem* **103**: 216-228.

Aston-Jones G, Cohen JD (2005). An integrative theory of locus coeruleus norepinephrine function: adaptive gain and optimal performance. *Annu Rev Neurosci* **28**: 403-450.

Attwell D, Laughlin SB (2001). An energy budget for signaling in the grey matter of the brain. *J Cereb Blood Flow Metab* **21**: 1133-1145.

Baker KB, Kim J (2002). Effects of stress and hippocampal NMDA receptor antagonism on recognition memory in rats. *Learn Mem* **9**: 58-65.

Baker KG, Tork I, Hornung JP, Halasz P (1989). The human locus coeruleus complex: an immunohistochemical and three-dimensional reconstruction study. *Exp Brain Res* **77**: 257-270.

Balducci C, Forloni G (2011). APP Transgenic mice: their use and limitations. *Neuromol Med* **13**: 117-137.

Ballatore C, Lee VM-Y, Trojanowski JQ (2007). Tau-mediated neurodegeneration in Alzheimer's disease and related disorders. *Nat Rev Neurosci* **8**: 663-672.

Barfield ET, Barry SM, Hodgkin HB, Thompson BM, Allen SS, Grisel JE (2010). β -endorphin mediates behavioral despair and the effect of ethanol on the tail suspension test in mice. *Alcohol Clin Exp Res* **34**: 1066-1072.

Barde YA, Edgar D, Thoenen H (1982). Purification of a new neurotrophic factor from mammalian brain. *EMBO* **1**: 549-553.

Bartus RT (2000). On neurodegenerative diseases, models and treatment strategies: lessons learned and lessons forgotten a generation following the cholinergic hypothesis. *Exp Neurol* **163**: 495-529.

Bartus RT, Dean III RL, Beer B, Lippa AS (1982). The cholinergic hypothesis of geriatric memory dysfunction. *Science* **217**: 408-417.

Bateman RJ, Aisen PS, De Strooper B, Fox NC, Lemere CA, Ringman JM *et al* (2011). Autosomal-dominant Alzheimer's disease: a review and proposal for the prevention of Alzheimer's disease. *Alzheimers Res Ther* **3**:1.

Bauer S, Moyse E, Jourdan F, Colpaert F, Martel JC, Marien M (2003). Effects of the α_2 -adrenoreceptor antagonist dexefaroxan on neurogenesis in the olfactory bulb of the adult rat in vivo: selective protection against neuronal death. *Neuroscience* **117**: 281-291.

Bekar LK, Wei HS, Nedergaard M (2012). The locus coeruleus-norepinephrine network optimizes coupling of cerebral blood volume with oxygen demand. *J Cereb Blood Flow Metab* **32**: 2135-2145.

Bellucci A, Luccarini I, Scali C, Prospero C, Giovannini MG, Pepeu G, Casamenti F (2006). Cholinergic dysfunction, neuronal damage and axonal loss in TgCRND8 mice. *Neurobiol Dis* **23**: 260-272.

Bellucci A, Rosi MC, Grossi C, Fiorentini A, Luccarini I, Casamenti F (2007). Abnormal processing of tau in the brain of aged TgCRND8 mice. *Neurobiol Dis* **27**: 328-338.

Belyaev ND, Kellet KAB, Beckett C, Makova NZ, Revett TJ, Nalivaeva NN (2010). The transcriptionally active amyloid precursor protein (APP) intracellular domain is preferentially produced from the 695 isoform of APP in a b-secretase-dependent pathway. *J Biol Chem* **285**: 41443-41454.

Benarroch EE (2009). The locus coeruleus norepinephrine system: functional organization and potential significance. *Neurology* **73**: 1699-1704.

Benice TS, Raber J (2008). Object recognition analysis in mice using nose-point digital video tracking. *J Neurosci Methods* **168**: 422-430.

Benilova I, Karran E, De Strooper B (2012). The toxic A β oligomer and Alzheimer's disease: an emperor in need of clothes. *Nat Neurosci* **15**: 349-357.

Benjamin S, Doraiswamy PM (2011). Review of the use of mirtazapine in the treatment of depression. *Expert Opin Pharmacother* **12**: 1623-1632.

Berridge CW, Waterhouse BD (2003). The locus coeruleus- noradrenergic system: modulation of behavioral state and state-dependent cognitive processes. *Brain Res Rev* **42**: 33-84.

Blier P (2003). The pharmacology of putative early-onset antidepressant strategies. *Eur Neuropsychopharmacol* **13**: 57-66.

Bonaventure N, Wioland N, Bigenwald J (1983). Involvement of GABAergic mechanisms in the optokinetic nystagmus of the frog. *Exp Brain Res* **50**: 433-441.

Bondareff W, Mountjoy CQ, Roth M (1981). Selective loss of neurons of origin of adrenergic projection to cerebral cortex (nucleus locus coeruleus) in senile dementia. *Lancet* **i**: 783-784.

Bondareff W, Mountjoy CQ, Roth M (1982). Loss of neurons of origin of the adrenergic projection to cerebral cortex (nucleus locus coeruleus) in senile dementia. *Neurology* **32**: 164-168.

Bondareff W, Mountjoy CQ, Roth M, Ressor MN, Iversen LL, Reynolds GP *et al* (1987). Neuronal degeneration in locus coeruleus and cortical correlates of Alzheimer's disease. *Alzheimer Dis Assoc Discord* **1**: 256-262.

Bosetti F, Brizzi F, Barogi S, Mancuso M, Siciliano G, Tendi E *et al* (2002). Cytochrome c oxidase and mitochondrial F1F0-ATPase (ATP synthase) activities in platelets and brain from patients with Alzheimer's disease. *Neurobiol Aging* **23**: 371-376.

Bossers K, Wirz KTS, Meerhoff GF, Essing AHW, Dongen JW, Houba P *et al* (2010). Concerted changes in transcripts in the prefrontal cortex precede neuropathology in Alzheimer's disease. *Brain* **133**: 3699-3723.

Bowen DM, Smith CB, White P, Davison AN (1976). Neurotransmitter-related enzymes and indices of hypoxia in senile dementia and other abiotrophies. *Brain* **99**: 459-496.

Bowling AC, Beal MF (1995). Bioenergetic and oxidative stress in neurodegenerative diseases. *Life Sciences* **56**: 1151-1171.

Braak H, Alafuzoff I, Arzberger T, Kretschmar H, Del Tredici K (2006). Staging of Alzheimer disease-associated neurofibrillary pathology using paraffin sections and immunocytochemistry. *Acta Neuropathol* **112**: 389-404.

Braak H, Braak E (1991). Neuropathological staging of Alzheimer-related changes. *Acta Neuropathol* **82**: 239-259.

Braak H, Del Tredici K (2004). Alzheimer's disease: intraneuronal alterations precede insoluble amyloid- β -formation. *Neurobiol Aging* **25**: 713-718.

Braak H, Del Tredici K (2011). Alzheimer's pathogenesis: is there neuron-to-neuron propagation? *Acta Neuropathol* **121**: 589-595.

Bramham CR, Messaoudi E (2005). BDNF function in adult synaptic plasticity: the synaptic consolidation hypothesis. *Prog Neurobiol* **76**: 99-125.

Brewer G, Wallimann T (2000). Protective effect of the energy precursor creatine against toxicity of glutamate and β -amyloid in rat hippocampal neurons. *J Neurochem* **74**: 1968-1978.

Broadbent NJ, Squire LR, Clark RE (2004). Spatial memory, recognition memory, and the hippocampus. *PNAS USA* **101**: 14515-14520.

Bruen PD, McGeown WJ, Shanks MF, Venneri A (2008). Neuroanatomical correlates of neuropsychiatric symptoms in Alzheimer's disease. *Brain* **131**: 2455-2463.

Bubber P, Haroutunian V, Fisch G, Blass JP, Gibson GE (2005). Mitochondrial abnormalities in Alzheimer brain: Mechanistic implications. *Ann Neurol* **57**: 695-703.

Bublak P, Redel P, Sorg C, Kurz A, Förstl H, Müller HJ, Schneider WX, Finke K (2011). Staged decline in visual processing capacity in mild cognitive impairment and Alzheimer's disease. *Neurobiol Aging* **32**: 1219-1230.

Burbach G, Hellweg R, Haas C, Del Turco D, Deicke U, Abramowski D *et al* (2004). Induction of Brain-derived neurotrophic factor in plaque-associated glial cells of aged APP23 transgenic mice. *J Neurosci* **24**: 2421-2430.

Bücheler MM, Hadamek K, Hein L (2002). Two α_2 -adrenergic receptor subtypes, α_{2A} - and α_{2C} -, inhibit transmitter release in the brain of gene-targeted mice. *Neuroscience* **109**: 819-826.

Bürklen TS, Schlattner U, Homayouni R, Gough K, Rak M, Szeghalmi A *et al* (2006). The creatine kinase/creatine connection to Alzheimer's disease: CK inactivation, APP-CK complexes, and focal creatine deposits. *J Biomed Biotechnol* Article ID: 35936

Burwell RD, Saddoris MP, Bucci DJ, Wiig KA (2004). Corticohippocampal contributions to spatial and contextual learning. *J Neurosci* **24**: 3826-3836.

Busch C, Bohl J, Ohm TJ (1997). Spatial, temporal and numeric analysis of Alzheimer changes in nucleus coeruleus. *Neurobiol Aging* **18**: 401-406.

Butterworth RF, Besnard AM (1990). Thiamine-dependent enzyme changes in temporal cortex of patients with Alzheimer's disease. *Metab Brain Dis* **5**: 179-184.

Bylund DB, Eikenberg DC, Hieble JP, Langer SZ, Lefkowitz RJ, Minneman KP *et al* (1994). International Union of Pharmacology nomenclature of adrenoceptors. *Pharmacol Rev* **46**: 121-136.

Cakir S, Kulaksizoglu IB (2008). The efficacy of mirtazapine in agitated patients with Alzheimer's disease: A 12-week open-label pilot study. *Neuropsychiatric Disease and*

Treatment 4: 963-966.

Calkins MJ, Reddy PH (2011). Amyloid beta impairs mitochondrial anterograde transport and degenerates synapses in Alzheimer's disease neurons. *Biochim Biophys Acta* **1812**: 507-513.

Capsoni S, Ugolini G, Comparini A, Ruberti F, Berardi N, Cattaneo A (2000). Alzheimer-like neurodegeneration in aged antinerve growth factor transgenic mice. *PNAS USA* **97**: 6826-6831.

Cardoso SM, Santana I, Swerdlow RH, Oliveira CR (2004). Mitochondria dysfunction of Alzheimer's disease hybrids enhances Abeta toxicity. *J Neurochem* **89**: 1417-26.

Casademont J, Miro O, Santiago B, Viedma P, Blesa R, Cardellach F (2003). Cholinesterase inhibitor rivastigmine enhances the mitochondrial electron transport chain in lymphocytes of patients with Alzheimer's disease. *J Neurol Sci* **206**: 23-26.

Cash AD, Aliev G, Siedlak SL, Nunomura A, Fujioka H, Zhu X et al. (2003). Microtubule reduction in Alzheimer's disease and aging is independent of tau filament formation. *Am J Pathol* **162**: 1623-1627.

Casley CS, Land JM, Sharpe MA, Clark JB, Duchen MR, Canevari L (2002). β -amyloid fragment 25-35 causes mitochondrial dysfunction in primary cortical neurons. *Neurobiol Dis* **10**: 258-267.

Caspersen C, Wang N, Yao J, Sosunov A, Chen X, Lustbader JW et al (2005). Mitochondrial Abeta: a potential focal point for neuronal metabolic dysfunction in Alzheimer's disease. *FASEB J* **19**: 2040-2041.

Chandrasekaran K, Hatanpaa K, Brady DR, Rapport SI (1996). Evidence for physiological downregulation of brain oxidative phosphorylation in Alzheimer's disease. *Exp Neurol* **142**: 80-88.

Chan-Palay V, Asan E (1989). Alterations in catecholamine neurons of the locus coeruleus in senile dementia of the Alzheimer type and in Parkinson's disease with and without dementia and depression. *J Comp Neurol* **287**: 373-392.

Charles DP, Browning PG, Gaffan D (2004). Entorhinal cortex contributes to object-in-place scene memory. *Eur J Neurosci* **20**: 3157-3164.

Chen L, Cagniard B, Mathews T, Jones S, Koh HC, Ding Y et al (2005). Age-dependent motor deficits and dopaminergic dysfunction in DJ-1 null mice. *J Biol Chem* **280**: 21418-21426.

Chen CT, Liu Z, Ouellet M, Calon F, Bazinet RP (2009). Rapid β -oxidation of eicosapentaenoic acid in mouse brain: An *in situ* study. *Prostaglandins Leukot Essent Fatty Acids* **80**: 157-163.

- Chen Q, Vasquez EJ, Moghaddas S, Hoppel CL, Lesnefsky EJ (2003). Production of reactive oxygen species by mitochondria: central role of complex III. *J Biol Chem* **278**: 36027-36031.
- Chetelat G, Baron J-C (2003). Early diagnosis of Alzheimer's disease: contribution of structural neuroimaging. *NeuroImage* **18**: 525-541.
- Chicco AJ, Sparagna GC (2006). Role of cardiolipin alterations in mitochondrial dysfunction and disease. *Am J Physiol Cell Physiol* **292**: 33-44.
- Chishti MA, Yang D, Janus C, Phinney A, Horne P, Pearson J *et al* (2001). Early-onset amyloid deposition and cognitive deficits in transgenic mice expressing a double mutant form of amyloid precursor protein 695. *J Biol Chem* **276**: 21562-21570.
- Chopin P, Colpaert F, Marien M (2002). Effects of acute and subchronic administration of dexefaroxan, an alpha2-adrenoceptor antagonist, on memory performance in young adult and aged rodents. *J Pharmacol Exp Ther* **301**: 187-196.
- Chopin P, Debeir T, Raisman-Vozari R, Colpaert FC, Marien MR (2004). Protective effect of the alpha2-adrenoceptor antagonist, dexefaroxan, against spatial memory deficit induced by cortical devascularization in the adult rat. *Exp Neurol* **185**: 198-200.
- Chow VW, Mattson MP, Wong PC, Gleichmann M (2010). An overview of APP processing enzymes and products. *Neuromol Med* **12**: 1-12.
- Christensen R, Marcussen AB, Wortwein G, Knudsen GM, Aznar S (2008). A β (1-42) injection causes memory impairment, lowered cortical and serum BDNF levels, and decreased hippocampal 5-HT_{2A} levels. *Exp Neurol* **210**: 164-171.
- Cocco T, Pacelli C, Sgobbo P, Villani G (2009). Control of OXPHOS efficiency by complex I in brain mitochondria. *Neurobiol Aging* **30**: 622-629.
- Colaianna M, Tucci P, Zotti M, Morgese MG, Schiavone S, Govoni S *et al* (2010). Soluble beta amyloid (1-42): a critical player in producing behavioural and biochemical changes evoking depressive-related state? *Br J Pharmacol* **159**: 1704-1715.
- Coleman M (2005). Axon degeneration mechanism: commonality amid diversity. *Nat Rev Neurosci* **6**: 889-898.
- Coleman PD, Yao PJ (2003). Synaptic slaughter in Alzheimer's disease. *Neurobiol Aging* **24**: 1023-1027.
- Connor B, Young D, Yan Q, Faull RL, Synek M, Dragunow M (1997). Brain-derived neurotrophic factor is reduced in Alzheimer's disease. *Mol Brain Res* **49**: 71-81.

- Contestabile A (2011). The history of the cholinergic hypothesis. *Behav Brain Res* **221**: 334-340.
- Counts S, Mufson E (2010). Noradrenaline activation of neurotrophic pathways protects against neuronal amyloid toxicity. *J Neurochem* **113**: 649-660.
- Coyle JT, Duman RS (2003). Finding the intracellular signaling pathways affected by mood disorder treatments. *Neuron* **38**: 57-160.
- Coyle JT, Price DL, DeLong MR (1983). Alzheimer's disease: a disorder of cortical cholinergic innervation. *Science* **219**: 1184-1190.
- Crews L, Rockenstein E, Masliah E (2010). APP transgenic modeling of Alzheimer's disease: mechanisms of neurodegeneration and aberrant neurogenesis. *Brain Struct Funct* **214**: 111-126.
- Cross AJ, Crow TJ, Perry EK, Perry RH, Blessed G, Tomlinson BE (1981). Reduced dopamine-beta-hydroxylase activity in Alzheimer's disease. *Br J Clin Res Ed* **282**: 93-94.
- Crouch PJ, Harding SE, White AR, Camakaris J, Bush AI, Masters CL (2008). Mechanisms of A β mediated neurodegeneration in Alzheimer's disease. *Int J Biochem Cell Biol* **40**: 181-198.
- Cruts M, Theuns J, Van Broeckhoven C (2012). Locus-specific mutation databases for neurodegenerative brain diseases. *Hum Mutat* **33**: 1340-1344.
- Cryan JF, Mombereau C, Vassout A (2005). The tail suspension test as a model for assessing antidepressant activity: review of pharmacological and genetic studies in mice. *Neurosci Biobehav Rev* **29**: 571-625.
- Cummings JL (2000). Cognitive and behavioural heterogeneity in Alzheimer's disease: seeking the neurobiological basis. *Neurobiol Aging* **21**: 845-861.
- Cummings JL, Kaufer D (1996). Neuropsychiatric aspects of Alzheimer's disease: The cholinergic hypothesis revisited. *Neurology* **47**: 876-883.
- Cunha C, Brambilla R, Thomas KL (2010). A simple role for BDNF in learning and memory? *Front Mol Neurosci* **3**: 1.
- David S, Shoemaker M, Haley BE (1998). Abnormal properties of creatine kinase in Alzheimer's disease brain: Correlation of reduced enzyme activity and active site photolabeling with aberrant cytosol-membrane partitioning. *Brain Research. Mol Brain Res* **54**: 276-287.
- Davies P, Maloney AJ (1976). Selective loss of central cholinergic neurons in Alzheimer's disease. *Lancet* **2**: 1403.

Davis CW, Hawkins BJ, Ramasamy S, Irrinki KM, Cameron BA, Islam K, Daswani VP, Doonan PJ, Manevich Y, Madesh M (2010). Nitration of the mitochondrial complex I subunit NDUFB8 elicits RIP1-and RIP3-mediated necrosis. *Free Radic Biol Med* **48**: 306-317.

Davis RE, Miller S, Herrnsstadt C, Ghosh SS, Fahy E, Shinobu LA *et al* (1997). Mutations in mitochondrial cytochrome c oxidase genes segregate with late-onset Alzheimer disease. *PNAS USA* **94**: 4526-31.

Davis KL, Mohs RC, Marin D, Purohit DP, Perl DP, Lantz M, Austin G, Haroutunian V (1999). Cholinergic markers in elderly patients with early signs of Alzheimer's disease. *JAMA* **281**: 1401-1406.

Debeir T, Marien M, Chopin P, Martel J-C, Colpaert F, Raisman- Vozari R (2002). Protective effects of the α_2 -adrenoceptor antagonist, dexefaroxan, against degeneration of the basalocortical cholinergic system induced by cortical devascularization in the adult rat. *Neuroscience* **115**: 41–53.

Debeir T, Marien M, Ferrario J, Rizk P, Prigent A, Colpaert F, Raisman-Vozari R (2004). In vivo upregulation of endogenous NGF in the rat brain by the α_2 -adrenoreceptor antagonist dexefaroxan: potential role in the protection of the basalocortical cholinergic system during neurodegeneration. *Exp Neurol* **190**: 384-395.

Decker MW, Gallagher M (1987). Scopolamine-disruption of radial arm maze performance: modification by noradrenergic depletion. *Brain Res* **417**: 59-69.

DeKosky ST, Ikonomic MD, Styren SD, Beckitt L, Wisniewski S, Bennett DA *et al* (2002). Upregulation of choline acetyltransferase activity in hippocampus and frontal cortex of elderly subjects with mild cognitive impairment. *Ann Neurol* **51**: 145-155.

Del Vecchio RA, Gold LH, Novick SJ, Wong G, Hyde LA (2004). Increased seizure threshold and severity in young transgenic CRND8 mice. *Neurosci Lett* **367**:164-167

Dere E, Huston JP, A De Souza Silva, M (2007). The pharmacology, neuroanatomy and neurogenetics of one-trial object recognition in rodents. *Neurosci Biobehav Rev* **31**: 673-704.

DeToledo-Morrell L, Sullivan MP, Morrell F, Wilson RS, Bennett DA, Spencer S (1997). Alzheimer's disease: in vivo detection of differential vulnerability of brain regions. *Neurobiol Aging* **18**: 463–468.

Deutsch JA (1971). The cholinergic synapse and the site of memory. *Science* **174**: 788-794.

Devanand DP, Bansal R, Liu J, Hao X, Pradhaban G, Petersen BS (2012). MRI hippocampal and entorhinal cortex mapping in predictive conversion to Alzheimer's disease. *NeuroImage* **60**: 1622-1629.

Devanand DP, Pradhaban G, Liu X, Khandji A, De Santi S, Segal S *et al* (2007). Hippocampal and entorhinal atrophy in mild cognitive impairment. Prediction of Alzheimer's disease. *Neurology* **68**: 828-836.

Devi L, Ohno M (2012). Mitochondrial dysfunction and accumulation of the β -secretase-cleaved C-terminal fragment of APP in Alzheimer's disease transgenic mice. *Neurobiol Disease* **45**: 417-424.

Devi L, Prabhu BM, Galati DF, Avadhani NG, Anandatheerthavarada HK (2006). Accumulation of amyloid precursor protein in the mitochondrial import channels of human Alzheimer's disease brain is associated with mitochondrial dysfunction. *J Neurosci* **26**: 9057-9068.

Dickson DW, Crystal HA, Mattiace LA, Masur DM, Blau AD, Davies P *et al* (1992). Identification of normal and pathological aging in prospectively studied nondemented elderly humans. *Neurobiol Aging* **13**: 179-189.

Diniz BS, Teixeira AL (2011). Brain-derived neurotrophic factor and Alzheimer's disease: Physiopathology and beyond. *Neuromol Med* **13**: 217-222.

Dodart JC, Mathis C, Bales KR, Paul SM (2002). Does my mouse have Alzheimer's disease? *Genes Brain Behav* **1**: 142-155.

Dodart JC, Mathis C, Ungerer A (1997). Scopolamine-induced deficits in a two-trial object recognition task in mice. *Neuroreport* **8**: 1173-1178.

Done D, Hajilou B (2005). Loss of high-level perceptual knowledge of object structure in DAT. *Neuropsychologia* **43**: 60-68.

Drachman DA (1977). Memory and cognitive function in man: does the cholinergic system have a specific role? *Neurology* **8**: 783-790.

Drachman DA, Leavitt J (1974). Human memory and the cholinergic system: a relationship to aging? *Arch Neurol* **30**: 113-121.

Dringenberg HC (2000). Alzheimer's disease: more than a 'cholinergic disorder'-evidence that cholinergic-monoaminergic interactions contribute to EEG slowing and dementia. *Behav Brain Res* **115**: 235-249.

Du J, Feng L, Zaitsev E, Je H-S, Liu X, Lu B (2003). Regulation of TrkB receptor tyrosine kinase and its internalization by neuronal activity and Ca^{2+} influx. *J Cell Biol* **163**: 385-395.

Duyckaerts C, Potier MC, Delatour B (2008). Alzheimer disease models and human neuropathology: similarities and differences. *Acta Neuropathol* **115**: 5- 38.

Eckert A, Schmitt K, Gotz J (2011). Mitochondrial dysfunction - the beginning of the end in Alzheimer's disease? Separate and synergistic modes of tau and amyloid- β toxicity. *Alzheimers Res Ther* **3**: 15.

Eisenhofer G, Kopin IJ, Goldstein DS (2004). Catecholamine metabolism: a contemporary view with implications for physiology and medicine. *Pharmacol Rev* **56**: 331-349.

Elder GA, Gama Sosa MA, De Gasperi R (2010). Transgenic mouse models of Alzheimer's disease. *Mt Sinai J Med* **77**: 69-81.

Emahazion T, Jobs M, Howell WM, Siegfried M, Wyoni P, Prince JA, Brookes AJ (1999). Identification of 167 polymorphisms in 88 genes from candidate neurodegeneration pathways. *Gene* **238**: 315-324.

Engberg G, Svensson TH (1980). Pharmacological analysis of a cholinergic receptor mediated regulation of brain norepinephrine neurons. *J Neural Transm* **49**: 137-150.

Ennaceur A, Delacour J (1988). A new one-trial test for neurobiological studies of memory in rats. 1: Behavioural data. *Behav Brain Res* **31**: 47-59.

Fawcett JP, Bamji SX, Causing CG, Aloyz R, Ase AR, Reader TA et al (1998). Functional evidence that BDNF is an anterograde neuronal trophic factor in the CNS. *J Neurosci* **18**: 2808-2821.

Feinstein DL, Heneka MT, Gavrilyuk V, Dello Russo C, Weinberg G, Galea E (2002). Noradrenergic regulation of inflammatory gene expression in brain. *Neurochem Int* **41**: 357-365.

Fernández M, Gobartt AL, Balana M, the COOPERA Study Group (2010). Behavioural symptoms in patients with Alzheimer's disease and their association with cognitive impairment. *BMC Neurology* **10**: 87.

Fernandez-Vizarra P, Fernandez AP, Castro-Blanco S, Serrano J, Bentura ML, Martinez-Murillo R et al (2004). Intra- and extracellular Abeta and PHF in clinically evaluated cases of Alzheimer's disease. *Histol Histopathol* **19**: 823-844.

Ferrer I, Marin C, Rey MJ, Ribalta T, Goutan E, Blanco R, Tolosa E, Marti E (1999). BDNF and full-length and truncated TrkB expression in Alzheimer's disease. *J Neuropathol Exp Neurol* **58**: 729-739.

Finkel SI (2004). Effects of rivastigmine on behavioral and psychological symptoms of dementia in Alzheimer's disease. *Clin Ther* **26**: 980-990.

- Flatmark T (2000). Catecholamine biosynthesis and physiological regulation in neuroendocrine cells. *Acta Physiol Scand* **168**: 1-17
- Folch J, Lees M, Sloane Stanley GH (1957). A simple method for the isolation and purification of total lipids from animal tissues. *J Biol Chem* **226**: 497-509.
- Foote SL, Bloom FE, Aston-Jones G (1983). Nucleus locus coeruleus: new evidence of anatomical and physiological specificity. *Physiol Rev* **63**: 844-914.
- Fornai F, Bassi L, Torracca MT, Alessandri MG, Scalori V, Corsini GU (1996). Region- and neurotransmitter-dependent species and strain differences in DSP-4-induced monoamine depletion in rodents. *Neurodegeneration* **5**: 241-249.
- Forno LS (1966). Pathology of Parkinsonism. *J Neurosurg* **24**: 266-271.
- Forno LS, Barbour PJ, Norville RL (1978). Presenile dementia with Lewy bodies and neurofibrillary tangles. *Arch Neurol* **35**: 818-822.
- Förstl H, Burns A, Luthert P, Cairns N, Lantos P, Levy R (1992). Clinical and neuropathological correlates of depression in Alzheimer's disease. *Psychol Med* **22**: 877-884.
- Francis BM, Kim J, Barakat ME, Fraenkl S, Yücel YH, Peng S, Michalski B, Fahnstock M, McLaurin J, Mount HTJ (2012a). Object recognition memory and BDNF expression are reduced in young TgCRND8 mice. *Neurobiol Aging* **33**: 555-563.
- Francis BM, Yang J, Hajderi E, Brown ME, Michalski B, McLaurin J, Fahnstock M, Mount HTJ (2012b). Reduced tissue levels of noradrenaline are associated with behavioural phenotypes of the TgCRND8 mouse model of Alzheimer's disease. *Neuropsychopharmacology* **37**: 1937-1944.
- Francis PT, Nordberg A, Arnold SE (2005). A preclinical view of cholinesterase inhibitors in neuroprotection: do they provide more than symptomatic benefits in Alzheimer's disease. *Trends Pharmacol Sci* **26**: 104-111.
- Francis PT, Palmer AM, Snape M, Wilcock GK (1999). The cholinergic hypothesis of Alzheimer's disease: a review of progress. *J Neurol Neurosurg Psychiatry* **66**: 137-147.
- Francis PT, Ramirez MJ, Lai MK (2010). Neurochemical basis for symptomatic treatment of Alzheimer's disease. *Neuropharmacology* **59**: 221-229.
- Friedman WJ (2000). Neurotrophins induce death of hippocampal neurons via the p75 receptor. *J Neurosci* **20**: 6340-6346.
- Fritschy JM, Grzanna R (1989). Immunohistochemical analysis of the neurotoxic effects of DSP-4 identifies two populations of noradrenergic axon terminals. *Neuroscience* **30**: 181-197.

Fukuyama H, Ogawa M, Yamauchi H, Yamaguchi S, Kimura J, Yonekura Y, Konishi J (1994). Altered cerebral energy metabolism in Alzheimer's disease: a PET study. *J Nucl Med* **35**: 1-6.

Fung J, Frost D, Chakrabartty A, McLaurin J (2004). Interaction of human and mouse A β peptides. *J Neurochem* **91**: 1398-1403.

Galeotti N, Ghelardini C (2012). Regionally selective activation and differential regulation of ERK, JNK and p38 MAP kinase signaling pathway by protein kinase C in mood modulation. *Int J Neuropsychopharmacol* **15**: 781-793.

Gallagher M, Koh MT (2011). Episodic memory on the path to Alzheimer's disease. *Curr Opin Neurobiol* **21**: 929-934.

Gallant M, Rak M, Szeghalmi A, Del Bigio MR, Westaway D, Yang J, Julian R, Gough KM (2006). Focally elevated creatine detected in amyloid precursor protein (APP) transgenic mice and Alzheimer's disease brain tissue. *J Biol Chem* **281**: 5-8

Gamblin TC, Chen F, Zambrano A, Abraha A, Lagalwar S, Guillozet AL *et al* (2003). Caspase cleavage of tau: linking amyloid and neurofibrillary tangles in Alzheimer's disease. *PNAS* **100**: 10032-10037.

Garzon DJ, Fahnstock M (2007). Oligomeric amyloid decreases basal levels of brain-derived neurotrophic factor (BDNF) mRNA via specific downregulation of BDNF transcripts IV and V in differentiated human neuroblastoma cells. *J Neurosci* **27**: 2628-2635.

Garzon D, Yu G, Fahnstock M (2002). A new brain-derived neurotrophic factor transcript and decrease in brain-derived neurotrophic factor transcripts 1, 2 and 3 in Alzheimer's disease parietal cortex. *J Neurochem* **82**: 1058-1064.

German DC, Manaye KF, White III CL, Woodward DJ, McIntire DD, Smith WK, Kalaria RN (1992). Disease-specific patterns of locus coeruleus cell loss. *Ann Neurol* **32**: 667-676.

German DC, Nelson O, Liang F, Liang C-L, Games D (2005). The PDAPP mouse model of Alzheimer's disease: Locus coeruleus neuronal shrinkage. *J Comp Neurol* **492**: 469-476.

German DC, Walker BS, Manaye K, Smith WK, Woodward DJ, North AJ (1988). The human locus coeruleus: computer reconstruction of cellular distribution. *J Neurosci* **8**: 1776-1788.

German DC, White CL, Sparkman DR (1987). Alzheimer's disease: neurofibrillary tangles in nuclei that project to the cerebral cortex. *Neuroscience* **21**: 305-312.

- Gesi M, Soldania P, Giorgia FS, Santinamia A, Bonaccorsib I, Fornaia BF (2000). The role of locus coeruleus in the development of Parkinson's disease. *Neurosci Biobehav Rev* **24**: 655-658.
- Gibson GE, Sheu KF, Blass JP, Baker A, Carlson KC, Harding B, Perrino P (1988). Reduced activities of thiamine-dependent enzymes in the brains and peripheral tissues of patients with Alzheimer's disease. *Arch Neurol* **45**: 836-840.
- Gibson GE, Sheu KF, Blass JP (1998). Abnormalities of mitochondrial enzymes in Alzheimer disease. *J Neural Transm* **105**: 855-870.
- Gillardon F, Rist W, Kussmaul L, Vogel J, Berg M, Danzer K, Kraut N, Hengerer B (2007). Proteomic and functional alterations in brain mitochondria from Tg2576 mice occur before amyloid plaque deposition. *Proteomics* **7**: 605-616.
- Gilsbach R, Hein L (2008). Presynaptic metabotropic receptors for acetyl- choline and adrenaline/noradrenaline. *Handb Exp Pharmacol* **184**: 261-288.
- Glavin GB (1985). Stress and Brain noradrenaline: a review. *Neurosci Biobehav Rev* **9**: 233-243.
- Glenner GG, Wong CW (1984). Alzheimer's disease: Initial report of the purification and characterization of a novel cerebrovascular amyloid protein. *Biochem Biophys Res Commun* **120**: 885-890.
- Gonzalo-Ruiz A, Gonzalez I, Sanz-Anquela JM (2003). Effects of b- amyloid protein on serotonergic, noradrenergic, and cholinergic markers in neurons of the pontomesencephalic tegmentum in the rat. *J Chem Neuroanat* **26**: 153-169.
- Görtz N, Lewejohann L, Tomm M, Ambrée O, Keyvani K, Paulus W et al (2008). Effects of environmental enrichment on exploration, anxiety, and memory in female TgCRND8 Alzheimer mice. *Behav Brain Res* **191**: 43-8.
- Götz J, Chen F, van Dorpe J, Nitsch RM (2001). Formation of neurofibrillary tangles in P301L tau transgenic mice induced by A β ₄₂ fibrils. *Science* **293**: 1491-1495.
- Götz J, Ittner LM, Kins S (2006). Do axonal defects in tau and amyloid precursor protein transgenic animals model axonopathy in Alzheimer's disease. *J Neurochem* **98**: 993-1006.
- Götz J, Schild A, Hoerndli F, Pennanen L (2004). Amyloid-induced neurofibrillary tangle formation in Alzheimer's disease: insight from transgenic mouse and tissue-culture models. *Int J Devl Neuroscience* **22**: 453-465.
- Greco SJ, Bryan KJ, Sarkar S, Zhu X, Smith MA, Ashford JW et al (2010). Leptin reduces pathology and improves memory in a transgenic mouse model of Alzheimer's disease. *J Alzheimer's Dis* **19**: 1155-1167.

Grudzien A, Shaw P, Weintraub S, Bigio E, Mash DC, Mesulam MM (2007). Locus coeruleus neurofibrillary degeneration in aging, mild cognitive impairment and early Alzheimer's disease. *Neurobiol Aging* **28**: 327-335.

Guan ZZ, Soderberg M, Sindelar P, Edlund C (1994). Content and fatty acid composition of cardiolipin in the brain of patients with AD. *Neurochem Int* **25**: 295-300.

Guérin D, Sacquet J, Mandairon N, Jourdan F, Didier A (2009). Early locus coeruleus degeneration and olfactory dysfunctions in Tg2576 mice. *Neurobiol Aging* **30**: 272-283.

Gulyás B, Brockschneider D, Nag S, Pavlova E, Kasa P, Beliczai Z *et al* (2010). The norepinephrine transporter (NET) ligand (S,S)-[18F]FMeNER-D2 shows significant decreases in NET density in the human brain in Alzheimer's disease: a post-mortem autoradiographic study. *Neurochem Int* **56**: 789-798.

Gunten A, Kovari E, Bussiere T, Rivara C, Gold G, Bouras C, Hof P, Giannakopoulos P (2006). Cognitive impact of neuronal pathology in the entorhinal cortex and CA1 field in Alzheimer's disease. *Neurobiol Aging* **27**: 270-277.

Haass C, Lemere CA, Capell A, Citron M, Seubert P, Schenk D, Lannfelt L, Selkoe DJ (1995). The Swedish mutation causes early-onset Alzheimer's disease by b-secretase cleavage within the secretory pathway. *Nature* **1**: 1291-1296.

Haass C, Koo EH, Mellon A, Hung AY, Selkoe DJ (1992). Targeting of cell-surface β -amyloid precursor protein to lysosomes: alternative processing into amyloid-bearing fragments. *Nature* **357**: 500-503.

Haass C, Selkoe DJ (2007). Soluble protein oligomers in neurodegeneration: lessons from the Alzheimer's amyloid β -peptide. *Nat Rev Mol Cell Biol* **8**: 101-112.

Hall CN, Klein-Flugge MC, Howarth C, Attwell D (2012). Oxidative phosphorylation, not glycolysis, powers presynaptic and postsynaptic mechanisms underlying brain information processing. *J Neurosci* **32**: 8940-8951.

Hallbook F, Ibanez CF, Persson H (1991). Evolutionary studies of the nerve growth factor family reveal a novel member abundantly expressed in *Xenopus* ovary. *Neuron* **6**: 845-858.

Hammerschmidt T, Kummer MP, Terwel D, Martinez A, Gorji A, Pape H-C *et al* (2013). Selective Loss of Noradrenaline Exacerbates Early Cognitive Dysfunction and Synaptic Deficits in APP/PS1 Mice. *Biol Psychiatry* **73**: 454-463.

Hammond RS, Tull LE, Stackman RW (2004). On the delay-dependent involvement of the hippocampus in object recognition memory. *Neurobiol Learn Mem* **82**: 26-34.

Hanna A, Horne P, Yager D, Eckman C, Eckman E, Janus C (2009). Amyloid- β and impairment in multiple memory systems in older transgenic APP TgCRND8 mice. *Genes Brain Behav* **8**: 676-684.

Hansson Petersen CA, Alikhani N, Behbahani H, Wiehager B, Pavlov PF, Alafuzoff I *et al* (2008). The amyloid beta-peptide is imported into mitochondria via the TOM import machinery and localized to mitochondrial cristae. *PNAS* **105**: 131450-13150.

Hansson CA, Frykman S, Farmery MR, Tjernberg LO, Nilsberth C, Pursglove SE *et al* (2004). Nicastrin, presenilin, APH-1, and PEN-2 form active gamma-secretase complexes in mitochondria. *J Biol Chem* **279**: 51654-51660.

Hardy J, Adolfsson R, Alafuzoff I, Bucht G, Marcusson J, Nyberg P *et al* (1985). Transmitter deficits in Alzheimer's disease. *Neurochem Int* **7**: 545-563.

Hardy JA, Higgins GA (1992). Alzheimer's disease: the amyloid cascade hypothesis. *Science* **256**: 184-185.

Hardy J, Selkoe DJ (2002). The amyloid hypothesis of Alzheimer's disease: progress and problems on the road to therapeutics. *Science* **297**: 353-356.

Harik SI, McCracken KA (1986). Age-related increase in presynaptic noradrenergic markers of the rat cerebral cortex. *Brain Res* **381**: 125-130.

Harley CW (2007). Norepinephrine and the dentate gyrus. *Prog Brain Res* **163**: 299-318.

Harris JA, Devidze N, Verret L, Ho K, Halabisky B, Thwin MT *et al.* (2010). Transsynaptic progression of amyloid- β -induced neuronal dysfunction within the entorhinal-hippocampal network. *Neuron* **68**: 428-441.

Hawkes CA, Deng L-H, Shaw JE, Nitz M, McLaurin J (2010). Small molecule β -amyloid inhibitors that stabilize protofibrillar structures *in vitro* improve cognition and pathology in a mouse model of Alzheimer's disease. *Eur J Neurosci* **31**: 203-213.

Heldt SA, Stanek L, Chhatwal JP, Ressler KJ (2007). Hippocampus-specific deletion of BDNF in adult mice impairs spatial memory and extinction of aversive memories. *Mol Psych* **12**: 656-670.

Heneka MT, Galea E, Gavrilyuk V, Dumitrescu-Ozimek L, Daeschner J, O'Banion MK *et al* (2002). Noradrenergic depletion potentiates beta-amyloid-induced cortical inflammation: implications for Alzheimer's disease. *J Neurosci* **22**: 2434-2442.

Heneka MT, Nadrigny F, Regen T, Martinez-Hernandez A, Dumitrescu-Ozimek L, Terwel D *et al* (2010). Locus coeruleus controls AD pathology by modulating microglial functions through norepinephrine. *PNAS* **107**: 6058-6063.

Heneka MT, O'Banion MK (2007). Inflammatory processes in Alzheimer's disease. *J Neuroimmunol* **184**: 69-91.

Heneka MT, Ramanathan M, Jacobs AH, Dumitrescu-Ozimek L, Bilkei-Gorzo A, Debeir T (2006). Locus coeruleus degeneration promotes Alzheimer pathogenesis in amyloid precursor protein 23 transgenic mice. *J Neurosci* **26**: 1343-1354.

Hennigan A, O'Callaghan RM, Kelly AM (2007). Neurotrophins and their receptors: roles in plasticity, neurodegeneration and neuroprotection. *Biochem Soc Trans* **35**: 424-427.

Henry RA, Hughes SM, Connor B (2007). AAV-mediated delivery of BDNF augments neurogenesis in the normal and quinolinic acid-lesioned adult rat brain. *Eur J Neurosci* **25**: 3513-3525.

Hensley K, Butterfield DA, Mattson M, Aksenova M, Harris M, Wu JF et al (1995). A model for beta-amyloid aggregation and neurotoxicity based on the free radical generating capacity of the peptide: Implications of "molecular shrapnel" for Alzheimer's disease. *Proc West Pharmacol Soc* **38**: 113-120.

Herrmann N, Lanctot KL, Khan LR (2004). The role of norepinephrine in the behavioural and psychological symptoms of dementia. *J Neuropsychiatry Clin Neurosci* **16**: 261-276.

Hickman SE, Allison EK, El Khoury J (2008). Microglial dysfunction and defective beta-amyloid clearance pathways in aging Alzheimer's disease mice. *J Neurosci* **28**: 8354-8360

Hock C, Heese K, Hulette C, Rosenberg C, Otten U (2000). Region-specific neurotrophin imbalances in Alzheimer disease: decreased levels of brain-derived neurotrophic factor and increased levels of nerve growth factor in hippocampus and cortical areas. *Arch Neurol* **57**: 846-851.

Hof PR, Bouras C (1991). Object recognition deficit in Alzheimer's disease: possible disconnection of the occipito-temporal component of the visual system. *Neurosci Lett* **122**: 53-56.

Hofer M, Pagliusi SR, Hohn A, Leibrock J, Barde YA (1990). Regional distribution of brain-derived neurotrophic factor mRNA in the adult mouse brain. *EMBO J* **9**: 2459-2464.

Holm PC, Rodriguez FJ, Kresse A, Canals JM, Silos-Santiago I, Arenas E (2003). Crucial role of TrkB ligands in the survival and phenotypic differentiation of developing locus coeruleus noradrenergic neurons. *Development* **130**: 3535-3545.

Holsinger RMD, Schnarr J, Henry P, Castelo VT, Fahnstock M (2000). Quantitation of BDNF mRNA in human parietal cortex by competitive reverse transcription-polymerase chain reaction: decreased levels in Alzheimer's disease. *Mol Brain Res* **76**: 347-354.

- Hoogendijk WJG, Pool CW, Troost D, van Zweiten E, Swaab DF (1995). Image analyzer-assisted morphology of the locus coeruleus in Alzheimer's disease, Parkinson's disease and amyotrophic lateral sclerosis. *Brain* **118**: 131-143.
- Hoyer S (1993). Brain oxidative energy and related metabolism, neuronal stress, and Alzheimer's disease: a speculative synthesis. *J Geriatr Psychiatry Neurol* **6**: 3-12.
- Hyde LA, Kazdoba TM, Grilli M, Lozza G, Brussa R, Zhang Q *et al* (2005). Age-progressing cognitive impairments and neuropathology in transgenic CRND8 mice. *Behav Brain Res* **160**: 344-355.
- Insua D, Suárez M-L, Santamarina G, Sarasa M, Pesini P (2010). Dogs with canine counterpart of Alzheimer's disease lose noradrenergic neurons. *Neurobiol Aging* **31**: 625-635.
- Ip NY, Ibanez CF, Nye SH, McClain J, Jones PF, Gies DR *et al* (1992). Mammalian neurotrophin-4: structure, chromosomal localization, tissue distribution and receptor specificity. *PNAS* **89**: 3060-3064.
- Ishida Y, Shirokawa T, Komatsu Y, Isobe K (2001). Changes in cortical noradrenergic axon terminals of locus coeruleus neurons in aged F344 rats. *Neurosci Lett* **307**: 197-199.
- Iversen LL, Rossor MN, Reynolds GP, Hills R, Roth M, Mountjoy CQ *et al* (1983). Loss of pigmented dopamine beta-hydroxylase positive cells from locus coeruleus in senile dementia of Alzheimer type. *Neurosci Lett* **39**: 95-100.
- Janus C (2004). Search Strategies Used by *APP* Transgenic Mice During Navigation in the Morris Water Maze. *Learn Mem* **11**: 337-346.
- Janus C, Pearson J, McLaurin J, Mathews PM, Jiang Y, Schmidt SD *et al.* (2000). A β peptide immunization reduces behavioural impairment and plaques in a model of Alzheimer's disease. *Nature* **408**: 979-982.
- Janus C, Welzl H, Hanna A, Lovasic L, Lane N, St George-Hyslop P, Westaway D (2004). Impaired conditioned taste aversion learning in *APP* transgenic mice. *Neurobiol Aging* **25**: 1213-1219.
- Jardanhazi-Kurutz D, Kummer MP, Terwel D, Vogel K, Dyrks T, Thiele A *et al* (2010). Induced LC degeneration in *APP/PS1* transgenic mice accelerates early cerebral amyloidosis and cognitive deficits. *Neurochem Int* **57**: 375-382.
- Jardanhazi-Kurutz D, Kummer MP, Terwel D, Vogel K, Thiele A, Heneka MT (2011). Distinct adrenergic system changes and neuroinflammation in response to induced locus coeruleus degeneration in *APP/PS1* transgenic mice. *Neuroscience* **176**: 396-407.
- Jawhar S, Trawicka A, Jenneckins C, Bayer TA, Wirths O (2012). Motor deficits, neuron

loss, and reduced anxiety coinciding with axonal degeneration and intraneuronal A β aggregation in the 5XFAD mouse model of Alzheimer's disease. *Neurobiol Aging* **33**: 196.e29–196.e40.

Jhaveri DJ, Mackay EW, Hamlin AS, Marathe SV, Nandam LS, Vaidya VA, Bartlett PF (2010). Norepinephrine Directly Activates Adult Hippocampal Precursors via β 3-Adrenergic Receptors. *J Neurosci* **30**: 2795-2806.

Jolas T, Zhang XS, Zhang Q, Wong G, Del Vecchio RA, Gold L, Priestley T (2002). Long-term potentiation is increased in the CA1 area of the hippocampus of APP^{swe}/ind CRND8 mice. *Neurobiol Dis* **11**: 394-409.

Jones TT, Brewer GJ (2010). Age-related deficiencies in complex I endogenous substrate availability and reserve capacity of complex IV in cortical neuron electron transport. *Biochim Biophys Acta* **1797**: 167-176.

Jucker M (2010). The benefits and limitations of animal models for translational research in neurodegenerative diseases. *Nature Med* **16**: 1210-1214.

Kalaria RN, Stockmeier CA, Harik SI (1989). Brain microvessels are innervated by locus coeruleus noradrenergic neurons. *Neurosci Lett* **97**: 203-208.

Kalinin S, Gavrilyuk V, Polak PE, Vasser R, Zhao J, Heneka MT *et al* (2007). Noradrenaline deficiency in brain increases beta- amyloid plaque burden in an animal model of Alzheimer's disease. *Neurobiol Aging* **28**: 1206-1214.

Kalinin S, Polak PE, Lin SX, Sakharkar AJ, Pandey SC, Feinstein DL (2012). The noradrenaline precursor L-DOPS reduces pathology in a mouse model of Alzheimer's disease. *Neurobiol Aging* **33**: 1651-1653.

Kar S, Slowikowski SPM, Westaway D, Mount HTJ (2004). Interactions between β -amyloid and central cholinergic neurons: implications for Alzheimer's disease. *J Psychiatry Neurosci* **29**: 427-441.

Kennedy AM, Frackowiak RSJ, Newman SK, Bloomfield PM, Seaward J, Roques P *et al* (1995). Deficits in cerebral glucose metabolism demonstrated by positron emission tomography in individuals at risk of familial Alzheimer disease. *Neurosci Lett* **186**: 17-20.

Kobayashi DT, Chen KS (2005). Behavioral phenotypes of amyloid-based genetically modified mouse models of Alzheimer's disease. *Genes Brain Behav* **4**: 173-96.

Koffie R, Hyman B, Spires-Jones T (2011). Alzheimer's disease: synapses gone cold. *Mol Neurodegener* **6**: 63-71.

Kokjohn TA, Roher AE (2009). Amyloid precursor protein transgenic mouse models and Alzheimer's disease: understanding the paradigms, limitations, and contributions. *Alzheimers Dement* **5**: 340-347.

- Kong Y, Ruan L, Qian L, Liu X, and Le Y (2010). Norepinephrine promotes microglia to uptake and degrade amyloid β peptide through upregulation of mouse formyl peptide receptor 2 and induction of insulin-degrading enzyme. *J Neurosci* **30**: 11848-11857.
- Kotani S, Yamauchi T, Teramoto T, Ogura H (2008). Donepezil, an acetylcholinesterase inhibitor, enhances adult hippocampal neurogenesis. *Chem Biol Interact* **175**: 227-230.
- Krantic S, Isorce N, Mechawar N, Davoli MA, Vignault E, Albuquerque M *et al* (2012). Hippocampal GABAergic neurons are susceptible to amyloid- β toxicity in vitro and are decreased in number in the Alzheimer's disease TgCRND8 mouse model. *J Alzheimers Dis* **29**: 293-308.
- Kulkarni VA, Jha S, Vaidya VA (2002). Depletion of norepinephrine decreases the proliferation, but does not influence the survival and differentiation, of granule cell progenitors in the adult rat hippocampus. *Eur J Neurosci* **16**: 2008-2012.
- Kumar P, Kumar A (2009). Protective effect of rivastigmine against 3-nitropropionic acid-induced Huntington's disease like symptoms: possible behavioural, biochemical and cellular alterations. *Eur J Pharmacol* **615**: 91-101.
- Kuzyk A, Kastyak M, Agrawal V, Gallant M, Sivakumar G, Rak M *et al* (2010). Association among amyloid plaque, lipid, and creatine in hippocampus of TgCRND8 mouse model for Alzheimer disease. *J Biol Chem* **285**: 31202-31207.
- Lambon Ralph MA, Patterson K, Graham N, Dawson K, Hodges JR (2003). Homogeneity and heterogeneity in mild cognitive impairment and Alzheimer's disease: a cross-sectional and longitudinal study of 55 cases. *Brain* **126**: 2350-2362.
- La Ferla FM (2002). Calcium dyshomeostasis and intracellular signaling in Alzheimer's disease. *Nat Rev Neurosci* **3**: 863-872.
- La Ferla FM, Green KM, Oddo S (2007). Intracellular amyloid- β in Alzheimer's disease. *Nat Rev Neurosci* **8**: 499-509.
- Lai AY, McLaurin J (2012). Inhibition of amyloid-beta peptide aggregation rescues the autophagic deficits in the TgCRND8 mouse model of Alzheimer's disease. *Biochim Biophys Acta* **1822**: 1629-1637.
- Lanari A, Amenta F, Silvestrelli G, Tomassoni D, Parnetti L (2006). Neurotransmitter deficits in behavioural and psychological symptoms of Alzheimer's disease. *Mech Ageing Dev* **127**: 158-165.
- Larson ME, Lesné SE (2012). Soluble A β production and toxicity. *J Neurochem* **120 (Suppl. 1)**: 125-139.

- Laske C, Stransky E, Leyhe T, Eschweiler G, Wittorf A, Richartz E *et al* (2006). Stage-dependent BDNF serum concentrations in Alzheimer's disease. *J Neural Transm* **113**: 1217-1224.
- Lazarou M, McKenzie M, Ohtake A, Thorburn DR, Ryan MT (2007). Analysis of the assembly profiles for mitochondrial-and nuclear-DNA-encoded subunits into complex I. *Mol Cell Biol* **27**: 4228-4237.
- Lenaz G, Baracca A, Barbero G, Bergamini C, Dalmonte ME, Del Sole M *et al* (2010). Mitochondrial respiratory chain super-complex I-III in physiology and pathology. *Biochim Biophys Acta* **1797**: 633-640.
- Levi-Montalcini R, Hamburger V (1951). Selective growth-stimulating effects of mouse sarcoma on the sensory and sympathetic nervous system of the chick embryo. *J Exp Zool* **116**: 321-361.
- Lewis J, Dickson DW, Lin W-L, Chisholm L, Corral A, Jones G *et al*. (2001). Enhanced neurofibrillary degeneration in transgenic mice expressing mutant tau and APP. *Science* **293**: 1487-1491.
- Leyhe T, Stransky E, Eschweiler GW, Buchkremer G, Laske C (2008). Increase of BDNF serum concentration during donepezil treatment of patients with early Alzheimer's disease. *Eur Arch Psychiatry Clin Neurosci* **258**: 124-128.
- Li C, Ebrahimi A, Schluesener H (2013). Drug pipeline in neurodegeneration based on transgenic mice models of Alzheimer's disease. *Ageing Res Rev* **12**: 116-140.
- Li N, Ragheb K, Lawler G, Sturgis J, Rajwa B, Melendez JA *et al* (2003). Mitochondrial complex I inhibitor rotenone induces apoptosis through enhancing mitochondrial reactive oxygen species production. *J Biol Chem* **278**: 8516-8525.
- Li Y-J, Oliveira SA, Xu P, Martin ER, Stenger JE, Scherzer CR *et al* (2003). Glutathione S-transferase omega-1 modifies age-at-onset of Alzheimer disease and Parkinson disease. *Hum Mol Genet* **12**: 3259-3267.
- Liang WS, Reiman EM, Valla J, Dunckley T, Beach TG, Grover A *et al* (2008). Alzheimer's disease is associated with reduced expression of energy metabolism genes in posterior cingulate neurons. *PNAS* **105**: 4441-4446.
- Lin MT, Beal MF (2006). Mitochondrial dysfunction and oxidative stress in neurodegenerative diseases. *Nature* **443**: 787-795.
- Lindvall O, Ernfors P, Bengzon J, Kokaia Z, Smith ML, Siesjo BK, Persson H (1992). Differential regulation of mRNAs for nerve growth factor, brain-derived neurotrophic factor, and neurotrophin 3 in the adult rat brain following cerebral ischemia and hypoglycemic coma. *PNAS USA* **89**: 648-652.

Li X, Bürklen T, Yuan X, Schlattner U, Desiderio DM, Wallimann T, Homayouni R (2006). Stabilization of ubiquitous mitochondrial creatine kinase preprotein by APP family proteins. *Mol Cell Neurosci* **31**: 263-272.

Liu Y, Fiskum G, Schubert D (2002). Generation of reactive oxygen species by the mitochondrial electron transport chain. *J Neurochem* **80**: 780-787.

Liu Y, Yoo MJ, Savonenko A, Stirling W, Price DL, Borchelt DR *et al* (2008). Amyloid pathology is associated with progressive monoaminergic neurodegeneration in a transgenic mouse model of Alzheimer's disease. *J Neurosci* **28**: 13805-13814.

Loughlin SE, Foote SL, Bloom FE (1986). Efferent projections of nucleus locus coeruleus: topographic organization of cells of origin demonstrated by three-dimensional reconstructions. *Neuroscience* **18**: 291-306.

Lovasic L, Bauschke H, Janus C (2005). Working memory impairment in a transgenic amyloid precursor protein TgCRND8 mouse model of Alzheimer's disease. *Genes Brain Behav* **4**: 197-208.

Ludwig V, Schwarting RKW (2007). Neurochemical and behavioural consequences of striatal injection of 5,7-dihydroxytryptamine. *J Neurosci Methods* **162**: 108-118.

Lue L-F, Kuo Y-M, Roher AE, Brachova L, Shen Y, Sue L *et al* (1999). Soluble amyloid β peptide concentration as a predictor of synaptic change in Alzheimer's disease. *Am J Pathol* **155**: 853-862.

Lustbader JW, Cirilli M, Lin C, Xu HW, Takuma K, Wang N *et al* (2004). A β AD directly links Abeta to mitochondrial toxicity in Alzheimer's disease. *Science* **304**: 448-452.

Lyness SA, Zarow C, Chui HC (2003). Neuron loss in key cholinergic and aminergic nuclei in Alzheimer's disease: a meta-analysis. *Neurobiol Aging* **24**: 1-23.

Ma K, Mount HTJ, McLaurin J (2011). Region-specific distribution of b-amyloid peptide and cytokine expression in TgCRND8 mice. *Neurosci Lett* **492**: 5-10.

Madrigal JLM, Kalinin S, Richardson JC, Feinstein DL (2007). Neuroprotective actions of noradrenaline: effects on glutathione synthesis and activation of peroxisome proliferator activated receptor delta. *J Neurochem* **103**: 2092-2101.

Madrigal JL, Leza JC, Polak P, Kalinin S, Feinstein DL (2009). Astrocyte-derived MCP-1 mediates neuroprotective effects of noradrenaline. *J Neurosci* **29**: 263-267.

Maeda T (2000). The locus coeruleus: history. *J Chem Neuroanat* **18**: 57-64.

Maisonpierre PC, Belluscio L, Squinto S, Ip NY, Furth ME, Lindsay RM, Yancopoulos GD (1990). Neurotrophin-3: a neurotrophic factor related to NGF and BDNF. *Science* **247**: 1446-1451.

Maj MC, MacKay N, Levandovskiy V, Addis J, Baumgartner ER, Baumgartner MR *et al* (2005). Pyruvate dehydrogenase phosphatase deficiency: Identification of the first mutation in two brothers and restoration of activity by protein complementation. *J Clin Endocrinol Metab* **90**: 4101-4107.

Maj M, Sriskandarajah N, Hung V, Browne I, Shah B, Weadge A *et al* (2011). Identification of drug candidates which increase cytochrome c oxidase activity in deficient patient fibroblasts. *Mitochondrion* **11**: 264-272.

Manaye KF, McIntire DD, Mann DM, German DC (1995). Locus coeruleus cell loss in the aging human brain: a non-random process. *J Comp Neurol* **358**: 79-87.

Manczak M, Anekonda TS, Henson E, Park BS, Quinn J, Reddy H (2006). Mitochondria are a direct site of Ab accumulation in Alzheimer's disease neurons: implications for free radical generation and oxidative damage in disease progression. *Hum Mol Gen* **15**: 1437-1449.

Manczak M, Park BS, Jung Y, Reddy H (2004). Differential expression of oxidative phosphorylation genes in patients with Alzheimer's disease. *Neuromol Med* **5**: 147-162.

Mann DMA, Lincoln J, Yates PO, Stamp JE, Toper S (1980). Changes in the monoamine containing neurons of the human CNS in senile dementia. *Brit J Psychiat* **136**: 533-541.

Mann DMA, Stanley M, Neophylides A, DeLeon MJ, Ferris SH, Gershon S (1981). Central amine metabolism in Alzheimer's disease: *in vivo* relationship to cognitive deficit. *Neurobiol Aging* **2**: 57-60.

Mann DMA, Yates PO, Hawkes J (1982). The noradrenergic system in Alzheimer and multi-infarct dementias. *J Neurol Neurosurg Psychiatry* **45**: 113-119.

Mann DMA, Yates PO, Marcyniuk B (1984a). A comparison of changes in the nucleus basalis and locus coeruleus in Alzheimer's disease. *J Neurol Neurosurg Psychiatry* **47**: 201-203.

Mann DMA, Yates PO, Marcyniuk B (1984b). Alzheimer's presenile dementia, senile dementia of Alzheimer type and Down's syndrome in middle age form an age related continuum of pathological changes. *Neuropath Appl Neurobiol* **10**: 185-207.

Marcyniuk B, Mann DMA, Yates PO (1986). Loss of nerve cells from locus coeruleus in Alzheimer's disease is topographically arranged. *Neurosci Lett* **64**: 247-252.

Marien MR, Colpaert FC, Rosenquist AC (2004). Noradrenergic mechanisms in neurodegenerative diseases: a theory. *Brain Res Rev* **45**: 38-78.

Maruszak A, Zekanowski C (2011). Mitochondrial dysfunction and Alzheimer's disease. *Prog Neuropsychopharmacol Biol Psychiatry* **35**: 320-330.

Marzo A, Bai J, Otani S (2009). Neuroplasticity Regulation by Noradrenaline in Mammalian Brain. *Curr Neuropharmacol* **7**: 286-295.

Mastrogiacomo F, Bergeron C, Kish SJ (1993). Brain alpha-ketoglutarate dehydrogenase complex activity in Alzheimer's disease. *J Neurochem* **61**: 2007-2014.

Mathew A, Yoshida Y, Maekawa T, Kumar DS (2011). Alzheimer's disease: cholesterol a menace? *Brain Res Bull* **86**: 1-12.

Matsunaga W, Shirokawa T, Isobe K (2004). BDNF is necessary for maintenance of noradrenergic innervations in the aged rat brain. *Neurobiol Aging* **25**: 341-348.

Matthews KL, Chen CP, Esiri MM, Keene J, Minger SL, Francis PT (2002). Noradrenergic changes, aggressive behaviour and cognition in patients with dementia. *Biol Psychiatry* **51**: 407-416.

Maurer K, Volk S, Gerbaldo H (1997). Auguste D and Alzheimer's Disease. *Lancet* **349**: 1546-1549.

McCandless DW, Stavinoha WB, Abel MS (1984). Maintenance of regional chemical integrity for energy metabolites in microwave heat inactivated mouse brain. *Brain Res Bull* **13**: 253-255.

McCool MF, Varty GB, Del Vecchio RA, Kazdoba TM, Parker EM, Hunter JC, Hyde LA (2003). Increased auditory startle response and reduced prepulse inhibition of startle in transgenic mice expressing a double mutant form of amyloid precursor protein. *Brain Res* **994**: 99-106.

McGowan E, Pickford F, Kim J, Onstead L, Eriksen J, Yu C *et al* (2005). A β_{42} is essential for parenchymal and vascular amyloid deposition in mice. *Neuron* **47**:191-199.

McKenzie M, Lazarou M, Thorburn DR, Ryan MT (2006). Mitochondrial respiratory chain supercomplexes are destabilized in Barth syndrome patients. *J Mol Biol* **361**: 462-469.

McKhann GM, Knopman DS, Chertkow H, Hyman BT, Jack Jr. CR, Kawas CH *et al*. (2011). The diagnosis of dementia due to Alzheimer's disease: Recommendations from the National Institute on Aging-Alzheimer's Association workgroups on diagnostic guidelines for Alzheimer's disease. *Alzheimers Dement* **7**: 263-269.

McLaurin J, Cecal R, Kierstead ME, Tian X, Phinney AL, Manea M *et al* (2002). Therapeutically effective antibodies against amyloid- β peptide target amyloid- β residues 4-10 and inhibit cytotoxicity and fibrillogenesis. *Nat Med* **8**: 1263-1269.

- McLaurin J, Kierstead ME, Brown ME, Hawkes CA, Lambermon MH, Phinney AL *et al* (2006). Cyclohexanehexol inhibitors of Abeta aggregation prevent and reverse Alzheimer phenotype in a mouse model. *Nat Med* **12**: 801-808.
- McMillan PJ, White SS, Franklin A, Greenup JL, Leverenz JB, Raskind MA, Szot P (2011). Differential response of the central noradrenergic nervous system to the loss of locus coeruleus neurons in Parkinson's disease and Alzheimer's disease. *Brain Res* **1373**: 240-252.
- Mejías-Aponte CA, Drouin C, Aston-Jones G (2009). Adrenergic and noradrenergic innervation of the midbrain ventral tegmental area and retrorubral field: prominent inputs from medullary homeostatic centres. *Neuroscience* **29**: 3613-3626.
- Meredith GE, Kang UJ (2006). Behavioral models of Parkinson's disease in rodents: a new look at an old problem. *Mov Disord* **21**: 1595-1606.
- Mesulam M (2004). The cholinergic lesion of Alzheimer's disease: pivotal factor or side show? *Learn Mem* **11**: 43-49.
- Michalski B, Fahnstock M (2003). Pro-brain-derived neurotrophic factor is decreased in parietal cortex in Alzheimer's disease. *Mol Brain Res* **111**: 148-154.
- Moreira PI, Carvalho C, Zhu X, Smith MA, Perry G (2010). Mitochondrial dysfunction is a trigger of Alzheimer's disease pathophysiology. *Biochem Biophys Acta* **1802**: 2-10.
- Morgan K (2011). The three new pathways leading to Alzheimer's disease. *Neuropathol Appl Neurobiol* **37**: 353-357.
- Mori K, Ozaki E, Zhang B, Yang L, Yokoyama A, Takeda I, Maeda N, Sakanaka M, Tanaka J (2002). Effects of norepinephrine on rat cultured microglial cells that express alpha1, alpha2, beta1 and beta2 adrenergic receptors. *Neuropharmacology* **43**: 1026-1034.
- Morilak DA, Barrera G, Echevarria DJ, Garcia AS, Hernandez A, Ma S, Petre CO (2005). Role of brain norepinephrine in the behavioral response to stress. *Prog Neuropsychopharmacol Biol Psychiatry* **29**: 1214-1224.
- Moroji T, Takahashi K, Ikeda C (1978). Levels of biogenic amines and their metabolites in rat whole brain after rapid tissue fixation with microwave irradiation. *No To Skinkei* **30**:1 303-1308.
- Morris JC, Storandt M, Miller P, McKeel DW, Price JL, Rubin EH, Berg L (2001). Mild cognitive impairment represents early-stage Alzheimer's disease. *Arch Neurol* **58**: 397-405.
- Mosconi L, Pupi A, De Leon MJ (2008). Brain glucose hypometabolism and oxidative stress in preclinical Alzheimer's disease. *Ann NY Acad Sci* **1147**: 180-95

- Mount HTJ, Martel J-C, Fluit P, Wu Y, Gallo-Hendrikx E, Cosi C *et al* (2004). Progressive sensorimotor impairment is not associated with reduced dopamine and high-energy phosphate donors in a model of ataxia-telangiectasia. *J Neurochem* **88**: 1449-1454.
- Mumby DG, Pinel JP (1994). Rhinal cortex lesions and object recognition in rats. *Behav Neurosci* **108**: 11-18.
- Murer MG, Boissiere F, Yan Q, Hunot S, Villares J, Faucheux B *et al* (1999). An immunohistochemical study of the distribution of brain-derived neurotrophic factor in the adult human brain, with particular reference to Alzheimer's disease. *Neuroscience* **88**: 1015-1032.
- Murphy EJ (2010). Brain fixation for analysis of brain lipid-mediators of signal transduction and brain eicosanoid requires head-focused microwave irradiation: An historical perspective. *Prostag Oth Lipid M* **91**: 63-67.
- Murray KD, Gall CM, Jones EG, Isackson PJ (1994). Differential regulation of brain-derived neurotrophic factor and type II calcium/calmodulin-dependent protein kinase messenger RNA expression in Alzheimer's disease. *Neuroscience* **60**: 37-48.
- Mutisya EM, Bowling AC, Beal MF (1994). Cortical cytochrome oxidase activity is reduced in Alzheimer's disease. *J Neurochem* **63**: 2179-84.
- Nagahara AH, Merrill DA, Coppola G, Tsukada S, Schroeder BE, Shaked GM *et al* (2009). Neuroprotective effects of brain-derived neurotrophic factor in rodent and primate models of Alzheimer's disease. *Nature Med* **15**: 331-337.
- Nagahara AH, Tuszynski MH (2011). Potential therapeutic uses of BDNF in neurological and psychiatric disorders. *Nat Rev Drug Discov* **10**: 209-219.
- Narisawa-Saito M, Wakabayashi K, Tsuji S, Takahashi H, Nawa H (1996). Regional specificity of alterations in NGF, BDNF and NT-3 levels in Alzheimer's disease. *Neuroreport* **7**: 2925-2928.
- Näslund J, Haroutunian V, Mohs R, Davis KL, Davies P, Greengard P, Buxbaum JD (2000). Correlation between elevated levels of amyloid β -peptide in the brain and cognitive decline. *JAMA* **283**: 1571-1577.
- Nilsson L, Nordberg A, Hardy J, Wester P, Winblad B (1986). Physostigmine restores ^3H -acetylcholine efflux from Alzheimer brain slices to normal level. *J Neural Transm* **67**: 275-285.
- Nixon RA (2007). Autophagy, amyloidogenesis and Alzheimer disease. *J Cell Sci* **120**: 4081-4091.

Nixon RA, Wegiel J, Kumar A, Yu WH, Peterhoff C, Cataldo A *et al* (2005). Extensive involvement of autophagy in Alzheimer disease: an immunoelectron microscopy study. *J Neuropathol Exp Neurol* **64**: 113-122.

Nixon RA, Yang DS (2011). Autophagy failure in Alzheimer's disease – locating the primary defect. *Neurobiol Disease* **43**: 38-45.

Oddo S, Billings L, Kesslak JP, Cribbs DH, LaFerla FM (2004). A β immunotherapy leads to clearance of early, but not late, hyperphosphorylated tau aggregates via the proteasome. *Neuron* **43**: 321-332.

Oddo S, Caccamo A, Shepherd JD, Murphy MP, Golde TE, Kaye R, Metherate R, Mattson MP, Akbari Y, LaFerla FM (2003). Triple transgenic model of Alzheimer's disease with plaques and tangles: intracellular A β and synaptic dysfunction. *Neuron* **39**: 409-421.

O'Donnell J, Zeppenfeld D, McConnell E, Pena S, Nedergaard M (2012). Norepinephrine: A Neuromodulator That Boosts the Function of Multiple Cell Types to Optimize CNS Performance. *Neurochem Res* DOI:10.1007/s11064-012-0818-x.

Ohm TG, Busch C, Bohl J (1997). Unbiased estimation of neuronal numbers in the human nucleus coeruleus during aging. *Neurobiol Aging* **18**: 393–399.

Ohno M, Yoshimatsu A, Kobayashi M, Watanabe S (1997). Noradrenergic DSP-4 lesions aggravate impairment of working memory produced by hippocampal muscarinic blockade in rats. *Pharmacol Biochem Behav* **57**: 257-261.

Palmer AM, Francis PT, Bowen DM, Benton JS, Neary D, Mann DM *et al* (1987a). Catecholaminergic neurones assessed ante-mortem in Alzheimer's disease. *Brain Res* **414**: 365-375.

Palmer AM, Wilcock GK, Esiri MM, Francis PT, Bowen DM (1987b). Monoaminergic innervations of the frontal and temporal lobes in Alzheimer's disease. *Brain Res* **401**: 231-238.

Papa S, Rasmø D, Scacco S, Signorile A, Technikova-Dobrova Z, Palmisano G *et al* (2008). Mammalian complex I: a regulable and pacemaker in mitochondrial respiratory function. *Biochem Biophys Acta* **1777**: 719-728.

Parron C, Poucet B, Save E (2006). Cooperation between the hippocampus and the entorhinal cortex in spatial memory: A disconnection study. *Behav Brain Res* **170**: 99-109.

Parihar MS, Brewer GJ (2007). Mitochondrial failure in Alzheimer's disease. *Am J Cell Physiol Cell Physiol* **292**: C8-C23.

Parker WD Jr., Filley CM, Parks JK (1990). Cytochrome oxidase deficiency in Alzheimer's disease. *Neurology* **40**: 1302-1303

Parker WD JR., Parks J, Filley CM, Klein-Schmidt-DeMasters BK (1994). Electron transport chain defects in Alzheimer's disease brain. *Neurology* **44**: 1090-1096.

Pathak RU, Davey GP (2008). Complex I and energy thresholds in the brain. *Biochim Biophys Acta* **1777**: 777-782.

Pavlov PF, Wiehager B, Sakai J, Frykman S, Behbahani H, Winblad B, Ankarcrona M (2011). Mitochondrial gamma-secretase participates in the metabolism of mitochondria-associated amyloid precursor protein. *FASEB J* **25**: 78-88.

Peng S, Garzon DJ, Marchese M, Klein W, Ginsberg SD, Francis BM, Mount HTJ *et al* (2009). Decreased brain-derived neurotrophic factor depends on amyloid aggregation state in transgenic mouse models of Alzheimer's disease. *J Neurosci* **29**: 9321- 9329.

Peng S, Wu J, Mufson EJ, Fahnstock M (2005). Precursor form of brain-derived neurotrophic factor and mature brain-derived neurotrophic factor are decreased in pre-clinical stages of Alzheimer's disease. *J Neurochem* **93**: 1412-1421.

Pereira C, Santos MS, Oliveira C (1998). Mitochondrial function impairment induced by amyloid beta-peptide on PC12 cells. *Neuroreport* **9**: 1749-1755.

Perier C, Tieu K, Guegan C, Caspersen C, Jackson-Lewis V, Carelli V, Martinuzzi A, Hirano M, Przedborski S, Vila M (2005). Complex I deficiency primes BAX-dependent neuronal apoptosis through mitochondrial oxidative damage. *PNAS* **102**: 19126-19131.

Perry EK, Blessed G, Tomlinson BE, Perry RH, Crow TJ, Cross AJ, Dockray GJ, Dimaline R, Arregui A (1981a). Neurochemical activities in human temporal lobe related to aging and Alzheimer type changes. *Neurobiol Aging* **2**: 251-256.

Perry EK, Perry RH, Blessed G, Tomlinson BE (1977). Necropsy evidence of central cholinergic deficits in senile dementia. *Lancet* **1**: 189.

Perry EK, Perry RH, Tomlinson BE, Blessed G, Gibson PH (1980). Coenzyme A acetylating enzymes in Alzheimer's disease: possible cholinergic compartments of pyruvate dehydrogenase. *Neurosci Lett* **18**: 105-110.

Perry EK, Tomlinson BE, Blessed G, Bergmann K, Gibson PH, Perry RH (1978). Correlation of cholinergic abnormalities with senile plaques and mental test scores in senile dementia. *BMJ* **2**: 1457-1459.

Perry EK, Tomlinson BE, Blessed G, Perry RH, Cross AJ, Crow TJ (1981b). Neuropathological and biochemical observations on the noradrenergic system in Alzheimer's disease. *J Neurol Sci* **51**: 279-287.

- Pertovaara A (2006) Noradrenergic pain modulation. *Prog Neurobiol* **80**: 53-83.
- Petersen RC, Smith GE, Waring SC, Ivnik RJ, Tangalos EG, Kokmen E (1999). Mild Cognitive Impairment: clinical characterization and outcome. *Arch Neurol* **56**: 303-308.
- Petersen RC (2011). Mild cognitive impairment. *N Engl J Med* **364**: 2227-2234.
- Pettegrew JW, Panchalingam K, Klunk WE, McClure RJ, Muenz LR (1994). Alterations of cerebral metabolism in probable Alzheimer's disease: A preliminary study. *Neurobiol Aging* **15**: 117-132.
- Phillips HS, Hains JM, Armanini M, Laramée JR, Johnson SA, Winslow JW (1991). BDNF mRNA is decreased in the hippocampus of individuals with Alzheimer's disease. *Neuron* **7**: 695-702.
- Pietrini P, Guazzelli M, Sarteschi P, Grady CL, Haxby JV, Swedo SE *et al* (1993). Positron Emission Tomography as a tool to investigate cerebral glucose metabolism in neurologic and psychiatric diseases: studies in Alzheimer's disease and in obsessive-compulsive disorder. *Psychiatry and Advanced Technologies*. Raven Press: New York.
- Pigino G, Morfini G, Atagi Y, Deshpande A, Yu C, Jungbauer L *et al.* (2009). Disruption of fast axonal transport is a pathogenic mechanism for intraneuronal amyloid beta. *PNAS USA* **106**: 5907-5912.
- Poon WW, Blurton-Jones M, Tu CH, Feinberg LM, Chabrier MA, Harris JW *et al* (2011). β -amyloid impairs axonal BDNF retrograde trafficking. *Neurobiol Aging* **32**: 821-833.
- Pope S, Land JM, Heales SJR (2008). Oxidative stress and mitochondrial dysfunction in neurodegeneration; cardiolipin a critical target? *Biochim Biophys Acta* **1777**: 794-799.
- Price JL, Morris JC (1999). Tangles and plaques in nondemented aging and "preclinical" Alzheimer's Disease. *Ann Neurol* **45**: 358-368.
- Prusky GT, Alam NM, Beekman S, Douglas RM (2004). Rapid quantification of adult and developing mouse spatial vision using a virtual optomotor system. *Invest Ophthalmol Vis Sci* **45**: 4611-4616.
- Pugh PL, Vidgeon-Hart MP, Ashmeade T, Culbert AA, Seymour Z, Perren MJ *et al* (2007). Repeated administration of the noradrenergic neurotoxin N-(2-chloroethyl)-N-ethyl-2-bromobenzylamine (DSP-4) modulates neuroinflammation and amyloid plaque load in mice bearing amyloid precursor protein and presenilin-1 mutant transgenes. *J Neuroinflamm* **4**: 8.
- Raji MA, Brady SR (2001). Mirtazapine for treatment of depression and comorbidities in Alzheimer disease. *Ann Pharmacother* **35**: 1024-1027

Rak M, Del Bigio MR, Mai S, Westaway D, Gough K (2007). Dense-core and diffuse Abeta plaques in TgCRND8 mice studied with synchrotron FTIR microspectroscopy. *Biopolymers* **87**: 207-212.

Reddy P, McWeeny S, Park BS, Manczak M, Gutala R, Partovi D *et al* (2004). Gene expression profiles of transcripts in amyloid precursor protein transgenic mice: upregulation of mitochondrial metabolism and apoptotic genes is an early cellular change in Alzheimer's disease. *Hum Mol Genet* **13**: 1225-1240.

Ressler KJ, Nemeroff CB (1999). Role of norepinephrine in the pathophysiology and treatment of mood disorders. *Biol Psychiatry* **46**: 1219-1233.

Rhein V, Baysang G, Rao S, Meier F, Bonert A, Müller-Spahn F, Eckert A (2009a). Amyloid-beta leads to impaired cellular respiration, energy production and mitochondrial electron chain complex activities in human neuroblastoma cells. *Cell Mol Neurobiol* **29**: 1063-1071.

Rhein V, Song X, Wiesner A, Ittner LM, Baysang G, Meier F *et al* (2009b). Amyloid- β and tau synergistically impair the oxidative phosphorylation system in triple transgenic Alzheimer's disease mice. *PNAS* **106**: 20057-20062.

Richter H, Ambrée O, Lewejohann L, Herring A, Keyvani K, Paulus W (2008). Wheel-running in a transgenic model of Alzheimer's disease: Protection or symptom? *Behav Brain Res* **190**: 74-84.

Rizk P, Salazar J, Raisman-Vozari R, Marien M, Ruberg M, Colpaert F *et al* (2006). The alpha2-adrenoceptor antagonist dexefaroxan enhances hippocampal neurogenesis by increasing the survival and differentiation of new granule cells. *Neuropsychopharmacology* **31**: 1146-1157.

Russo Neustadt A, Cotman CW (1997). Adrenergic receptors in Alzheimer's disease brain: Selective increases in the cerebella of aggressive patients. *J Neurosci* **17**: 5573-5580.

Rylett RJ, Ball MJ, Colhoun EH (1983). Evidence for high affinity choline transport in synaptosomes prepared from hippocampus and neocortex of patients with Alzheimer's disease. *Brain Res* **289**: 169-175.

Sairanen M, Lucas G, Ernfors P, Castren M, Castren E (2005). Brain-derived neurotrophic factor and antidepressant drugs have different but coordinated effects on neuronal turnover, proliferation, and survival in the adult dentate gyrus. *J Neurosci* **25**: 1089-1094.

Scharfman H, Goodman J, Macleod A, Phani S, Antonelli C, Croll S (2005). Increased neurogenesis and the ectopic granule cells after intra-hippocampal BDNF infusion in adult rats. *Exp Neurol* **192**: 348-356.

Sara SJ (2009). The locus coeruleus and noradrenergic modulation of cognition. *Nat rev Neurosci* **10**: 211-223.

Sara SJ, Bouret S (2012). Orienting and reorienting: the locus coeruleus mediates cognition through arousal. *Neuron* **76**: 130-141.

Schallert T, Upchurch M, Lobaugh N, Farrar SB, Spirduso WW, Gilliam P et al (1982). Tactile extinction: distinguishing between sensorimotor and motor asymmetries in rats with unilateral nigrostriatal damage. *Pharmacol Biochem Behav* **16**: 455-462.

Scheibner J, Trendelenburg AU, Hein L, Starke K (2001). Stimulation frequency-noradrenaline release relationships examined in alpha2A-, alpha2B- and alpha2C-adrenoceptor-deficient mice. *Naunyn Schmiedebergs Arch Pharmacol* **364**: 321-328.

Schindowski K, Belarbi K, Buée L (2008). Neurotrophic factors in Alzheimer's disease: role of axonal transport. *Genes Brain Behav* **7**: 43-56.

Schliebs R, Arendt T (2006). The significance of the cholinergic system in the brain during aging and in Alzheimer's disease. *J Neural Transm* **113**: 1625-1644.

Schmechel DE, Saunders AM, Strittmatter WJ, Crain BJ, Hulette CM, Joo SH et al (1993). Increased amyloid beta-peptide deposition in cerebral cortex as a consequence of apolipoprotein E genotype in late-onset Alzheimer disease. *PNAS* **90**: 9649-9653.

Scullion GA, Kendall DA, Marsden CA, Sunter D, Pardon MC (2011). Chronic treatment with the alpha(2)-adrenoceptor antagonist fluparoxan prevents age-related deficits in spatial working memory in APPxPS1 transgenic mice without altering beta-amyloid plaque load or astrogliosis. *Neuropharmacology* **60**: 223-234.

Schwartzing RKW, Thiel CM, Muller CP, Huston JP (1998). Relationship between anxiety and serotonin in the ventral striatum. *Neuroreport* **9**: 1025-1029.

Selkoe DJ (2002). Alzheimer's disease is a synaptic failure. *Science* **298**: 789-791.

Serrano-Pozo A, Frosch MP, Masliah E, Hyman BT (2011). Neuropathological alterations in Alzheimer's disease. *Cold Spring Harb Perspect Med* **1**: a006189.

Seyda A, Newbold RF, Hudson TJ, Verner A, MacKay N et al (2001). A novel syndrome affecting multiple mitochondrial functions, located by microcell-mediated transfer to chromosome 2p14-2p13. *Am J Hum Genet* **68**: 386-396.

Shankar GM, Walsh DM (2009). Alzheimer's disease: synaptic dysfunction and A β . *Mol Neurodegener* **4**: 48.

Sharma Y, Xu T, Graf WM, Fobbs A, Sherwood CC, Hof PR, Allman JM, Manaye KF (2010). Comparative anatomy of the locus coeruleus in humans and nonhuman primates. *J Comp Neurol* **518**: 963-971.

Shepherd JK, Grewal SS, Fletcher A, Bill DJ, Dourish CT (1994). Behavioural and pharmacological characterization of the elevated “zero-maze” as an animal model of anxiety. *Psychopharmacology* **116**: 56-64.

Siegel GJ, Chauhan NB (2000). Neurotrophic factors in Alzheimer’s and Parkinson’s disease brain. *Brain Res Rev* **33**: 199-227.

Sik A, Nieuwehuizen P, Prickaerts J, Blockland A (2003). Performance of different mouse strains in an object recognition task. *Behav Brain Res* **147**: 49-54.

Sipos E, Kurunczi A, Kasza A, Horvath J, Felszeghy K, Laroche S *et al* (2007). β -amyloid pathology in the entorhinal cortex of rats induces memory deficits: Implications for Alzheimer’s disease. *Neuroscience* **147**: 28-36.

Sirk D, Zhu Z, Wadia JS, Shulyakova N, Phan N, Fong J, Mills LR (2007). Chronic exposure to sub-lethal beta-amyloid ($A\beta$) inhibits the import of nuclear-encoded proteins to mitochondria in differentiated PC12 cells. *J Neurochem* **103**: 1989-2003

Sisodia SS, St. George-Hyslop PH (2002). γ -secretase, notch, $A\beta$ and Alzheimer’s disease: where do the presenilins fit in? *Nat Rev Neurosci* **3**: 281-290.

Sitsen JMA, Moors J (1994). Mirtazapine, a novel antidepressant, in the treatment of anxiety symptoms. *Drug Invest* **8**: 339-344.

Small GW, Ercoli LM, Silverman DH, Huang SC, Komo S, Bookheimer SY *et al.* (2000). Cerebral metabolic and cognitive decline in persons at genetic risk for Alzheimer’s disease. *PNAS USA* **97**: 6037-6042.

Smiley JF, Subramanian M, Mesulam MM (1999). Monoaminergic-cholinergic interactions in the primate basal forebrain. *Neuroscience* **93**: 817-829.

Sorbi S, Bird ED, Blass JP (1983). Decreased pyruvate dehydrogenase complex activity in Huntington and Alzheimer brain. *Ann Neurol* **13**: 72-78.

Spires TL, Meyer-Luehmann M, Stern EA, McLean PJ, Skoch J, Nguyen PT *et al* (2005). Dendritic spine abnormalities in amyloid precursor protein transgenic mice demonstrated by gene transfer and intravital multiphoton microscopy. *J Neurosci* **25**: 7278–7287

Srivareerat M, Tran TT, Salim S, Aleisa AM, Alkadhi KA (2011). Chronic nicotine restores normal $A\beta$ levels and prevents short-term memory and E-LTP impairment in $A\beta$ rat model of Alzheimer’s disease. *Neurobiol Aging* **32**: 834-844.

Strazielle C, Strurchler-Pierrat C, Staufenbiel M, Lalonde R (2003). Regional brain cytochrome oxidase activity in β -amyloid precursor protein transgenic mice with the Swedish mutation. *Neuroscience* **118**: 1151-1163.

- Steckler T, Drinkenburg WHIM, Sahgal A, Aggleton JP (1998). Recognition memory in rats – II. Neuroanatomical substrates. *Prog Neurobiol* **54**: 313-332.
- Steru L, Chermat R, Thierry B, Simon P (1985). The tail suspension test: a new method for screening antidepressants in mice. *Psychopharmacology* **85**: 367-370.
- Stimmel GL, Dopheide JA, Stahl SM (1997). Mirtazapine: an antidepressant with noradrenergic and specific serotonergic effects. *Pharmacotherapy* **17**: 10-21.
- Stokin GB, Lillo C, Falzone TL, Brusch RG, Rockenstein E, Mount SL *et al* (2005). Axonopathy and Transport Deficits Early in the Pathogenesis of Alzheimer's Disease. *Science* **307**: 1282-1288.
- Stoub TR, Rogalski EJ, Leurgans S, Bennett DA, DeToledo-Morrell L (2010). Rate of entorhinal and hippocampal atrophy in incipient and mild AD: relation to memory function. *Neurobiol Aging* **31**: 1089-1098.
- Strong R, Huang JS, Huang SS, Chung HD, Hale C, Burke WJ (1991). Degeneration of the cholinergic innervation of the locus coeruleus in Alzheimer's disease. *Brain Res* **542**: 23-28.
- Su JH, Cummings BJ, Cotman CW (1998). Plaque biogenesis in brain aging and Alzheimer's disease. II. Progressive transformation and developmental sequence of dystrophic neurites. *Acta Neuropathol* **96**: 463-471.
- Sullivan PG, Brown MR (2005). Mitochondrial aging and dysfunction in Alzheimer's disease. *Prog Neuropsychopharmacol Biol Psychiatry* **29**: 407-410.
- Supnet C, Grant J, Kong H, Westaway D, Mayne M (2006). Amyloid- β -(1-42) increases ryanodine receptor-3 expression and function in neurons of TgCRND8 mice. *J Biol Chem* **281**: 38440-38447.
- Swerdlow RH (2012). Mitochondria and cell bioenergetics: Increasingly recognized components and a possible etiologic cause of Alzheimer's disease. *Antioxid Redox Signaling* **16**: 1434-1455.
- Szot P, Leverenz JB, Peskind ER, Kiyasu E, Rohde K, Miller MA, Raskind MA (2000). Tyrosine hydroxylase and norepinephrine transporter mRNA expression in the locus coeruleus in Alzheimer's disease. *Mol Brain Res* **84**: 135-140.
- Szot P, Miguelez C, White SS, Franklin A, Sikkema C, Wilkinson CW *et al* (2010). A comprehensive analysis of the effect of DSP4 on the locus coeruleus noradrenergic system in the rat. *Neuroscience* **166**: 279-291.
- Szot P, White SS, Greenup JL, Leverenz JB, Peskind ER, Raskind MA (2006). Compensatory changes in the noradrenergic nervous system in the locus coeruleus and

hippocampus of postmortem subjects with Alzheimer's disease and dementia with Lewy bodies. *J Neurosci* **26**: 467-478.

Szot P, White SS, Greenup JL, Leverenz JB, Peskind ER, Raskind MA (2007). Changes in the adrenoceptors in the prefrontal cortex of subjects with dementia: evidence of compensatory changes. *Neuroscience* **146**: 471-480.

Szapacs ME, Numis AL, Andrews AM (2004). Late onset loss of hippocampal 5-HT and NE is accompanied by increases in BDNF protein expression in mice co-expressing mutant APP and PS1. *Neurobiol Dis* **16**: 572-580.

Tanghe A, Termont A, Merchiers P, Schilling S, Demuth H, Scrocchi L et al (2010). Pathological Hallmarks, clinical parallels, and value for drug testing in Alzheimer's disease of the APP[V717I] London transgenic mouse model. *Int J Alzheimer Dis* 2010: 417314.

Tanzi RE, Bertram L (2005). Twenty years of the Alzheimer's disease amyloid hypothesis: a genetic perspective. *Cell* **120**: 545-555.

Tapia-Arancibia L, Aliaga E, Silhol M, Arancibia S (2008). New insights into brain BDNF function in normal aging and Alzheimer disease. *Brain Res Rev* **59**: 201-220.

Tellez S, Colpaert F, Marien M (1997). Acetylcholine release in the rat prefrontal cortex in vivo: modulation by α_2 -adrenoceptor agonists and antagonists. *J Neurochem* **68**: 778-785.

Tellez S, Colpaert F, Marien M (1999). α_2 -Adrenoceptor modulation of cortical acetylcholine release *in vivo*. *Neuroscience* **89**: 1041-1050.

Terry RD, Masliah E, Salmon DP, Butters N, DeTeresa R, Hill R et al (1991). Physical basis of cognitive alteration in Alzheimer's disease: synapse loss is the major correlate of cognitive impairment. *Ann Neurol* **30**: 572-580.

Terwel D, Bothmer J, Wolf E, Meng F, Jolles J (1998). Affected enzyme activities in Alzheimer's disease are sensitive to ante mortem hypoxia. *J Neurolog Sci* **16**: 147-156.

Thal DR, Capetillo-Zarate E, Tredici K, Braak H (2006). The development of amyloid β -protein deposits in the aged brain. *Science of Aging Knowledge Environment* **6**: 1-9.

Thal DR, Rüb U, Schultz C, Sassin I, Ghebremedhin E, Del Tredici K et al (2000). Sequence of abeta-protein deposition in the human medial temporal lobe. *J Neuropathol Exp Neurol* **59**: 733-748.

Thal DR, Rüb U, Orantes M, Braak H (2002). Phases of A β -deposition in the human brain and its relevance for the development of AD. *Neurology* **58**: 1791-1800.

Thomas BB, Seiler MJ, Sadda SR, Coffey PJ, Aramant RB (2004). Optokinetic test to evaluate visual acuity of each eye independently. *J Neurosci Methods* **138**: 7-13.

Tillement L, Lecanu L, Papadopoulos V (2011). Alzheimer's disease: effects of β -amyloid on mitochondria. *Mitochondrion* **11**: 13-21.

Tomlinson BE, Irving D, Blessed G (1981). Cell loss in the locus coeruleus in senile dementia of Alzheimer type. *J Neurol Sci* **49**: 419-428.

Tong L, Balazs R, Thornton PL, Cotman CW (2004). β -amyloid peptide at sublethal concentrations downregulates brain-derived neurotrophic factor functions in cultured cortical neurons. *J Neurosci* **24**: 6799-6809.

Tong L, Thornton PL, Balazs R, Cotman CW (2001). Beta-amyloid-(1–42) impairs activity-dependent cAMP-response element-binding protein signaling in neurons at concentrations in which cell survival is not compromised. *J Biol Chem* **276**: 17301-17306.

Traver S, Marien M, Martin E, Hirsch EC, Michel PP (2006). The phenotypic differentiation of locus coeruleus noradrenergic neurons mediated by brain-derived neurotrophic factor is enhanced by corticotropin releasing factor through the activation of a cAMP-dependent signaling pathway. *Mol Pharmacol* **70**: 30–40.

Traver S, Salthun-Lassalle B, Marien M, Hirsch EC, Colpaert F, Michel PP (2005). The neurotransmitter noradrenaline rescues septal cholinergic neurons in culture from degeneration caused by low-level oxidative stress. *Mol Pharmacol* **67**: 1882-1891.

Troade J-D, Marien M, Darios F, Hartmann A, Ruberg M, Colpaert F *et al* (2001). Noradrenaline provides long-term protection to dopaminergic neurons by reducing oxidative stress. *J Neurochem* **79**: 200-210.

Trushina E, Nemutlu E, Zhang S, Christensen T, Camp J, Mesa J *et al* (2012). Defects in mitochondrial dynamics and metabolomic signatures of evolving energetic stress in mouse models of familial Alzheimer's disease. *PLoS ONE* **7**: e32737.

Tully K, Bolshakov VY (2010). Emotional enhancement of memory: how norepinephrine enables synaptic plasticity. *Mol Brain* **3**:15.

Vacher B, Funes P, Chopin P, Cussac D, Heusler P, Tourette A, Marien M (2010). Rigid analogues of the α_2 -adrenergic blocker atipamezole: small changes, big consequences. *J Med Chem* **53**: 6986-6995.

Valla J, Schneider L, Niedzielko T, Coon KD, Caselli R, Sabbagh MN, *et al* (2006). Impaired platelet mitochondrial activity in Alzheimer's disease and mild cognitive impairment. *Mitochondrion* **6**: 323-330.

Van Dam D, Abramowski D, Staufienbiel M, De Deyn PP (2005). Symptomatic effect of donepezil, rivastigmine, galantamine and memantine on cognitive deficits in the APP23 model. *Psychopharmacology* **180**: 177–190.

- Van Dam D, De Deyn PP (2006). Drug discovery in dementia: the role of rodent models. *Nat Rev Drug Discov* **5**: 956-970.
- Van Dam D, D'Hooge R, Staufenbiel M, Van Ginneken C, Van Meir F, De Deyn PP (2003). Age-dependent cognitive decline in the APP23 model precedes amyloid deposition. *Eur J Neurosci* **17**: 388-396.
- Vannucci M, Pezer N, Helmstaedter C, Schaller K, Viggiano M, Elger C, Grunwald T (2008). Hippocampal response to visual objects is related to visual memory functioning. *Neuroreport* **19**: 965-968.
- Vaucher E, Fluit P, Chishti MA, Westaway D, Mount HTJ, Kar S (2002). Object recognition memory and cholinergic parameters in mice expressing human presenilin 1 transgenes. *Exp Neurol* **175**: 398-406.
- Veyrac A, Didier A, Colpaert F, Jourdan F, Marien M (2005). Activation of noradrenergic transmission by α_2 -adrenoceptor antagonists counteract deafferentation-induced neuronal death and cell proliferation in the adult mouse olfactory bulb. *Exp Neurol* **194**: 444-456.
- Viggiano M, Galli G, Righi S, Brancati C, Gori G, Cincotta M (2008). Visual recognition memory in Alzheimer's disease: Repetition-lag effects. *Exp Aging Res* **34**: 267-281.
- Vijayashankar N, Brody H (1979). A quantitative study of the pigmented neurons in the nuclei locus coeruleus and subcoeruleus in man as related to aging. *J Neuropathol Exp Neurol* **38**: 490-497.
- Vogel RO, Smeitink JAM, Nijtmans LGJ (2007). Human mitochondrial complex I assembly: A dynamic and versatile process. *Biochim Biophys Acta* **1767**: 1215-1227.
- Von Gunten A, Kövari E, Bussi re T, Rivara C-B, Gold G, Bouras C, Hof PR, Giannakopoulos P (2006). Cognitive impact of neuronal pathology in the entorhinal cortex and CA1 field in Alzheimer's disease. *Neurobiol Aging* **27**: 270-277.
- Votyakova TV, Reynolds IJ (2001). DeltaPsi(m)-dependent and- independent production of reactive oxygen species by rat brain mitochondria. *J Neurochem* **79**: 266-277.
- Walker JM, Fowler SW, Sun AY, Weisman GA, Wood WG, Sun GY et al (2011). Spatial learning and memory impairment and increased locomotion in a transgenic amyloid precursor protein mouse model of Alzheimer's disease. *Behav Brain Res* **222**: 169-175.
- Wallimann T, Wyss M, Brdiczka D, Nicolay K, Eppenberger HM (1992). Intracellular compartmentation structure and function of creatine kinase isoenzymes in tissues with high and fluctuating energy demands: the 'phosphocreatine circuit' for cellular energy homeostasis. *Biochem J* **281**: 21-40.

Walsh DM, Teplow DB (2012). Alzheimer's disease and the amyloid- β protein. *Prog Mol Biol Transl Sci* **107**: 101-124.

Wenge B, Bönisch, H., 2009. Interference of the noradrenergic neurotoxin DSP4 with neuronal and non-neuronal monoamine transporters. *Naunyn Schmiedebergs Arch Pharmacol* **380**: 523-529.

Westerman MA, Cooper-Blacketer D, Mariash A, Kotilinek L, Kawarabayashi T, Younkin LH *et al* (2002). The relationship between A β and Memory in the Tg2576 mouse model of Alzheimer's disease. *J Neurosci* **22**: 1858-1867.

Whitehouse PJ, Price DL, Struble RG, Clark AW, Coyle JT, De Long MR (1982). Alzheimer's disease and senile dementia- loss of neurons in the basal forebrain. *Science* **215**: 1237-1239.

Wilcock GK, Esiri MM, Bowen DM, Smith CC (1982). Alzheimer's disease. Correlation of cortical choline acetyltransferase activity with the severity of dementia and histological abnormalities. *J Neurol Sci* **57**: 407-417.

Wills LP, Trager RE, Beeson GC, Lindsey CC, Peterson YK, Beeson CC, Schnellmann RG (2012). The β_2 -adrenoceptor agonist formoterol stimulates mitochondrial biogenesis. *J Pharmacol Exp Therap* **342**: 106-118.

Winters BD, Forwood SE, Cowell RA, Saksida LM, Bussey TJ (2004). Double dissociation between the effects of peri-postrhinal cortex and hippocampal lesions on tests of object recognition and spatial memory: heterogeneity of function within the temporal lobe. *J Neurosci* **24**: 5901-5908.

Wirhns O, Bayer TA (2010). Neuron loss in transgenic mouse models of Alzheimer's disease. *Int J Alzheimers Dis* **2010**: ID: 723782.

Wood PL, Altar CA (1988). Dopamine release in vivo from nigrostriatal, mesolimbic and mesocortical neurons: utility of 3-methoxytyramine measurements. *Pharmacol Rev* **40**: 163-187.

Wood PL, Kim HS, Altar CA (1987). In Vivo assessment of dopamine and noradrenaline release in rat neocortex: gas chromatography-mass spectrometry measurement of 3-Methoxytyramine and normetanephrine. *J Neurochem* **48**: 574-579.

Woodhouse A, Vickers JC, Adlard PA, Dickson TC (2009). Dystrophic neurites in TgCRND8 and Tg2576 mice mimic human pathological brain aging. *Neurobiol Aging* **30**: 8640-874.

Xu F, Ackerley C, Maj MC, Addis JB, Levandovskiy V, Lee J *et al* (2008). Disruption of a mitochondrial RNA-binding protein gene results in decreased cytochrome b expression and a marked reduction in ubiquinol-cytochrome c reductase activity in mouse heart mitochondria. *Biochem J* **416**: 15-26.

- Yamaguchi H, Yamazaki T, Ishiguro K, Shoji M, Nakazato Y, Hirai S (1992). Ultrastructural localization of Alzheimer amyloid beta/A4 protein precursor in the cytoplasm of neurons and senile plaque-associated astrocytes. *Acta Neuropathol* **85**: 15-22.
- Yamamoto-Sasaki M, Ozawa H, Saito T, Rosler M, Riederer P (1999). Impaired phosphorylation of cyclic AMP response element binding protein in the hippocampus of dementia of the Alzheimer type. *Brain Res* **824**: 300-303.
- Yan Q, Rosenfeld RD, Matheson CR, Hawkins NA, Lopez OT, Bennett L, Welcher AA (1997). Expression of brain-derived neurotrophic factor protein in the adult rat central nervous system. *Neuroscience* **78**: 431-448.
- Yang D-S, Stavrides P, Mohan PS, Kaushik S, Kumar A, Ohno M *et al* (2011). Reversal of autophagy dysfunction in the TgCRND8 mouse model of Alzheimer's disease ameliorates amyloid pathologies and memory deficits. *Brain* **134**: 258-277.
- Yanpallewar SU, Fernandes K, Marathe SV, Vadodaria KC, Jhaveri D, Rommelfanger K *et al* (2010). α_2 -adrenoceptor blockade accelerates the neurogenic, neurotrophic, and behavioral effects of chronic antidepressant treatment. *J Neurosci* **30**: 1096-1109.
- Yates CM, Butterworth J, Tennant MC, Gordon A (1990). Enzyme activities in relation to pH and lactate in postmortem brain in Alzheimer-type and other dementias. *J Neurochem* **55**: 1624-1630.
- Ye X, Tai W, Zhang D (2012). The early events of Alzheimer's disease pathology: from mitochondrial dysfunction to BDNF axonal transport deficits. *Neurobiol Aging* **33**: 1122.e1-1122.e10.
- Yiu AP, Rashid AJ, Josselyn SA (2011). Increasing CREB Function in the CA1 Region of Dorsal Hippocampus Rescues the Spatial Memory Deficits in a Mouse Model of Alzheimer's Disease. *Neuropsychopharmacology* **36**: 2169-2186.
- Yu J-T, Wang N-D, Ma T, Jiang H, Guan J, Tan L (2011). Roles of β -adrenergic receptors in Alzheimer's disease: Implications for novel therapeutics. *Brain Res Bull* **84**: 114-117.
- Yücel YH, Jardon B, Kim MS, Bonaventure N (1990). Directional asymmetry of the horizontal monocular head and eye optokinetic nystagmus: Effects of picrotoxin. *Vision Res* **30**: 549-555.
- Yuede CM, Zimmerman SD, Dong H, Kling MJ, Bero AW, Holtzman DM *et al* (2009). Effects of voluntary and forced exercise on plaque deposition, hippocampal volume, and behavior in the Tg2576 mouse model of Alzheimer disease. *Neurobiol Dis* **35**: 426-432.

- Zaborszky L, Rosin DL, Kiss J (2004). Alpha-adrenergic receptor (α_{2A}) is colocalized in basal forebrain cholinergic neurons: A light and electron microscopic double immunolabeling study. *J Neurocytol* **33**: 265-276.
- Zahs KR, Ashe KH (2010). 'Too much good news'—are Alzheimer mouse models trying to tell us how to prevent, not cure, Alzheimer's disease? *Trends Neurosci* **33**: 381-389.
- Zarow C, Lyness SA, Mortimer JA, Chui HC (2003). Neuronal loss is greater in the locus coeruleus than nucleus basalis and substantia nigra in Alzheimer and Parkinson diseases. *Arch Neurology* **60**: 337-341.
- Zhang Y, Marcillat O, Giulivi C, Ernster L, Davies KJA (1990). The oxidative inactivation of mitochondrial electron transport chain components and ATPase. *J Biol Chem* **265**: 16330-16336.
- Zhang Y, Thompson R, Zhang H, Xu H (2011). APP processing in Alzheimer's disease. *Mol Brain* **4**: 3.
- Zhang YJ, Xu YF, Chen XQ, Wang XC, Wang JZ (2005a). Nitration and oligomerization of tau induced by peroxynitrite inhibit its microtubule-binding activity. *FEBS Lett* **579**: 2421-2427.
- Zhang YJ, Xu YF, Liu YH, Yin J, Wang JZ (2005b). Nitric oxide induces tau hyperphosphorylation via glycogen synthase kinase-3 β activation. *FEBS Lett* **579**: 6230-6236.
- Zheng F, Luo Y, Wang H (2009). Regulation of brain-derived neurotrophic factor-mediated transcription of the immediate early gene *Arc* by intracellular calcium and calmodulin. *J Neurosci Res* **87**: 380-392.
- Zweig RM, Ross CA, Hedreen JC, Steele C, Cardillo JE, Whitehouse PJ *et al* (1988). The neuropathology of aminergic nuclei in Alzheimer's disease. *Ann Neurol* **24**: 233-242.

Copyright Acknowledgements

RightsLink – Your Account

13-04-26 3:50 PM


[My Orders](#)
[My Library](#)
[My Profile](#)

Welcome beverly.francis@utoronto.ca

[Log out](#) | [Help](#)
[My Orders](#) > [Orders](#) > [All Orders](#)

License Details

This is a License Agreement between Beverly M Francis ("You") and Elsevier ("Elsevier"). The license consists of your order details, the terms and conditions provided by Elsevier, and the [payment terms and conditions](#).

[Get the printable license.](#)

License Number	3136611194172
License date	Apr 26, 2013
Licensed content publisher	Elsevier
Licensed content publication	Brain Research Bulletin
Licensed content title	Alzheimer's disease: Cholesterol a menace?
Licensed content author	Anila Mathew, Yasuhiko Yoshida, Toru Maekawa, D. Sakthi Kumar
Licensed content date	10 August 2011
Licensed content volume number	86
Licensed content issue number	1-2
Number of pages	12
Type of Use	reuse in a thesis/dissertation
Portion	figures/tables/illustrations
Number of figures/tables/illustrations	1
Format	both print and electronic
Are you the author of this Elsevier article?	No
Will you be translating?	No
Order reference number	None
Title of your thesis/dissertation	Noradrenergic deficits contribute to impairment in the TgCRND8 mouse model of Alzheimer's disease
Expected completion date	Jun 2013
Estimated size (number of pages)	240
Elsevier VAT number	GB 494 6272 12
Permissions price	0.00 USD
VAT/Local Sales Tax	0.00 USD
Total	0.00 USD

[← Back](#)



RightsLink®

[My Orders](#)

[My Library](#)

[My Profile](#)

Welcome [beverly.francis@utoronto.ca](#)

[Log out](#) | [Help](#)

[My Orders](#) > [Orders](#) > [All Orders](#)

License Details

This is a License Agreement between Beverly M Francis ("You") and Elsevier ("Elsevier"). The license consists of your order details, the terms and conditions provided by Elsevier, and the [payment terms and conditions](#).

[Get the printable license.](#)

License Number	3136640382091
License date	Apr 26, 2013
Licensed content publisher	Elsevier
Licensed content publication	Neuroscience
Licensed content title	α 2-Adrenoceptor modulation of cortical acetylcholine release <i>in vivo</i>
Licensed content author	S Tellez, F Colpaert, M Marien
Licensed content date	April 1999
Licensed content volume number	89
Licensed content issue number	4
Number of pages	10
Type of Use	reuse in a thesis/dissertation
Portion	figures/tables/illustrations
Number of figures/tables/illustrations	1
Format	both print and electronic
Are you the author of this Elsevier article?	No
Will you be translating?	No
Order reference number	None
Title of your thesis/dissertation	Noradrenergic deficits contribute to impairment in the TgCRND8 mouse model of Alzheimer's disease
Expected completion date	Jun 2013
Estimated size (number of pages)	240
Elsevier VAT number	GB 494 6272 12
Permissions price	0.00 USD
VAT/Local Sales Tax	0.00 USD
Total	0.00 USD



RightsLink®

[My Orders](#)

[My Library](#)

[My Profile](#)

Welcome beverly.francis@utoronto.ca

[Log out](#) | [Help](#)

[My Orders](#) > [Orders](#) > [All Orders](#)

License Details

This is a License Agreement between Beverly M Francis ("You") and Elsevier ("Elsevier"). The license consists of your order details, the terms and conditions provided by Elsevier, and the [payment terms and conditions](#).

[Get the printable license.](#)

License Number	3136650486489
License date	Apr 26, 2013
Licensed content publisher	Elsevier
Licensed content publication	Neurobiology of Aging
Licensed content title	Object recognition memory and BDNF expression are reduced in young TgCRND8 mice
Licensed content author	Beverly M. Francis, John Kim, Meredith E. Barakat, Stephan Fraenkl, Yeni H. Yücel, Shiyong Peng, Bernadeta Michalski, Margaret Fahnestock, JoAnne McLaurin, Howard T.J. Mount
Licensed content date	March 2012
Licensed content volume number	33
Licensed content issue number	3
Number of pages	9
Type of Use	reuse in a thesis/dissertation
Portion	full article
Format	both print and electronic
Are you the author of this Elsevier article?	Yes
Will you be translating?	No
Order reference number	None
Title of your thesis/dissertation	Noradrenergic deficits contribute to impairment in the TgCRND8 mouse model of Alzheimer's disease
Expected completion date	Jun 2013
Estimated size (number of pages)	240
Elsevier VAT number	GB 494 6272 12
Permissions price	0.00 USD
VAT/Local Sales Tax	0.00 USD
Total	0.00 USD

[← Back](#)